

Anaerobic Protein Degradation for Resources Recovery from Nitrogen-Loaded Residual Streams

Deng, Z.

DOI

[10.4233/uuid:0fbfd624-39a0-45f7-8046-c90e854baca6](https://doi.org/10.4233/uuid:0fbfd624-39a0-45f7-8046-c90e854baca6)

Publication date

2023

Document Version

Final published version

Citation (APA)

Deng, Z. (2023). *Anaerobic Protein Degradation for Resources Recovery from Nitrogen-Loaded Residual Streams*. [Dissertation (TU Delft), Delft University of Technology]. <https://doi.org/10.4233/uuid:0fbfd624-39a0-45f7-8046-c90e854baca6>

Important note

To cite this publication, please use the final published version (if applicable). Please check the document version above.

Copyright

Other than for strictly personal use, it is not permitted to download, forward or distribute the text or part of it, without the consent of the author(s) and/or copyright holder(s), unless the work is under an open content license such as Creative Commons.

Takedown policy

Please contact us and provide details if you believe this document breaches copyrights. We will remove access to the work immediately and investigate your claim.

**Anaerobic Protein Degradation for
Resources Recovery from
Nitrogen-Loaded Residual Streams**

Zhe Deng

Propositions accompanying the thesis:

Anaerobic Protein Degradation for Resources Recovery from Nitrogen-Loaded Residual Streams

Zhe Deng

1. Anaerobic digestion is an advantageous pre-treatment for ammoniacal nitrogen recovery especially for protein-rich and high solids streams, because it transforms the organic nitrogen into ammoniacal nitrogen while reducing COD and solids concentration (this thesis).
2. Two main factors constraining the reuse of ammoniacal nitrogen are the quantity and the quality of ammoniacal nitrogen that can be recovered from the residual streams (this thesis).
3. The retardation of protein degradation by the presence of carbohydrate is due to 1) the substrate-preference of the dominant bacteria, including the facultative bacteria and the sugar fermenters, and 2) the higher growth rate and yield of the dominant bacteria (this thesis).
4. AnSBR can be an effective alternative to optimise protein conversion, as the feast and famine operational scheme allows the depletion of easily degradable substrates and provides an interval for slowly degradable substrates (this thesis).
5. Proper prediction of organic nitrogen mineralization into ammonium during anaerobic digestion is required for optimizing substitution of mineral fertilizer by digestates (Bareha et al., 2018).
6. The knowledge and understanding of wastewater treatment has advanced extensively and moved away from empirically based approaches to a fundamentally based 'first principles' approach embracing chemistry, microbiology, physical and bioprocess engineering, and mathematics (Henze et al., 2008).
7. Science is both a way of thinking about the natural world and the sum of the information and theories that result from such thinking (Nelson and Cox, 2017).
8. To obtain labelled casein, we need to label the whole cow (Prof. Jeppe Lund Nielsen, Aalborg University).
9. Everyone can start a PhD, but not everyone can finish it.
10. The best time to start anything is now.

These propositions are regarded as opposable and defensible, and have been approved as such by the promoters, Prof.dr.ir. J.B. van Lier and Dr.ir. H.L.F.M. Spanjers.

**Anaerobic Protein Degradation for
Resources Recovery from
Nitrogen-Loaded Residual Streams**

Dissertation

For the purpose of obtaining the degree of doctor
at Delft University of Technology
by the authority of the Rector Magnificus Prof.dr.ir. T.H.J.J. van der Hagen
chair of the Board for Doctorates
to be defended publicly on

Tuesday 3 October 2023 at 15:00 o'clock

by

Zhe DENG

Master of Science in Civil Engineering,
Delft University of Technology, the Netherlands

Born in Guangxi, China

This dissertation has been approved by the promotor.

Composition of the doctoral committee:

Rector Magnificus,	Chairperson
Prof.dr.ir. J.B. van Lier	Delft University of Technology, promotor
Dr.ir. H.L.F.M. Spanjers	Delft University of Technology, promotor

Independent members:

Dr.ir. S. Pacheco Ruiz	Biothane-Veolia
Prof.dr.ir. L. Appels	Katholieke Universiteit Leuven, Belgium
Prof.dr.ir. D. Machado De Sousa	Wageningen University
Prof.dr.ir. D.G. Weissbrodt	Norwegian University of Science and Technology, Norway
Prof.dr.ir. M.K. de Kreuk	Delft University of Technology

Reserve member:

Prof.dr. H.M. Jonkers	Delft University of Technology
-----------------------	--------------------------------

Printed by: Proefschrift-aio.nl

ISBN: 978-94-93353-16-9

Copyright © 2023 by Zhe Deng

Email: dengzhe2017@hotmail.com

All rights reserved. No part of the material protected by this copyright may be reproduced or utilized in any form or by any means, electronic or mechanical, including photocopying, recording, or by any information storage and retrieval system, without the written permission from the copyright owner.

SUMMARY

Summary

The demand for reactive nitrogen, i.e., ammonia (NH_3), is constantly growing as the global population grows, especially in the nitrogen (N) fertiliser production sector. Simultaneously, the reactive nitrogen in residual streams, i.e., mainly ammonium (NH_4^+) and nitrate (NO_3^-), has caused serious environmental issues, e.g., eutrophication and species diversity loss.

NH_3 is produced from non-reactive nitrogen gas (N_2) by means of the energy-intensive Haber-Bosch process. Typically, reactive nitrogen is converted back to the non-reactive N_2 by nitrification and denitrification in wastewater treatment plants at the cost of energy. To reduce the overall energy demand and reduce the pool of reactive nitrogen in the environment, a potential solution can be the recovery and reuse of NH_3 and NH_4^+ (Total Ammoniacal nitrogen, TAN) from N-loaded residual streams.

Ongoing TAN recovery research has mainly focused on the efficiency of different available technologies from the perspective of a specific application of the recovered TAN. One important aspect, the availability of N-loaded residual streams and their compositions, is overlooked: there is a lack of identification and characterisation of the potential streams for TAN recovery.

Therefore, an analysis of the whole TAN recovery chain was carried out, from identifying and categorising the potential N-loaded residual streams, evaluating the available technologies for TAN recovery, to the possibilities of TAN reuse. The overview of the whole TAN recovery chain provided a roadmap for TAN recovery based on both the characteristics of the N-loaded residual streams and the TAN format of the local demand, such as, fertiliser, fuel, etc.

Additionally, protein-rich streams were identified as a typical N-loaded residual stream with high potential for TAN recovery, that received less attention in TAN recovery research. In most of the N-loaded residual streams, the directly recoverable TAN is mainly produced from anaerobic digestion (AD) of proteins. Prior to recovery, organic nitrogen compounds in protein-rich streams need to be converted to TAN. Therefore, efficient anaerobic conversion of proteins is considered of prime importance for TAN recovery.

AD is advantageous for converting protein to TAN, as it simultaneously lowers the chemical oxygen demand (COD) and total suspended solids content (TSS). Anaerobic conversion of

proteins to methane (CH₄) can be simplified into three steps: 1) hydrolysis of proteins to amino acids, 2) acidification or deamination of amino acids to NH₄⁺ and volatile fatty acids (VFAs), and 3) methanogenesis of VFAs. Notably, the conversion of proteins to TAN is often observed retarded in the presence of carbohydrates. Besides, the rate-limiting step of the anaerobic protein degradation is still in dispute.

To investigate the effects of the presence of carbohydrates and identify the rate-limiting step in anaerobic protein degradation, a kinetic study was performed with model proteins, i.e., bovine serum albumin (BSA) and casein (CAS). The reaction rates of hydrolysis, deamination and methanogenesis were compared between the presence and absence of carbohydrates in batch experiments. Application of the modified Gompertz model showed that the presence of carbohydrates increased the hydrolysis rate and methanogenesis rate significantly, but slightly decreased the deamination rate. Methanogenesis limited the conversion during the first 20 hours of batch incubation, whereas deamination was identified as the rate-limiting step in AD of soluble proteins.

To further study the mechanism of the retardation of anaerobic protein degradation in the presence of carbohydrates, a comparison between the microbiota acclimated to protein or carbohydrate was conducted in a continuously fed acidification reactor. CAS was used as the model protein and lactose (LAC) was the model carbohydrate, both presenting the main components in protein-rich dairy wastewaters. Results showed a low similarity between the microbial communities adapted to CAS and those adapted to LAC. The presence of LAC deteriorated the anaerobic protein degradation and shifted the microbial community towards the one adapted to LAC. The dominant genera, in the presence and absence of carbohydrates, were found to be able to ferment both proteins and carbohydrates.

Moreover, to directly identify the active protein degraders and deduce their metabolic pathways, ecophysiological analysis was performed by metaproteomics. ¹³C-labelled protein substrate was applied in batch incubations and proteins extracted from the biomass were analysed. Taxonomic annotation of the proteins through the overlapping of the proteome and metagenome¹ led to the identification of the most active genus, *Acinetobacter*. Similar to the dominant genera in CAS, *Acinetobacter* is also able to ferment both proteins and carbohydrates. Results showed that the outer membrane-bound proteins and porin proteins

Overlapping of the proteome and metagenome¹: combining protein analysis data and metagenomic data as a reference of the whole microbiome present in the experimental environment.

Summary

were the most frequently found incorporating the ^{13}C -substrate. These proteins are associated with the proteinases or the amino acids transportation channel across the cell wall. The results confirmed that the retardation of anaerobic protein degradation by the presence of carbohydrates could be attributed to the substrate preference of the protein degraders.

Accordingly, an anaerobic sequencing batch reactor (AnSBR) was tested as a competitive alternative for efficient protein conversion. Theoretically, the feast and famine operation of AnSBR can provide a time-phased degradation of proteins and carbohydrates, allowing the depletion of more rapidly degradable carbohydrates and providing intervals for the degradation of more slowly degradable proteins. The applied AnSBR achieved 90% TCOD removal and 85% protein degradation without pre-treatment at an organic loading rate (OLR) up to $6.2 \text{ kg COD}\cdot\text{L}^{-1}\cdot\text{d}^{-1}$. Furthermore, correlation analysis showed that hydraulic retention time (HRT), OLR, and solids retention time (SLR) were key operational parameters for TCOD removal efficiency and sludge settling performance. For protein-rich residual streams, protein degradation shall be considered as the key process in the reactor design and operation.

Overall, AD of protein-rich streams, which is upstream of TAN recovery, has a high potential to recover TAN. Although the anaerobic protein to TAN conversion is retarded by the presence of carbohydrates, AnSBR can be an effective alternative to optimise protein conversion.

SAMENVATTING

Samenvatting

Naarmate de wereldbevolking groeit, groeit ook de vraag naar reactieve stikstof, oftewel ammoniak (NH_3). Dit is vooral het geval in de stikstof (N) meststof productiesector. Tegelijkertijd leidt reactieve stikstof in restwaters, voornamelijk ammonium (NH_4^+) en nitraat (NO_3^-), echter tot ernstige milieuproblemen zoals eutrofiëring en verlies van soortenrijkdom.

NH_3 wordt geproduceerd uit niet-reactief stikstofgas (N_2) door middel van het energie-intensieve Haber-Bosch proces. Gewoonlijk wordt reactieve stikstof weer omgezet naar het niet reactieve N_2 door nitrificatie en denitrificatie in afvalwaterzuiveringsinstallaties, ten koste van energie. Om de totale energievraag en de pool van reactieve stikstof in het milieu te verminderen, is een mogelijke oplossingsrichting het terugwinnen en hergebruiken van NH_3 en NH_4^+ (TAN) uit N-rijk restwater.

Lopend onderzoek naar het terugwinnen van TAN was voornamelijk gericht op de efficiëntie van verschillende beschikbare technologieën, waarbij een specifieke toepassing van de teruggewonnen TAN werd aangehouden. Een belangrijk aspect dat over het hoofd wordt gezien betreft de beschikbare N-rijke restwaters en hun samenstelling: er is een gebrek aan de identificatie en karakterisering van de potentiële restwateren voor TAN-terugwinning.

Daarom is een analyse van de gehele TAN-terugwinning uitgevoerd, van het identificeren en categoriseren van de potentiële N-rijke restwaters, het evalueren van de beschikbare technologieën voor TAN-terugwinning, tot de mogelijkheden voor het opnieuw gebruiken van TAN. Het resulterende overzicht van de gehele TAN-terugwinning gaf een routekaart voor TAN-terugwinning aan de hand van zowel de karakteristieken van het N-rijke restwater als de lokale vraag naar een bepaald type TAN, bijvoorbeeld voor bemesting, brandstof, enz.

Daarnaast werd eiwitrijk restwater geïdentificeerd als een typisch N-rijke restwater met hoog potentieel voor TAN-terugwinning, dat tot nog toe minder aandacht kreeg in het onderzoek naar TAN-terugwinning. In de meeste N-rijke restwateren wordt het direct terug te winnen TAN hoofdzakelijk geproduceerd door anaerobe afbraak (anaerobic digestion, AD) van eiwitten. Voor terugwinning moeten organische stikstofverbindingen in eiwitrijk restwater worden omgezet naar TAN. Daarom wordt efficiënte anaerobe omzetting van eiwitten beschouwd als van primair belang voor TAN-terugwinning.

AD voor het omzetten van eiwitten naar TAN heeft het bijkomende voordeel dat het tegelijkertijd het chemisch zuurstofverbruik (chemical oxygen demand, COD) en het totaal aan gesuspenderde stoffen (total suspended solids, TSS) verlaagt. De anaerobe omzetting van eiwitten naar methaan (CH_4) kan vereenvoudigd worden weergegeven door drie stappen: 1) de hydrolyse van eiwitten naar aminozuren, 2) de verzuring ofwel de de-aminering van aminozuren naar NH_4^+ en vluchtige vetzuren (volatile fatty acids, VFAs), en 3) methanogenese van VFA's. Opmerkelijk is dat de omzetting van eiwitten naar TAN vaak wordt geremd in aanwezigheid van koolhydraten. Bovendien is de beperkende stap van de anaerobe afbraak van eiwitten nog steeds onderwerp van discussie.

Om het effecten van de aanwezigheid van koolhydraten te onderzoeken en de beperkende stap in anaerobe eiwitdegradatie te identificeren, is een kinetische studie uitgevoerd met modelproteïnen, te weten: bovine serum albumine (BSA) en caseïne (CAS). De reactiesnelheden van hydrolyse, de-aminering en methanogenese werden vergeleken in batch-experimenten met en zonder koolhydraten. Toepassing van het gewijzigde Gompertz-model liet zien dat de aanwezigheid van koolhydraten de hydrolysesnelheid en de methanogenesesnelheid significant verhoogde, maar de de-amineringsnelheid licht verlaagde. Methanogenese was beperkend voor het proces gedurende de eerste 20 uur van de batchincubatie, terwijl de-aminering werd geïdentificeerd als de limiterende stap bij AD van opgeloste proteïnen.

Om het mechanisme van de vertraging van anaerobe eiwitafbraak in aanwezigheid van koolhydraten verder te bestuderen, werd een vergelijking gemaakt tussen de microbiota geacclimatiseerd aan eiwitten of aan koolhydraten, in een continu gevoede verzuringreactor. CAS werd gebruikt als modeleiwit en lactose (LAC) als modelkoolhydraat, beide belangrijke componenten in eiwitrijk zuivelafvalwater. De resultaten toonden een lage gelijkenis tussen de microbiële gemeenschappen die aangepast waren aan CAS en die aangepast waren aan LAC. De aanwezigheid van LAC verslechterde de anaerobe eiwitafbraak en verschoof de microbiële gemeenschap naar die aangepast aan LAC. De dominante geslachten, in aanwezigheid en afwezigheid van koolhydraten, bleken beide eiwitten en koolhydraten te kunnen fermenteren.

Samenvatting

Om de actieve eiwitdegraderende organismen direct te identificeren en hun metaboliseroute af te leiden, werd een ecofysiologische analyse uitgevoerd door middel van meta-proteomica. ¹³C-gelabeld eiwitrijk substraat werd toegepast in batch-incubaties en proteïnen die uit de biomassa werden geëxtraheerd werden geanalyseerd. Taxonomische annotatie van de proteïnen door middel van overlapping van het proteome en het metagenoom¹ leidde tot de identificatie van het meest actieve geslacht, *Acinetobacter*. Resultaten toonden aan dat proteïnen aan de buitenste membraan en porineproteïnen het meest frequent de ¹³C-substraat bevatten. Deze proteïnen zijn geassocieerd met de proteasen van de aminozuurtransportkanalen langs de celwand. Net als de dominante geslachten in CAS is *Acinetobacter* ook in staat om zowel eiwitten als koolhydraten te fermenteren. De resultaten bevestigden dat de vertraging van de anaerobe eiwitdegradatie door de aanwezigheid van koolhydraten toegeschreven kon worden aan de voorkeur voor substraten van de eiwitdegraderende organismen.

Vervolgens werd een anaerobe sequencing batch reactor (AnSBR) getest als een concurrerend alternatief voor efficiënte eiwitconversie. Theoretisch kan het 'feast and famine' regime van de AnSBR een scheiding mogelijk maken in de tijd voor de afbraak van zowel eiwitten als koolhydraten. Hierdoor worden de sneller afbreekbare koolhydraten opgebruikt en intervallen voor de afbraak van langzamer afbreekbare eiwitten gecreëerd. De toegepaste AnSBR verwijderde 90% van het totaal COD met een 85% eiwitdegradatie, zonder voorbehandeling bij een organische belasting (organic loading rate, OLR) tot 6.2 kg COD·L⁻¹·d⁻¹. Bovendien liet de correlatieanalyse zien dat de hydraulische verblijftijd (HRT), OLR en biomassaverblijftijd belangrijke operationele waren voor de TCOD-verwijderingsefficiëntie en de slibbezinkingresultaat. Voor eiwitrijke restwater wordt eiwitdegradatie beschouwd als het sleutelproces bij het ontwerp en de operationele van de uitvoering van de reactor.

Al met al biedt de AD van eiwitrijk restwater als voorbehandeling bij de terugwinning van TAN, een groot potentieel voor de terugwinning van TAN. Hoewel de anaerobe conversie van eiwit naar TAN wordt vertraagd door de aanwezigheid van koolhydraten kan de AnSBR een effectieve technologie zijn om de eiwitconversie te optimaliseren.

Overlapping van het proteoom en het metagenoom¹: Het combineren van proteïne-analysegegevens en metagenomische gegevens als referentie voor het gehele microbiom dat aanwezig is in de experimentele omgeving.

CONTENTS

Chapter 1	Introduction	1
Chapter 2	Recovery and applications of ammoniacal nitrogen from nitrogen-loaded residual streams: A review	9
Chapter 3	Anaerobic protein degradation: Effects of protein structural complexity, protein concentrations, carbohydrates, and volatile fatty acids	61
Chapter 4	Characterisation of microbial communities in anaerobic acidification reactors fed with casein and/or lactose	85
Chapter 5	Identification of protein-degraders in an anaerobic digester by protein stable isotope (protein-SIP) combined with metagenomics	111
Chapter 6	Effect of operational parameters on the performance of an anaerobic sequencing batch reactor (AnSBR) treating protein-rich wastewater	153
Chapter 7	Conclusions and recommendations	181
	Bibliography	185
	Acknowledgement 致谢	219
	Curriculum vitae	223

CHAPTER 1

INTRODUCTION

1 Total ammoniacal nitrogen recovery from nitrogen-loaded residual streams

- Demand for nitrogen for food production

Nitrogen (N) is a critical substance for life, and the availability of reactive nitrogen determines the productivity of agricultural lands (Vitousek et al. 2002). Most of the N on earth is present as non-reactive nitrogen gas (N_2) and is not useable for metabolic purposes for most organisms. The growing food demand of the population has led to a significant alteration of the natural N cycle, initiated in 1913 when the Haber-Bosch process was developed to produce ammonia (NH_3) from N_2 and hydrogen gas (H_2) (Smil 2004). About 80% of the synthesised NH_3 was used as agricultural fertiliser. The production of artificial N-fertiliser boosted food production in the 20th century, which brought great prosperity to human society (Erisman et al. 2008).

- Pollution by overuse of nitrogen-fertiliser

However, the overuse of N-fertilisers is creating environmental and human health problems (Ju et al. 2016). For example, NH_3 can directly evaporate into the atmosphere or be flushed away from the soil by rainfall and end up in water bodies in the form of nitrates and ammoniacal nitrogen or TAN (the sum of dissolved ammonium NH_4^+ and ammonia NH_3), causing eutrophication (Erisman et al. 2007). Some scientists suggest that the planetary limit for tolerable anthropogenic changes in the N-cycle has already been crossed (Rockström et al. 2009).

- Necessity of ammoniacal nitrogen recovery

To protect the environment, NH_4^+ is usually removed from residual waters by nitrification and denitrification (N/DN). This biochemical conversion of NH_4^+ into N_2 at the expense of energy, excludes the potential to recover and reuse TAN. Actually, the recovered TAN can be a versatile resource: 1) for N-fertiliser production, 2) energy production, 3) chemical and biochemical processes, e.g., wool & textile industry, detergent synthesis, and pre-treatment of lignin (Deng et al. 2021). To avoid environmental damage, stricter disposal regulations for N-containing waste (or residues) should be met, while the sustainability of the NH_3 -cycle must be improved and removal and recovery of TAN is required (Galloway et al. 2008).

- Knowledge gap: potential nitrogen-loaded residual streams for ammonical nitrogen recovery

In the past decades, research has been conducted on the recovery of TAN from residual waters by both mature technologies, such as chemical precipitation and stripping, and novel technologies such as reverse osmosis (RO) and electro dialysis (ED) (Mehta et al. 2015, Xie et al. 2016). More recent reviews discuss the ongoing research on the different available technologies from the perspective of one specific TAN application, i.e., as a fertiliser (Mehta et al. 2015), or as an energy carrier (Valera-Medina et al. 2018). Moreover, published reviews overlook or do not explore one important aspect of the TAN recovery potential, which is the existing available nitrogen-loaded residual streams and their composition, especially the N-speciation. Currently, there is neither a clear identification of potential streams, nor related indicators to classify them according to their treatment requirements proposed or discussed so far.

2 Identification and categorisation of nitrogen-loaded residual streams

- Defining nitrogen-loaded residual streams

Based on data collected from literature, $0.5 \text{ g}\cdot\text{L}^{-1}$ is the minimum nitrogen concentration that is considered for TAN recovery (Deng et al. 2021). Therefore, in this thesis, a nitrogen-loaded (hereafter referred to as N-loaded) residual stream, which has a potential for TAN recovery, is defined as a residual stream containing a total Kjeldahl nitrogen (TKN) concentration of at least $0.5 \text{ g}\cdot\text{L}^{-1}$ or $\text{g}\cdot\text{kg}^{-1}$.

- Three categories of nitrogen-loaded residual streams

Approximately 150 studies reporting on potential N-loaded residual streams were collected, these streams include waste and wastewater from domestic, agricultural, and industrial sources (Deng et al. 2021). Based on selected three main characteristics, including solids content, chemical oxygen demand (COD), and TAN/TKN ratios, as well as the required treatment steps, these streams were categorised into three groups: 1) Residual streams with a TAN/TKN ratio lower than 0.5, which can be considered as protein-rich streams ; 2) Residual streams with a TAN/TKN higher than 0.5 and TSS higher than $1 \text{ g}\cdot\text{L}^{-1}$; 3) Residual streams

with a TAN/TKN higher than 0.5 and total suspended solids (TSS) lower than $1 \text{ g}\cdot\text{L}^{-1}$, suitable for direct TAN recovery (Deng et al. 2021).

- Knowledge gap: upstream conversion of proteins to ammoniacal nitrogen for recovery

TAN is not directly available in the protein-rich streams, a conversion of proteins to TAN is required before recovery. According to literature, researchers only consider TAN concentration as the only parameter for TAN recovery potential assessment (Deng et al. 2021). Therefore, although the protein-rich streams have a potential for TAN recovery, these streams have not been considered in the recovery of TAN previously.

3 Challenges of recovering ammoniacal nitrogen from protein-rich streams

- Conversion of protein to ammoniacal nitrogen by anaerobic digestion

Anaerobic digestion (AD) is predominantly used in the treatment of protein-rich streams (Deng et al. 2021). The full conversion of proteins into TAN is called ammonification and it includes two main steps: 1) hydrolysis of the proteins to peptides and subsequently to amino acids by proteases and peptidases (i.e., proteinases); and 2) the deamination of the amino acids to TAN, volatile fatty acids (VFAs), and H_2 (McInerney 1988). The amino groups ($-\text{NH}_2$) are mainly removed from the amino acids during the deamination (Dakin 1920, Ladd and Jackson 1982). The conversion of protein to TAN during AD can be simplified as: proteins (hydrolysis) \rightarrow amino acids (deamination) \rightarrow TAN (Bareha et al. 2019, Batstone et al. 2002).

- Advantages & disadvantages of applying anaerobic digestion for protein to ammoniacal nitrogen conversion

When AD is applied for the conversion of protein to TAN, the TAN/TKN can be increased from below 0.3 to 0.5-1.0, and simultaneously, the TSS and COD of the residual streams can be greatly reduced (up to two orders of magnitude) (Deng et al. 2021). Both the increase in TAN/TKN and the decrease in TSS and COD are favourable for the TAN recovery. Nonetheless, it is also reported that the conversion of protein to TAN is often limited to a

range of 18 - 77% and largely depends on the substrate and the operational conditions of AD (Bareha et al. 2018). In addition, the produced TAN can also negatively affect the stability of AD by inhibiting the methanogenesis (Jiang et al. 2019).

- Knowledge gap: rate-limiting step, impact factors on anaerobic protein degradation and mechanisms

To improve the conversion of protein to TAN, the rate-limiting step must be identified. Hydrolysis is generally considered the rate-limiting step in AD of complex substrates, such as food waste and algal biomass (Kobayashi et al. 2015, Zhang et al. 2014). Conversely, in AD of a soluble model proteins, i.e., gelatine, deamination is reported to be the rate-limiting step (Duong et al. 2019). Generally, CH₄ production is the ultimate goal in applying AD for treatment of organic residues, and the methanogens are known to be slow-growing microbiota (Meegoda et al. 2018). There is a lack of comparison between the reaction rates of the three steps during anaerobic protein degradation.

Additionally, the factors limiting anaerobic protein degradation and the mechanisms must be investigated. Previous studies focus on the inhibition of NH₃/NH₄⁺ on methanogens, and attempt to co-digest protein-rich streams with carbohydrate-rich streams to reduce inhibition by preventing a pH rise and increasing the C/N ratio (Mata-Alvarez et al. 2014, Rajagopal et al. 2013). However, carbohydrates are reported to retard protein degradation because they can suppress protease production (Glenn 1976), and it is observed that carbohydrates are degraded prior to protein in both chemostat and batch reactors (Breure et al. 1986, Yu and Fang 2001). It is yet to discover whether the presence of carbohydrates or their intermediates have an impact on protein degradation, and what the mechanisms are (Duong et al. 2019).

4 Research scope and thesis framework

This thesis, in chapter 2, first gives an overview of TAN recovery from residual streams by identifying potential N-loaded residual streams and providing information on the available technologies for TAN recovery and reuse from the different residual streams. This is followed by a comprehensive investigation into the upstream processes prior to TAN recovery, i.e., anaerobic conversion of protein to TAN. To fully understand the anaerobic protein

degradation and seek for possibilities to improve protein conversion, the following research questions were proposed and addressed in the chapters of the thesis:

Research question 1: Which step is rate-limiting during anaerobic protein degradation, and what is the effect of the presence of carbohydrates and their intermediates on the reaction rates?

Chapter 3 investigates the effect of protein structural complexity, protein concentration, presence of carbohydrates, and VFAs on anaerobic protein degradation rates. To compare the degradation rates of different protein-rich wastewaters, two types of proteins with different structural complexities, representing the main protein in slaughterhouse and dairy wastewater, were used in the experiments. Additionally, modified Gompertz kinetic model was used to describe and compare the hydrolysis, deamination and methanogenesis rates in the presence and absence of carbohydrate and VFAs. The negative effect of the presence of carbohydrates was described by reaction rates and the rate-limiting step was identified. This chapter provides a theoretical background for the design of anaerobic reactors for treating protein-rich wastewaters.

Research question 2: What is the mechanism of retardation of anaerobic protein degradation in the presence of carbohydrates?

Chapter 4 identifies and compares the dominant microorganisms in the presence and absence of carbohydrates and correlates the shift in microbial community with the changing reactor performance. Casein and lactose as substrates, representing proteins and carbohydrates, respectively, were used in continuous incubation experiments. By characterizing the dominating genus and their ability to ferment proteins/carbohydrates, we intended to reveal the mechanism of the carbohydrates' impact on the anaerobic protein degradation in a mixed culture. These results would lead to a better understanding of anaerobic protein degradation at the microbial level and would support the future design and operation of AD reactors to support the core microbiome for the treatment of protein-rich streams.

Chapter 5 applies the novel proteogenomics technology, to directly identify the active protein degraders in a complex anaerobic microbiota. Batch incubations were carried out. ¹³C

labelled substrate, with a protein content of higher than 97%, was applied to identify the active protein degraders. The identified protein degraders in the presence and absence of carbohydrates were compared. Finally, the substrate utilization abilities of the identified protein degraders were characterized. The results of microbial community analysis and metagenomics analysis confirmed the phylogenetic annotation of the active protein degraders which was proposed in **Chapter 4**.

Research question 3: Is anaerobic sequencing batch reactor (AnSBR) an appropriate operational scheme to reduce the retardation of anaerobic protein degradation in the presence of carbohydrates?

Chapter 6 applies a non-conventional lab-scale anaerobic sequencing batch reactor (AnSBR) to treat protein-rich slaughterhouse wastewater (SWW). Theoretically, proteins and carbohydrates degradation can be separated in time. Such separation can be accomplished by the feast-and-famine operation of an AnSBR, allowing the depletion of more rapidly degradable carbohydrates and providing intervals for the degradation of more slowly degradable proteins. This chapter demonstrates a stable and robust AnSBR, without pre-treatment or the addition of chemicals, for the treatment of SWW, and identifies the key operational parameters that influence the reactor performance by correlation analysis.

Chapter 7 summarises the main conclusions of this thesis and presents recommendations for future research and applications.

CHAPTER 2

RECOVERY AND APPLICATIONS OF AMMONIACAL NITROGEN FROM NITROGEN-LOADED RESIDUAL STREAMS: A REVIEW

This chapter is based on: Deng, Z., van Linden, N., Guillen, E., Spanjers, H., & van Lier, J.B. (2021). Recovery and applications of ammoniacal nitrogen from nitrogen-loaded residual streams: A review. *Journal of Environmental Management*, 295, 113096.

Abstract

Total ammoniacal nitrogen (TAN) is a pollutant but is also a versatile resource. This review presents an overview of the TAN recovery potentials from nitrogen (N)-loaded residual streams by discussing the sources, recovery technologies and potential applications. The first section of the review addresses the fate of TAN after its production. The second section describes the identification and categorisation of N-loaded ($\geq 0.5 \text{ g}\cdot\text{L}^{-1}$ of reduced N) residual streams based on total suspended solids (TSS), chemical oxygen demand (COD), total Kjeldahl nitrogen (TKN), TAN, and TAN/TKN ratio. Category 1 represents streams with a low TAN/TKN ratio (< 0.5) that need conversion of organic-N to TAN prior to TAN recovery, for example by anaerobic digestion (AD). Category 2 represents streams with a high TAN/TKN ratio (≥ 0.5) and high TSS ($> 1 \text{ g}\cdot\text{L}^{-1}$) that require a decrease of the TSS prior to TAN recovery, whereas category 3 represents streams with a high TAN/TKN ratio (≥ 0.5) and low TSS ($\leq 1 \text{ g}\cdot\text{L}^{-1}$) that are suitable for direct TAN recovery. The third section focuses on the key processes and limitations of AD, which is identified as a suitable technology to increase the TAN/TKN ratio by converting organic-N to TAN. In the fourth section, TAN recovery technologies are evaluated in terms of the feed composition tolerance, the required inputs (energy, chemicals, etc.) and obtained outputs of TAN (chemical form, concentration, etc.). Finally, in the fifth section, the use of recovered TAN for three major potential applications (fertiliser, fuel, and resource for chemical and biochemical processes) is discussed. This review presents an overview of possible TAN recovery strategies based on the available technologies, but the choice of the recovery strategy shall ultimately depend on the product characteristics required by the application. The major challenges identified in this review are the lack of information on enhancing the conversion of organic-N into TAN by AD, the difficulties in comparing the performance and required input of the recovery technologies, and the deficiency of information on the required concentration and quality of the final TAN products for reuse.

1 Introduction

1.1 Production and fate of ammonia

Ammonia (NH_3) is the world's second most produced chemical, of which major use is as nitrogen (N) fertiliser. About 80% of the NH_3 produced by industry is used in agriculture while the rest (20%) is used as raw material for the fabrication of chemical compounds and explosives (**Figure 1**) (Erisman et al. 2008, Galloway et al. 2004). Nearly 1 – 2% of the total world energy production is used in the Haber-Bosch (HB) process to produce N-fertilisers, which represents a 3 – 5% of the global annual natural gas consumption and generates 4 – 8 ton CO_2eq (equivalent carbon dioxide) per ton N-fertiliser per year. The well-established HB process synthesises NH_3 from nitrogen (N_2) and hydrogen (H_2) at high temperatures and under high pressure. The generation of H_2 accounts for the largest part of the energy consumption of the process. When the H_2 is generated via methane (CH_4) reforming, the energy consumption of the HB is $28 \text{ MJ}\cdot\text{kg N}^{-1}$; if the H_2 is generated via water electrolysis, the energy consumption of the HB is $107 \text{ MJ}\cdot\text{kg N}^{-1}$ (Cherkasov et al. 2015). Even though the HB process has been largely improved and is very efficient and economically attractive, alternative methods for NH_3 production such as electrochemical-routes are being actively studied and developed (Garagounis et al. 2019, Giddey et al. 2013).

The successful synthesis of artificial NH_3 boosted the food production in the 20th century and brought great prosperity to the human society. Nowadays, more than 189 Million ton of NH_3 are synthesised annually (FAO 2019). However, the overuse of N-fertilisers is creating an environmental and human health problem. For example, N can directly evaporate into the atmosphere or be flushed away from the soil by rainfall and end up in water bodies in the form of nitrates and ammoniacal nitrogen or TAN (the sum of dissolved ammonium NH_4^+ and ammonia NH_3), causing eutrophication (Erisman et al. 2007). Statistics show that only 16% of the total amount of annually applied fertilisers are consumed as vegetable and animal proteins (**Figure 1**), the rest is lost into water bodies and the atmosphere. In the EU, 11 Million $\text{ton}\cdot\text{year}^{-1}$ of N is currently applied to the crops, and 18-46% of the N are not being recovered from agriculture, sewage and food chain (especially slaughterhouses) waste streams (Buckwell and Nadeu 2016).

About 10 - 40% of the lost N-fertilisers is denitrified (converted to N_2) either by vegetation or in wastewater treatment plants (WWTPs) (Erisman et al. 2007, Galloway et al. 2004, Matassa et al. 2015). They may also contribute to global warming and atmospheric pollution when transformed into gaseous oxidised-N species (Ju et al. 2016), such as nitrogen oxide (NO), nitrogen dioxide (NO_2), nitrous oxide (N_2O). In fact, some scientists suggest that the planetary limit for tolerable anthropogenic changes in the N-cycle has already been crossed (Rockström et al. 2009). To avoid environmental damage, stricter disposal regulations for N-containing waste (or residues) should be met, while the sustainability of the NH_3 -cycle must be improved and removal and recovery of TAN is required (Galloway et al. 2008).

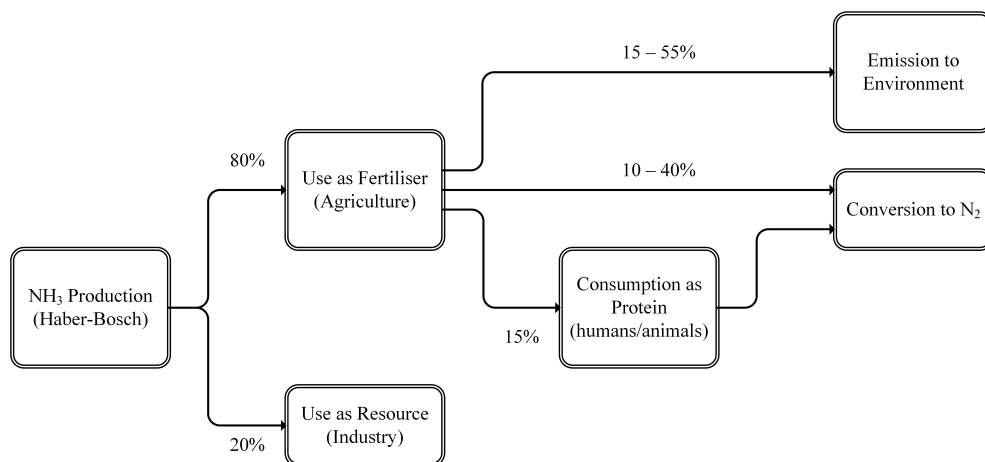


Figure 1 - Fate of produced NH_3 from Haber-Bosch (Erisman et al. 2008, Galloway et al. 2004).

1.2 Treatment of residual waters that contain ammoniacal nitrogen

Conventionally, the ammonium (NH_4^+) is removed from residual waters by nitrification in combination with denitrification (N/DN). To achieve sufficient N removal, N/DN reactors require high hydraulic and solids retention times, which results in large footprints. Besides, nitrification needs abundant supply of oxygen (O_2) by addition of air, attaining liquid dissolved O_2 concentrations of $> 2 \text{ mg}\cdot\text{L}^{-1}$, which represents up to 80% of the total energy consumption of sewage treatment plants (Siegrist et al. 2008).

Removal of NH_4^+ can also be achieved by the combination of partial nitrification and anammox (PN/A), which is typically applied to treat residual streams with relatively high

NH_4^+ concentrations ($0.5 - 2.5 \text{ g}\cdot\text{L}^{-1}$), such as reject water of digested manure, waste activated sludge or landfill leachate (Gonzalez-Martinez et al. 2018, Lackner et al. 2014, Magrí et al. 2013). Because during PN/A, NH_4^+ is only partially oxidised, less energy for aeration is required than for N/DN. According to Lackner et al. (2014) and Schaubroeck et al. (2015), the energy consumption of NH_4^+ removal from reject water by N/DN is reported to be $57 \text{ MJ}\cdot\text{kg N}^{-1}$, whereas the application of PN/A to remove NH_4^+ from reject water requires $3 - 15 \text{ MJ}\cdot\text{kg N}^{-1}$. Despite the energetic advantage of PN/A over N/DN, the application of PN/A is currently limited to (warm) side streams with low carbon to N ratios (C/N), as the preferred operating temperature of anammox bacteria is about $35 \text{ }^\circ\text{C}$ and the growth of these bacteria is outcompeted by other bacteria species in the presence of high concentrations of organic carbon in the feed water (Gonzalez-Martinez et al. 2018). Besides, Lackner et al. (2014) reported that the stable operation of PN/A systems can be challenging due to the accumulation of solids, insufficient retention of the biomass and the accumulation of nitrite and nitrate.

Another challenge for the application of N/DN and PN/A is the generation and emission of gaseous oxidised N species, such as N_2O , NO and NO_2 . Especially the emission of N_2O is undesirable, because it is a potent greenhouse gas, having a 296 times higher global warming potential than CO_2 (Prather et al. 2001). According to the review of Desloover et al. (2012), the emission of N_2O during biochemical processes can contribute to 80% of the total greenhouse gas emissions of water treatment plants that process sewage, manure, landfill leachate or industrial effluents. The fraction of N_2O -N emission relative to the total N load of full-scale biochemical N removal systems is reported to be $0 - 14.6\%$ (Kampschreur et al. 2009, Vasilaki et al. 2019). In general, currently available literature shows that biochemical removal of NH_4^+ consumes energy and results in the emission of strong greenhouse gases.

1.3 Aim of the review

The biochemical conversion of NH_4^+ into N_2 at the expense of energy, excludes the potential to recover and reuse TAN. To this end, more focus has been brought onto the recovery of TAN from residual waters by both mature technologies such as chemical precipitation and stripping, as well as novel technologies such as reverse osmosis (RO) and electrodialysis (ED) (Mehta et al. 2015, Xie et al. 2016). However, recent reviews discuss the ongoing research

or the different available technologies from the perspective of one specific TAN application, i.e., as a fertiliser (Mehta et al. 2015), or as energy carrier (Valera-Medina et al. 2018).

Moreover, published reviews overlook or do not explore one important aspect of the TAN recovery potential, which is the existing available N-loaded residual streams and their composition, especially the N-speciation. N is mainly present in residual streams in two forms: organic and inorganic. Organic N refers to organic nitrogenous compounds such as proteins, whereas inorganic N refers to nitrite, nitrate and TAN.

In general, TAN concentration is the only considered parameter for TAN recovery potential assessment. According to a study by Mulder (2003), the treatment of residual streams with TAN concentrations $< 0.1 \text{ g}\cdot\text{L}^{-1}$ is only cost-effective if biochemical TAN removal technologies are used. TAN recovery from streams with concentrations between $0.1 - 5 \text{ g}\cdot\text{L}^{-1}$ is technically possible but not cost-effective and only TAN recovery from streams with concentrations $> 5 \text{ g}\cdot\text{L}^{-1}$ is economically feasible. However, this study was published in 2003 and ever since, water treatment and TAN recovery technologies made great progress, not to mention the changes in the regulatory framework with regard to N emissions (Lymperatou et al. 2015, Pikaar et al. 2018).

Currently, there is neither a clear identification of potential streams, nor related indicators to classify them according to their treatment requirements proposed or discussed so far. For example, residual streams rich in organic N could also be considered for TAN recovery if anaerobic digestion (AD) is applied first. Therefore, the presence of organic N and TAN in residual streams, quantified by the total Kjeldahl nitrogen (TKN, including organic N and TAN) content, should be considered as an important indicator for TAN potential classification of streams.

This chapter:

- Identifies existing and potential N-loaded residual streams for TAN recovery.
- Proposes a parameter-based categorisation for their treatment.
- Discusses the available TAN recovery technologies based on their principle (concentrate TAN as NH_4^+ , NH_3 or separate TAN as NH_3 from the liquid), main energy input, end product and challenges.

- Summarises the possible uses of the recovered TAN including specific requirements in terms of quantity and quality, and challenges for the TAN reuse technologies.

During the identification of suitable residual streams, we came across a wide range of descriptions of the term “nitrogen-loaded”: “nitrogen rich”, “high nitrogen content” and “high strength nitrogen”. In this chapter, the term “nitrogen-loaded” (hereafter N-loaded) refers to residual streams containing TKN concentrations of at least $0.5 \text{ g}\cdot\text{L}^{-1}$ or $\text{g}\cdot\text{kg}^{-1}$. The overall aim of this chapter was to provide an objective and complete overview, without judgement on the preferable recovery techniques and application. Additionally, economic aspects were not discussed due to lack of information from collected literature preventing a fair and objective comparison.

2 Characterisation and categorisation of N-loaded residual streams

2.1 Parameters for characterisation of N-loaded residual streams

To characterise the N-loaded residual streams, we collected data on various key parameters to be considered for their treatment to allow for TAN recovery. These parameters are: the total suspended solids (TSS), the chemical oxygen demand (COD), the TKN and the TAN. To report consistently, we normalised the TSS, COD, TKN and TAN to parts per thousand, which corresponds to $\text{g}\cdot\text{kg}^{-1}$ and $\text{g}\cdot\text{L}^{-1}$ for solid and liquid streams (assuming a liquid density of $1,000 \text{ g}\cdot\text{L}^{-1}$), respectively. The TSS indicates the feasibility to use directly physicochemical technologies for the recovery of TAN or the need for pre-treatment (e.g., filtration). The COD is an indication of the presence of organic matter, which must be decreased before discharge to receiving water bodies. Also, a high COD is likely to induce fouling in the physicochemical technologies for TAN recovery, indicating the need for pre-treatment.

The absolute TKN content is an indication of the amount of N that is present as both organic N and TAN. The TAN/TKN ratio indicates the dominant present form of N. Data collected in this chapter suggests that physicochemical technologies, such as stripping and precipitation, can be used for direct TAN recovery, i.e., pre-treatment steps such as conversion of organic N to TAN or solids removal is not needed, at a TAN/TKN ratio higher

than 0.5; TAN/TKN ratios lower than 0.5 suggest that the organic N must be first converted to TAN to allow for recovery of TAN.

When it is necessary to convert organic N to TAN, the COD/N ratio must also be considered. Typically, when the COD/N ratio of residual streams falls within a certain range (i.e., 20 - 30), biochemical technologies such as AD are suitable to decrease the organic matter content, without potential problems of N shortage or inhibition (Rajagopal et al. 2013). Besides, the COD/N ratio is an indicator of fouling proneness in membrane operations (Feng et al. 2012). Although the C/N and COD/N are both used (Khalid et al. 2011, Mata-Alvarez et al. 2014, Rajagopal et al. 2013), there are some differences. Compared to the COD/N ratio, the C/N ratio is less convenient to use because it cannot be directly related to CH₄ production (van Lier et al. 2020). In contrast, the COD can be used to estimate the CH₄ production, design and calculate the conversion efficiency of anaerobic systems (André et al. 2017). Regarding the N in the COD/N ratio, this could refer to either the TN (including both organic N and inorganic N) or the TKN. It must be noted that under anaerobic conditions the TKN is assumed to be equal to the TN so the COD/N ratio can be calculated with the TKN or TN.

2.2 Identification of N-loaded residual streams

We collected data on N-loaded residual streams obtained from approximately 150 studies, all using real (not synthetic) residual streams either for analytical or experimental research purposes. For each identified N-loaded residual stream, we used at least three independent references and report the average, minimum and maximum values of the characteristic parameters. We divided the N-loaded residual streams in four different groups, based on their origins: solid residual streams, manure, liquid residual streams (all domestic) and residual streams reported to originate from industrial processes. The obtained average, minimum and maximum values are presented in **Figure 2**. In the text, we only refer to the average values. More details on the consulted references, such as the TSS, COD, TKN and TAN content, the respective units, used treatment technologies and reference details can be found in the Supporting information.

2.2.1 Solid residual streams

The first group includes: bio- and food waste, the organic fraction of municipal solid waste (OFMSW) and spent biomass, such as the waste activated sludge from wastewater treatment

plants (WWTPs) and algal sludge (Mata-Alvarez et al. 2000). Typical TSS values for bio- and food waste and OFMSW are 269 and 333 $\text{g}\cdot\text{kg}^{-1}$ (ranges can be consulted in **Figure 2**), respectively, while the COD content is 428 and 644 $\text{g}\cdot\text{kg}^{-1}$, respectively. For the spent biomass streams, the TSS and COD are considerably lower than for bio- and food waste and OFMSW: 49 and 50 $\text{g}\cdot\text{kg}^{-1}$, respectively. The typical TAN content of the solid residual streams is 1 $\text{g}\cdot\text{kg}^{-1}$. Furthermore, the TKN ranges between 3 – 12 $\text{g}\cdot\text{kg}^{-1}$ and is mainly represented by the presence of proteins (Braguglia et al. 2018, Ganesh Saratale et al. 2018). The relatively low TAN/TKN ratios (ranging 0 – 0.3) indicate that direct TAN recovery will be challenging. To allow for effective TAN recovery, the TAN/TKN ratio must be increased by converting organic N to TAN. For bio- and food waste and OFMSW, the COD/N ratio is 47 and 60, respectively, whereas for spent biomass the COD/N ratio is 14, because of the lower COD content. Anaerobic (co-)digestion is a widely applied technology to treat these solid residual streams, due to the relatively high COD ($> 10 \text{ g}\cdot\text{kg}^{-1}$) and N contents ($> 0.5 \text{ g}\cdot\text{kg}^{-1}$) (Hartmann and Ahring 2005, Keucken et al. 2018). Anaerobic (co-)digestion allows for the simultaneous decrease of the solids and COD content of the residual streams, while the organic N is converted to TAN, increasing the TAN/TKN ratio. More information on the use of AD to convert organic N to TAN is presented in Section 3.

2.2.2 Manure

The second group concerns manure, which is frequently reported to contain high levels of TAN and TSS, and is often considered to be problematic for its treatment via AD (Massé et al. 2014, Rodriguez-Verde et al. 2018). Manure is divided into poultry, cattle, and swine manure. Poultry manure has the highest TSS, COD and TKN: 521, 661 and 35 $\text{g}\cdot\text{kg}^{-1}$, respectively. Despite the low TAN/TKN ratio (TAN/TKN~0) of poultry manure, its absolute TAN content is high, i.e., 2 $\text{g}\cdot\text{kg}^{-1}$, practically 92% N is present as organic N in poultry manure. Cattle and swine manure have a much lower content of TSS, i.e., 81 and 24 $\text{g}\cdot\text{kg}^{-1}$, respectively, COD, i.e., 58 and 36 $\text{g}\cdot\text{kg}^{-1}$, respectively, and TKN, i.e., 4 $\text{g}\cdot\text{kg}^{-1}$. The TAN of cattle manure is 1 $\text{g}\cdot\text{kg}^{-1}$, whereas swine manure has a TAN of 4 $\text{g}\cdot\text{kg}^{-1}$. The N in cattle manure is predominantly present as organic N (TAN/TKN ratio is 0.4), whereas in swine manure N is already present predominantly as TAN (TAN/TKN ratio is 0.7). The COD/N ratio of the various types of manure ranges between 8 - 32. According to the consulted studies, manure is mainly treated by AD but, due to the high level of TAN, is often co-digested with

other organic residues to suppress the negative effects of the presence of TAN during the AD processes (Hartmann and Ahring 2005, Mata-Alvarez et al. 2014).

2.2.3 Liquid residual streams

The third group includes: leachate, the liquid fraction of raw swine manure (swine liquid) and human (source-separated) urine. The TSS of swine liquid and urine streams is below $1 \text{ g}\cdot\text{L}^{-1}$, whereas conversely, leachates can contain high amounts of suspended solids ($19 \text{ g}\cdot\text{L}^{-1}$). Regarding COD, leachates and swine liquid contain 26 and $31 \text{ g}\cdot\text{L}^{-1}$, respectively, whereas human urine ranges between $5 - 10 \text{ g}\cdot\text{L}^{-1}$. The TKN content for all the liquid N-loaded residual streams ranges between $3 - 7 \text{ g}\cdot\text{L}^{-1}$. For leachate, swine liquid and stored human urine, the TAN/TKN is at least 0.8 . Fresh human urine, however, has a TAN/TKN ratio of 0.0 , because N is still present as urea. When urine is stored, urea is hydrolysed to TAN, increasing the TAN/TKN ratio (Udert et al. 2003). When leachates contain high TSS and COD, and have a high COD/N ratio, anaerobic (co-)digestion can be applied for the treatment of the organic fraction (Lei et al. 2018, Montusiewicz et al. 2018).

2.2.4 Industrial residual streams

The fourth group concerns those N-loaded residual streams that have an industrial origin, such as mining and fertiliser industry and fish/fishmeal processing. Amongst these industrial N-loaded residual streams, fishery residual water has the highest COD content ($110 \text{ g}\cdot\text{L}^{-1}$) and TKN content ($3 \text{ g}\cdot\text{L}^{-1}$), and the TKN is mostly present as organic N (TAN/TKN ratio of 0.3). Residual streams originating from mining and fertiliser industries have a much lower COD content (1 and $0 \text{ g}\cdot\text{L}^{-1}$, respectively), while all N is present as TAN (TAN/TKN is 1.0). The TAN content of mining and fertiliser industry residual streams is 5 and $2 \text{ g}\cdot\text{L}^{-1}$, respectively. For the treatment of fishery residual streams, AD has been used (Guerrero et al. 1999), whereas physicochemical TAN recovery technologies and biological oxidation processes were used to treat mining and fertiliser wastewater (Huang et al. 2011, Noworyta et al. 2003). Finally, there are also specific (industrial) residual streams that are not represented in **Figure 2** but are considered to be N-loaded and therefore potentially interesting for recovery. For example, TAN content of glutamate wastewater ranges between $16 - 19 \text{ g}\cdot\text{L}^{-1}$ (Wang et al. 2011, Yang et al. 2005); pectin wastewater can contain around $1.4 \text{ g}\cdot\text{L}^{-1}$ (Degn Pedersen et al. 2003); slaughterhouse wastewater $\sim 0.7 \text{ g}\cdot\text{L}^{-1}$ (Kundu et al. 2013); nuclear wastewater $\sim 35 \text{ g}\cdot\text{L}^{-1}$ (Gain et al. 2002); coking wastewater can contain between 0.2

- 0.6 g·L⁻¹ (Jin et al. 2013, Lin et al. 2018) and ion exchange brine up to 3.9 g·L⁻¹ (Vecino et al. 2019). These residual streams also have a high potential for TAN recovery, but insufficient information on their composition and current treatment is available to consider them in this chapter.

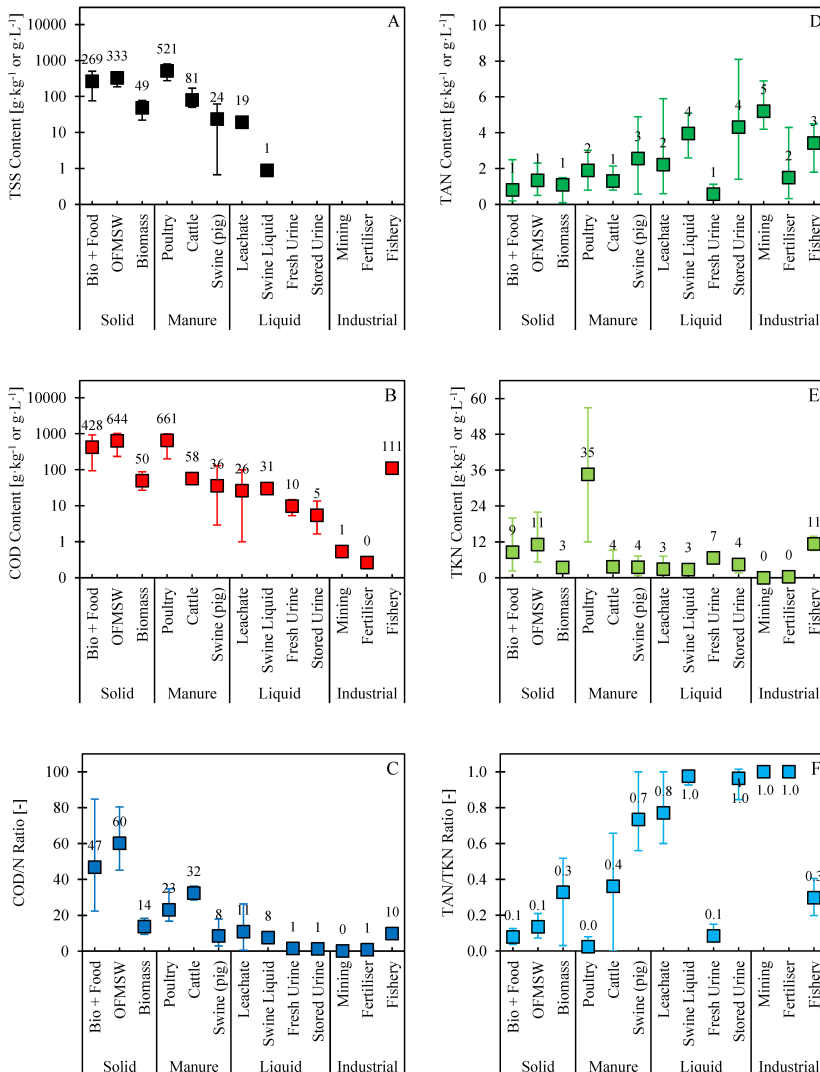


Figure 2 - An overview of the identified N-loaded residual streams and their characteristics in terms of TSS (A), COD (B), TKN (D) and TAN (E) content, and the respective calculated COD/N (C) and TAN/TKN (F) ratios. The presented values and error bars represent the averages and minimum and maximum values of at least three independently consulted references. The consulted references are extensively presented and referred to in the Supporting Information.

2.3 Discussion on categorisation of N-loaded residual streams

Based on their characteristics related to the required (pre-)treatment before TAN recovery, the N-loaded residual streams are divided into three categories:

1. Residual streams with a TAN/TKN ratio lower than 0.5.
2. Residual streams with a TAN/TKN higher than 0.5 and TSS higher than $1 \text{ g}\cdot\text{L}^{-1}$.
3. Residual streams with a TAN/TKN higher than 0.5 and TSS lower than $1 \text{ g}\cdot\text{L}^{-1}$, suitable for direct TAN recovery.

Figure 3 presents a strategic distribution of these various categories, based on the need of (pre-)treatment before subsequent technologies can be applied for the recovery of TAN.

2.3.1 Category 1: TAN/TKN < 0.5

Category 1 contains N-loaded residual streams with a TAN/TKN ratio < 0.5 and a TSS and COD content both higher than 24 and 36 $\text{g}\cdot\text{kg}^{-1}$, respectively. For these streams, the TAN/TKN must be increased to at least 0.5 to allow for subsequent effective TAN recovery; Christiaens et al. (2019b) reported 0.5 as the lowest TAN/TKN ratio for which TAN recovery is applied from biomass digestate. The N-loaded residual streams that require this organic N to TAN conversion step are bio- and food waste, OFMSW, spent biomass, poultry, and cattle manure. Various biochemical and physicochemical processes, such as AD, can be used to increase the TAN/TKN ratio by conversion of organic N to TAN, while simultaneously the TSS and COD content is decreased. The conversion of organic N to TAN by AD is more extensively discussed in Section 3.

2.3.2 Category 2: TAN/TKN ≥ 0.5 , TSS $> 1 \text{ g}\cdot\text{L}^{-1}$

Category 2 contains N-loaded residual streams with a TAN/TKN ratio greater than 0.5 and TSS concentrations higher than $1 \text{ g}\cdot\text{L}^{-1}$. The application of AD to treat various organic N-loaded residual streams from category 1 leads to the generation of digestate (which falls into this category), having a TAN/TKN ratio greater than 0.5. Direct TAN recovery is possible by solids-tolerant recovery technologies, such as struvite precipitation and air stripping (see Section 4) for digestate with TSS up to $1 \text{ g}\cdot\text{L}^{-1}$. However, for recovery technologies that are prone to fouling (mostly membrane-based technologies), the feed stream must be made free

from solids by using solid-liquid separation (centrifugation or belt-press filtration), sedimentation, sand filtration, micro- or ultrafiltration.

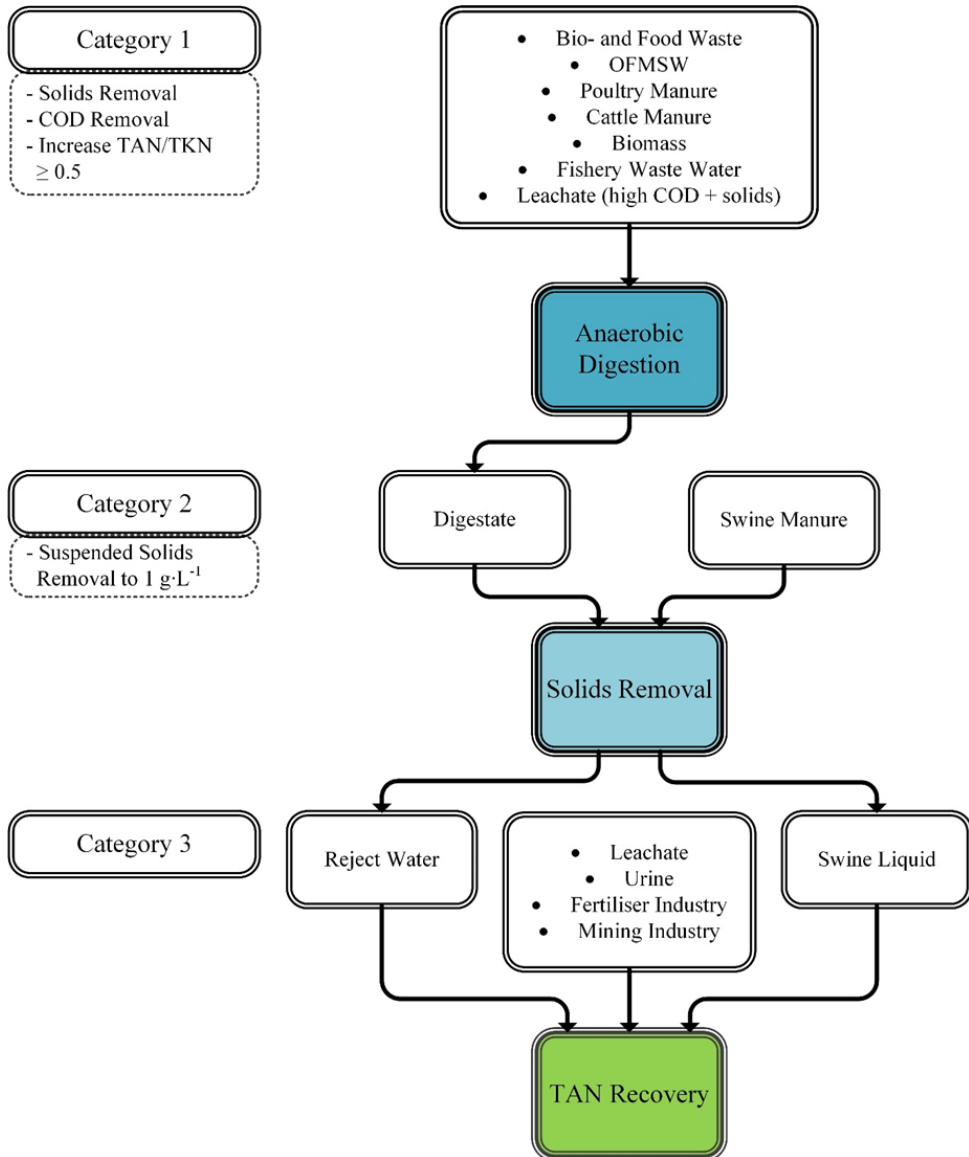


Figure 3 - A strategic categorisation of the various N-loaded residual streams, based on their characteristics and required (pre-)treatment before TAN recovery.

2.3.3 Category 3: TAN/TKN ≥ 0.5 , TSS $\leq 1 \text{ g}\cdot\text{L}^{-1}$

Category 3 contains N-loaded residual streams with a TAN concentration higher than $0.5 \text{ g}\cdot\text{L}^{-1}$, a TAN/TKN ratio greater than 0.5 and TSS $\leq 1 \text{ g}\cdot\text{L}^{-1}$. Within category 3, the liquid residual streams, such as solids free leachate, filtered swine liquid and urine, and various industrial N-loaded residual streams originating from mining and fertiliser industry are placed. According to the obtained data with respect to applied treatment technologies, these residual streams are considered suitable for direct TAN recovery by technologies discussed in Section 4.

2.3.4 Categorisation of N-loaded residual streams

The proposed categories indicate the suitability and the path for TAN recovery. If we take category 1 (rich in organic N and low TAN/TKN ratio) as an example, the organic N needs to be converted firstly to TAN to increase the TAN/TKN ratio, usually carried out by AD, then the TAN in the effluent must be separated from the solids, and finally the liquid stream is suitable for TAN recovery. Therefore, category 1 streams require the most (pre-)treatment steps, whereas category 3 streams, on the other hand, require the least. The streams in category 3 can be found in specific industries, e.g., mining and chemical industries, and have a high potential for TAN recovery because of their high TAN concentrations and low TSS content. However, the access to this information is usually limited. Therefore, the streams from category 2 are commonly considered as having the greatest potential for TAN recovery.

3 Conversion of organic nitrogen to ammoniacal nitrogen by anaerobic digestion

3.1 Conversion of organic nitrogen to ammoniacal nitrogen

Both biochemical and physicochemical processes can be used to convert organic N to TAN. Biochemical processes, in particular AD, is predominantly used in commercial applications. Besides the conversion of organic N to TAN, AD allows for resource recovery from rather diluted streams, i.e., biogas production and nutrient recovery during post-treatment, while having low operational costs (Oladejo et al. 2018). On the other hand, biochemical processes have slow kinetics resulting in long residence times, ranging between one to five weeks for AD digesters, and consequently large reactor footprints.

When dealing with poorly biodegradable substrates, e.g., spent biomass, physicochemical processes such as pyrolysis, gasification and wet air oxidation might be preferred over AD (Oladejo et al. 2018). The conversion time of these processes ranges from seconds to minutes and 80 - 90% conversion efficiencies can be achieved (Oladejo et al. 2018). However, physicochemical processes require extensive pre-treatment (e.g., exhaustive drying) and complex reactor designs to handle high temperatures and pressures. For example, hydrothermal liquefaction of algae requires temperatures in the range of 250 - 350 °C and pressures in the range of 40 – 250 bar (Jazrawi et al. 2015). Furthermore, large chemical and/or energy inputs are required, and sometimes expensive catalyst must be used (Elliott et al. 2013, Oliviero et al. 2003). Therefore, even though physicochemical processes allow for higher organic N to NH₃ conversion rates and efficiencies, their practical application is rather limited.

Besides the mentioned treatment methods, hydrothermal pre-treatment and alkali dosage are also frequently discussed (Ahmad et al. 2018, Carrere et al. 2016). These methods are proven to be suitable for enhancing the hydrolysis of various complex substrates, especially biomass, and therefore can be used to enhance the organic N conversion. However, no data is found on organic N or protein conversion efficiency.

Figure 4 shows the effect of the application of AD by comparing the characteristics of the residual streams (raw substrates) before and after AD, referred to as digestate and reject water, the latter being the liquid fraction of the digestate obtained after solid-liquid separation by centrifuges, screw presses, etc. When AD is used, the TSS and COD of the residual streams are reduced by 30-85% depending on the streams. A high degree of removal is especially desirable when membrane-based TAN recovery technologies are considered, because of reduced fouling risks (Zarebska et al. 2015). The TSS of the untreated streams, which ranges between 24 - 81 g·kg⁻¹ or g·L⁻¹, is reduced to 16 - 20 g·L⁻¹ in the digestate and to a range of 4 - 11 g·L⁻¹ in the reject water (see **Figure 4A**). Regarding COD, the initial content of the residual streams is reduced from 36 - 58 to 11 – 15 g·kg⁻¹ or g·L⁻¹ in the digestate and to 6 - 7 g·L⁻¹ in the reject water after AD (see **Figure 4B**). The decrease in COD content ultimately results in a decrease of the overall COD/N ratio, as presented in **Figure 4D**, since the total N content remains unaffected (only transformed into TAN) by AD.

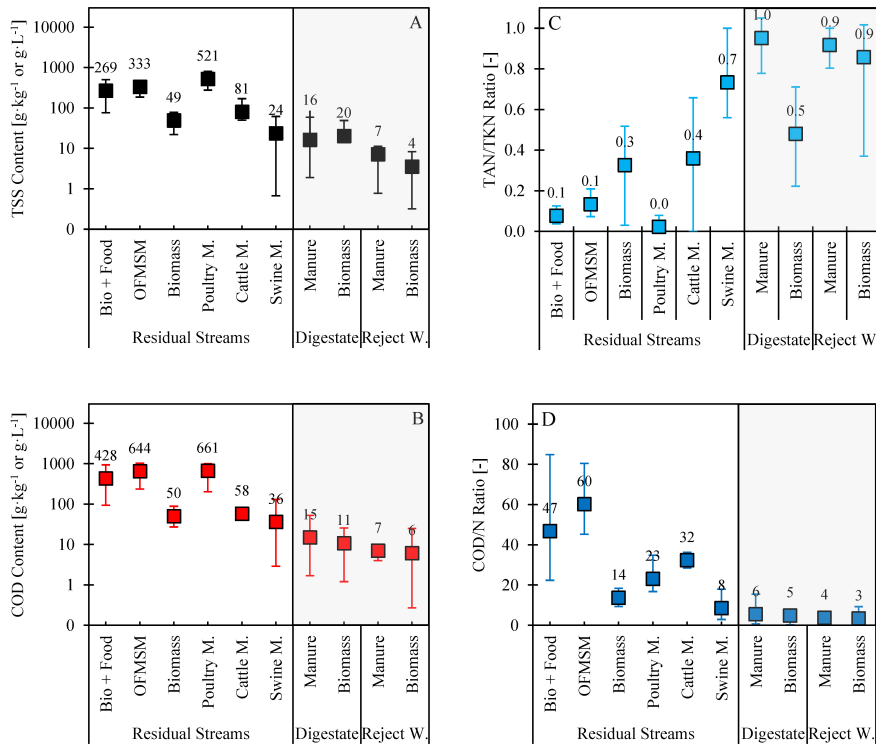


Figure 4 - Change in the solids content (A), COD content (B), TAN/TKN ratio (C), and COD/N content (D) in the obtained digestates and reject waters resulting from AD applied to biomass and manure. Note the exponential y-axis in figures A and B. The presented values and error bars represent the averages and minimum and maximum values of at least three independently consulted references. The consulted references are extensively presented and referred to in the Supporting Information.

Furthermore, **Figure 4C** shows that the application of AD leads to a substantial increase in the TAN/TKN ratio, up to 0.9 - 1 in both digester and reject water, for most of the residual streams here considered, indicating the effective conversion of organic N to TAN. Only biomass appears to be a substrate for which limited conversion can take place, as the TAN/TKN ratio of its digester is only 0.5. Note that swine manure possesses already a high TAN/TKN ratio (0.7) before AD, whereas the TAN/TKN ratio for biomass and cattle manure does not exceed 0.5.

Because AD is widely applied commercially and as seen here, it can be considered an effective method to convert organic N to TAN. The next subsection will further elaborate on its mechanisms and limitations in the conversion of organic N to TAN.

3.2 Mechanism for biochemical conversion of organic nitrogen to ammoniacal nitrogen during anaerobic digestions

Proteins are the most common organic N compound present in wastewaters. Except proteins, organic N can also exist as urea, quaternary ammonium salts (such as betaine), and melanoidins. The amount of urea present in animal manure is prominent, but it is easily hydrolysed into TAN without additional conversion steps. Betaine is present in low concentrations (0.8 - 1.6 % dry weight of sugar-beet) (Thalasso et al. 1999) and melanoidins have a poor biodegradability (6 - 7%) (Pazouki et al. 2008). Both groups of compounds have a low potential for TAN recovery and were not further considered in this chapter. In fact, only protein-rich streams have been considered as the main organic N-loaded residual streams that need a conversion step before TAN recovery.

The conversion of proteins to TAN under anaerobic conditions has been widely studied (Kayhanian 1999, McInerney 1988) and is schematically represented in **Figure 5**. The full conversion of protein into TAN is called ammonification. The ammonification process includes two main steps: the hydrolysis of the proteins to peptides and subsequently to amino acids by proteases and peptidases (i.e., proteinases); and the deamination of the amino acids to TAN, volatile fatty acids (VFAs), and H_2 (McInerney 1988). The deamination process is included in the acidogenesis process, in which the amino groups ($-NH_2$) are removed from the amino acids (Ladd and Jackson 1982). TAN is partly produced (0.4%) during hydrolysis, while the major part (99.6%) is produced during deamination assuming a 100% protein to TAN conversion efficiency (Dakin 1920). Therefore, the conversion of organic N to TAN in AD can be simplified as proteins (hydrolysis) \rightarrow amino acids (deamination) \rightarrow TAN (Bareha et al. 2019, Batstone et al. 2002).

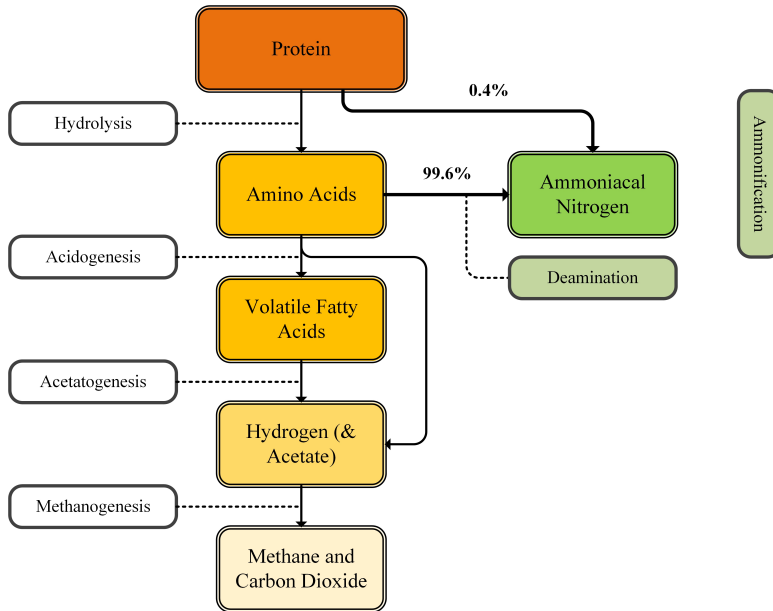


Figure 5 - Schematic representation of protein degradation during AD. Formation of TAN particularly occurs during the first stages of AD (assuming 100% protein to TAN conversion efficiency), adapted from (Kayhanian 1999, McInerney 1988).

3.3 Limiting factors of conversion of organic nitrogen to ammoniacal nitrogen by anaerobic digestion

The conversion of organic N to TAN mostly is not fully completed during AD of non-synthetic residual streams; its efficiency has been reported to be in the range of 18 - 77% and depends largely on the substrate and the operational conditions (Bareha et al. 2018). According to literature, the rate-limiting step of the conversion is hydrolysis, specifically for complex substrates, e.g., food waste and algal biomass (Kobayashi et al. 2015, Zhang et al. 2014). When hydrolysis is impeded, the availability of amino acids is limited, and the subsequent deamination can only take place to a certain degree.

Proteins are complex molecules that can contain more than 100 amino acids and can roughly be divided into insoluble fibroid and soluble globular proteins (Powar and Chatwal 2007). Fibroid proteins, e.g., in manure fibres, are more resistant to hydrolysis because they are less soluble than globular proteins (Sanders 2001). Besides, humic acids can decrease the solubility of proteins when binding to them, forming larger and more complex molecules. In

fact, Sanders (2001) reported that the hydrolysis of protein is inhibited at humic acids concentrations higher than $1 \text{ g}\cdot\text{L}^{-1}$.

A recent study revealed that the N biodegradability (understood as organic N conversion potential) varies before and after storage (Bareha et al. 2018). The potential can be roughly indicated by TAN/TKN. If the TAN/TKN is higher than 0.3 before AD (e.g., during storage of manure or food wastes), the organic N left in the substrate is more resistant to degradation. This could be attributed to certain uncontrolled storage conditions (e.g., decreasing pH) that can promote partial conversion of the organic N to TAN, while the unconverted remaining organic N can form more stable compounds, which impedes the hydrolysis (Bareha et al. 2018). Uncontrolled storage of complex substrates seems to be less preferable in terms of organic N conversion.

Besides the impeded hydrolysis of proteins, also the produced TAN from proteins is regarded as a problem for AD. In earlier studies, TAN is believed to inhibit mainly the methanogenesis phase (Angelidaki and Ahring 1993). Whereas in later studies, TAN is also found to affect the overall AD processes. For example, Niu et al. (2014) found similar IC_{50} values (i.e., half-maximal inhibitory concentrations, in this case TAN, for which the conversion efficiency is reduced by 50%) for methanogenesis, acidogenesis and hydrolysis, which were 5.1 , 5.3 and $5.7 \text{ g N}\cdot\text{L}^{-1}$, respectively. According to Nakakubo et al. (2008), the addition of TAN caused a decrease in CH_4 production, but no immediate VFA accumulation was observed, indicating that hydrolysis and acidogenesis were also inhibited. Protein conversion rates and efficiencies were found inhibited by TAN at concentrations above $2 \text{ g N}\cdot\text{L}^{-1}$ (Chen et al. 2018, Gallert et al. 1998, Krylova et al. 1997). Krylova et al. (1997) reported that TAN concentrations ranging between $2.6 - 8 \text{ g N}\cdot\text{L}^{-1}$ significantly reduce the population of the proteolytic group (i.e., microbial group producing protease). Gallert et al. (1998) found 50% inhibition of deamination at TAN concentrations of $3.0 \text{ g N}\cdot\text{L}^{-1}$ and NH_3 concentration of $95 \text{ mg N}\cdot\text{L}^{-1}$ under mesophilic conditions, and at TAN concentrations of $2.0 \text{ g N}\cdot\text{L}^{-1}$ and NH_3 concentration of $274 \text{ mg N}\cdot\text{L}^{-1}$ under thermophilic conditions. Similarly, Niu et al. (2013) reported a rapid decrease in protein conversion efficiency when TAN was above $5.0 \text{ g N}\cdot\text{L}^{-1}$. **Table 1** presents an overview of the TAN and NH_3 concentrations, as well as the operational conditions (i.e., pH and temperature), and their effect on the conversion of organic N to TAN found in literature.

Table 1 - Effect of TAN and NH₃ concentrations (under certain pH and temperature) on organic N conversion by AD.

pH	Temp.	TAN	NH ₃	Impact on conversion of organic N	Reference
-	°C	g N·L ⁻¹	g N·L ⁻¹		
7.4 - 8.3	55	3.0	0.3 - 1.3	0% inhibition	(Niu et al. 2014)
7.4 - 8.3	55	6.0	0.5 - 2.6	75% inhibition	
<7.0	37 or 55	7.9	0.1 - 0.2	10% reduction of proteolytic group	(Krylova et al. 1997)
<7.0	37 or 55	13.2	0.2 - 0.5	40% reduction of proteolytic group	
8.0 - 8.2	35	3.0 - 5.0	0.3 - 0.5	40% inhibition	(Niu et al. 2013)
8.0 - 8.2	35	5.0 - 15.0	0.5 - 1.5	80% inhibition	
7.3	37	2.0	0.1	50% reduction of proteobacteria	(Chen et al. 2018)
7.3	37	7.8	0.2	100% inhibition	
7.2	37	3.0	0.1	50% inhibition	(Gallert et al. 1998)
7.2	55	2.0	0.3	50% inhibition	

3.4 Methods to enhance the conversion of organic nitrogen to ammoniacal nitrogen

To deal with the protein-rich streams, many methods have been applied, such as co-digestion, pre-/side-treatments and adaption, to stabilise the AD system and promote CH₄ production. In general, protein is only considered part of the total COD and few studies were found that especially focused on protein conversion. Therefore, we have summarised the effect of the most often applied or studied methods for protein conversion.

Co-digestion with carbohydrate-rich streams, such as starch or glycerine, is applied to increase the C/N ratio to avoid TAN inhibition. Based on the collected data, co-digestion is detrimental to protein conversion rate and efficiency. The presence of carbohydrates suppress the production of protease and the increased C/N ratio induces a lower protein solubilisation rate (Glenn 1976, Wang et al. 2014). Besides, increasing the C/N by co-digestion promotes bacterial growth and TAN concentration might be reduced by the N consumption during this growth (Verma 2002).

Pre-treatment methods are also applied, to improve the CH₄ production during anaerobic treatment of protein-rich streams. Guerrero et al. (1999) found that 80% protein conversion can be achieved by the acidification of fishmeal wastewater. Microwave pre-treated sewage sludge showed a 10% higher solubility of organic N compared to the untreated sludge, but still the effect on its conversion efficiency is not clear (Gil et al. 2018). Side-treatments (e.g., side-stripping, side-adsorption) are used to reduce the NH₃ accumulation in AD systems, especially when TAN/TKN ratio is above 0.5 (Kabdashlı et al. 2000, Resch et al. 2011). The effect of these side-treatments on the organic N conversion has not been studied. Only one study reported that increased temperature and alkalinity of the side-stripping stream improved the organic N solubility, resulting in a 20 - 33% increase in the organic N conversion efficiency (Serna-Maza et al. 2014).

In the past decade, adaption of AD biomass towards inhibitive TAN concentrations has been studied, aiming at restoring the CH₄ production after an episode of TAN inhibition. The activity of the proteolytic group is found closely related to the protein conversion rate, therefore, adaption is considered to promote the restoration of the protein conversion rate of TAN inhibited biomass (Chen et al. 2018). The successful adaption of methanogens to a TAN concentration of 5 g N·L⁻¹ in an AD reactor was reported by Fotidis et al. (2014). Without interrupting the process or replacing the substrate, they observed a 30% higher CH₄ production in the bio-augmentation reactor (with addition of methanogenic culture) than the control reactor within 41 days. Chen et al. (2018) reported that protein degradation decreased noticeably when TAN increased to 5.5 g N·L⁻¹, but 90% protein conversion rate (relative to the conversion rate of the non-inhibited biomass) can be restored after adaption. Likewise, Kovács et al. (2013) found 3.5 - 5 times higher protease activity in the biomass after adapted to increasing protein concentrations.

3.5 Discussion on anaerobic digestion to convert organic nitrogen to ammoniacal nitrogen

AD is used to convert the organic N to TAN, while reducing COD and TSS simultaneously. However, the N contained in the protein was not always completely converted to TAN. For complex substrates like spent biomass, the maximum conversion of TKN to TAN is only 50% (Christiaens et al. 2019b). Recently, studies are trying to predict the fate of N during

anaerobic digestion, Bareha et al. (2018) estimated the accessibility of organic N in complex substrates by chemical extraction methods (Van Soest fraction and EPS fraction). Their study reports that the organic N conversion efficiency cannot be accurately predicted by the biodegradability or chemical accessibility of the substrate. Therefore, for evaluating the potential recovery of TAN from organic N-loaded streams, there is a need for estimating the actual TAN potential of these streams.

The wide range in the reported organic N conversion efficiencies (18-77%) might be caused by limited hydrolysis of complex proteins but can also be attributed to the inhibitory effects of accumulating TAN. Although extensive work was done to study TAN inhibition effects and mechanisms, there is no agreement on either the 'intrinsic' TAN inhibitory concentration, nor the inhibitory form of TAN (NH_4^+ or NH_3). Probably because these studies were done with various substrates and under various operational conditions (pH and/or temperature), which make it difficult to compare the results. Moreover, studies reporting on the effect of TAN on organic N or protein conversion are rather limited, increasing the difficulties for a systematic analysis or review.

Unsurprisingly, the currently applied or studied methods to relieve the stress that protein-rich streams pose on AD, such as co-digestion, pre/side-treatments and adaption, are all focusing on the CH_4 yield. Based on the collected data, no firm conclusion can be made. Generally, studies show that increasing C/N (or COD/N) ratio by co-digestion can negatively affect the organic N conversion efficiency, and more importantly, this method dilutes the TAN concentration in the AD, which has an additional impact on the potential TAN recovery efficiency downstream. Side-stripping removes NH_3 from the AD system, and therefore is supposed to improve the organic N conversion: on the one hand it reduces the inhibition by NH_3 , and on the other hand it enhances the protein hydrolysis efficiency by applying higher temperatures and pH than in the AD reactor. However, the improvement (10 - 33%) reported might be less attractive considering the required energy input (further elaborated in Section 4). Direct NH_3 stripping in AD reactors is also being studied, however, AD reactors are rather unstable at high temperatures ($> 55\text{ }^\circ\text{C}$) and high pH (> 8) that is needed for the stripping process (Gebreyessus and Jenicek 2016). Combining the two technologies can either result in AD reactor failure or low concentration NH_3 -containing end products. Adaption does not improve the conversion efficiency but allows for restoration of the conversion after TAN

inhibition. Although the process takes longer, adaption might be advantageous for maintaining both the conversion efficiency and keeping the concentrated TAN in the effluent, which might be advantageous for TAN recovery after AD.

4 Technologies to recover ammoniacal nitrogen from residual streams

4.1 Technologies to concentrate ammoniacal nitrogen

Solid – liquid separation or complete solids removal is suggested prior to TAN recovery; mature technologies such as centrifugation, media (sand) filtration or microfiltration and ultrafiltration, can be applied to reduce an initial TSS to below $1 \text{ g}\cdot\text{L}^{-1}$ (2%) (Masse et al. 2007, Zarebska et al. 2015). The technologies discussed below are used at a TSS concentration lower than $1 \text{ g}\cdot\text{L}^{-1}$ or else after solids removal technologies.

4.1.1 Reverse and forward osmosis

In reverse osmosis (RO), the residual water is pressurised to allow for water permeation through a membrane that rejects practically all dissolved substances. To effectively use RO as concentration technology by rejecting TAN and decrease the volume of the residual, TAN must be present as NH_4^+ , because uncharged NH_3 can easily permeate through the membrane (Masse et al. 2008). For example, Mondor et al. (2008) and Gong (2013) reported final TAN concentrations of 12.8 and $12 \text{ g}\cdot\text{L}^{-1}$ in the concentrate after using RO to treat filtered swine manure reject water, respectively. The concentration factor (CF), relating the final achieved concentration to the ingoing concentration of the respective residual water, was 1.5 and 3.6, respectively. Ledda et al. (2013) achieved TAN concentrations of 5.7 and $7.3 \text{ g}\cdot\text{L}^{-1}$, with a CF of 4, after treating cow and swine reject water pre-treated by ultrafiltration, respectively. In addition, Schoeman and Strachan (2009) obtained $1.8 \text{ g}\cdot\text{L}^{-1}$, CF of 2, after concentrating solid waste leachate by RO. Finally, Fu et al. (2011) used RO to concentrate TAN in simulated acid scrubber effluent and reported a final TAN concentration of $12.6 \text{ g}\cdot\text{L}^{-1}$ (CF of 3, based on the reported volume reduction and NH_4^+ rejection) and Noworyta et al. (2003) produced an RO concentrate with a TAN concentration of $11 \text{ g}\cdot\text{L}^{-1}$ (CF of 8) after treating NH_4NO_3 condensate from fertiliser industry.

Forward osmosis (FO) uses a saline draw solution to force water permeation from the feed water by osmosis, while most (except volatile) dissolved substances are rejected by a membrane. Holloway et al. (2007) reported a water recovery of 70% and a NH_4^+ rejection of 92% for the use of FO to concentrate nutrients in filtered sludge reject water, resulting a final TAN concentration of $4 \text{ g}\cdot\text{L}^{-1}$ (CF of 3). Interestingly, even though the same water recovery was achieved on manure digestate by Li et al. (2020), the authors did not succeed to concentrate TAN by FO as the rejection of NH_4^+ was less than 40%.

According to the consulted studies, the maximum CF that can be achieved by RO and FO for TAN in residual streams is about 6 and 3, respectively. The CF for RO and FO is mainly limited by the water recovery. Furthermore, as a result of the effective rejection (and thus concentration) of substances such as humic acids and multivalent ions by RO and FO, membrane fouling was observed in many studies (Holloway et al. 2007, Li et al. 2020, Masse et al. 2007, Xie et al. 2016), even when pre-treatment by (membrane) filtration was applied. Hence, extensive membrane cleaning is required, to allow for stable operation to concentrate TAN by RO and FO when substances in the feed stream are present that induce particulate fouling, scaling, or organic fouling. Finally, because the membranes reject practically everything, also other concentrated compounds (organics and salts) are present in the concentrated NH_4^+ solution.

4.1.2 (Bio-)electrochemical cells

In (bio-)electrochemical cells ((B)ECs), TAN is transported as NH_4^+ from the anode compartment, through a cation exchange membrane, to the cathode compartment when an electric current is applied. In the last decade, these technologies have been widely applied to recover TAN from residual streams as urine and reject water, containing NH_4^+ feed concentrations up to $4 \text{ g}\cdot\text{L}^{-1}$ (Kuntke et al. 2018, Rodríguez Arredondo et al. 2015). The various types of (B)ECs comprise microbial fuel cells (MFCs), microbial electrolysis cells (MECs) and electrochemical cells (ECs). While MFCs are actually able to recover TAN and simultaneously produce energy, the highest reported NH_4^+ fluxes ($0.08 \text{ kg N}\cdot\text{m}^{-2}\cdot\text{d}^{-1}$) are 6.5 times lower than for MECs ($0.52 \text{ kg N}\cdot\text{m}^{-2}\cdot\text{d}^{-1}$) and 4.8 times lower than for ECs ($0.38 \text{ kg N}\cdot\text{m}^{-2}\cdot\text{d}^{-1}$) (Kuntke et al. 2018). The higher NH_4^+ fluxes in MECs and ECs are attained at the expense of external electricity supply, which results in a higher energy consumption for MECs ($4 - 22 \text{ MJ}\cdot\text{kg}^{-1} \text{ N}$) and ECs ($18 - 94 \text{ MJ}\cdot\text{kg}^{-1} \text{ N}$) compared to the energy producing

MFCs ($-10 \text{ MJ}\cdot\text{kg}^{-1} \text{ N}$) (Kuntke et al. 2018). The wide range of reported energy consumptions by the (B)ECs can be explained by the very wide range of achieved TAN removal efficiencies (1 – 100%). Based on the reported (B)ECs data, the efforts to decrease the electrode and membrane areas, for which increased NH_4^+ fluxes are required, led to higher energy consumptions.

(B)ECs are actually used to concentrate TAN, and are mostly combined with stripping and scrubbing of NH_3 , allowing for actual TAN recovery (Kuntke et al. 2018). Hence, very little attention is paid to the concentrations of TAN obtained in the cathode compartment. The study of Ledezma et al. (2017) reported a final concentration of $26.2 \text{ g N}\cdot\text{L}^{-1}$ (CF of 4.5) in the cathode during the recovery of TAN from synthetic urine by a novel MEC, while Kuntke et al. (2014) achieved a concentration of $7 \text{ g N}\cdot\text{L}^{-1}$ when concentrating TAN in an MEC (CF of 10). A convenient aspect of (B)ECs is the reduction of water at the cathode side, resulting in the generation of OH^- , allowing for an in-situ pH increase while no chemicals are needed. Hence, the concentrated TAN solution produced by (B)ECs contains dissolved NH_3 . Interestingly, no limitations by fouling were reported in the reviews of Kuntke et al. (2018) and Rodríguez Arredondo et al. (2015) while urine, (pig) digestate, reject water leachate were used as feed streams. The apparent tolerance of (B)ECs to blockage by solids and fouling is possibly explained by the relatively wide anode compartments and the fact that the feed water is not pressurised and forced through the membrane.

4.1.3 (Bipolar membrane) electro dialysis

Similar as in (B)ECs, TAN is transported as NH_4^+ from the residual water when an electric current is applied in electro dialysis (ED). However, because ED contains alternating cation and anion exchange membranes, alternating feed water and concentrate channels are formed. Eventually, the transported NH_4^+ ends up as concentrated TAN in the ED concentrate. Pronk et al. (2006a) applied ED to concentrate 93% of the TAN from source-separated urine and achieved a final concentration of $14.2 \text{ g}\cdot\text{L}^{-1}$ (CF of 2.9). Studies performed by Mondor et al. (2008) and Ippersiel et al. (2012) showed that ED can be used to remove NH_4^+ by 75 – 85% from filtered manure reject water and that final TAN concentrations between $14 - 21 \text{ g}\cdot\text{L}^{-1}$ can be achieved (CF up to 5.6) for an energy consumption ranging $66 - 71 \text{ MJ}\cdot\text{kg}^{-1} \text{ N}$. Furthermore, Ward et al. (2018) achieved a CF of 8.5 in the ED concentrate of 120 L by removing 23% of the NH_4^+ from 5,400 L sludge reject water at an energy consumption of 18

MJ·kg⁻¹ N, leading to a final TAN concentration of 7 g·L⁻¹. Furthermore, by optimising the applied current density (which will minimise osmotic water transport and ion back-diffusion), the TAN concentration can be increased from 1.5 to 10 g·L⁻¹ (CF of 6.7) for 90% TAN removal at energy consumption of 5 MJ·kg⁻¹ N (van Linden et al. 2019).

By using bipolar membrane electro dialysis (BPMED), TAN can be transported from the residual stream as NH₄⁺ and simultaneously be concentrated as dissolved NH₃ due to the production of OH⁻ by bipolar membranes, which only requires electricity (van Linden et al. 2020). According to the study of van Linden et al. (2020), at least 85% TAN removal can be achieved by BPMED for the production of 5 g·L⁻¹ of NH₃ at the expense of 19 MJ·kg⁻¹ N. Dissolved NH₃ concentrations of 46 and 54 g NH₃·L⁻¹ starting from synthetic NH₄Cl and NH₄NO₃ solutions containing 37 and 45 g NH₄⁺·L⁻¹, respectively, were achieved by Li et al. (2016) and Gain et al. (2002), respectively. A study performed by Pronk et al. (2006b) resulted in the production of a solution containing 2.5 g NH₃·L⁻¹ after treating diluted urine with an initial TAN concentration of 4.9 g·L⁻¹ by BPMED, whereas Shi et al. (2018) used BPMED to completely remove NH₄⁺ from synthetic pig manure reject water at the expense of 58 MJ·kg⁻¹ N, reaching a final concentration of 13.8 g NH₃·L⁻¹.

Similar to FO and RO, feed waters with low solids concentrations are desired for ED and BPMED, to avoid particulate fouling between the spacers and membranes. Besides, in available studies on ED to concentrate TAN, organic fouling and scaling on the membranes was reported (Mondor et al. 2009, Shi et al. 2019). Fouling in ED can be reversed and limited by chemical cleaning, reversing the electrode polarity (Shi et al. 2019) or by avoiding the transport of scaling substances (multivalent ions) and humic acids by using selective membranes (Kim et al. 2002). In the few published studies on BPMED to recover TAN from residual streams, no information on fouling was found.

4.2 Technologies to recover ammoniacal nitrogen

4.2.1 Struvite precipitation

The addition of magnesium to residual waters containing both TAN and phosphate within the optimum pH range (pH = 8 – 9) leads to the precipitation of struvite crystals (MgNH₄PO₄·6H₂O, having an NH₄⁺ content of 7 m%), which can be used as fertiliser (Mehta et al. 2015, Zarebska et al. 2015). Struvite precipitation is widely applied to avoid undesired

scaling in pipelines during the transport of digestate and for the recovery of phosphorus. Moreover, struvite formation can directly be achieved in manure reject water, suggesting that struvite precipitation has a high tolerance to the presence of solids in the residual water (Mehta et al. 2015, Zarebska et al. 2015). However, in N-loaded residual waters, TAN is present in excess molar concentrations with respect to phosphate (equal molar concentrations required to form struvite) resulting in a TAN removal efficiency of struvite precipitation limited to 15 - 30% (Mehta et al. 2015, Zarebska et al. 2015). The energy consumption of chemical precipitation for the removal and recovery of TAN was reported by Magrí et al. (2013) to be $59 \text{ MJ}\cdot\text{kg}^{-1} \text{ N}$, taking the use of chemicals into account.

4.2.2 (Air) stripping and acid scrubbing

TAN can also be recovered as NH_3 by air stripping (AS), for example from manure and sludge reject water (Magrí et al. 2013, Zarebska et al. 2015) and recovery of TAN from cathode solutions produced by (B)ECs (Kuntke et al. 2018). Because the vapour pressure of NH_3 in fresh air is negligibly low, NH_3 transport from the residual water to the air takes place. TAN recovery by AS in stripping towers has a high tolerance of solids as studies reported that no pre-treatment of digestate was required (Mehta et al. 2015, Zarebska et al. 2015), while it should be noted that accumulation and scaling of minerals requires cleaning. However, before NH_3 effectively can be stripped, the pH of the residual water must be increased to convert NH_4^+ to NH_3 , by means of chemical addition, CO_2 stripping or electrochemical reactions (water reduction or water dissociation).

The actual concentrations of NH_3 in the air after NH_3 stripping according to the study of Wang et al. (2010) are below 9,000 ppm (corresponding to 0.9 m%). Besides, based on the reported NH_3 mass flows and the used air flow rates, the concentration of NH_3 in the air is well below 1 m% according to the studies of Bonmatí and Flotats (2003) and Lei et al. (2007). Hence, by using AS, only diluted gaseous NH_3 is obtained. By subsequent scrubbing of the NH_3 gas-containing air with acid, dissolved NH_4^+ solutions or even solid NH_4^+ salts such as ammonium sulphate ($(\text{NH}_4)_2\text{SO}_4$), ammonium bicarbonate (NH_4HCO_3) or ammonium nitrate (NH_4NO_3) can be obtained (Bonmatí and Flotats 2003, Kuntke et al. 2018, Ukwuani and Tao 2016). The energy consumption of AS and subsequent scrubbing in acid ranges from 14 to $50 \text{ MJ}\cdot\text{kg}^{-1} \text{ N}$ and depends strongly on the TAN concentration and temperature of the residual

water (Mehta et al. 2015, Zarebska et al. 2015). However, not all reported values consistently consider the energy for the addition of heat and the addition of chemicals.

By using hydrophobic membranes, which are impermeable for liquids, but permeable for vapours and gases, to separate the liquid and gas phase, small installation footprints can be realised by providing a large contact area per unit of volume between the feed water and the permeate. Moreover, the pressure of the liquid can be controlled independently of the pressure of the gas. When an acidic solution is recirculated in the permeate side and the feed water contains dissolved NH_3 , stripping and direct scrubbing takes place, resulting in the direct production of solution containing NH_4^+ . This configuration of NH_3 stripping and scrubbing is called direct membrane contactors (DMCS) or transmembrane chemisorption (TMCS).

According to the review studies of Zarebska et al. (2015), Mehta et al. (2015) and Kuntke et al. (2018), the DMCS or TMCS was widely applied to directly scrub the stripped NH_3 from digestates, reject waters, stored urine and from the cathode compartment solutions from (B)ECs, even though TSS concentrations of up to $20 \text{ g}\cdot\text{L}^{-1}$ were present. The review of Beckinghausen et al. (2020) reported that the energy consumption was about $4 \text{ MJ}\cdot\text{kg}\cdot\text{N}^{-1}$, but it remains unclear whether this includes the use of heat and chemicals such as H_2SO_4 .

4.2.3 Vacuum (membrane) stripping

Finally, stripping of NH_3 also can be achieved by applying vacuum, which avoids the presence of air in the vapour that contains the stripped NH_3 . Ukwuani and Tao (2016) successfully used vacuum stripping (VS) in combination with acid scrubbing to recover NH_3 from water at various feed water temperatures and vacuum pressures from manure, food waste, sludge digestate and landfill leachate (containing $1.0 - 6.4 \text{ g}\cdot\text{L}^{-1}$ of NH_3). According to the review of Beckinghausen et al. (2020), the required energy for TAN recovery by VS was $215 \text{ MJ}\cdot\text{kg}\cdot\text{N}^{-1}$, which is mainly required for increasing the feed water temperature. However, besides the stripping of NH_3 , also water is evaporated during VS and vacuum membrane stripping (VMS) resulting in a gaseous NH_3 and water vapour mixture (He et al. 2018). In fact, the ratio of the NH_3 flux to the total flux (water and NH_3) during VMS to recover at NH_3 at TAN feed concentrations ranging $1 - 4 \text{ g}\cdot\text{L}^{-1}$ was only 1% (NH_3 concentration of 1 m%) in unfiltered digestate in the studies of He et al. (2018), (2017a).

However, according to the study of El-Bourawi et al. (2007), the NH_3 in the recovered gas increases from 1.2 m% to 6.8 m% when the concentration of NH_3 in the liquid feed is increased from 4.9 to 20 $\text{g NH}_3\cdot\text{L}^{-1}$, respectively.

4.3 Discussion on ammoniacal nitrogen concentration and recovery technologies

Table 2 presents an overview of all discussed TAN recovery technologies, including the tolerance to the presence of solids in the feed/source water, the required inputs (i.e., energy, chemicals, etc.), the obtained outputs (i.e., TAN chemical form, concentration, etc.). In addition, **Figure 6** presents an overview of the applications of the various TAN recovery technologies to obtain the various TAN products. The most suitable approach to recover TAN is very location-specific because the local situation determines the characteristics of the residual stream, discharge restrictions, the available resources (energy, financial, etc.) and the possibilities for reuse/recovery. Therefore, this chapter presents the technology sequence in an objective manner by only providing the information for decision making, which relates to input, product, and qualities, as shown in **Table 2**.

For almost all technologies (except for struvite precipitation), the actual energy consumption depends heavily on the feed water characteristics, the operational conditions, and the actual performance. In current available literature, the energy consumption for RO and FO is not directly reported. Hence, to concentrate TAN by RO and FO, high TAN rejections and water recoveries must be achieved, leading to an increase in osmotic pressure throughout the operation, which will ultimately translate to a higher energy consumption. Also, the required information to determine the energy consumption to concentrate TAN is lacking. Therefore, there is a need to assess and normalise the energy consumption to concentrate TAN (in $\text{MJ}\cdot\text{kg}^{-1}\text{ N}$) by RO and FO, which will be a function of the TAN feed concentration and rejection, the water recovery and flow rate, transmembrane membrane pressure and pump efficiency. The same holds for (B)ECs and (BPM)ED, for which the energy consumption to concentrate TAN strongly depends on the feed concentration, the amount of TAN transported, the efficiency of using electric charge and the resistance of the cell and membrane stacks. When sufficient data is available, there is potential to normalise the data and derive technology-specific energy values to concentrate TAN. Eventually, the normalisation of the required

energy input for the recovery of TAN can be based on the respective feed concentration and the removal or recovery efficiency.

Table 2 - An overview of the various technologies that can be used to concentrate or recover TAN from residual waters.

Technology	TAN Feed Conc. g·L ⁻¹	Required Input -	Solids Tolerance -	End products -	TAN Product Conc. m% TAN	Energy Consumption MJ·kg ⁻¹ N	Reference
Technologies to concentrate TAN	RO	0.9 – 8.5	Electricity	Low	NH ₄ ⁺ (aq)	1.3	^a n.r. (Mondor et al. 2008, Schoeman and Strachan 2009)
	FO	1.3	Elec. + salt solution	Low	NH ₄ ⁺ (aq)	0.4	n.r. (Holloway et al. 2007)
	(B)ES	0.7 – 5.8	Electricity	Low	NH ₃ (aq)	0.7 - 2.6	^b -10 - 94 (Kuntke et al. 2018)
	ED	0.8 – 4.9	Electricity	Low	NH ₄ ⁺ (aq)	0.7 - 2.1	18 - 71 (Ippersiel et al. 2012, Mondor et al. 2008, Ward et al. 2018)
	BP MED	4.9 - 45	Electricity	Low	NH ₃ (aq)	0.5 - 1.4	58 (Shi et al. 2018)
Technologies to recover TAN	Precipitation	n.r.	Base and salt	High	MgNH ₄ PO ₄ ·(6 H ₂ O) (s)	7	59 (Magrí et al. 2013)
	AS (+ Scrub)	0.5 – 6.7	Electricity, heat and base (acid)	High	NH ₃ -air (g) (NH ₄ ⁺ (aq))	0.9 (7 - 14)	14 - 50 (Mehta et al. 2015, Zarebska et al. 2015)
	V(M)S	1 - 12	Electricity, heat and base	High	NH ₃ -water (g)	1.0 - 6.8	215 (Beckinghausen et al. 2020)

^a n.r. – not reported; ^b - negative energy consumption means energy production.

Finally, to recover TAN as gaseous NH₃, NH₄⁺ solution or solid NH₄⁺ crystals, the energy consumption must be expressed including the required amount of heat and energy to produce chemicals and to increase the pH and scrub the NH₃. Only when normalised information is available on the various strategies and technologies to recover TAN, fair comparisons between technologies can be made. Eventually, the choice to use a certain technology or combination of technologies will depend on the availability of local resources, the potential to use the recovered products and the financial implications.

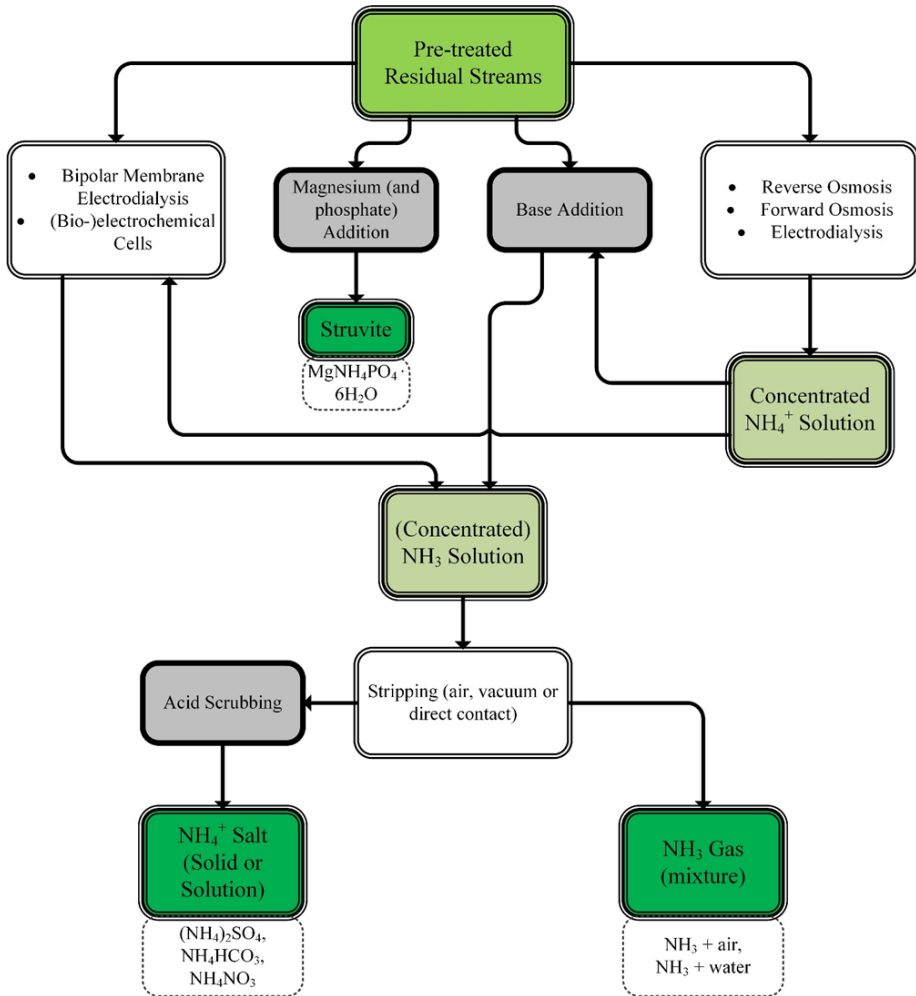


Figure 6 - A schematic overview of the various TAN recovery technologies to obtain various TAN products, such as concentrated NH_4^+ solutions, NH_3 solutions, struvite, solid or dissolved NH_4^+ salts and gaseous NH_3 .

5 Use of the recovered ammoniacal nitrogen

5.1 N-fertiliser production

Among the plant nutrients, N is the most important one for crop yield and plant growth and accounts for the majority (>50%) of the total crop fertiliser consumption. N-fertilisers can be produced in various chemical forms such as: urea, $(\text{NH}_4)_2\text{SO}_4$, NH_4NO_3 , and urea ammonium nitrate. A higher crop growth rate is forecasted for urea, since it has the highest N content (~46 m% of N) (Chien et al. 2011). The potentially recovered TAN can be used to produce any of these N-fertilisers, shortcutting the artificial N-cycle and partially meeting the fertiliser demand.

Although there is an increasing interest in the production of bio-based fertilisers in the emerging circular economy (Sigurnjak et al. 2016), there is also a lack of information about the resulting end-products and their performance. In fact, the European fertiliser legislation (Regulation (EU) No. 2003/2003) still identifies these products as animal manure, hindering their market potential. One of the few and most recent studies on the production and testing of ammonia-based fertilisers from agricultural waste is that of Sigurnjak et al. (2016), where the authors found no performance differences between the bio-based produced NH_4NO_3 and $(\text{NH}_4)_2\text{SO}_4$ and the synthetic fertilisers when applied in crops of *Lactuca sativa* L.. However, a high N-content variability for bio-based $(\text{NH}_4)_2\text{SO}_4$ (30 – 86 g N·kg⁻¹) and NH_4NO_3 (132 – 198 g N·kg⁻¹) recovered at different installations was found. Similar conclusions were reached by Szymańska et al. (2019) in a very similar study for maize and grass. The work of Sigurnjak et al. (2016) is part of the EU funded project SYSTEMIC that aims at recovery and recycle of valuable mineral components from organic waste streams into new products including fertilisers at large scale. During the project, extensive characterisation and performance assessment was done for the end-products ($(\text{NH}_4)_2\text{SO}_4$ and NH_4NO_3) of several ammonia stripping installations from anaerobic digesters in Europe.

The most common approach for production of fertilisers from recovered TAN is the stripping-scrubbing approach, where either $(\text{NH}_4)_2\text{SO}_4$ or NH_4NO_3 are produced. Both end-products have a high N-concentration, yet most implemented stripping units produce $(\text{NH}_4)_2\text{SO}_4$. Worldwide, $(\text{NH}_4)_2\text{SO}_4$ represents only 4% of the N-fertiliser production because of its relatively low N-concentration as compared to urea (21 m% and 45 m%, respectively)

(Vaneekhaute et al. 2017). However, the demand for $(\text{NH}_4)_2\text{SO}_4$ has raised recently because of an increased necessity for S-nutrition, due to that better air quality results in less S deposition on agricultural land (Chien et al. 2011). Typically, commercial ammonia stripping systems can achieve $(\text{NH}_4)_2\text{SO}_4$ concentrations between 25 – 40 m% (equivalent to 6-10% of N), which is often marketed as a liquid fertiliser (Vaneekhaute et al. 2017). Although granular (>1.8 mm crystals) $(\text{NH}_4)_2\text{SO}_4$ is preferred because of its higher market price, the techno-economic feasibility of producing it from residual water requires more investigation (Hofmann et al. 2009, Vaneekhaute et al. 2017). According to the former European regulation (Regulation (EU) 2003/2003), fertilisers should have a minimum N-concentration of 15 m%, which is more easily reachable by NH_4NO_3 due to the additional presence of N as NO_3 . In the new EU regulation for fertiliser products (Regulation (EU) 2019/1009) lower N-concentration concentrations (1.5 – 3 m%) are required for liquid inorganic macronutrient fertilisers, which can easily be produced with $(\text{NH}_4)_2\text{SO}_4$ solutions. In any case, if both $(\text{NH}_4)_2\text{SO}_4$ and NH_4NO_3 are obtained from residual streams, their use in crops is limited and regulated by the current European nitrates' directive (Directive 91/676/EEC, 1991).

Besides the recovery of $(\text{NH}_4)_2\text{SO}_4$, TAN is also recovered in full-scale applications as struvite, which can be used as a slow-release fertiliser. However, the struvite precipitation only recovers a limited fraction of TAN in the residual streams due to the off-balance in molar concentrations of TAN and phosphate (as discussed in 4.2.1). Regarding urea, no literature or projects have been found, probably because of the technical difficulties for its synthesis entailing high temperatures (i.e., 160-180°C) and pressures (i.e., 110 atm). A very interesting work is presented by He et al. (2017b), who described ammonia water recovery from biogas digestate via VMS, which is subsequently used for the upgrade of biogas (i.e., CO_2 capture). The by-product of the process is aqueous NH_4HCO_3 , an inexpensive N-fertiliser that is commonly used as a substitute of urea in China.

Finally, an important aspect for the commercialisation of bio-based fertilisers is the presence of impurities and their potential long-term environmental impact. Impurities caused by organics, metals, pathogens and other contaminants may occur and must be, therefore, assessed (Vaneekhaute et al. 2017). To this end, Laurenzi et al. (2013) assessed the influence of the COD content of the feed streams (pig manure and reject water) on the organic contamination (TOC and VOCs) of the recovered $(\text{NH}_4)_2\text{SO}_4$ via ammonia stripping. The

degree of impurity depended greatly on the initial organic matter content of the streams and to some extent on the pH used to strip NH_3 . In general, reject water (i.e., low COD) and high pH is preferred. The authors also propose the use of basic traps downstream to increase the organics abatement. Besides, a few researchers investigated the properties of recovered struvite (Rahman et al. 2014) and $(\text{NH}_4)_2\text{SO}_4$ (El Diwani et al. 2007, Möller and Müller 2012, Vaneckhaute et al. 2014) as fertilisers.

5.2 Energy carrier

NH_3 was recently identified as a suitable energy carrier, as an alternative to carbon-based fuels such as oil and natural gas, because it is carbon-free and the storage and transportation systems are already established (Valera-Medina et al. 2018). Therefore, NH_3 can also be used as a fuel to produce both heat and power. Based on collected data, a general overview of direct NH_3 fuel cells and their operational characteristics and peak power densities is provided in **Table 3** (Afif et al. 2016, Lan and Tao 2014, Ni et al. 2009).

Table 3 - Various direct NH_3 fuel cells and their operational characteristics and peak power densities according to the review studies of Afif et al. (2016), Lan and Tao (2014), and Ni et al. (2009).

Type	Operating Temperature	Electrolyte	Mobile ion	Peak Power Density
AMFC	25 °C	Anion Exchange Membrane	OH^-	16 $\text{mW}\cdot\text{cm}^{-2}$
AFC	50 – 450 °C	Dissolved/molten OH^-	OH^-	40 $\text{mW}\cdot\text{cm}^{-2}$
SOFC-H	450 – 750 °C	Ceramic Membrane	H^+	580 $\text{mW}\cdot\text{cm}^{-2}$
SOFC-O	500 – 1,000 °C	Ceramic Membrane	O^{2-}	1,190 $\text{mW}\cdot\text{cm}^{-2}$

5.2.1 Combustion technologies

NH_3 can be used as fuel in thermal combustion and propulsion technologies. This is normally done in combination with other fuels, such as H_2 , CH_4 or other carbon-based fuels (Valera-Medina et al. 2018). The inherent efficiency of combustion-based technologies is limited. Moreover, according to the review studies of Kobayashi et al. (2019) and Dimitriou and Javaid (2020), there are additional challenges when using NH_3 regarding low flammability, emission of unprocessed NH_3 and oxidised nitrogen species (NO_x , N_2O , etc.). No studies on the use of recovered NH_3 in energy generation with combustion-based technologies could be found.

Recent developments in the maritime shipping industry are focusing on using ammonia in internal combustion engines (Lesmana et al. 2019). In fact, ammonia is regarded as a key carbon neutral player, particularly in the retrofitting of the existing fleet. According to a recent market outlook (DNV·GL 2020), to achieve the UN-IMO (International Maritime Association) targets, ammonia (dual-fuel) internal combustion engines could have a share between 30 – 60 % of the total maritime fuel mix by 2050.

5.2.2 Alkaline (membrane) fuel cells

Alkaline fuel cells (AFCs) use dissolved or molten hydroxide for the transport of hydroxide (OH^-) from the cathode to the anode, whereas alkaline membrane fuel cells (AMFCs) use an anion exchange membrane. In both AFCs and AMFCs, NH_3 is directly electrochemically oxidised by OH^- at the anode, while at the cathode O_2 and water react together with the supplied electrons to OH^- (Lan and Tao, 2014). However, Lan and Tao (2010) mentioned that the low operational temperature of 25 °C resulted in a long stabilisation time of the established electric potential difference between the anode and cathode of their AMFC, indicating slow kinetics of the processes. Furthermore, research conducted by Suzuki et al. (2012) showed that the performance of AMFCs is limited by fuel cross-over, caused by diffusion of NH_3 from the anode to the cathode. Moreover, Suzuki et al. (2012) also showed that poisoning of the metal catalysts with adsorbed N species takes place at the anode. Finally, the reported maximum power densities for AFCs and AMFCs are only 40 and 16 $\text{mW}\cdot\text{cm}^{-2}$, respectively, (Ganley 2008, Lan and Tao 2010), which is an order of magnitude lower than high temperature fuel cells.

5.2.3 Solid oxide fuel cells

SOFCs can be divided, based on their ability, to either conduct protons (SOFC-H) or oxygen ions (SOFC-O) through the solid ceramic electrolyte. Because in both SOFC types the operational temperature is well above 500 °C, NH_3 is spontaneously cracked at the anode in the presence of a nickel catalyst, resulting in the production of H_2 and N_2 . Initially, nickel was used as a catalyst for H_2 -fueled SOFCs (Mahato et al. 2015) and later also appeared to be a good catalyst to crack NH_3 (Fournier et al. 2006). In SOFC-Hs, the electrolyte is proton-conducting, while in SOFC-Os, the electrolyte is oxygen-conducting, implying different reactions to take place. According to the study of Ni et al. (2008), the application of SOFC-Hs could lead to higher electrical efficiencies than SOFC-Os when using NH_3 as fuel due to

the place where the oxidation reaction takes place, which affects the activity of the reactants. However, available literature reports higher power densities for SOFC-Os than for SOFC-Hs (Afif et al. 2016, Ni et al. 2009), which is mainly attributed to the low resistance of the oxygen-conducting electrolytes. A maximum power density of $1,190 \text{ mW}\cdot\text{cm}^{-2}$ for SOFC-Os was reported by Meng et al. (2007), compared to $580 \text{ mW}\cdot\text{cm}^{-2}$ for SOFC-Hs (Aoki et al. 2018), both using NH_3 directly (without external cracking) as fuel. The higher power density reported for SOFC-O is probably a result of more intensive research activities. Based on review papers of (Ni et al. 2009) and (Afif et al. 2016), it can be concluded that also the design of the cell is important, as the use of anode-supported planar cells results in superior power densities, compared to the use of tubular-supported or tubular cells. Unfortunately, most research on NH_3 -fueled SOFCs only report the achieved power density. In addition to the maximum power density, it is also important how efficient the fuel is used, to determine the actual electrical efficiency. Only a limited number of studies reported the actual electrical efficiency (i.e., conversion of chemical energy to electrical energy), which can go up to 70% (Dekker and Rietveld 2006). A more general review paper on SOFCs by Stambouli and Traversa (2002) also reported that electrical efficiencies of 60% are feasible, while an additional 30% of the chemical energy from the fuels can be used as a high-grade heat. Therefore, SOFCs can potentially effectively use 90% of the total energy content of NH_3 , making the SOFC the most efficient technology to reclaim energy from NH_3 .

Another advantage of SOFCs over combustion-based technologies and A(M)FCs is the negligible production of oxidised N species (NO_x). Staniforth and Ormerod (2003), Ma et al. (2006) and Okanishi et al. (2017) analysed the anode off-gas, and concluded that the concentration of oxidised N-species is below the detection limit, and 0.5 ppm by Dekker and Rietveld (2006). Moreover, the application of SOFC-Hs using NH_3 as fuel will even less likely produce oxidised N species, because N_2 and O_2 will not be in direct contact, as only H^+ is transported through the proton-conducting electrolyte (Ni et al. 2009). However, a potential challenge for the use of SOFCs is nickel nitridation, which is the formation of nickel-nitrogen (Ni_3N) species at the anode. Nitridation of nickel at the nickel/yttria-stabilised zirconia anode was observed by Yang et al. (2015a), who linked this to a decrease in electric potential over the operational run time at an operational temperature ranging 600 – 700 °C. These findings were confirmed by Stoeckl et al. (2019b), who also observed a

decrease in electric potential at 700 °C, while using a nickel/yttria-stabilised zirconia anode. However, interestingly, Stoeckl et al. (2019b) also observed a stable electric potential at an operational temperature of 800 °C. In a subsequent study of Stoeckl et al. (2020), the electric potential decreased only by 1% over an operational run time of 1,000 hours, when an operational temperature ranging 815 – 845 °C was maintained. The authors reported that no structural damage was observed at the anode. However, in this study, a nickel/gadolinium-doped ceria anode was used. Therefore, it remains unclear under what operational conditions and for what anode materials nickel nitridation threatens the stable operation of NH₃ in SOFC-Os. For SOFC-Hs, we found no studies reporting on nitridation or the production of oxidised N species.

To the best of our knowledge, there are no studies that use NH₃ recovered from residual streams as a fuel in a fuel cell. In case of recovery from residual water, NH₃ will be accompanied by water vapour and potentially other contaminants. Interestingly, the main components of biogas (CH₄ and CO₂), can also be fed to the SOFC-Os, because after CH₄ reforming with steam or CO₂, the produced H₂ and CO also serve as fuel (Gür 2016, Saadabadi et al. 2019). However, research conducted by Papadimas et al. (2012) showed that SOFCs are especially sensitive to contaminants such as H₂S (typically present in biogas), HCl and siloxanes, which deactivate the nickel catalyst and decrease the effective surface of the anode, suggesting that gas cleaning is required before using recovered gases as fuels. Finally, studies on SOFC-Os conducted by Wojcik et al. (2003), Cinti et al. (2016), Stoeckl et al. (2019a) and Stoeckl et al. (2020) showed that it is actually feasible to use mixtures of NH₃ and water vapour as fuel for SOFC-Os. However, the minimum concentration of NH₃ in the fuel was 17% (Wojcik et al. 2003) and it remains unclear whether NH₃ in this concentration can (directly) be recovered from water. Therefore, more research is required to determine what concentrations of NH₃ can be realised when NH₃ is recovered as a gas from (residual) water and whether SOFCs can work with these concentrations.

5.3 Resource for chemical and biochemical processes

Besides its use as (resource for) fertilisers, NH₃ is also widely used as a refrigerant gas, for purification of water supplies, and in the manufacture of plastics, explosives, textiles, pesticides, dyes, and other chemicals. Besides, NH₃ is found in household and many

industrial-strength cleaning solutions. In general, NH_3 is the precursor of most of the N-containing compounds synthesised by the industry. Important derivatives of NH_3 are nitric acid (for the fabrication of explosives and fertilisers), hydrazine (used as foaming agent, for pharmaceuticals, insecticides and as rocket fuel) and hydroxylamine (used in the preparation of oximes, precursors of nylon). Industrial NH_3 for chemical application is normally sold as NH_3 liquor or sometimes called ammonium hydroxide (an aqueous solution with a 25-33% concentration of NH_3) or as pressurised/refrigerated anhydrous liquid NH_3 .

Low concentrated (4-28 m%) aqueous ammonia solutions are also used for CO_2 capture. Compared to the amine-based traditional capture solvents, aqueous ammonia is cheaper, not easily decomposed by other flue gases and less corrosive. However, aqueous ammonia has a lower CO_2 absorption rate and its higher vapour pressure leads to ammonia losses in the flue gas (Yang et al. 2014). Recent studies have proposed process modifications (e.g., Lean vapour compression, Rich solvent split, etc.) to overcome these drawbacks, showing promising results (Obek et al. 2019), even at pilot plant level (Yu et al. 2018). Additionally, selective reduction (Catalytic and Non-Catalytic) is a well-known chemical process for NO_x abatement in flue or exhaust gas streams in both vehicles and industrial processes. Numerous commercial products use an ammonia or a urea liquid solution as reducing agents. Ammonium sulphate solutions from recovered NH_3 also can be used for this purpose (Ellersdorfer 2018, Lubensky et al. 2019).

Recently, the possibility of shortcutting the anthropogenic N cycle via direct production of edible proteins with NH_3 recovered from residual streams is being explored (Pikaar et al. 2018). The concept involves the production of high-value protein (single-cell protein) via biosynthesis, using lithotrophic H_2 -oxidising bacteria in a reactor. For the bacteria to synthesise proteins, NH_3 , H_2 and CO_2 are required as raw materials. According to Matassa et al. (2015), the physical footprint of such a system can surpass that of the plant-based one by several orders of magnitude. The authors theorised a potential yield, assuming wind energy-powered H_2 production at an average power of $2\text{W}\cdot\text{m}^{-2}$ and a recovery of 1235 ton $\text{NH}_3\text{-N}$ per year from Amsterdam-West WWTP, up to $3120\text{ ton}\cdot\text{Ha}^{-1}\cdot\text{y}^{-1}$ of microbial protein, which would be 3 orders of magnitude more efficient than actual soy productivity (currently around $3\text{ ton}\cdot\text{Ha}^{-1}\cdot\text{y}^{-1}$). The results of the first phase (proof-of-concept in a 5 L reactor operating in batch and continuous mode) showed H_2 conversion efficiencies ranging between 65 - 81%

and protein concentrations between 78 - 375 g cell dry weight·m⁻³·h⁻¹ with very good nutritional properties comparable to those of high-quality fishmeal, showing the potential of this concept (Matassa et al. 2015).

Finally, recovered aqueous NH₃ can also be used as biomass feedstock (e.g., wheat straw) pre-treatment prior AD in biogas plants (Wang and Serventi 2019), or to enhance the production of functionalised carbonaceous materials (biochar) via hydrothermal carbonisation (Latham et al. 2018).

5.4 Discussion on the use of recovered TAN

As above discussed, TAN is a very versatile commodity that has many applications. Moreover, all the mentioned applications have or will have important roles in the future CO₂-neutral and circular economy scenario. It seems logical to pursue closing the N-cycle by increasing the recovery of the TAN and eventually reducing the industrial NH₃ production. However, the amount and quality standards of the current and future ammonia applications are challenging.

In this chapter, two main challenges hindering the practical use of the recovered TAN were identified: 1) the maximum amount of TAN that the combination of the recovery technologies and the TAN concentrations in the identified sources can provide and 2) the quality and/or concentration of the recovered TAN. In marketable terms, fertilisers are the main share (i.e., 80%) as mentioned in previous sections (Galloway et al. 2008). However, there is an important lack of information regarding impurities/pollutant content and agronomic performance. Although the recovery technologies here mentioned showed very high selectivity towards TAN, most of the studies lack detailed chemical analysis and/or field trials. Parameters such as acidity and COD are likely of interest to the agronomic community, and other parameters such as heavy metal content (e.g., Cd, Cr, Hg, Ni, Pb, etc.), microbiological parameters (e.g., Salmonella, E. coli), etc. have maximum limits established by law. This is probably the reason why the legislators and the consumers are hesitant towards the application in the fields of fertilisers produced from recovered TAN. In fact, the current fertiliser regulation framework in the EU, although moving towards a circular economy scenario, shows some incongruences between the classification and applicability criteria and reduces the financial value of these products. Moreover, in most of the studies the final

product was liquid, whereas a solid fertiliser is mostly preferred. A liquid product has much higher transportation and storage costs and may have stability problems over time.

If used as a fuel, the obtained NH_3 concentration is a key factor. The presence of water vapour or any other additional non-oxidizable gas stream will reduce the performance of the technology. Gas upgrading by reducing the water content needs to be explored. Additionally, for the fuel cells and in particular for the SOFC technology, certain chemical compounds such as H_2S might deactivate the catalysts (catalyst poisoning) and may necessitate gas cleaning before it enters the cell (Wasajja H. et al. 2021). In the case of the ammonia fuelled combustion engines, NO_x formation and low performance related to the low ammonia combustion rate are the main challenges. The use of combustion promoters (i.e., a second fuel) or partial ammonia cracking prior the combustion are the approaches being explored for the latter challenge (Lesmana et al. 2019). Direct electrification will always be the most energy efficient option, however in the case of transportation and specifically in long-haul or freight trips, ammonia combustion engines can offer a better alternative.

The application of ammonia solutions to capture CO_2 and eventually produce ammonium carbonate or even urea is gaining interest, however, NH_3 slips in the flue gas and its relatively lower absorption capacity are the main development barriers. Additionally, the influence of other impurities or gases in the recovered TAN solutions is unknown and could be considerable, given the delicate thermodynamic equilibrium of the $\text{NH}_3\text{-CO}_2\text{-H}_2\text{O}$ system.

The application of ammonia, urea or ammonium sulphate solutions to NO_x abatement is also very interesting but NH_3 slip is an important issue. The same issue applies regarding the unknown effects of other impurities or gases present in the recovered TAN solutions, especially in the case of the catalytic selective reduction, where a solid catalyst is employed.

In order to gain the trust of the end-users and the authorities and advance towards a real circular economy, an effort from the scientific community towards a detailed and application-oriented characterisation of the quantity and the quality of the recovered TAN and its performance is needed. We have summarised in **Table 4** the various applications discussed here, as well as the form of TAN, the (minimum) required concentrations for each application and their main challenges.

Table 4 - An overview of the various applications for recovered TAN, including the respective ammonia forms, concentrations, and main product challenges.

Application	TAN Form	Concentration Required	Challenges/opportunities	Reference
Fertiliser	NH ₄ ⁺ (aq.) or NH ₄ ⁺ (s) (urea, ammonium sulphate, struvite, etc.)	6 – 10 m% (15 m% required by EU regulation)	Possible presence of pollutants and lack of end product performance assesment Use in crops is limited and regulated by the European nitrates' directive Big market (Million ton·year ⁻¹)	(Vaneeckhaute et al. 2017), (Regulation (EU) 2003/2003, Directive 91/676/EEC, 1991)
CO ₂ capture	NH ₃ (aq.)	4 - 18 g N·L ⁻¹	Market dominated by amines Lower CO ₂ absorption capacity Ammonia gas leaks	(He et al. 2017b)
Chemical industry (chemical precursor)	NH ₃ (aq.) NH ₃ (g.)	25-33 m%	High purity and concentration needed Big market (Million ton·year ⁻¹)	(Mysoreammonia 2020, Steelmangas 2020, Yara 2020)
Biomass pre-treatment processes (biorefineries)	NH ₃ (aq.)	0.7 m%	Small market	(Wang et al. 2019)
NO _x abatement (flue gas)	NH ₃ (aq.) NH ₄ ⁺ (aq.) urea or ammonium sulphate	20-32 m%	High purity and concentration needed Big market (ktons·year ⁻¹)	(Lubensky et al. 2019)
Energy Generation	NH ₃ (-H ₂ O mixture) (g)	>17 m%	Possible presence of poisoning pollutants for fuel cells (S)	(Wojcik et al. 2003)

6 Conclusions

- In this chapter, residual streams with a minimum TKN of 0.5 g N·L⁻¹ are identified as N-loaded residual streams and categorised by their TAN recovery potential. Three different categories are established according to the TAN/TKN ratio and TSS content. Category 1 as streams with TAN/TKN < 0.5, category 2 as streams with TAN/TKN ≥ 0.5 and TSS > 1 g·L⁻¹ and category 3 as streams with TAN/TKN ≥ 0.5 and TSS ≤ 1 g·L⁻¹. Category 1 streams usually need a conversion of organic N to TAN before TAN recovery, whereas category 2 streams require the removal of solids to enhance the TAN recovery efficiency and category 3 streams are suitable for direct TAN recovery.

- AD is an advantageous pre-treatment for TAN recovery especially for category 1 streams, because it transforms the organic N into TAN while reducing COD and TSS. However, AD sometimes faces slow organic-N conversion rates and limited efficiencies. Incomplete hydrolysis and TAN inhibition are generally identified as the main causes. In general, further research is needed to identify methods for enhancing the organic-N conversion during AD.
- TAN recovery can be done via several technologies requiring different inputs (i.e., electricity, heat, chemicals, etc.), resulting in several end-products (i.e., TAN solutions, NH_3 gas, solid NH_4^+ salts, etc.). Complete information about quality and TAN concentration of end-products, energy and chemical inputs and operational costs is limited and therefore reliable comparisons are difficult to make. Therefore, the energy consumption must be normalised to the respective TAN concentration in the feed and the removal or recovery efficiency.
- Various applications to use the recovered TAN have been identified and discussed in this chapter, including N-fertiliser production, energy generation, industrial processes usage and some novel ones like microbial protein production. Two main factors constraining the reuse of TAN were identified: the actual TAN that can be recovered from the residual streams and the quality of this recovered TAN. Especially in the case of N-fertiliser production, which use is linked to its quality, a lack of information on product quality and performance has been reported.

Supporting information

Table S1 - The TSS, COD, TKN and TAN content, the respective units, used treatment technologies of N-loaded residual streams obtained from approximately 150 studies.

Solid waste	Solids Content	COD Content	TKN Content	TAN Content	TAN/TKN Ratio	COD/N Ratio	Treatment	Reference
Bio + Food Waste								
Biowaste	44.3%	772.0 g/kg	20.0 g/kg	2.5 g/kg	0.1	39	Anaerobic digestion	(Bayard et al. 2015)
Biowaste	50.4%	933.0 g/kg	11.0 g/kg	1.0 g/kg	0.1	85	Anaerobic digestion	(Bayard et al. 2015)
Food waste	18.1%	238.5 g/L	5.4 g/L	0.2 g/L	0.0	44	Anaerobic co-digestion	(Zhang et al. 2011)
Food waste	7.62%	101.2 g/L	2.3 g/L	0.2 g/L	0.1	44	Anaerobic digestion	(Wu et al. 2015)
Food waste	140 g/L	94 g/L	4.2 g/L	0.2 g/L	0.0	22	Anaerobic co-digestion	(Silva et al. 2018)
Biomass								
Waste activated sludge	7.81%	88.2 g/L	4.8 g/L	1.5 g/L	0.3	18	Anaerobic digestion	(Tao et al. 2016)
Raw sewage sludge	21.943 g/L	27.5 g/L	2.9 g/L	1.3 g/L	0.4	9	Semi-continuous anaerobic digestion	(Gil et al. 2018)
Pre-treated sewage sludge	22.031 g/L	27.1 g/L	2.9 g/L	1.5 g/L	0.5	9	Semi-continuous anaerobic digestion	(Gil et al. 2018)
Mixed sludge	73.6 g/kg	57.2 g/L	3.3 g/L	0.1 g/L	0.0	17	Anaerobic co-digestion	(Keucken et al. 2018)

Solid waste	Solids Content	COD Content	TKN Content	TAN Content	TAN/TKN Ratio	COD/N Ratio	Treatment	Reference
Municipal Solid Waste								
Residual municipal waste	33.9 %	1026 g/kg	22.0 g/kg	1.6 g/kg	0.1	47	Anaerobic digestion	(Bayard et al. 2015)
Residual municipal waste	45.1 %	885.0 g/kg	11.0 g/kg	2.3 g/kg	0.2	80	Anaerobic digestion	(Bayard et al. 2015)
OFMSW	35.60%	431.0 g/kg	6.3 g/kg	1.0 g/kg	0.2	68	Thermophilic anaerobic co-digestion	(Hartmann & Ahring 2005)
OFMSW	186 g/kg	235.0 g/L	5.2 g/L	0.5 g/L	0.1	45	Anaerobic co-digestion	(Keucken et al. 2018)
Poultry								
Manure	Solids Content	COD Content	TKN Content	TAN Content	TAN/TKN Ratio	COD/N Ratio	Treatment	Reference
Poultry manure	806 g/kg	783.0 g/kg	22.5 g/kg	0.8 g/kg	0.0	35	Anaerobic co-digestion	(Rodriguez-Verde et al. 2018)
Poultry manure	TS = 30%	1000 g/kg	56.9 g/kg	-	0.0	18	Anaerobic co-digestion	(Bres et al. 2018)
Poultry manure	277 g/kg	201 g/kg	12 g/kg	-	0.0	17	Anaerobic co-digestion	(Borowski et al. 2014)
Poultry litter	VS = 77%	-	38.3 g/kg	3.03 g/kg	0.1	-	Direct contact membrane stripping	(Rothrock Jr et al. 2010)
Broiler manure	45%	-	43.7 g/kg	-	0.0	-	Composting	(Ho et al. 2013)

Manure	Solids Content	COD Content	TKN Content	TAN Content	TAN/TKN Ratio	COD/N Ratio	Treatment	Reference
Cattle								
Cow manure	50 g/L	58 g/L	1.6 g/L	-	0.0	36	Anaerobic digestion	(Karim et al. 2007)
Cattle manure	50 g/L	57 g/L	2 g/L	0.9 g/L	0.5	29	Anaerobic digestion	(El-Mashad et al. 2004)
Cattle manure	79 g/L	-	3.27 g/L	2.15 g/L	0.7	-	Bipolar bioelectrodialysis	(Zhang & Angelidaki 2015)
Cattle manure	17%	-	9.3 g/L	0.8 g/L	0.1	-	Anaerobic digestion	(Omar et al. 2008)
Cattle manure	55 g/L	-	2.3 g/L	1.4 g/L	0.6	-	Anaerobic digestion	(Nielsen et al. 2004)
Swine (Pig)								
Piggery wastewater	6.18 %	130.8 g/L	7.3 g/L	4.8 g/L	0.7	18	Anaerobic digestion	(Ahn et al. 2006)
Piggery wastewater	5.64 %	92.8 g/L	7.3 g/L	4.9 g/L	0.7	13	Anaerobic co-digestion	(Zhang et al. 2011)
Piggery wastewater	18.6 g/kg	14792 mg/kg	1963 mg/kg	1264 mg/kg	0.6	8	Nitrification – denitrification	(Tilche et al. 1999)
Pig slurry	52.97 g/kg	70.59 g/kg	5.63 g/kg	3.39 g/kg	0.6	13	Air stripping	(Bonmatí & Flotats 2003)
Swine manure	17.3 g/kg	24.3 g/kg	3.3 g/kg	3.1 g/kg	0.9	7	Anaerobic co-digestion	(Rodríguez-Verde et al. 2018)
Swine manure	TSS = 6.29 g/L	12.56 g/L	1293 mg/L	724 mg/L	0.6	10	Flocculation + Solid liquid separation	(Vanotti et al. 2002)
Swine manure	14.4 g/L	16780 mg/L	2700 mg/L	2390 mg/L N	0.9	6	Direct contact membrane stripping (+ aeration)	(García-González et al. 2015)
Swine manure	8.60 g/L	6880 mg/L	1890 mg/L	1280 mg/L	0.7	4	Direct contact membrane stripping	(García-González & Vanotti 2015)

Manure	Solids Content	COD Content	TKN Content	TAN Content	TAN/TKN Ratio	COD/N Ratio	Treatment	Reference
Swine (Pig)								
Swine manure (low strength)	4.90 g/L	4520 mg/L	1340 mg/L	1070 mg/L	0.8	3	Direct contact membrane stripping	(Garcia-González & Vanotti 2015)
Swine manure (medium strength)	17.4 g/L	24580 mg/L	2740 mg/L	1680 mg/L	0.6	9	Direct contact membrane stripping	(Garcia-González & Vanotti 2015)
Swine manure (high strength)	24.9 g/L	34080 mg/L	3700 mg/L	2290 mg/L	0.6	9	Direct contact membrane stripping	(Garcia-González & Vanotti 2015)
Swine manure	TSS = 31346 mg/L	59.6 g/L	3939 mg/L	2804 mg/L	0.7	15	Reverse osmosis	(Masse et al. 2013)
Swine manure	40 g/L	33.5 g/L	5.7 g/L	4.6 g/L	0.8	6	Electrodialysis and reverse osmosis	(Mondor et al. 2008)
Swine wastewater	TSS = 667 mg/L	BOD = 2912 mg/L	TN = 707 mg/L	579 mg/L	0.8	4	Nitrification – denitrification	(Chen et al. 2004)

Digestate	Solids Content	COD Content	TKN Content	TAN Content	TAN/TKN Ratio	COD/N Ratio	Treatment	Reference
Manure Digestate								
Chicken manure biogas slurry	TSS = 1920 mg/L	4850 mg/L	TN = 2000 mg/L	2100 mg/L	1.1	2	Extensive pre-treatment + reverse osmosis	(Zhou et al. 2019)
Digested pig slurry	0.83%	7951 mg/kg	-	1121 mg/L	1.0	7	Microbial fuel cell	(Cerrillo et al. 2016)
Digested pig slurry	1.7%	25 g/kg	-	1.8 g/L	1.0	14	Microbial fuel cell	(Cerrillo et al. 2017)
Digested swine manure	8.5 g/L	1685 mg/L	2459 mg/L	2097 mg/L	0.9	1	Direct contact membrane stripping (+ aeration)	(Dube et al. 2016)
Digested swine manure	6.42 g/L	2485 mg/L	1752 mg/L	1465 mg/L	0.8	1	Direct contact membrane stripping (+ aeration)	(Dube et al. 2016)
Pig hydrolysate	TSS = 5.9 %	52.7 g/L	-	3.4 g/L	1.0	16	Extensive pre-treatment + Bipolar membrane electrodialysis	(Shi et al. 2018)
Pig manure digestate	TSS = 19.3 g/L	2.9 g/L	-	2575 mg/L	1.0	1	Electrodialysis	(Shi et al. 2019)
Pig manure slurry	TS = 4387 mg/L	2912 mg/L	-	2.0 g/L	1.0	1	Vacuum membrane distillation	(He et al. 2017a)
Pig manure slurry	TS = 6387 mg/L	7451 mg/L	-	2.5 g/L	1.0	3	Vacuum membrane distillation	(He et al. 2018)
Pig slurry digestate	31.72 g/kg	41.23 g/kg	4.73 g/kg	3.68 g/kg	0.8	9	Air stripping	(Bonmati & Flotats 2003)
Biomass Digestate								
Organic waste digestate	2.89%	-	2.8 g/kg	1.99 g/kg	0.7	-	Air stripping	(Provolo et al. 2017)
Digested sludge	23.5 g/kg	25.5 g/kg	6.7 g/kg	2.1 g/kg	0.3	4	Anaerobic co-digestion	(Forster-Carneiro et al. 2007)
Digested sludge	49.37 g/kg	1.2 g/L	4.5 g/L	2.2 g/L	0.5	0	Anaerobic ureolysis	(Christiaens et al. 2019a)
Digested microalgae	-	6.9 g/L	0.9 g/L	0.2 g/L	0.2	8	Anaerobic digestion	(Ras et al. 2011)
Digested microalgae	-	9.3 g/L	1.2 g/L	0.8 g/L	0.7	8	Anaerobic digestion	(Ras et al. 2011)

Reject water	Solids Content	COD Content	TKN Content	TAN Content	TAN/TKN Ratio	COD/N Ratio	Treatment	Reference
Manure Reject Water								
Liquid fraction digestate poultry manure	TSS = 7240 mg/L	7467 mg/L	TN = 3600 mg/L	3347 mg/L	0.9	2	Reverse osmosis	(Gong 2013)
Liquid fraction pig slurry	TSS = 0.78%	6908 mg/kg	1068 mg/L	858 mg/L	0.8	6	Microbial fuel and electrolysis cell	(Sotres et al., 2015)
Liquid fraction swine manure digestate	9077 mg/L	9550 mg/L	-	2276 mg/L	1.0	4	Forward osmosis	(Li et al., 2020)
Centrifuged piggery wastewater digestate	11.2 g/L	3969 mg/L	TN = 1700 mg/L	1650 mg/L	1.0	2	Nitrification – denitrification	(Obaja et al., 2003)
Filtered swine manure digestate	TSS = 772 mg/L	-	2814 mg/L	2475 mg/L	0.9	-	Reverse osmosis	(Masse, 2008)
Biomass Reject Water								
Sludge reject water	2.1 g/L	270 mg/L	820 mg/L	740 mg/L	0.9	0	Reverse osmosis and various recovery technologies	(Ek et al., 2006)
Sludge liquor	TSS = 320 mg/L	1160 mg/L	-	1247 mg/L	1.0	1	Nitritation - denitritation	(Jenicek et al., 2004)
Supernatant digested sludge (reject water)	-	369 mg/L	-	847 mg/L	1.0	0	Electrodialysis	(Ward et al., 2018)
Supernatant hydrothermal sludge		25,000 mg/L	TN = 2,700 mg/L	1,000 mg/L	0.4	9	Hydrothermal pre-treatment + anaerobic digestion	(Qiao et al., 2011)
Anaerobic digester supernatant	TSS = 8317 mg/L	3491 mg/L	609 mg/L	609 mg/L	1.0	6	Nitritation - denitritation	(Gil & Choi, 2004)

Urine	Solids Content	COD Content	TKN Content	TAN Content	TAN/TKN Ratio	COD/N Ratio	Treatment	Reference
Swine Liquid								
Liquid fraction raw swine manure	TSS = 0.67 g/L	40.3 g/L	-	5.1 g/L	1.0	8	Electrodialysis	(Mondor et al. 2009)
Liquid fraction raw swine manure	TSS = 1148 mg/L	21.3 g/L	2806 mg/L	2601 mg/L	0.9	8	Nanofiltration + Reverse osmosis	(Masse et al. 2013)
Liquid fraction raw swine manure	TSS = 0.87 g/L	30 g/L	3.5 g/L	4.2 g/L	1.0	7	Electrodialysis and reverse osmosis	(Mondor et al. 2008)
Fresh Human Urine								
Fresh urine	-	7.0 g/L	5.3 g/L	0.3 g/L	0.1	1	Electrochemical cell + stripping	(Luther 2015)
Fresh urine	-	12110 mg/L	TN = 7284 mg/L	490 mg/L	0.1	2	Direct contact membrane stripping	(Xu et al. 2019)
Fresh urine	-	TOC = 5298 mg/L	TN = 7523 mg/L	1125 mg/L	0.1	1	Forward osmosis	(Liu et al. 2016a)
Fresh urine	-	14.9 g/L	6.5 g/L	0.4 g/L	0.1	2	Struvite precipitation	(Wei et al. 2018)
Stored Urine								
Stored urine	-	1650 mg/L	-	1720 mg/L	1.0	1	No treatment	(Udert et al. 2003)
Stored urine	-	10 g/L	-	8,100 mg/L N	1.0	1	Urea hydrolysis (after)	(Udert et al. 2006)
Stored urine	-	6978 mg/L	TN = 5911 mg/L	6006 mg/L	1.0	1	Direct contact membrane stripping	(Xu et al. 2019)
Hydrolysed urine	-	6.8 g/L	5.8 g/L	4.9 g/L	0.8	1	Electrochemical cell + stripping	(Luther 2015)
Centrifuged urine	-	3.9 g/L	-	4.05 g/L	1.0	1	Microbial fuel cell	(Kuntke et al. 2012)
Urine	-	3460 mg/L	-	3820 mg/L	1.0	1	Electrochemical cell + direct contact membrane stripping	(Tarpeh et al. 2018)
Urine	-	2.6 g/L	2.7 g/L	2.5 g/L	0.9	1	Reverse Osmosis + various recovery technologies	(Ek et al. 2006)
Urine	-	4.5 g/L	-	4.0 g/L	1.0	1	Microbial electrolysis cell	(Zamora et al. 2017)
Urine	-	4360 mg/L	-	4850 mg/L	1.0	1	Electrodialysis	(Pronk et al. 2006a)

Urine	Solids Content	COD Content	TKN Content	TAN Content	TAN/TKN Ratio	COD/N Ratio	Treatment	Reference
Stored Urine								
Urine	-	4.7 g/L	-	4.9 g/L	1.0	1	Bipolar membrane electro dialysis	(Pronk et al. 2006b)
Stored urine	-	3.3 g/L	1.6 g/L	1.4 g/L	0.9	2	Struvite precipitation	(Wei et al. 2018)
Stored urine	-	13.5 g/L	6.2 g/L	5.6 g/L	0.9	2	Struvite precipitation	(Wei et al. 2018)
Organic Industrial Wastes	Solids Content	COD Content	TKN Content	TAN Content	TAN/TKN Ratio	COD/N Ratio	Treatment	Reference
Fish Meal								
Fish meal wastewater	-	86.6 g/L	9.1 g/L	1.8 g/L	0.2	10	Anaerobic hydrolysis and acidification	(Guerrero et al. 1999)
Fish meal wastewater	-	105.0 g/L	11.1 g/L	4.5 g/L	0.4	9	Anaerobic hydrolysis and acidification	(Guerrero et al. 1999)
Fish meal wastewater	-	142.8 g/L	13.9 g/L	4.0 g/L	0.3	10	Aerobic degradation	(Kim et al. 2007)
Tannery								
Tannery wastewater	-	2990 mg/L	-	174 mg/L	1.0	17	Membrane Bioreactor + Reverse Osmosis	(Scholz et al. 2005)
Tannery wastewater	TSS = 463 mg/L	2514 mg/L	224 mg/L	126 mg/L	0.6	11	Nitrification – denitrification	(Murat et al. 2002)
Tannery wastewater	TSS = 592 – 998 mg/L	1340 – 2514 mg/L	123 – 185 mg/L	65 – 128 mg/L	0.6	13	Nitrification – denitrification	(Murat et al. 2006)

Inorganic Industrial Wastewater	Solids Content	COD Content	TKN Content	TAN Content	TAN/TKN Ratio	COD/N Ratio	Treatment	Reference
Fertiliser								
Fertiliser industry (urea)	-	-	-	824 mg/L	1.0	-	Struvite precipitation	(Machdar et al. 2018)
Fertiliser industry	-	-	-	325 mg/L	1.0	-	Ion exchange	(Leaković et al. 2000)
Fertiliser industry	TSS = 2.3 mg/L	267 mg/L	357 mg/L	357 mg/L	1.0	1	Nitritation - denitritation + zeolite	(Chung et al. 2000)
Fertiliser industry	-	-	-	1.1 – 1.8 g/L	1.0	-	Reverse osmosis	(Noworyta et al. 2003)
Fertiliser industry	-	-	-	2.8 – 5.8 g/L	1.0	-	Electrodialysis	(Hikmawati et al. 2019)
Rare-earth mining								
Rare-earth wastewater	-	-	-	6.9 g/L	1.0	-	Leaching	(Qiu et al. 2014)
Rare-earth wastewater	-	TOC = 582 mg/L	-	4535 mg/L	1.0	0	Struvite precipitation	(Huang et al. 2011)
Rare-earth wastewater	-	TOC = 494 mg/L	-	4200 mg/L	1.0	0	Struvite precipitation	(Huang et al. 2009)

CHAPTER 3

ANAEROBIC PROTEIN DEGRADATION: EFFECTS OF PROTEIN STRUCTURAL COMPLEXITY, PROTEIN CONCENTRATION, CARBOHYDRATES, AND VOLATILE FATTY ACIDS

This chapter is based on: Deng, Z., Ferreira, A.L.M., Spanjers, H., & van Lier, J.B. (2023). Anaerobic protein degradation: effects of protein structural complexity, protein concentration, carbohydrates, and volatile fatty acids. *Bioresource Technology Reports* 22, 101501.

Abstract

The anaerobic degradation of proteins is often retarded by the presence of carbohydrates. In this chapter, the effects of the presence of carbohydrates and volatile fatty acids (VFAs) on protein degradation was investigated and the rate-limiting step was identified. Bovine serum albumin (BSA) and casein (CAS) were used in batch tests to compare the protein degradation in the presence and absence of carbohydrates and VFAs. The modified Gompertz model was applied to estimate reaction rates. The results showed that deamination was the rate-limiting step, with a rate ranging between 2.7 - 12.7 mg N·h⁻¹. Higher protein structural complexity negatively affected protein hydrolysis, deamination, and methanogenesis by a factor of 1.6 – 3.8; whereas a higher protein concentration improved the conversion rates. A carbohydrate : protein COD ratio of 1 improved the hydrolysis rate of BSA from 26 mg·h⁻¹ to 45 mg·h⁻¹, and that of CAS from 98 mg·h⁻¹ to 157 mg·h⁻¹; whereas the deamination rate slightly decreased from 2.7 mg N·h⁻¹ to 2.5 mg N·h⁻¹ and from 6.0 mg N·h⁻¹ to 5.6 mg N·h⁻¹. In addition, an initial VFAs : protein COD ratio of 1 decreased the CAS deamination rate by 17%. It is postulated that the design of anaerobic reactors, treating protein-rich wastewaters, should be based on the attainable deamination rate, and high VFA concentrations must be avoided.

1 Introduction

The global meat production in 2018 was 342 million tons·year⁻¹ (FAO 2020) and the milk production was 354 million tons·year⁻¹ (Eurostats 2018). More than 30% of the animal weight ends up as protein-rich waste and 2.5 L of wastewater is produced per L of processed milk, resulting in abundant production of protein-rich streams annually (Eurostats 2018). The protein content can be 40% of the dry weight in dairy wastewater and 90% in slaughterhouse wastewater (Salminen and Rintala 2002, Slavov 2017). Protein-rich streams have been considered as potential feedstock for biogas production. A lab-scale protein-fed reactor is confirmed to be stable and can produce biogas (Kovács et al. 2013); as such, the protein-rich stream can be used for bioenergy and ammonia recovery (Kovács et al. 2015).

Anaerobic protein degradation can be generalised into three steps, hydrolysis of protein to amino acids, deamination (or acidification) of amino acids into ammonium and volatile fatty acids (VFAs), and methane (CH₄) production from VFAs (i.e., methanogenesis). The presence of proteins can be problematic in anaerobic digestion (AD), due to 1) occurrence of foaming, 2) incomplete degradation of organic nitrogenous compounds (Bareha et al. 2018), 3) increase in total ammoniacal nitrogen concentration, which may result in inhibition of methanogenesis (Jiang et al. 2019), 4) deterioration of the morphological sludge properties (Liu et al. 2019). According to the reviews of Mata-Alvarez et al. (2014) and (Rajagopal et al. 2013), previous studies focus on the inhibition of NH₃/NH₄⁺ on methanogens, and attempt to co-digest protein-rich streams with carbohydrate-rich streams to reduce inhibition by preventing a pH rise and increasing the C/N ratio.

In fact, carbohydrates are reported to have a negative impact on protein degradation because they can suppress protease production (Glenn 1976). Breure et al. (1986a) and Yu and Fang (2001) observed that carbohydrate is degraded prior to protein: in their chemostat, glucose was completely acidified whereas gelatine was barely acidified; and in batch reactors, proteins only started to be degraded when carbohydrates were depleted. A possible explanation is that carbohydrates, especially glucose, are thermodynamically preferred by microorganisms since their fermentation yields more energy than fermenting amino acids. Bacterial cells gain 1-2 mol ATP·mol⁻¹ glucose compared to 0.5 mol ATP·mol⁻¹ amino acids (Barker 1981, Zhou et al. 2018). Nonetheless, the protein degradation rates in the presence

and absence of carbohydrates are not yet investigated, as well as the step that is affected by the presence of carbohydrates and limiting the protein conversion.

To optimise the degradation of proteins, it is important to understand the effects of the presence of carbohydrates and their intermediates, i.e., volatile fatty acids (VFAs), on protein degradation, and to identify the rate-limiting step for methane (CH₄) production from protein-rich streams. The anaerobic conversion of proteins to CH₄ mainly consists of three steps: hydrolysis, acidification, and methanogenesis. The release of the amino group (-NH₂) from the amino acids is known as the deamination, which is part of the acidification process (Ladd and Jackson 1982). It is generally agreed that hydrolysis is the rate-limiting step during AD of complex feedstock (Kobayashi et al. 2015), whereas Duong et al. (2019) found that acidification is the rate-limiting step during anaerobic digestion of dissolved proteins. Additionally, most methanogens are known to be sensitive to process perturbations and have a slow growth rate (Meegoda et al. 2018). Thus, next to hydrolysis and acidification, methanogenesis is also considered the potential limiting step. However, instead of the CH₄ production rate, previous research mainly focused on the CH₄ potential or yield (Braguglia et al. 2018, Mata-Alvarez et al. 2014).

To identify the rate-limiting step during anaerobic protein degradation, it is essential to compare the rates of the three reaction steps. Previous studies considered either acidification or CH₄ production, the comparison of the three reaction steps was overlooked. Moreover, gelatine (GEL) was the most used model protein, but it is only a mixture of peptides, and it is not representative for the complex structures of most proteins in waste streams. Protein in real wastewaters varies in type and concentration, e.g., casein (CAS) is the most abundant protein in dairy wastewater (80% of total protein), and it consists of four types of CAS (Atamer et al. 2017); whereas albumin accounts for 55% of total protein in blood (Smith et al. 2013), and is supposed to be the most abundant in wastewater from animal slaughterhouses. The different types and concentrations of proteins also impact the anaerobic digestion performance. For example, although both fish ensilage and manure are regarded protein-rich streams, Vivekanand et al. (2018) reported 4.7 times higher methane yield from fish ensilage compared to manure. According to Elbeshbishy and Nakhla (2012), the methane yield at a protein concentration of 1.0 g COD·L⁻¹ is 1.5 times higher than that at a protein concentration of 5.0 g COD·L⁻¹. However, the underlying mechanism is to be revealed.

This chapter aimed to investigate the effect of different types of protein, different concentrations of protein, and presence of carbohydrates and VFAs on anaerobic protein degradation. To compare the protein degradation rates of different protein-rich wastewaters, bovine serum albumin (BSA) and CAS, with different structural complexities and representing the main protein in slaughterhouse and dairy wastewater, were used in the experiments. Additionally, the modified Gompertz kinetic model was used to describe and compare the hydrolysis rates, deamination rates, i.e., ammonium release rate during fermentation minus ammonium consumption rate for bacterial growth, and methanogenesis rates, when protein was degraded in the presence and absence of carbohydrates and VFAs.

2 Materials and Methods

2.1 Inoculum and (co-)substrates

The inoculum used in this chapter was collected from an anaerobic digester of a full-scale treatment plant in the Netherlands. The inoculum had an average total solids (TS) and volatile solids (VS) content of $155 \pm 10 \text{ g} \cdot \text{kg}^{-1}$ wet weight and $122 \pm 1 \text{ g} \cdot \text{kg}^{-1}$ wet weight, respectively. The inoculum was stored at room temperature and was washed three times with tap water before use.

Two model proteins were used: bovine serum albumin (BSA, A7030, Sigma Aldrich, Germany) and CAS (9000-71-9, Fisher Scientific, Germany). Likewise, two model carbohydrates were used: D-(+)-Glucose (GLU, G8270, Sigma Aldrich) and α -Lactose monohydrate (LAC, L3625, Sigma Aldrich, Germany). Acetate (C2, Sigma Aldrich, Germany) and propionate (C3, Sigma Aldrich, Germany) served as model VFAs. Gelatine (GEL, G2500, Sigma Aldrich, Germany) was used as a positive control for proteins, due to its wide application as a representative protein in wastewaters and has a high biodegradability (Breure and van Anandel 1984, Duong et al. 2019). BSA and GLU were used to represent the main protein and carbohydrate in slaughterhouse wastewater, especially from the slaughter line (Ruiz et al. 1997). CAS and LAC were used to represent the main protein and carbohydrate in dairy wastewater. The VFA compositions (C2 : C3 was 1:3, based on chemical oxygen demand (COD)) were determined based on the composition found in pre-acidified dairy wastewater in Biothane – Veolia Water Technologies Techno Center Netherlands B.V Research Facilities (Delft, The Netherlands).

The characteristics of the four protein feeds and six co-substrate feeds are listed in **Table 1**, the target COD of the feeds was $6.0 \text{ g}\cdot\text{L}^{-1}$, or, in the case of the low concentration protein feeds BSA₁ and CAS₁, $3 \text{ g}\cdot\text{L}^{-1}$ (**Table 1**). The concentration of protein and carbohydrate used in this chapter were based on the measurement of real slaughterhouse and dairy wastewaters. the reference wastewaters, with a total COD of $5,000 - 6,000 \text{ mg}\cdot\text{L}^{-1}$ and a protein content of 50% COD, were described in details in the study of Deng et al. (2023b) and Tan et al. (2021). The protein concentration in the BSA₂ and CAS₂ was twice that in the BSA₁ (and BSA₁ co-substrates feeds) and CAS₁ (and CAS₁ co-substrates feeds). The total nitrogen (TN) of the added protein is also listed in **Table 1**. NH₄Cl was added to adjust the COD : N ratio of the co-substrate feeds to 10-11, which was the same as pure protein feeds. Due to the heterogeneity of the casein solution and potential systematic COD measurement error, there was a variation of 3 – 15% difference among the total COD of the CAS and co-substrate feeds.

The macronutrients added were $20 \text{ mg}\cdot\text{L}^{-1}$ of KH₂PO₄ (7778-77-0, Sigma Aldrich, the Netherlands), $15 \text{ mg}\cdot\text{L}^{-1}$ of MgSO₄·7H₂O (10034-99-8, Sigma Aldrich, the Netherlands), and $10 \text{ mg}\cdot\text{L}^{-1}$ of CaCl₂ (10043-52-4, Sigma Aldrich, the Netherlands). The pH of the feeds was adjusted to 7.5 with $0.1 \text{ mol}\cdot\text{L}^{-1}$ NaOH or HCl solutions, and finally $3.5 \text{ g}\cdot\text{L}^{-1}$ of NaHCO₃ (144-55-8, Sigma Aldrich, the Netherlands) was added as a buffer.

2.2 Anaerobic batch test

Batch tests were carried out in duplicates with 600 mL glass bottles, the working volume was 500 mL, and the headspace was 100 mL. In each bottle, 44 g of inoculum and one feed were added, resulting in an initial biomass concentration of $12 \text{ gVS}\cdot\text{L}^{-1}$ and a feed COD concentration of $6 \text{ g}\cdot\text{L}^{-1}$ ($3 \text{ g}\cdot\text{L}^{-1}$ for BSA₁ and CAS₁). Hereafter the bottles were closed with a screw cap and butyl rubber septum and flushed with nitrogen gas for 1 min before incubation at 37 °C and under continuous stirring at 100 rpm.

2.3 Sampling and analysis

Liquid sampling was carried out at 1 h, 15 h, 25 h, 45 h, 70 h, and 140 h with a syringe. Samples were analysed for pH, COD, TN, NH₄⁺-N, VFA composition, and protein. After pH measurement, samples were first centrifuged at $13,500 \times g$ for 5 min and filtered through

0.45 µm membrane filters (Whatman, Sigma Aldrich, the Netherlands). COD, TN, and NH₄⁺-N were measured with HACH-Lange kits (Sigma Aldrich, the Netherlands) LCK014, LCK338, and LCK302, respectively.

Table 1 - Composition and characteristics of the blank, control, five BSA feeds and five CAS feeds.

Feeds	COD (%)			COD	°TN
	Protein	Carbohydrate	VFAs	(g·L ⁻¹)	(mg·L ⁻¹)
^a Blank	0	0	0	0	0
^b GEL	100	0	0	6.0 ± 0%	936 ± 4%
1 BSA ₂	100	0	0	6.2 ± 0%	804 ± 9%
2 BSA ₁	100	0	0	3.2 ± 1%	322 ± 2%
3 BSA ₁ +GLU	50	50	0	6.0 ± 0%	395 ± 0%
4 BSA ₁ +GLU+VFA	50	25	25	6.2 ± 1%	312 ± 1%
5 BSA ₁ +VFA	50	0	50	6.2 ± 0%	318 ± 3%
6 CAS ₂	100	0	0	7.8 ± 0%	809 ± 9%
7 CAS ₁	100	0	0	3.2 ± 1%	292 ± 3%
8 CAS ₁ +LAC	50	50	0	6.8 ± 0%	465 ± 0%
9 CAS ₁ +LAC+VFA	50	25	25	5.6 ± 1%	334 ± 6%
10 CAS ₁ +VFA	50	0	50	5.2 ± 0%	355 ± 5%

^aonly inoculum and NaHCO₃ buffer were added to the blank.

^bGEL was used as a positive control, blank and control were used to validate the CH₄ production registration. Blanks should be below 20% of total methane production in the positive control, and methane production in positive control shall be between 85% and 100% of the theoretical biomethane potential (BMP) (Holliger et al. 2016).

°TN is the total nitrogen of added protein.

Feed 1, 2, 6, and 7 were the pure protein substrate, feed 1 and 6 had a protein concentration twice as that of feed 2 and 7, as indicated by the subscription.

Feed 3-5, with the same BSA protein concentration as in feed 2, were BSA₁ co-substrates.

Feed 8-10, with the same CAS protein concentration as in feed 7, were CAS₁ co-substrates.

Protein concentrations were assessed following the manufacturer protocol of the bicinchoninic acid kit (BCA protein assay, BCA1-1KT, Sigma Aldrich, the Netherlands), measured by a spectrometer at 562 nm, with either BSA or CAS as standard.

The VFAs composition, including C2, C3, C4 (butyrate), iC4 (iso-butyrate), C5 (valerate), iC5 (iso-valerate), iC6 (iso-caproate), was analysed by a gas chromatograph (GC, 7820A, Agilent Technologies, Amstelveen, the Netherlands) equipped with a CP 7614 column (WCOT Fused Silica 25 m × 0.55 mm, CP-wax 58 FFAP capillary, Agilent Technologies) and flame ionization detector. The injector temperature was 250°C, and nitrogen gas (28.5 mL·min⁻¹) with a split ratio of 10 was used as a carrier. The GC oven method sequence was started at 100 °C, held for 2 min; and then increased to 140 °C and held for 6 min. An internal standard was prepared with 100 mg·L⁻¹ iC5 in 5% formic acid. Cumulative CH₄ production was recorded every hour with AMPTS-II (BPC instruments, Sweden), and converted to mg COD using 0.35 L CH₄ = 1 g COD.

The hydrolysis, deamination, and methanogenesis rates were described by the modified Gompertz model, which has been widely used for describing the biogas production process (Liu et al. 2023). The used equations and parameters are presented in **Table 2**. The nonlinear least-squares method was used for model fitting in MATLAB (R2016b), and the coefficient of determination (R²) and root-mean-square error (RMSE) were used to evaluate the goodness of the fit (details of results can be found in **Figure S1**).

Table 2 - Modified Gompertz models used to describe the hydrolysis, deamination and methanogenesis rates.

Step	Equation	Parameters
Hydrolysis	$P_{(t)} = P_m \times \exp \left(-\exp \left[\frac{R_P e(\lambda - t)}{P_m} + 1 \right] \right)$	P_m, R_P, λ
Deamination	$N_{(t)} = N_m \times \exp \left(-\exp \left[\frac{R_N e(\lambda - t)}{N_m} + 1 \right] \right)$	N_m, R_N, λ
Methanogenesis	$C_{(t)} = C_m \times \exp \left(-\exp \left[\frac{R_C e(\lambda - t)}{C_m} + 1 \right] \right)$	C_m, R_C, λ

P_m , N_m and C_m represent the maximum hydrolysed protein (mg), ammonium production (mg N) and methane production (mg COD), respectively.

R_P , R_N and R_C represent the maximum reaction rates (mg·h⁻¹) of hydrolysis, deamination and methanogenesis following the Modified Gompertz model, respectively.

λ is the delay of the reaction (h).

3 Results and discussion

3.1 Effect of protein structural complexity and protein concentration

To compare protein degradation in the different protein-rich wastewaters, the tertiary-structured BSA and simple secondary-structured CAS, were used in the batch tests. In addition, the effect of protein concentrations on the conversion rates was studied. The added protein concentrations in the BSA₂ and CAS₂ were twice that in the BSA₁ and CAS₁, while the COD in the BSA₂ and CAS₂ was 6.0 g·L⁻¹, and the COD in the BSA₁ and CAS₁ was 3.0 g·L⁻¹.

3.1.1 Hydrolysis

Figure 1A shows the degraded protein (mg) in BSA₁ and BSA₂ at each sampling time. The degraded protein was calculated as initial protein minus the measured protein; results of the duplicates are presented together with simulated results. **Figure 1A** also presents the reaction rate obtained from the modified Gompertz model fitting. Results clearly show that the protein hydrolysis rate in BSA₂ ($75 \pm 28 \text{ mg}\cdot\text{h}^{-1}$) was higher than in BSA₁ ($26 \pm 9 \text{ mg}\cdot\text{h}^{-1}$). **Figure 1B** shows the degraded protein (mg) in CAS₁ and CAS₂, as well as the obtained reaction rates. Like in the BSA incubations, CAS₂ also had a somewhat higher hydrolysis rate than CAS₁, which were $155 \pm 173 \text{ mg}\cdot\text{h}^{-1}$ and $98 \pm 79 \text{ mg}\cdot\text{h}^{-1}$, respectively, but observed differences were much less than with BSA.

The higher initial protein concentrations in BSA₂ and, to a lesser extent, CAS₂ led to a higher hydrolysis rate. According to Guo et al. (2021), protease activity is induced by protein concentration and consequently higher protein concentration leads to higher protease activity, and therefore higher hydrolysis rate. Additionally, the hydrolysis rates of BSA substrates were 2.0–3.8 times lower than that of CAS substrates, indicating a negative impact of protein structural complexity on the protein hydrolysis rate. Notably, the difference of protein concentration between the duplicates was 200-500 mg·L⁻¹ and 400-600 mg·L⁻¹ in BSA₂ and CAS₂, as a result, the hydrolysis rate given by the modified Gompertz model had a wide 95% confidence bound. To have an accurate protein hydrolysis rate, a better protein measurement is needed, especially at high protein concentrations (e.g., 6000 g·L⁻¹) and when proteins have a lower solubility (e.g., casein).

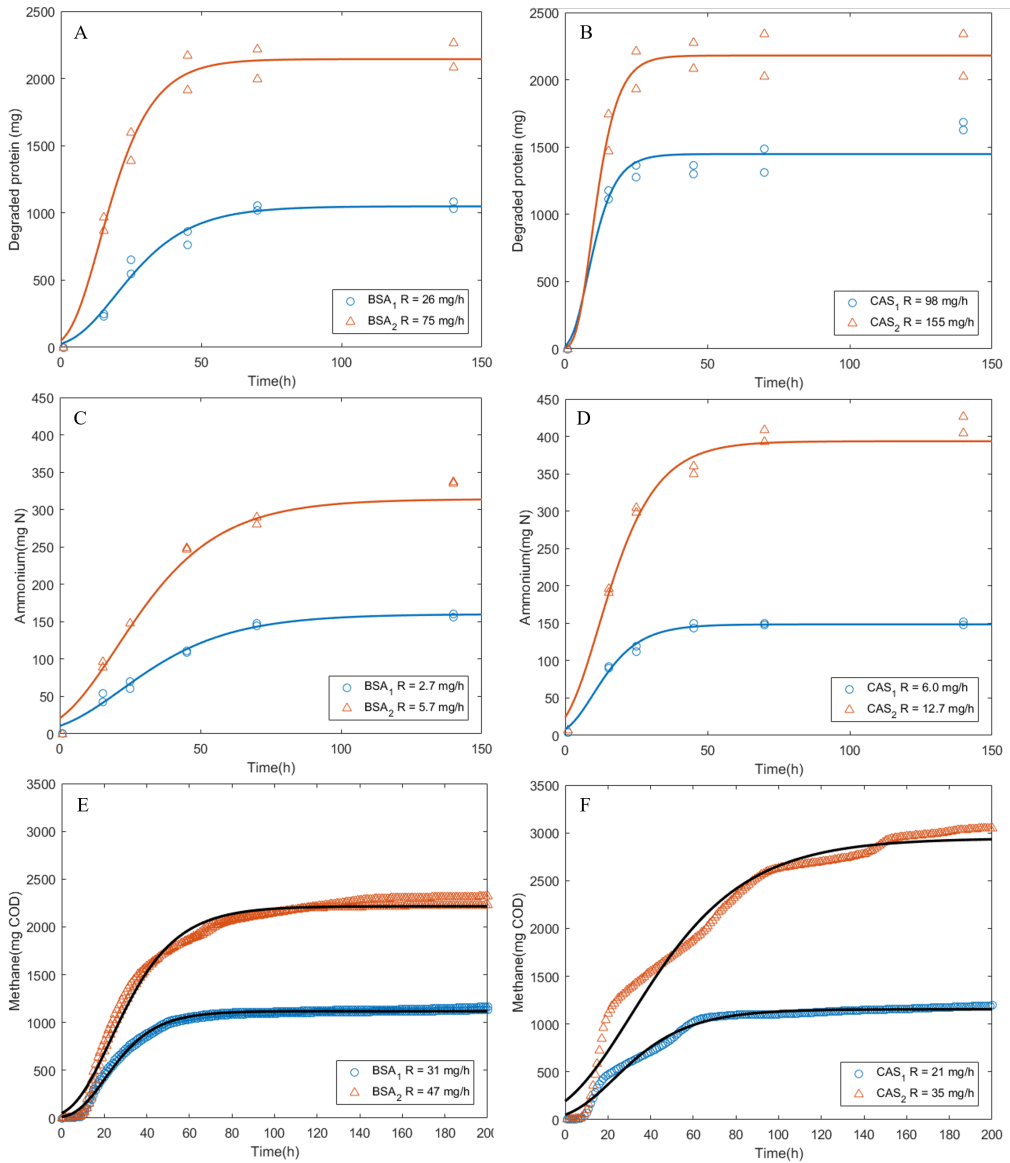


Figure 1 - Profile and reaction rates of A) BSA hydrolysis and B) CAS hydrolysis, C) BSA deamination and D) CAS deamination, E) BSA methanogenesis and F) CAS methanogenesis in pure protein feeds. Measurements of duplicates were presented as scattered plot, and modelled values were presented as solid lines, along with the overall reaction rates ($\text{mg} \cdot \text{d}^{-1}$) of hydrolysis, deamination and methanogenesis obtained from the modified Gompertz models. BSA₁ and CAS₁ indicated a substrate protein COD concentration of $3 \text{ g} \cdot \text{L}^{-1}$, and BSA₂ and CAS₂ indicated a substrate protein COD concentration of $6 \text{ g} \cdot \text{L}^{-1}$.

3.1.2 Deamination

Figure 1C presents the produced ammonium (mg N) in BSA₁ and BSA₂ at each sampling time. The ammonium consumption was ignored, because it is low in anaerobic digestion of protein rich wastes, i.e., about 5% of the COD is used for bacterial growth, and the C:N ratio of the biomass is 5:1 (van Lier et al. 2020). As shown in the figure, the reaction rates obtained from the modified Gompertz model clearly showed that BSA₂ had a deamination rate 2.1 times higher than that of BSA₁, which were $5.7 \pm 2 \text{ mg N}\cdot\text{h}^{-1}$ and $2.7 \pm 0.6 \text{ mg N}\cdot\text{h}^{-1}$, respectively. In addition, a lower percentage (84%, calculated as produced ammonium in mg N divided by TN in mg N in the initial protein) of the initial protein in BSA₂ was converted to ammonium at the end of the experiment (140 h), compared to that of BSA₁ (91%).

Figure 1D shows the produced ammonium (mg N) in CAS₁ and CAS₂ at each sampling time. The reaction rates obtained from the modified Gompertz model were $12.7 \pm 5 \text{ mgN}\cdot\text{h}^{-1}$ in CAS₂ and $6.0 \pm 1 \text{ mgN}\cdot\text{h}^{-1}$ in CAS₁, respectively. In CAS₂, 97% of the nitrogen in the added protein was released as ammonium, and 100% of nitrogen in the added protein in CAS₁ was released as ammonium.

Like hydrolysis, CAS showed about 2.2 times higher deamination rate than BSA at the same initial protein concentrations. The protein hydrolysis and deamination of CAS stabilised at approximately 50 – 70 hours, whereas it took 70 – 100 hours for the deamination of BSA. According to Bhat et al. (2016) and Bevilacqua et al. (2020), the conversion of proteins can be affected by the protein structure or the amino acids compositions. However, the effect of protein structural complexity and amino acids composition on the protein conversion rate was not investigated before. The β -CAS used in this chapter had a plain secondary structure (Dickinson 2003), making it structurally simpler compared to the tertiary-structured BSA (Varga et al. 2016). Consequently, the protease was able to more efficiently break down the peptide linkages in CAS, requiring less energy and time compared to the unfolding of the BSA peptide chain to release the amino acids and amino groups. With a sequence length of 607 amino acids for BSA and 225 amino acids for CAS, the interactions between BSA amino acids side chains are more intricate, contributing to the reported inert nature of BSA (Bourassa et al. 2010). In conclusion, the lower degradation rate of BSA was attributed to the higher structural complexity. Based on the amino acids composition (in % of mass) in BSA and CAS (GMIA 2019, Nightingale et al. 2017), the major difference is the fraction of

cysteine. Cysteine accounts for 5.51% of amino acids in BSA, whereas it is 0.00% in CAS. Cysteine is known to form intramolecular and intermolecular di-sulphide bonds and is the key contributor to protein strength and rigidity (Miniaci et al. 2016), e.g., the structural protein, keratin, contains 7 – 20% cysteine (Numata 2021). In conclusion, the higher fraction of cysteine in BSA, which very likely contributed to a higher protein structural complexity, may have resulted in the observed lower degradation rate.

3.1.3 Methanogenesis

The methane production in the positive control (GEL) was 96% of the added COD, and the CH₄ production in the blank was 12% of that in the positive control.

Figure 1E shows the cumulative CH₄ production (mg COD) in BSA₁ and BSA₂. Based on the modified Gompertz model, BSA₂ had a higher overall methanogenesis rate (during 0 – 200 h incubation time) of 47 ± 1 mg COD·h⁻¹ than that of BSA₁, which was 31 ± 1 mg COD·h⁻¹. However, it should be noted that the modified Gompertz model was not able to fully capture all the experimental data. BSA conversion did not follow the expected first-order reaction kinetics, especially at the high BSA concentration. To evaluate the conversion of protein to CH₄, the conversion efficiency was calculated by dividing the cumulative CH₄ production (mg COD) at 140 h by the initial COD (mg). BSA₂ and BSA₁ had a similar conversion efficiency of 70 – 71%. The conversion efficiency of protein to CH₄ was not affected by the initial protein concentration in the absence of carbohydrates.

Figure 1F shows the cumulative CH₄ production (mg COD) in CAS₁ and CAS₂. As obtained from the modified Gompertz model, the overall methanogenesis rate in CAS₂ was 35 ± 2 mg COD·h⁻¹ and that of CAS₁ was 21 ± 1 mg COD·h⁻¹. However, compared to BSA, the deviation from the first-order reaction kinetics was much larger in the case of CAS as the substrate. In addition, the COD to CH₄ conversion efficiency of CAS₂ (75%) was slightly higher than that of CAS₁ (72%). Based on the overall methanogenesis rate of CAS, the initial protein concentration had a slightly positive effect on the CAS conversion to CH₄ rate and efficiency.

Regardless of the type and concentration of proteins, the four protein feeds all showed a lag phase of approximately 10 h, as shown in **Figure 1E** and **1F**. The CH₄ production profiles of CAS₂ and CAS₁ showed two different stages with distinct rates: an initial rapid production

stage followed by a much slower production stage. CAS₁ and CAS₂ showed a substantially lower CH₄ production rate during 20 – 100 h, simultaneously, VFAs accumulation was observed. As shown in **Figure 2A** and **2B**, the total VFA concentrations in BSA₁ remained at a level of 100 mg COD·L⁻¹ during 0 – 70 h, whereas the total VFA in CAS₁ quickly increased to 440 mg COD·L⁻¹ at 15 h, and remained between 350 and 500 mg COD·L⁻¹ until 45 h. Although the measured VFA concentration was likely not inhibiting at a pH above 7 (Siegert and Banks 2005), the VFA accumulation and concomitantly lower methanogenesis rate suggested a negative effect of CAS, being a protein with a simpler structure, on the methanogenesis rate (**Figure 1F** and **2B**).

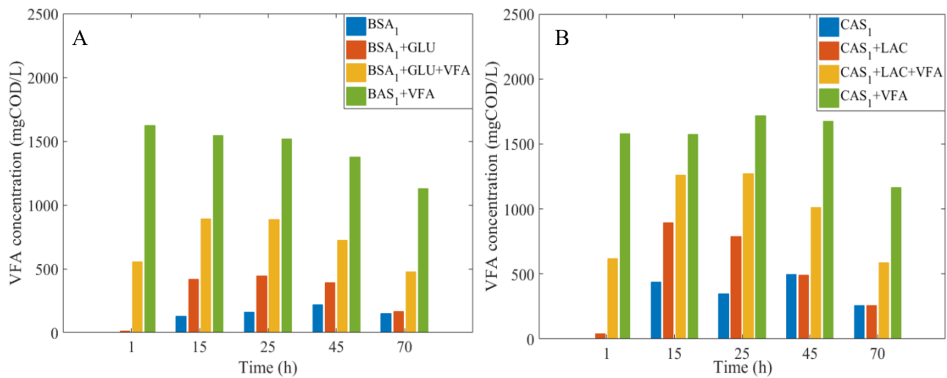


Figure 2 - Total VFA concentrations (in mg COD·L⁻¹) in A) BSA incubations, and B) CAS incubation, at different time instants during the batch tests. Incubations consisted of pure proteins, as well as proteins with co-substrates (GLU = glucose, LAC = lactose, VFA = volatile fatty acids).

This seemingly staged conversion could indicate the presence of two different CAS protein fractions: one fraction was easily degradable and showed a fast CH₄ production (0 - 20 h), whereas the other fraction showed slower CH₄ production (20 - 100h). After 100 hours of incubation, a third even slower conversion could be identified, possibly indicating a third protein fraction. Results suggest that methanogenesis could have been the rate-limiting step during 0 - 20 h, but step(s) prior to methanogenesis were certainly limiting the methane production during 20 - 100 h.

In this chapter, the cumulative methane production profile was divided into two different stages, which were modelled separately for obtaining a better estimation of the maximum

methane production rate (**Figure S1**). The incubation period of 0 – 40 h in BSA batch tests and 0 – 20 h in CAS batch tests were designated as the rapid reaction stage, during which the high reaction rate was modelled; concurrently, the 40 – 200 h and 20 – 200 h for CAS were designated as the slow reaction stage, characterised by a low reaction rate. By modelling the two methane production stages separately, the lag phase given by the model was close to 10 h and the R^2 was significantly improved (**Table S1**). The results of the high and low methane production rates are shown in **Table 3**. Notably, the overall methanogenesis rate of BSA was about 25% - 30% higher than that of CAS at the same initial protein concentrations, but the maximum methanogenesis rate of BSA was 40% - 46% lower than that of CAS at the same initial protein concentration. Therefore, it was concluded that a high protein structural complexity had a negative effect on the maximum methanogenesis rate, and a higher protein concentration had a positive effect on the methanogenesis.

Table 3 - Methanogenesis rate (in $\text{mg}\cdot\text{h}^{-1}$) during the fast and slow methane production stages with 95% confidence bounds.

	BSA ₂	BSA ₁	BSA ₁ +GLU	BSA ₁ +GLU+VFA	BSA ₁ +VFA
Overall reaction rate ($\text{mg}\cdot\text{h}^{-1}$)	47±1	31±1	78±2	49±2	22±1
High reaction rate ($\text{mg}\cdot\text{h}^{-1}$)	66±3	34±1	99±8	85±6	48±2
Low reaction rate ($\text{mg}\cdot\text{h}^{-1}$)	26±2	24±4	36±3	41±2	21±1
	CAS ₂	CAS ₁	CAS ₁ +LAC	CAS ₁ +LAC+VFA	CAS ₁ +VFA
Overall reaction rate ($\text{mg}\cdot\text{h}^{-1}$)	35±2	21±1	72±4	37±2	20±1
High reaction rate ($\text{mg}\cdot\text{h}^{-1}$)	122±3	57±2	181±12	95±4	45±4
Low reaction rate ($\text{mg}\cdot\text{h}^{-1}$)	23±1	19±1	33±1	23±1	18±1

The overall reaction rate is the average methanogenesis rate during 0 – 200h. The high reaction rate is the methanogenesis rate during 0 – 40 h in BSA batch tests and 0 – 20 h in CAS batch tests; concurrently, the low reaction rate is the methanogenesis rate during 40 – 200 h and or 20 – 200 h, for BSA and CAS, respectively.

In summary, compared to the reaction rates of hydrolysis and methanogenesis, the deamination rates were found to be the lowest with both BSA and CAS as the substrates. Additionally, as shown in **Figure 2** (blue bars), the increase of VFAs was below $100 \text{ mg}\cdot\text{L}^{-1}$ after 15 h, indicating minor accumulation of VFAs during this period. Therefore, deamination was potentially the rate-limiting step during the degradation of BSA and CAS, especially

after 20 h of batch incubation. The applied protein measurement considered all non-monomers, i.e., protein and peptides, and gave a good indication of the hydrolysis of protein to amino acids. Measuring the protein concentration in time series can be a proper method to describe the protein hydrolysis rate. However, it is recommended to include amino acids measurement in future studies to examine the accumulation of amino acids.

Besides, our results clearly showed that the applied modified Gompertz model, which is based on first-order conversion kinetics, was not able to describe the two-three different stages of CAS degradation, the computed results were an average of the entire conversion. It is suggested to model the different degradation stages separately or develop a model that can describe protein conversion with different degradation stages, to better estimate the maximum methane production rates.

3.2 Effect of glucose, lactose, and volatile fatty acids

To investigate the effect of the presence of carbohydrates and their intermediates (i.e., VFAs) on anaerobic protein degradation, GLU or LAC and VFAs were added to be co-digested with the model proteins, BSA and CAS. The protein hydrolysis, deamination and methanogenesis rates were compared between pure protein feeds and co-substrates feeds.

3.2.1 Hydrolysis

Figure 3A shows the degraded BSA protein (mg) in all BSA₁ incubations; measurements of the duplicates are shown in scattered plots, with the modelled results as solid lines. Based on the obtained reaction rates from the modified Gompertz model, BSA₁+GLU had the highest hydrolysis rate ($45 \pm 35 \text{ mg}\cdot\text{h}^{-1}$), followed by BSA₁+GLU+VFA ($32 \pm 15 \text{ mg}\cdot\text{h}^{-1}$), whereas BSA₁+VFA had a similar hydrolysis rate ($24 \pm 7 \text{ mg}\cdot\text{h}^{-1}$) as BSA₁ ($26 \pm 9 \text{ mg}\cdot\text{h}^{-1}$).

Figure 3B shows the degraded CAS protein (mg) in all CAS₁ incubations; duplicate measurements are shown as scattered plots, with solid lines representing the modelled results. The reaction rates obtained from the modified Gompertz model are also shown in the figure. Like the batch test with BSA, CAS₁+LAC had the highest hydrolysis rate ($157 \pm 185 \text{ mg}\cdot\text{h}^{-1}$), and the CAS₁+VFA had a similar hydrolysis rate ($99 \pm 80 \text{ mg}\cdot\text{h}^{-1}$) as CAS₁. However, CAS₁+LAC+VFA had the lowest hydrolysis rate of $94 \pm 165 \text{ mg}\cdot\text{h}^{-1}$.

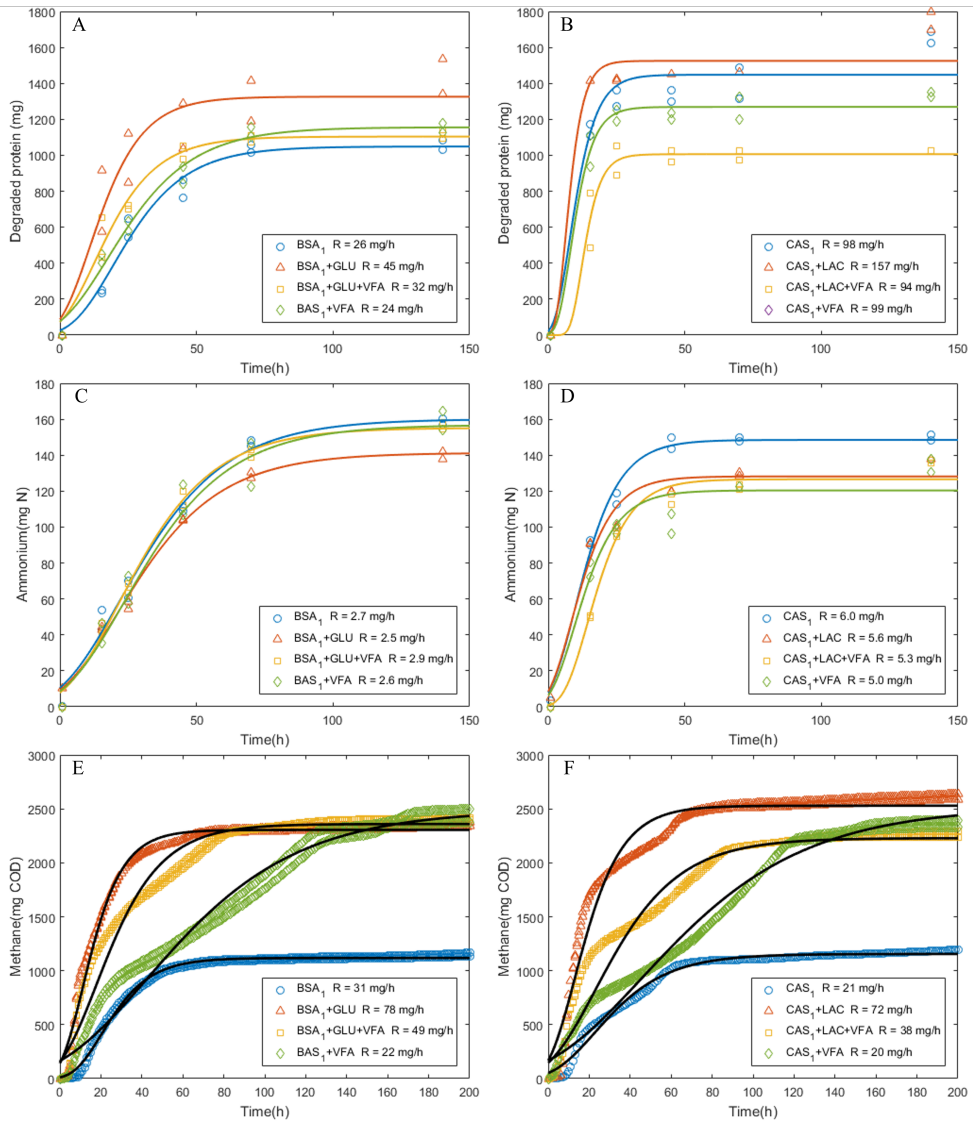


Figure 3 - Profile and reaction rates of protein hydrolysis. Figure 3A and 3B, deamination, Figure 3C and 3D, and methanogenesis, Figure 3E and 3F, in BSA and CAS incubations including co-substrates, respectively, compared with BSA₁ and CAS₁ as the sole substrate. Measurements of duplicates were presented as scattered plot, and modelled values were presented as solid lines, along with the overall reaction rates (mg·d⁻¹) of hydrolysis, deamination and methanogenesis obtained from the modified Gompertz models. (GLU = glucose, LAC = lactose, VFA = volatile fatty acids).

Contrary to previous studies reporting an inhibition behaviour of carbohydrates on protein hydrolysis (Yang et al. 2015b, Yu and Fang 2001), the presence of GLU and LAC improved the BSA and CAS hydrolysis rates by a factor of 1.6 - 1.7 in this chapter, indicating a positive effect on protein hydrolysis. The present results are in agreement with the study of Elbeshbishy and Nakhla (2012), in which 1.5 fold higher hydrolysis rate was observed when starch was added in anaerobic degradation of BSA. In addition, the carbohydrate to protein ratio is 1 in terms of COD in this chapter. Wang et al. (2022) reported that such a carbohydrate to protein ratio optimise protease activity. In contrast, the carbohydrate to protein ratios in previous studies were either below or above 1, resulting in reduced protease activity and consequently lower hydrolysis rates (Yang et al. 2015b, Yu and Fang 2001).

The presence of VFAs had an ignorable effect on protein hydrolysis, whereas the co-presence of carbohydrates and VFAs had a negative effect on protein hydrolysis. Duong et al. (2022) reported an inhibitive effect of VFAs on gelatine hydrolysis at a VFA:GEL COD ratio of 2.2. Likely, the synergetic effect of a lower protease activity and VFA inhibition at a CAS:LAC:VFA COD ration of 1:0.5:0.5 lead to the lower hydrolysis rate in CAS₁+LAC+VFA. Whereas in BSA₁+GLU+VFA, the BSA hydrolysis rate and acidification rate were lower than that of CAS (**Figure 2**), and therefore the protein hydrolysis was not inhibited by VFAs at a lower concentration.

Figure 3C presents the ammonium production (mg N) in all BSA₁ incubations at each sampling time. The obtained reaction rates applying modified Gompertz model fittings are shown in the same figure. The deamination rates of BSA₁+GLU, BSA₁+GLU+VFA and BSA₁+VFA were $2.5 \pm 0.2 \text{ mg N} \cdot \text{h}^{-1}$, $2.9 \pm 0.5 \text{ mg N} \cdot \text{h}^{-1}$ and $2.7 \pm 0.9 \text{ mg N} \cdot \text{h}^{-1}$, respectively. The lowest value found for BSA₁+GLU (7% lower than solely BSA₁) indicated that the presence of glucose had a slightly negative effect on the BSA deamination. Both the deamination rates of BSA₁+GLU and BSA₁+VFA were lower than solely BSA₁, whereas the deamination rates of BSA₁+GLU+VFA was 7% higher. The observed phenomenon may be attributed to the initial concentrations of GLU and VFA. Specifically, in the BSA₁+GLU+VFA batch test, the COD contents of GLU and VFA were half that of BSA₁+GLU and BSA₁+VFA batch tests. According to Duong et al. (2022), the activity of methanogens helps mitigate the negative impact of starch on protein deamination. The moderate concentrations of GLU and VFA in BSA₁+GLU+VFA could have activated the

acid-forming bacteria and methanogens, and resulting in a positive effect on the deamination reaction.

3.2.2 Deamination

In **Figure 3D**, the ammonium production (mg N) in all CAS₁ incubations at each sampling time is shown, as well as the reaction rates of the modified Gompertz model. The deamination rates of CAS₁+LAC, CAS₁+LAC+VFA, and CAS₁+VFA were 5.6 ± 2 mg N·h⁻¹, 5.3 ± 2 mg N·h⁻¹, and 5.0 ± 3 mg N·h⁻¹, respectively. The presence of LAC alone led to a 7% lower deamination rate compared to CAS₁, the presence of both LAC and VFAs caused a 12% lower deamination rate compared to that of CAS₁, and the presence of VFAs alone led to a 17% lower deamination rate. The presence of LAC had a minor impact on the CAS deamination, whereas VFAs had a negative effect on the CAS deamination rates.

Both the presence of glucose and lactose showed a negative effect on BSA and CAS deamination. As also observed by Duong et al. (2022), deamination rate reduced to 40% at a starch:GEL COD ratio of 1. In all our incubations, the pH was maintained above 7 (**Figure S2**), and the C2-iC6 VFA composition did not vary notably during the experiment (data not shown), only a delay in VFA production was observed in BSA₁+VFA and CAS₁+VFA (**Figure 2A** and **2B**), which indicated that VFA production (i.e., deamination) was negatively affected by the presence of high initial VFA concentration. Possibly, the excessively available VFAs inhibited the protein hydrolysis and affected the bioactivity of the acid-forming bacteria, and therefore limited the acidification of CAS (Duong et al. 2022, Wang et al. 2022).

3.2.3 Methanogenesis

Figure 3E presents the cumulative CH₄ production (mg COD) in BSA₁ co-substrate feeds and BSA₁, as well as the obtained methanogenesis rates from the modified Gompertz model. Again, the model was not able to capture the data accurately. The highest deviation was found in incubations with the BSA₁+GLU+VFA, which had two-three methane production stages with different rates. Therefore, the overall methanogenesis rate estimated by the model was rejected, and instead, the maximum methanogenesis rate was used for comparison (data shown in **Table 3**).

The presence of GLU had a significant positive effect on methanogenesis, the maximum methanogenesis rate in BSA₁+GLU and BSA₁+GLU+VFA was 99 ± 8 mg COD·h⁻¹ and 85 ± 6 mg COD·h⁻¹, which was 2.5-2.9 times higher than that in the BSA₁ incubation (34 ± 1 mg COD·h⁻¹). The maximum methanogenesis rate in BSA₁+VFA was 48 ± 2 mg COD·h⁻¹, indicating that the presence of high initial VFAs concentration also had a slightly positive effect on the methanogenesis. Additionally, the lag phase in the BSA co-substrates incubations were shorter than that in the BSA₁ incubations, indicating that methanogenesis of protein started later than that of the GLU and VFAs.

Figure 3F shows the cumulative CH₄ production (mg COD) in CAS₁ with co-substrate incubations and CAS₁ as the sole substrate, along with the overall methanogenesis rates obtained from the modified Gompertz model. Like the results of the BSA batch tests, the modified Gompertz model also showed a high deviation from the measured data, and the overall methanogenesis rate was regarded as not representative of the methanogenesis step. Therefore, the fast methane production stage was fitted separately to obtain the maximum methanogenesis rate (see **Table 3**). CAS₁+LAC showed the highest methanogenesis rate of 181 ± 12 mg COD·h⁻¹, followed by CAS₁+LAC+VFA, with a rate of 95 ± 4 mg COD·h⁻¹. Although the maximum methanogenesis rate in CAS₁+VFA (45 ± 4 mg COD·h⁻¹) was lower than that in CAS₁ (57 ± 2 mg COD·h⁻¹), it showed the shortest lag phase of less than 5 h (**Figure 3F**). The pH was maintained between 7.0 - 8.0 in all incubations (**Supplementary Figure S₂**), being in the optimal range for methanogenesis (Jones et al. 1987). The reduced methanogenesis rate in CAS₁+VFA might have been caused by the high initial propionate concentration of 1500 mg·L⁻¹ (**Figure 2B**). Notably, propionate concentrations exceeding 900 mg·L⁻¹ at pH 7.0 may lead to inhibition of methanogens, resulting in VFAs accumulation (Wang et al. 2009). In general, the presence of LAC increased the methanogenesis rate by 3.2 times, and the high initial VFA concentrations had a negative effect on the methanogenesis rate but a positive effect on shortening the lag phase.

Like the tests with sole proteins (section 3.1.3, **Figure 1F**), fast and slow methane production stages were observed in the CH₄ production profiles of CAS co-substrates. Moreover, a staged pattern was more clearly observed with BSA₁ and co-substrates compared to BSA₁ as the sole substrate, particularly when VFA was added as a co-substrate (**Figure 3E**). Likely, methane was mainly produced from the available carbohydrates and VFA in the fast

production stage, whereas methane was produced from proteins during the slow production stage and at the end of the slow production stage (**Figure S₃**). As already mentioned in section 3.1.3, methanogenesis was seemingly the rate-limiting step during the fast methane production stage. However, another step was limiting the degradation rate during the slow production stage. Hence further study is needed to investigate the reaction rates of the intermediates degradation prior to methanogenesis.

Based on our present results, it can be concluded that degradation of intermediates, i.e., deamination, was the rate-limiting step in the presence and absence of carbohydrates and VFAs. It must be noted that commonly, hydrolysis is considered to be the rate-limiting step in AD (Pavlostathis and Giraldo-Gomez 1991), and therefore solid-state digesters are designed based on attainable hydrolysis rates. However, in the anaerobic treatment of wastewaters from dairy processing or slaughterhouses, deamination is apparently limiting the conversion of proteins to CH₄. Therefore, it can be postulated that reactor designs, e.g., dilution rate or hydraulic retention times, rather should be based on attainable deamination rate. Moreover, VFAs showed a negative effect on protein hydrolysis and deamination, therefore, high VFA concentrations should be avoided to achieve high reaction rates during protein degradation.

4 Conclusions

- Deamination of protein was identified as the rate-limiting step.
- Compared to CAS, BSA showed lower hydrolysis and deamination rates, suggesting that proteins with a higher structural complexity have a lower degradation rate. Reaction rates obtained from the modified Gompertz model also showed that carbohydrates had a positive effect on the protein hydrolysis rate and methanogenesis rate, but a negative effect on the deamination rate.
- A high initial VFA concentration had a negative effect on the protein hydrolysis and deamination rates. It is postulated that the design of anaerobic reactors, treating protein-rich wastewaters, should be based on the attainable deamination rate, and high VFA concentrations must be avoided.

Supporting information

Table S1 - Evaluation parameters of model fitting (part 1)

Hydrolysis	BSA ₂	BSA ₁	BSA ₁ + GLU	BSA ₁ + GLU+VFA	BSA ₁ + VFA
R _p (mg · h ⁻¹)	75.2	25.9	44.8	32.0	24.4
R ²	0.98	0.97	0.87	0.96	0.98
RMSE (mg)	119	68	174	78	62
Deamination	BSA ₂	BSA ₁	BSA ₁ + GLU	BSA ₁ + GLU+VFA	BSA ₁ + VFA
R _N (mg · h ⁻¹)	5.7	2.7	2.5	2.9	2.7
R ²	0.96	0.99	0.99	0.99	0.97
RMSE (mg)	25	7	4	5	10
Methanogenesis	BSA ₂	BSA ₁	BSA ₁ + GLU	BSA ₁ + GLU+VFA	BSA ₁ + VFA
R _C (mg · h ⁻¹)	47.2	30.8	77.7	48.8	21.8
R ²	0.98	0.99	0.98	0.96	0.97
RMSE (mg)	78	25	66	114	127
Hydrolysis	CAS ₂	CAS ₁	CAS ₁ + LAC	CAS ₁ + LAC + VFA	CAS ₁ + VFA
R _p (mg · h ⁻¹)	155.4	97.8	156.8	94.0	99.5
R ²	0.96	0.92	0.93	0.94	0.97
RMSE (mg)	156	139	135	88	72
Deamination	CAS ₂	CAS ₁	CAS ₁ + LAC	CAS ₁ + LAC + VFA	CAS ₁ + VFA
R _N (mg · h ⁻¹)	12.7	6.0	5.6	5.3	5.0
R ²	0.96	0.99	0.95	0.98	0.92
RMSE (mg)	28	6	10	7	12
Methanogenesis	CAS ₂	CAS ₁	CAS ₁ + LAC	CAS ₁ + LAC + VFA	CAS ₁ + VFA
R _C (mg · h ⁻¹)	35.4	21.3	71.7	37.5	20.4
R ²	0.97	0.99	0.96	0.95	0.98
RMSE (mg)	149	40	124	127	106

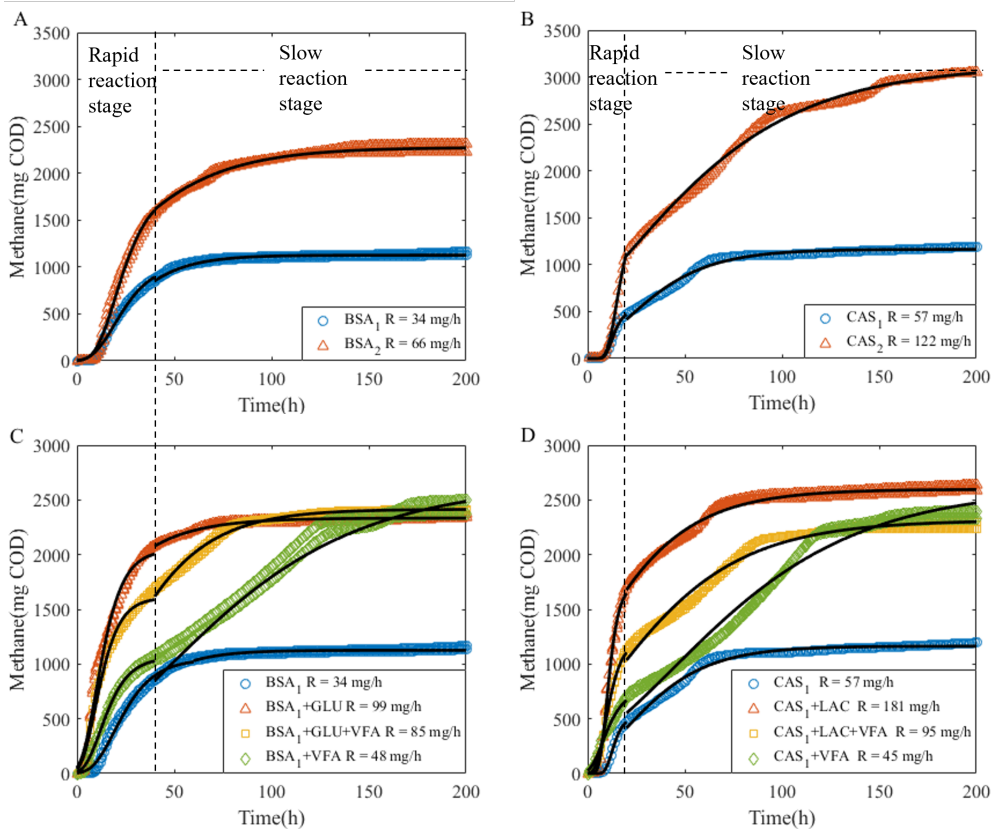


Figure S1 - Two-stage methane production rates simulated by the Modified Gompertz model. The incubation period of 0 – 40 h in BSA batch tests and 0 – 20 h in CAS batch tests were designated as the rapid reaction stage, during which the high reaction rate was modelled; concurrently, the 40 – 200 h for BSA and 20 – 200 h for CAS were designated as the slow reaction stage, characterised by a low reaction rate. The high reaction rates for each incubation are listed in the legend.

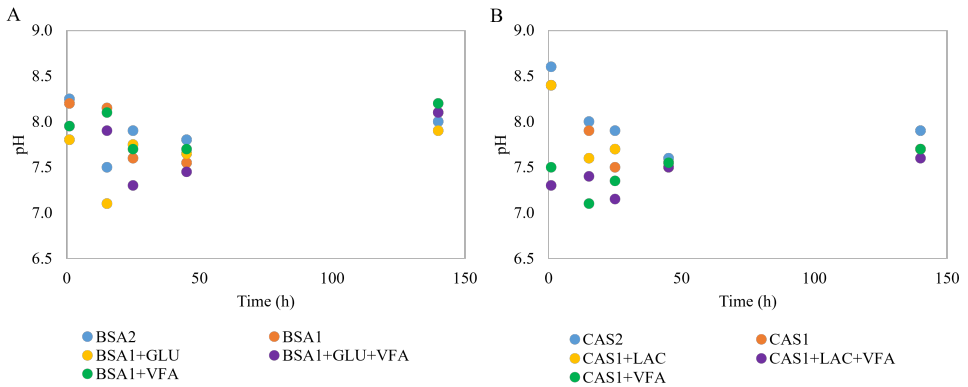


Figure S₂ - pH measurement in A) BSA and co-substrates incubations and B) CAS and co-substrates incubations. Relative deviation ≤ 0.01 .

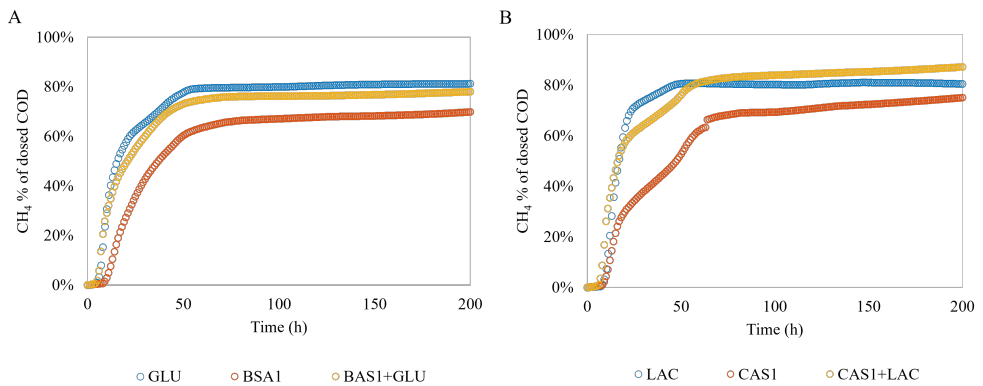


Figure S₃ - Methane production (% of dosed COD) in A) GLU, BSA, and BSA+GLU incubations, and B) LAC, CAS and CAS+LAC incubations. Results were averaged and has a relative deviation ≤ 0.01 , methane production from blank control was subtracted.

CHAPTER 4

CHARACTERISATION OF MICROBIAL COMMUNITIES IN ANAEROBIC ACIDIFICATION REACTORS FED WITH CASEIN AND/OR LACTOSE

This chapter is based on: Deng, Z., Ferreira, A.L.M., Spanjers, H., & van Lier, J.B. (2022). Characterization of microbial communities in anaerobic acidification reactors fed with casein and/or lactose. *Applied Microbiology and Biotechnology*, 106(18), 6301-6316.

Abstract

Protein-rich agro-industrial waste streams are high in organic load and represent a major environmental problem. Anaerobic digestion is an established technology to treat these streams, however, retardation of protein degradation is frequently observed when carbohydrates are present. This chapter investigated the mechanism of the retardation by manipulating the carbon source fed to an anaerobic mixed culture and linking the reactor performance to the variation of the microbial community. Two anaerobic acidification reactors were first acclimated either to casein (CAS reactor) or lactose (LAC reactor), and then fed with mixtures of casein and lactose. Results showed that when lactose was present, the microbial community acclimated to casein shifted from mainly *Chloroflexi* to *Proteobacteria* and *Firmicutes*, the degree of deamination in the CAS reactor decreased from 77% to 15%, and the VFA production decreased from 75% to 34% of the effluent COD. A decrease of 75 % in protease activity and 90% in deamination activity of the biomass was also observed. The microorganisms that can ferment both proteins and carbohydrates were predominant in the microbial community, and from a thermodynamical point of view, they consumed carbohydrates prior to proteins. The frequently observed negative effect of carbohydrates on protein degradation can be mainly attributed to the substrate preference of these populations.

1 Introduction

Proteins are complex molecules that can contain more than 50 amino acids. They can be roughly divided into insoluble fibroid proteins and soluble globular proteins. The fibroid proteins, e.g., in manure fibres, are more resistant to hydrolysis due to the lower solubility than globular proteins (Sanders 2001). Proteins are abundantly found in food processing industries, for example, dairy and meat, and therefore end up in waste and wastewaters of dairy, slaughterhouse, and fishery industries, as well as in food residues (Braguglia et al. 2018, Wang et al. 2005). Being an important component of cells, proteins are also found in biomass, such as algae and spent biomass of biological treatment processes (Ganesh Saratale et al. 2018, Magdalena et al. 2018, Mata-Alvarez et al. 2014).

These protein-rich streams are usually high in organic load and represent a major environmental problem, especially regarding the growth of the global population and increasing demand for food protein (Bustillo-Lecompte and Mehrvar 2015, Hassan and Nelson 2012). Direct discharge of protein-rich streams into surface water can lead to severe damage to the water quality, i.e., causing eutrophication and aquatic life extinction (Baker et al. 2021). The stricter discharge standards and the decreasing availability of freshwater contribute to the requirement for both wastewater treatment and resources recycling (Bustillo-Lecompte and Mehrvar 2015). Due to the high organic load, the protein-rich streams are preferably treated by anaerobic digestion (AD), which can purify the wastewater by converting the organic matters to a gaseous energy carrier, i.e., biogas (Adhikari et al. 2018).

Anaerobic protein degradation generally consists of four steps, which are hydrolysis of protein to amino acids, deamination and acidogenesis of amino acids to ammonium and VFAs, acetogenesis of VFAs to acetic acid, and methanogenesis (Hassan and Nelson 2012). Previous studies found that protein hydrolysis is slower than that of carbohydrates, and its efficiency decreases with the increase in the availability of carbohydrates (Wang et al. 2014, Yu and Fang 2001). The mechanism of this impact is unclear. Although the Stickland reaction pathways and involved microorganisms were reported in the 1960s (Barker 1961), the conclusions were based on studies on culturable bacteria that account for a small fraction of the total diversity (Stewart 2012). Generally, it is believed that in an AD reactor, there is a

specific group that converts proteins (Barker 1961), and this group is reported to have a slower growth rate than the carbohydrates fermenting bacteria, i.e., protein-fermenting mixed culture $\mu_{\max} = 0.08 - 0.15 \text{ d}^{-1}$, carbohydrates-fermenting mixed culture $\mu_{\max} = 0.3 - 1.25 \text{ h}^{-1}$ (Pavlostathis and Giraldo-Gomez 1991, Tang et al. 2005). There is a lack of information to identify and characterise the protein-fermenting microorganisms (hereafter referred to as protein degraders) and to link the microbial process performance with the microbial community during anaerobic protein conversion.

With the development of genetic technologies, it is possible to analyse the entire microbial community and identify the dominant microorganisms. In the present chapter, we aimed to identify the dominant microorganisms under three circumstances, i.e., protein as the sole substrate, carbohydrate as the sole substrate, and a mixture of protein and carbohydrate as the substrate. In the experiments, we used casein and lactose as substrates representing proteins and carbohydrates, respectively. By characterizing the dominating genus and their ability to ferment proteins/carbohydrates, we intended to reveal the mechanism of the carbohydrates' impact on the anaerobic protein degradation in a mixed culture. These results will lead to a better understanding of anaerobic protein degradation at a microbial level and would support the future design and operations of anaerobic digestion reactors for the treatment of protein-rich streams.

2 Materials and methods

2.1 Materials

Anaerobic mixed culture of a flocculent treatment system fed with dairy wastewater was used, taken at Biothane - Veolia Water Technologies Techno Center Netherlands B.V Research Facilities, in Delft, The Netherlands. The solids content of the biomass was $14.5 \text{ g VSS} \cdot \text{kg}^{-1}$ wet weight, and 3 g VSS was added to each reactor (working volume of 2 L) to achieve an inoculum concentration of $1.5 \text{ g VSS} \cdot \text{L}^{-1}$.

Three substrates were used in the experiment: A) casein (Fisher Scientific), with casein as the sole carbon source, B) lactose (Sigma Aldrich), with lactose as the sole carbon source, and C) mixture of casein and lactose as carbon sources, further referred to as MIX, with a

ratio of 50%: 50% in terms of chemical oxygen demand (COD). The addition of nutrients was based on the anaerobic fermentation process growth media protocol of Hendriks et al. (2018). The substrates contained $6000 \pm 100 \text{ mg COD}\cdot\text{L}^{-1}$ and $800 \pm 50 \text{ mg N}\cdot\text{L}^{-1}$.

2.2 Operation of acidification reactors

The reactors were mounted in parallel as shown in **Figure 1**, each reactor set-up had a feed tank, a 3.5 L double layer (water jacketed) glass vessel, and an effluent tank. The feed tanks were stored in a fridge at $4 \text{ }^\circ\text{C}$ to minimise biological processes. The two vessels of 2 L working volume, were operated as acidification reactors at $25 \pm 3 \text{ }^\circ\text{C}$ and an HRT of 24 h. The temperature in the acidification reactors was controlled by using a recirculating water bath (Thermo Haake DC10), the pH in each tank was measured with a probe (Hamilton pH sensor), and a controller (Hach SC200 Universal Controller, USA) was used to control the pH in both reactors at 6 ± 0.2 by adding $0.5 \text{ mol}\cdot\text{L}^{-1}$ NaOH (Yu and Fang 2003). The volumetric loading rate (VLR) was $8 \text{ kg COD}\cdot\text{m}^{-3}\cdot\text{d}^{-1}$.

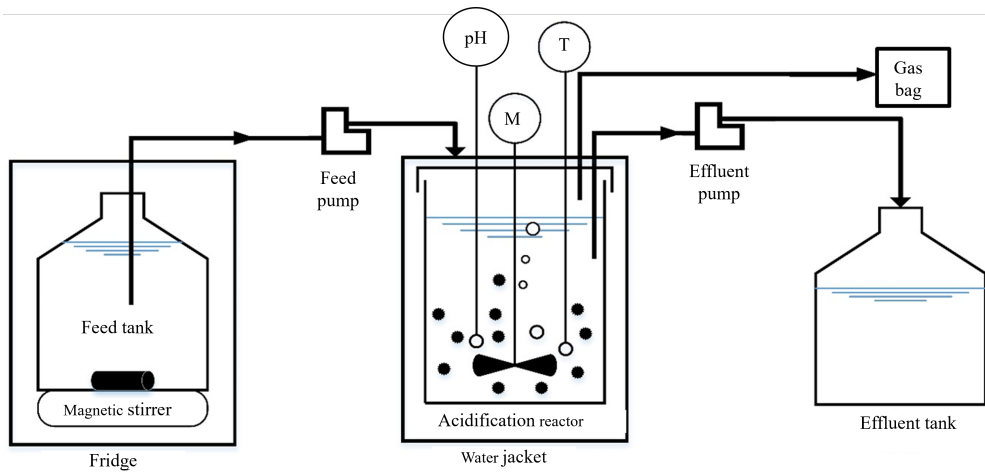


Figure 1 - Schematic diagram of the reactor set-up.

The operation of the reactors was divided into two stages. In the first stage, the CAS reactor, fed with substrate A) casein, was acclimated to pure protein substrate, whereas the LAC reactor, fed with substrate B) lactose, was acclimated to pure carbohydrate substrate. At the beginning of stage II, the feed of both reactors (CAS and LAC) was switched to substrate C) the mixture of casein and lactose (MIX), and the biomass was acclimated to the mixture of

protein and carbohydrate. Magnetic stirrers were used to ensure the mixing of the feed, while two stirring blades connected to motors were used for mixing the reactors at 50 rpm. Four peristaltic pumps (Longer L100-18-2 with FG25-13 pump head, China) were used for influent feeding and effluent extraction. The operational conditions were constant during all stages, controlled by LabVIEW.

Effluent samples were taken twice a week, and the reactors were considered stable when the difference between daily feed COD and effluent COD was less than 2% and the variation in total VFA production and deamination was less than 10% in a week. The reactors were operated for 132 days. To acclimate the biomass towards a specific substrate, stage I lasted 84 days, whereas stage II started from day 86 and lasted 46 days.

2.3 Deamination activity tests

To investigate the deamination activity of the biomass, batch tests were carried out in duplicates with biomass samples taken from the reactor at the end of each stage. Glass bottles with a total volume of 350 mL were used for the batch test. The biomass concentration in each bottle was $1.5 \text{ g VSS}\cdot\text{L}^{-1}$. Substrate A) of $190 \pm 0.2 \text{ mL}$ and buffer solution ($3.5 \text{ g NaHCO}_3\cdot\text{L}^{-1}$) was added to achieve a total liquid volume of $200 \pm 0.5 \text{ mL}$. All bottles were incubated at $25 \text{ }^\circ\text{C}$, with manual shaking before sampling. Liquid samples of 2 mL were taken from each bottle with syringes at 0 h, 1 h, 4 h, 8 h, 12 h, 20 h, and 24 h, and COD, total Kjeldahl nitrogen (TKN), VFAs, and ammonium (NH_4^+) were measured.

2.4 Analysis

The solids contents (TSS and VSS), TKN, and NH_4^+ of the reactor effluent were analysed following standard methods (APHA, 1998). The COD measurements were done with HACH-Lange kits (LCK014) without pre-treatment. VFAs, including acetic acid (C2), propionic acid (C3), iso-butyric acid (iC4), butyric acid (C4), iso-valeric acid (iC5), valeric acid (C5), and hexanoic acid (C6), were measured by gas chromatography (GC, Agilent Technologies 7820A) equipped with a CP 7614 column (WCOT Fused Silica $25 \text{ m} \times 0.55 \text{ mm}$, CP-wax 58 FFAP capillary, Agilent Technologies) and flame ionization detector. The injector temperature was 250°C , and nitrogen gas ($28.5 \text{ mL}\cdot\text{min}^{-1}$) with a split ratio of 10 was used as a carrier. The GC oven method sequence was started at $100 \text{ }^\circ\text{C}$ and held for 2 min, then

increased to 140 °C and held for 6 min. The VFA production was calculated by first converting the measured VFAs (C2-C6) concentrations ($\text{mg}\cdot\text{L}^{-1}$) to COD ($\text{mgCOD}\cdot\text{L}^{-1}$), then divided by the COD of the effluent and times 100%.

The protease activity was measured with the PierceTM Fluorescent Protease Activity kit (Thermo Scientific, USA), including contents of FTC-Casein, TPKC Trypsin, and BupHTM Tris-buffered saline. Measurement was carried out in triplicates, 100 μL sample taken directly from the reactors was mixed with 100 μL FTC-Casein working reagent (10 $\mu\text{g}\cdot\text{mL}^{-1}$ FTC-Casein in 25mM Tris, 0.15M NaCl, pH 7.2 assay buffer) in a 96-well plate (Pierce White Opaque 96-Well Plates). The plate was incubated for 2 h at 25 °C inside the fluorometer (FLUOstar, galaxy), the fluorescence was read every 120 seconds, and the fluorescein filter was set between 485 nm excitation wavelength and 520 nm emission wavelength. The reads of each sample were converted to BAEE (fluorescence unit, Na-Vebzoyl-L-Arginine Ethyl Ester, $\text{units}\cdot\text{L}^{-1}$), based on the calibration curve built with reference protease, Trypsin, and the conversion factor between its concentration and BAEE (14,000 BAEE $\text{units}\cdot\text{L}^{-1}$ equivalent can be produced by 50 $\text{mg}\cdot\text{L}^{-1}$ Trypsin). Final protease activity was calculated by linear fitting of the BAEE measurements and then normalised with the COD concentration of the sample.

For microbial community analysis, samples were taken at the beginning and the end (stable operation) of each stage, as shown in **Table 1**. Aliquots of 2 mL liquid sample were centrifuged at 14,000 x g for 5 min, the supernatant was removed, and the biomass was stored at -20 °C before DNA extraction with FastDNATM Spin Kit for Soil (MP BIOMEDICALS). The extracted DNA concentrations in all samples were checked by the Qubit 3 Fluorometer (Thermo Fisher Scientific, USA) to ensure a DNA concentration higher than 20 $\text{ng}\cdot\mu\text{L}^{-1}$. The DNA samples were then sent for amplicon sequencing by Illumina NovaSeq 6000 platform (Novogene, UK), using the primers 341F [(5'-3')CCTAYGGGRBGCASCAG] and 806R [(5'-3') GGACTACNNGGGTATCTAAT] for bacteria/archaea in the V3-V4 regions. Paired-end reads were merged using FLASH (V1.2.7) (Magoč and Salzberg 2011), and the splicing sequences were called raw tags. High-quality clean tags (Bokulich et al. 2013) were obtained by quality filtering on the raw tags according to the QIIME (V1.7.0) (Caporaso et al. 2010). The clean tags were compared with the Gold database (see details http://drive5.com/uchime/uchime_download.html) using UCHIME algorithm (Edgaret al.

2011) to detect and remove chimera sequences (Haaset al. 2011) to obtain the effective tags. Sequences analysis were performed by Uparse (V7.0.1001) (Edgar 2013) using the effective tags. Sequences with $\geq 97\%$ similarity were assigned to the same Operational Taxonomic Unit (OTU) and screened for further annotation by Mothur software against the SSUrRNA database of SILVA Database (Wanget al. 2007). Phylogenetic relationship of all OTUs was obtained by the MUSCLE (Version 3.8.31) (Edgar 2004). The sequences were deposited at DDBJ/EMBL/GenBank under the accession KFUH00000000.

OTUs abundance information was normalized using a standard of sequence number corresponding to the sample with the least sequences. Subsequent analysis of alpha diversity and beta diversity were all performed based on this output normalized data. Alpha diversity is applied in analysing biodiversity through observed species, Chao1, and phylogenetic diversity (PD). The indices in the samples were calculated with QIIME (V 1.7.0) and displayed with R software (V 2.15.3). Beta diversity analysis on weighted unifracs was calculated by QIIME (V 1.7.0). Principal Coordinate Analysis (PCoA) based on the weighted unifracs distance matrix of OTUs was performed and displayed by WGCNA package, stat packages and ggplot2 package in R software (V 2.15.3).

Table 1 - Biomass samples taken at the beginning and end of each stage for microbial community analysis

		STAGE I				STAGE II		
		Inoculum	Day 62	Day 84	Day 112	Day 132		
CAS	Sample No.	/	C1.2	C1.3	/	C2.2	C2.3	
	Sample content		^a Suspended biomass	Suspended biomass		Suspended biomass	^b Biofilm	
LAC	Sample No.	L1.1	L1.2	L1.3	L1.4	L2.1	L2.2	L2.3
	Sample content	Suspended biomass	Suspended biomass	Suspended biomass	Biofilm	Suspended biomass	Suspended biomass	Biofilm

^a Suspended biomass was the suspended solids in the effluent;

^b Biofilm sample was the biomass attached to the inner wall of the reactor.

/: Sample not valid due to low DNA concentration

3 Results and discussion

The COD balance in the two acidification reactors during the operation period of 132 days is shown in **Figure 2A**, the COD in the effluents was higher than 93 % of the influent CODs of both the CAS and LAC reactors. The pH in the reactors was well regulated at 6 (**Figure 2B**). Limited biogas gas production was expected at pH 6 (Holliger et al. 2016). Therefore, the COD in the two acidification reactors during the operation period was balanced with a maximum gap of 5%.

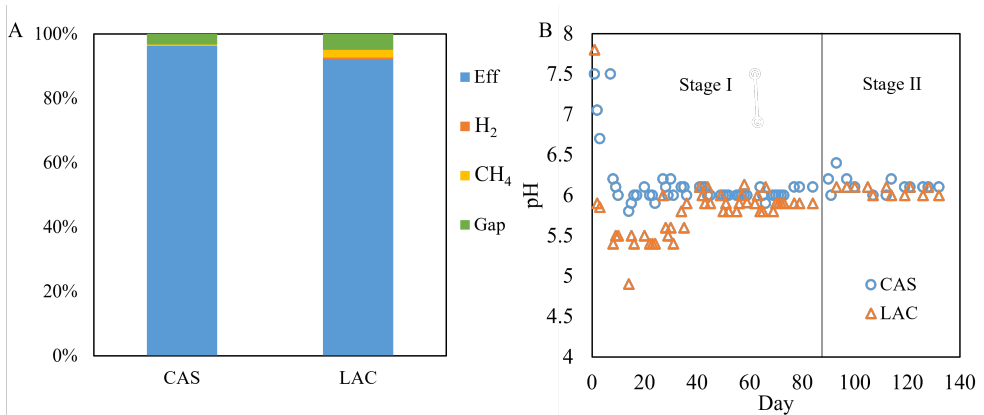


Figure 2 - Average COD balance in the CAS and LAC reactors (A), where Eff, H₂, and CH₄ represent the output COD in the liquid effluent, and resulting biogas (H₂ and CH₄), the Gap represents the difference between the total output COD and input COD in the influent; pH in the two reactors recorded by the online pH probes (B).

3.1 Effect of the presence of lactose on deamination and VFA production

3.1.1 Deamination

Figure 3A shows the deamination efficiency of the two acidification reactors during the two stages. In stage I, casein was fed as the sole carbon and nitrogen source to the CAS reactor, and the deamination efficiency was calculated as the percentage of NH₄⁺ released from the fed protein. The deamination efficiency increased from only 40% to almost 100% during the start-up period (day 0 - 20) and fluctuated between 60 - 80% during days 20 - 64. During days 70 - 84, a relatively stable period was observed, the average deamination degree was 77%, with a relative standard deviation of less than 5%. In the LAC reactor, lactose was fed as the carbon source and NH₄⁺ was added as a nitrogen source, and therefore the deamination efficiency was 0%.

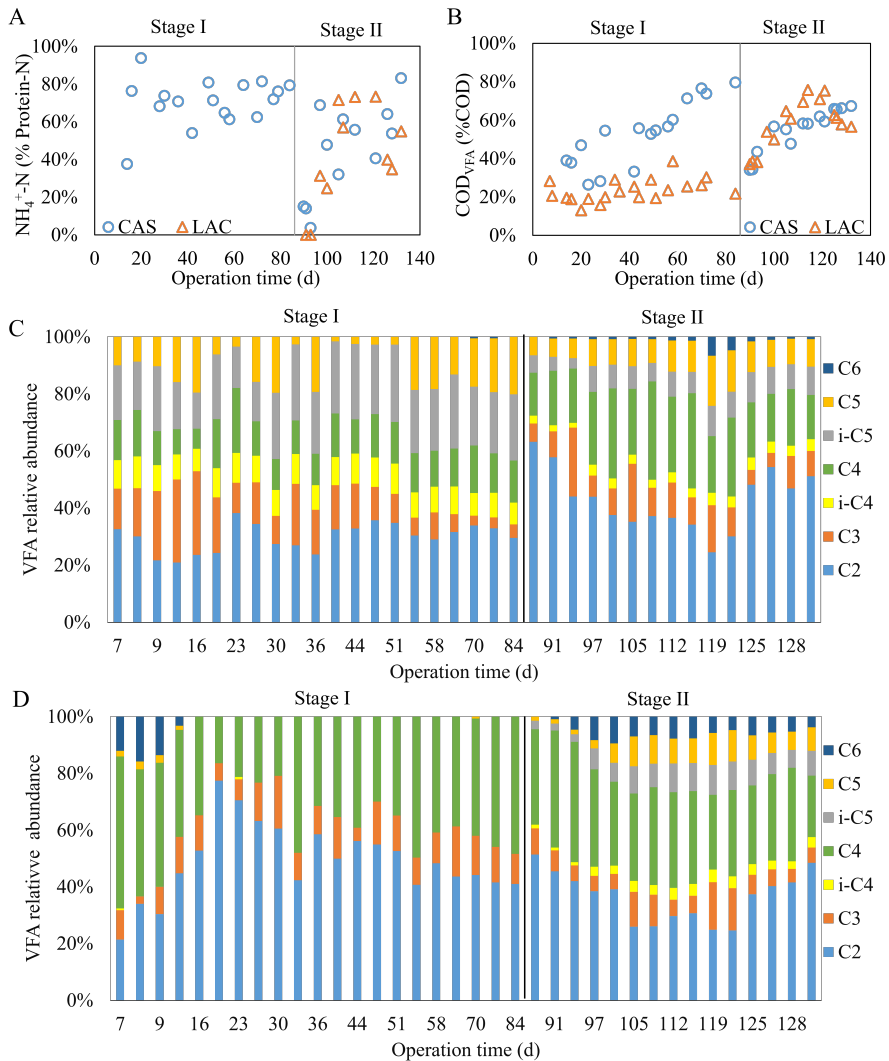


Figure 3 - Deamination (A) and VFA production as % of effluent COD (B) in CAS reactor and LAC reactor during the operational period, VFA relative abundance in the CAS reactor (C), and VFA relative abundance in the LAC reactor (D).

In stage II, both reactors were fed with the MIX (substrate C). The deamination efficiency in the CAS reactor dropped to 15% at the beginning of stage II. Subsequently, an increasing trend with fluctuations (between 41 - 64%) was observed, and a similar deamination efficiency as in stage I was achieved at the end of stage II (80%). Similarly, the deamination

efficiency of the LAC reactor also increased from 4% to 73% during days 86 - 120 but decreased to 35 - 55% during days 120 - 132.

3.1.2 VFA production

Figure 3B shows that the effluent VFA content of the CAS reactor fluctuated between 30 – 55% of the effluent COD during days 0 – 49 (VFA concentration data can be found in supplementary material **Table S1**). It increased steadily from 51 % to 64 % of the effluent COD during days 49 – 64 and stabilised at $75 \pm 5\%$ during days 64 - 84. Whereas in the LAC reactor, the VFA production was relatively stable between 20 – 39% of the effluent COD throughout stage I, with an average of $23 \pm 6\%$. The difference in VFA production efficiency between the CAS and LAC reactor was 40% in stage I.

In stage II, VFAs production in the CAS reactor initially decreased to 34% of the effluent COD, followed by a gradual increase to 67 % during days 120 - 132. The variation in VFAs production agreed with the variation in deamination efficiency, that is: a sudden decrease in protein degradation at the beginning of stage II. The VFAs production in the LAC reactor considerably increased from 37% to 76% of the effluent COD during days 86 – 114; however, it started dropping to $60 \pm 2\%$ by the end of stage II. The observed increased COD to VFA conversion efficiency could be attributed to the production of the more reduced VFAs iC5, C5, and C6 (**Figure 3D**) coinciding with protein degradation. The presence of lactose reduced the degradation efficiency of casein, resulting in a decreased deamination efficiency and VFAs production in the CAS reactor in stage II.

Figure 3C presents the VFA composition as the percentage of total VFA-COD in the CAS reactor during stage I and stage II. During days 56 – 84, the VFA production and composition were considered stable in stage I. The relative abundance of VFAs was similar to the fermentation products of gelatine at pH 6 in the study of Breure and van Anandel (1984). When the substrate was changed to the MIX in stage II, the composition of VFAs during stable operation performance (days 125 – 132) had changed compared to that in stage I. The C2 increased from $30\% \pm 9\%$ to $50 \pm 3\%$, and C4 increased from $14 \pm 3\%$ to $23 \pm 5\%$.

As shown in **Figure 3D**, the fluctuations in VFA composition in the LAC reactor mainly concerned C2 and C4 during stage I. A relatively stable VFA composition was observed from day 64 to day 84, where the most abundant VFAs were C2 ($43 \pm 2 \%$) and C4 ($44 \pm 4 \%$). In

stage II, the VFA composition in the LAC reactor gradually changed with the increasing production of iC4, iC5 and C5, and C6. This trend was also observed in the CAS reactor, and the identified main VFA products during stage II were C2 ($42 \pm 5 \%$) and C4 ($28 \pm 5 \%$).

3.2 Effect of the presence of lactose on protease activity and deamination activity

3.2.1 Protease activity

At the end of experimental stage I (day 84), the protease activity of the samples from both reactors was analysed. As shown in **Figure 4**, protease activity of 0.18 ± 0.01 BAEE unit·mgCOD⁻¹·h⁻¹ was observed in the CAS reactor, whereas no protease activity was detected in the LAC reactor sample. During stage II (day 91 and day 132), the CAS and LAC reactors were both found to have protease activity but at a level lower than 0.04 ± 0.01 BAEE unit·mgCOD⁻¹·h⁻¹.

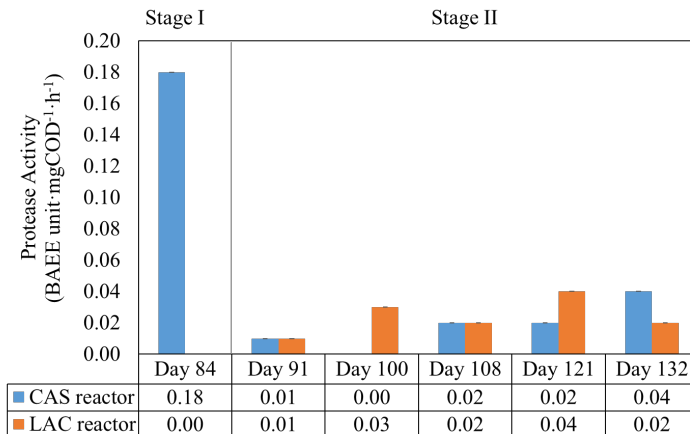


Figure 4 - Protease activity measured in stage I and stage II (the column represents the average protease activity in BAEE unit·mgCOD⁻¹·h⁻¹, error bars represent the standard deviation).

The results showed that with the presence of lactose, the protease activity decreased to lower than 25% of that in stage I in the CAS reactor, indicating a negative effect of lactose on the protease activity. Whereas in the LAC reactor, protease activity was slowly developed under the presence of protein.

3.2.2 Deamination activity

At the end of each stage, microbiota samples were taken from the reactor for assessing the deamination activity in batch tests. **Figure 5A** shows the ammonium production by the microbiota sample taken from the CAS and LAC reactors at the end of stage I. The deamination activity was calculated by linear fitting of the scattered plot of NH_4^+ concentrations as a function of time and divided by the microbiota concentration, $1.5 \text{ g VSS}\cdot\text{L}^{-1}$. Only suspended microbiota was found and collected from the CAS reactor (CAS microbiota) during this stage, whereas suspended microbiota (LAC suspended microbiota) and biofilm (LAC biofilm) were found and collected from the LAC reactor. The CAS microbiota had the highest deamination activity of $10.6 \text{ mg N}\cdot\text{g VSS}^{-1}\cdot\text{h}^{-1}$. In contrast, no deamination activity of the LAC suspended microbiota and LAC biofilm was observed.

Figure 5B shows the ammonium production by the microbiota samples collected from both reactors at the end of stage II, including CAS suspended microbiota, CAS biofilm, LAC suspended microbiota and LAC biofilm. Compared to the deamination activity of CAS microbiota from stage I, the four microbiota samples from stage II showed a similarly low level of deamination activity, which was $1.2 \text{ mg N}\cdot\text{g VSS}^{-1}\cdot\text{h}^{-1}$.

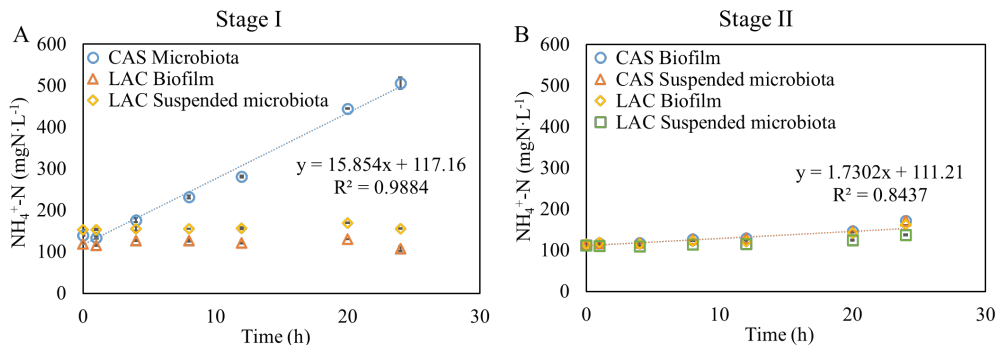


Figure 5 - Ammonium production by microbiota sample taken at the end of stage I - 84 days (A) and stage II - 132 days (B). The ammonium production rate was derived from the linear fitting of the plots; error bars represent the standard deviation.

3.3 Effect of the presence of lactose on microbial community

3.3.1 Microbial community composition in stage I and stage II

Alpha diversity of the samples were compared using three indices, the observed species, chao1 and phylogenetic diversity indices. As can be seen in **Figure 6A**, samples from the CAS reactor, especially during stage I, showed a higher diversity. In **Figure 6B**, the PCoA analysis illustrated the similarity of the microbial communities in all samples that are indicated in **Table 1**. The distance between samples indicates their similarity in microbial community, the shorter the distance, the higher the similarity, and vice versa. As shown in the figure, samples C1.2 and C1.3 taken from the CAS reactor stage I, displayed the longest distance to the rest of the samples, indicating that the microbial community under casein-fed conditions had a very different composition than the lactose-fed or MIX-fed conditions. The samples L2.2 and L2.3, taken from the LAC reactor, displayed the shortest distance, indicating that the microbial community can be considered similar in the suspended microbiota and biofilm in this reactor by the end of stage II. Remarkably, suspended microbiota L1.3 had a shorter distance to stage I samples, whereas biofilm sample L1.4 was closer to stage II samples. This means that the microbial community composition in the biofilm samples of stage I became predominant in stage II in LAC reactor.

Figure 6C shows the relative abundance at phylum level in each sample. When comparing the difference between stage I and stage II in the CAS reactor, the phyla *Firmicutes* and *Proteobacteria* were promoted by the presence of lactose and increased from 5.5% and 11.5% OTUs (average of C1.2 and C1.3) to 41% and 42% OTUs (C2.3), respectively. At the same time, the phyla *Chloroflexi* and *Euryarchaeota* (Archaea) were predominant in stage I but decreased in relative abundance in stage II from 23.5% and 18.5% OTUs (average of C1.2 and C1.3) to 1% and 4% OTUs (C2.3), respectively. Microorganisms belonging to these phyla had a slower growth rate than the acid producing bacteria at pH 6. The phylum *Bacteroidetes* exhibited first an increase from 14% OTUs (average of C1.2 and C1.3) to 24% OTUs (C2.2) and then decreased to 7% OTUs (C2.3). With the feed changed from casein to the MIX, the composition of the microbial community in the CAS reactor significantly changed at the phylum level, and the presence of lactose promoted the growth of bacteria affiliated to phyla *Proteobacteria* and *Firmicutes*.

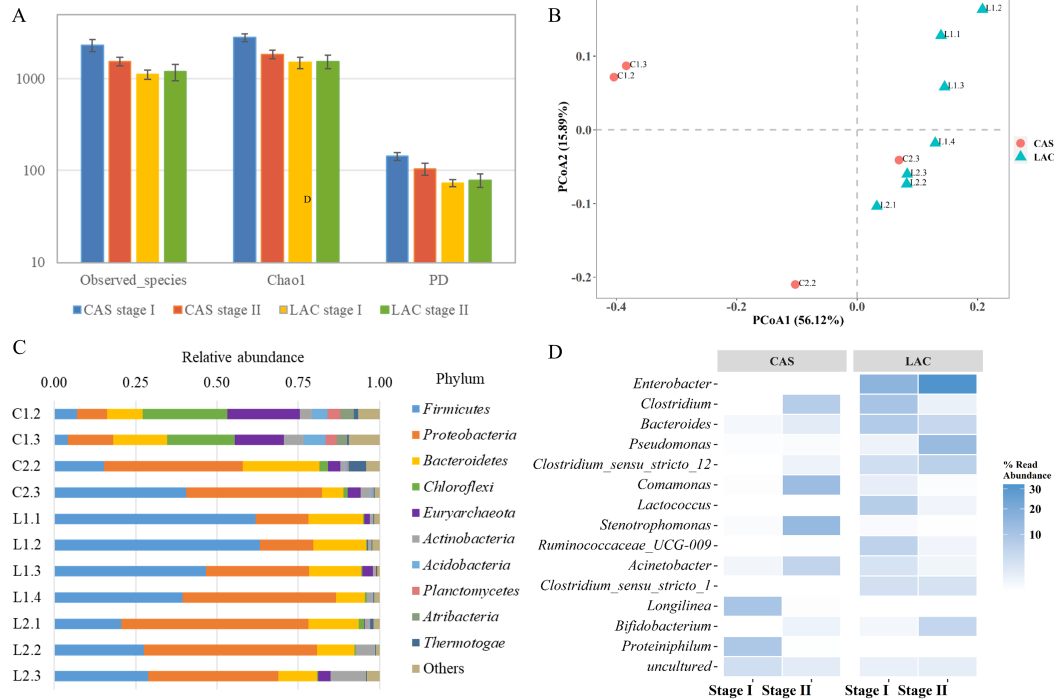


Figure 6 - Alpha diversity of the microbial community in CAS and LAC reactors during stage I and stage II, average values of the observed species, Chao1, and phylogenetic diversity (PD) are presented and the error bars indicate the minimum and maximum values of the samples in each stage (A), Principal coordinates analysis (PCoA) ordination based on the weighted unfrac distance matrix of OTUs comparing all samples taken from CAS and LAC reactors during stage I and stage II. The PCoA is coloured by reactor: red symbols indicate CAS; the green ones indicate LAC. The percentage of the variation explained by the plotted principal coordinates is indicated on the axes (B), phylum relative abundance of microbiota in samples from CAS and LAC reactors during stage I and stage II (C), and top 15 dominant genera in CAS and LAC reactors during stage I and stage II (D).

When comparing the differences in microbial community composition between stage I and stage II in the LAC reactor, the phylum *Firmicutes* was found to be predominant in stage I, accounting for more than 60% OTUs in L1.1 and L1.2, 47% OTUs in L1.3, and 39% OTUs in L1.4. However, in stage II, *Firmicutes* decreased to 29% OTUs (L2.3). The phylum *Proteobacteria* were the second most abundant in L1.1 and L1.2 (16% OTUs) and gradually became more abundant than *Firmicutes* in L1.4, with a relative abundance of 47% OTUs, and was maintained above 40% OTUs during stage II. Bacteria from the phylum *Bacteroidetes* was also abundantly present in all the LAC samples, it accounted for 17% OTUs in L1.1 and 12% OTUs in L2.3, and the composition of the microbial community in the LAC reactor remained relatively stable during the two different stages.

According to the alpha and beta diversity analysis, the microbiota, that was acclimated to casein as the sole substrate, was significantly different from the microbial community acclimated to lactose as the sole substrate. The phyla *Chloroflexi* and *Euryarchaeota* (Archaea) were predominant in the casein-fed reactor, whereas *Proteobacteria* and *Firmicutes* were predominant when lactose was present in the reactor. In general, the microbial community had a higher similarity in stage II, when lactose was present.

3.3.2 Characterization of predominant genera

Figure 6D presents the top 15 predominant genera in stage I and stage II in CAS and LAC reactors. In the CAS reactor, it was found that genera *Longilinea*, *Proteiniphilum*, and *midas_g_156* were predominant in stage I. Whereas genera *Stenotrophomonas*, *Comamonas*, *Clostridium*, *Acinetobacter*, and *Bacteroides* were dominating in stage II. Among the dominating genera found in CAS reactor, the genera *Longilinea*, *Proteiniphilum*, *Stenotrophomonas*, *Acinetobacter*, and *Clostridium sensu stricto* are identified as facultative, i.e., being able to ferment both sugars and proteins/amino acids (see **Table 2**). Whereas genus *Comamonas* is identified as only able to ferment proteins/amino acids, genus *Bacteroides* is identified as only able to ferment sugars (Dueholm et al. 2021).

During stage I of the LAC reactor, the dominating genera included *Enterobacter*, *Clostridium*, *Bacteroides*, *Lactococcus*, *Ruminococcaceae UCG 009*, *Acinetobacter*, *Clostridium sensu stricto 1*, and *Clostridium sensu stricto 12*. The dominating genera in stage II were *Enterobacter*, *Pseudomonas*, *Clostridium sensu stricto 12*, *Bacteroides*, *Bifidobacterium*,

and *Clostridium sensu stricto 1*. As shown in **Table 2**, in addition to the genera mentioned in the previous paragraph, genera *Proteiniphilum*, *Pseudomonas*, *Ruminococcaceae UCG 009*, and *Bifidobacterium* are reported to be only able to ferment sugars. Whereas *Lactococcus* is identified as a facultative genus, which can ferment both proteins/amino acids and sugars.

Results in **Table 2** show the 33 dominating genera identified in the collected samples, which had a relative abundance higher than 0.1% in at least one sample, and their ability to ferment sugars and proteins/amino acids is also presented. According to the abundance and substrate utilization information, the top 33 genera from all samples were categorised into 4 groups: 1) facultative bacteria, able to ferment both sugars and proteins; 2) sugar fermenting bacteria, able to ferment sugars but not proteins; 3) protein fermenting bacteria, able to ferment proteins but not sugars; and 4) not available, substrate utilization information was not available. We calculated the percentage of each group in the top 33 genera by counting the number of genera in each group and divided it by the total number of genera (33), and plotted the results as shown in **Figure 7**. Half of the identified genera (49%) are reported to be facultative. Due to the limited availability of systematic genome analysis of some genera, the ability, to ferment proteins/amino acids, of some sugar-fermenting genera could not be fully confirmed, e.g., *Bifidobacterium* and *Ruminococcaceae UCG 009*, meaning that they could possibly be assigned to the facultative category as well.

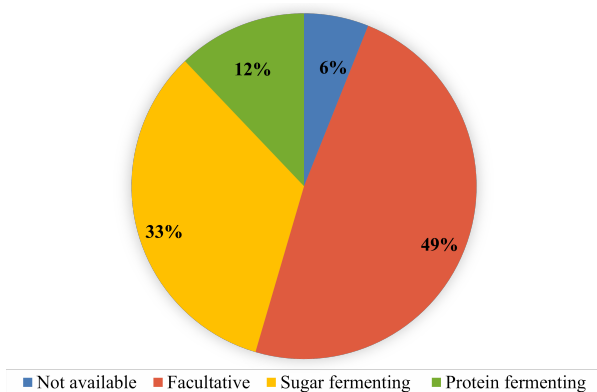


Figure 7 - Categorization of the top 33 genera in all samples according to substrate utilization characteristics. Facultative indicates the percentage of genera that can ferment both proteins and sugars, sugar fermenting indicates the percentage of genera that can only ferment sugars, protein fermenting indicates the percentage of genera that can only ferment proteins, and not available indicates the percentage of genera that could not be characterised.

Table 2 - Substrate-utilization of the identified top 33 predominant genera

Phylum	Genus	Substrate-utilization		Environment	Reference
		Sugar	Proteins/ amino acids		
<i>Actinobacteria</i>	<i>Bifidobacterium</i>	n.a.	n.a.	^a Stage II Mixture-feeding	(Dueholm et al. 2021)
		Y	n.a.	Animal gut	(Milani et al. 2014)
<i>Atribacteria</i>	<i>Candidatus caldatribacterium</i>	n/a	n.a.	^a Stage I Protein-feeding	(Dueholm et al. 2021)
		Y	n.a.	Glucose (and chemicals)-feeding AD reactor	(Schwan et al. 2020)
<i>Bacteroidetes</i>	<i>Acetobacteroides</i>	Y	Y	Stage II Mixture-feeding	(Dueholm et al. 2021)
	<i>Bacteroides</i>	Y	N	Stage I Sugar-feeding	(Dueholm et al. 2021)
	<i>Elizabethkingia</i>	n.a.	n.a.	Stage I Sugar-feeding	(Dueholm et al. 2021)
	<i>Macellibacteroides</i>	n.a.	n.a.	Stage II Mixture-feeding	(Dueholm et al. 2021)
		Y	Y	Slaughterhouse wastewater feeding UFMB reactor	(Jabari et al. 2012)
	<i>Petrimonas</i>	n.a.	n.a.	Stage II Mixture-feeding	(Dueholm et al. 2021)
		Y	N		(Hahnke et al. 2016)
	<i>Prevotella (9)</i>	Y	Y	Stage II Mixture-feeding	(Dueholm et al. 2021)
	<i>Proteiniphilum</i>	Y	Y	Stage I Protein-feeding	(Dueholm et al. 2021)
	<i>Sphingobacterium</i>	n.a.	n.a.	Stage I Sugar-feeding	(Dueholm et al. 2021)
Y		Y	Human gut	(Yabuuchi et al. 1983)	
<i>Chloroflexi</i>	<i>Longilinea</i>	Y	Y	Stage I Protein-feeding	(Dueholm et al. 2021)
<i>Firmicutes</i>	<i>Acetoanaerobium</i>	n.a.	n.a.	Stage II Mixture-feeding	(Dueholm et al. 2021)
		Y	Y	oil exploration drilling site; Pulp and paper mill-feeding AD reactor	(Duan et al. 2016, Sleat et al. 1985)
	<i>Blautia</i>	n.a.	n.a.	Stage I Sugar-feeding	(Dueholm et al. 2021)
		Y	n.a.	Human gut	(Maturana and Cárdenas 2021)

<i>Caproiciproducens</i>	n.a.	n.a.	Stage I Sugar-feeding; Stage II Mixture-feeding	(Dueholm et al. 2021)
	Y	Y	Galactitolivorans wastewater treatment plant	(Kim et al. 2015)
<i>Clostridium sensu stricto 1</i>	Y	Y	Stage I Sugar-feeding; Stage II Mixture-feeding	(Dueholm et al. 2021)
<i>Clostridium sensu stricto 2</i>	n.a.	n.a.	Stage I Sugar-feeding; Stage II Mixture-feeding	(Dueholm et al. 2021)
	Y	Y		(Udaondo et al. 2017)
<i>Clostridium sensu stricto 9</i>	n.a.	n.a.	Stage II Mixture-feeding	(Dueholm et al. 2021)
	Y	Y		(Udaondo et al. 2017)
<i>Clostridium sensu stricto 12</i>	Y	Y	Stage I Sugar-feeding; Stage II Mixture-feeding	(Dueholm et al. 2021)
<i>Erysipelotrichaceae (UCG-004)</i>	n.a.	n.a.	Stage II Mixture-feeding	(Dueholm et al. 2021)
	Y	n.a.	Jersey cows' diet-feeding	(Deusch et al. 2017)
<i>Lactococcus</i>	Y	Y	Stage I Sugar-feeding	(Dueholm et al. 2021)
<i>Lachnoclostridium (5)</i>	Y	N	Stage I Sugar-feeding; Stage II Mixture-feeding	(Dueholm et al. 2021)
<i>Lactobacillus</i>	n.a.	n.a.	Stage II Mixture-feeding	(Dueholm et al. 2021)
	Y	n.a.	Fermented food production	(Salveti et al. 2012)
<i>Pygmaibacter</i>	n.a.	n.a.	Stage I Sugar-feeding	(Dueholm et al. 2021)
	N	Y	Human gut	(Bilen et al. 2016)
<i>Ruminococcaceae (UCG-009)</i>	n.a.	n.a.	Stage I Sugar-feeding	(Dueholm et al. 2021)
	Y	n.a.	animal gut	(Bäckhed et al. 2004)
<i>Acinetobacter</i>	Y	Y	Stage II Mixture-feeding	(Dueholm et al. 2021)
	N	Y	Human microbiome	(Bouvet and Jeanjean 1989)
<i>Proteobacteria Comamonas</i>	N	Y	Stage II Mixture-feeding	(Dueholm et al. 2021)
	n.a.	n.a.	Stage II Mixture-feeding	(Dueholm et al. 2021)
<i>Delftia</i>	n.a.	n.a.	Stage II Mixture-feeding	(Dueholm et al. 2021)
	n.a.	Y		(Braña et al. 2016)

	<i>Hydrogenophaga</i>	n.a.	n.a.	Stage I Sugar-feeding	(Dueholm et al. 2021)
		Y	N		(Willems et al. 1989)
	<i>Parasutterella</i>	n.a.	n.a.	Stage II Mixture-feeding	(Dueholm et al. 2021)
		Y	n.a.	Human and mouse gut	(Ju et al. 2019)
	<i>Pseudomonas</i>	Y	Y	Stage II Mixture-feeding	(Dueholm et al. 2021)
	<i>Stenotrophomonas</i>	n.a.	n.a.	Stage II Mixture-feeding	(Dueholm et al. 2021)
<i>Synergistetes</i>	<i>JGI-0000079-D21</i>	n.a.	n.a.	Stage I Protein-feeding	(Dueholm et al. 2021)
		N	Y	Terephthalate degrading reactor	(Chen et al. 2020)
<i>Thermotogae</i>	<i>Mesotoga</i>	n.a.	n.a.	Stage II Mixture-feeding	(Dueholm et al. 2021)
		Y	Y		(Nesbø et al. 2019)

^a Stage I and Stage II refers to this chapter.

n.a.: not available.

Y: yes.

N: no.

3.4 Discussion

As reported in previous studies, the presence of carbohydrates retards the production of protease, limits protein solubility and hydrolysis, and restricts the acidification of amino acids (Breure et al. 1986b, Glenn 1976, Yang et al. 2015a). In this chapter, it was found that when the carbon source was changed from casein to the mixture of casein and lactose, the efficiency of deamination in the protein-fed reactor decreased from 77% to 15% and the VFA production decreased from 75% to 34% of the effluent COD (**Figure 3**).

Additionally, a decrease in protease activity and deamination activity of the microbiota was also observed in the presence of lactose (**Figure 4 and 5**), which has not been reported before. The deamination activity was $10.6 \text{ mg N} \cdot \text{gVSS}^{-1} \cdot \text{h}^{-1}$ when the microbiota was acclimated to pure casein, it decreased to about 10% after the microbiota was acclimated to the MIX, and it took at least a month to acclimate the microbial community to the MIX to achieve a similar deamination efficiency as in stage I. Although the protein concentration in stage II was half that in stage I, it was not the reason for the lower deamination efficiency, as casein is completely deaminated within 20 h at both $6.0 \text{ g} \cdot \text{L}^{-1}$ and $3.0 \text{ g} \cdot \text{L}^{-1}$ (Deng et al. 2023a). In the presence of lactose, the microbial community has a low protease activity and deamination activity, and only degraded casein to a limited extent. These results are in agreement with the study carried out by Breure et al. (1986a), which shows that gelatine degradation is retarded when glucose is present as a second carbon source.

Although the retardation of protein degradation by the presence of carbohydrates was frequently observed, the mechanism of the phenomenon has not been revealed. This chapter investigated the effect of lactose on the microbial community and found that when lactose was present, the microbial community, previously acclimated to casein, became similar to the microbial community acclimated to lactose (**Figure 6A**). The results indicated a selection of microorganisms by the presence of lactose. Generally, *Firmicutes* are the most abundant under various environmental conditions in anaerobic reactors (Pasalari et al. 2021), *Chloroflexi* and *Firmicutes* are dominant in protein-fed reactors (Kovács et al. 2013, Palatsi et al. 2011). The phyla *Chloroflexi*, *Proteobacteria*, and *Bacteroidetes* were predominant in the casein-fed reactor, whereas *Proteobacteria* and *Firmicutes* were predominant when

lactose was present in the reactor. The observed retardation of protein degradation can be correlated to the shift in the microbial community in the presence of lactose.

Furthermore, among the identified microorganisms, genera that can ferment both proteins/amino acids and carbohydrates were the predominant population in the microbial community (**Table 2**). Thermodynamically, sugar fermentation yields more energy than proteins/amino acids: cells gain 1-2 mol ATP·mol⁻¹ glucose (Zhou et al. 2018) compared to 0.5 mol ATP·mol⁻¹ amino acids (Barker 1981). The bacteria that can ferment sugars, including the facultative bacteria and the sugar fermenters, have a higher growth rate and biomass yield than the bacteria that are only fermenting proteins/amino acids (Pavlostathis and Giraldo-Gomez 1991, Tang et al. 2005), and it is, therefore, expected that the former can outgrow the latter during the mixture-feeding conditions at a specified solids retention time. Consequently, lactose was degraded prior to casein.

To confirm that the predominant facultative microorganisms are the active protein degraders, further research on the functional analysis of the microbial community is recommended. In addition, microbial community analysis has been focused on the methane-producing archaea and the granulation-involving filamentous (De Vrieze and Verstraete 2016), and less attention has been given to the protein degraders in a complex microbiota. To better manage and control the AD process for the treatment of protein-rich streams, an in-depth understanding of the protein degraders in complex microbiota is required.

4 Conclusions

- In conclusion, the retardation of casein degradation by the presence of lactose was due to 1) the substrate-preference of the dominant bacteria, including the facultative bacteria and the sugar fermenters, and 2) the higher growth rate and yield of the dominant bacteria.
- Overall, this chapter offers a better understanding of the mechanisms behind the retardation of protein degradation by the presence of carbohydrates, which can provide insights into the design of the anaerobic digestion process of protein-rich streams to improve protein degradation.

Supporting information

Table S1 - VFA concentration in CAS and LAC effluent (part 1 – CAS)

Stage	Day	CSTR 1 (CAS Effluent)															
		C2	C3	i-C4	C4	i-C5	C5	C6	Tot VFA	C2	C3	i-C4	C4	i-C5	C5	C6	check
		mg/L	mg/L	mg/L	mg/L	mg/L	mg/L	mg/L	^a mg COD/L	^b 1.07 %	1.51 %	1.82 %	1.82 %	2.04 %	2.04 %	2.20 %	%
	7	1025	315	185	260	315	165	0	3362	33%	14%	10%	14%	19%	10%	0%	100%
	8	440	175	96	140	130	67	0	1566	30%	17%	11%	16%	17%	9%	0%	100%
	9	788	623	195	254	433	196	0	3884	22%	24%	9%	12%	23%	10%	0%	100%
	14	525	517	129	130	217	209	0	2683	21%	29%	9%	9%	17%	16%	0%	100%
	16	503	442	98	88	142	218	0	2279	24%	29%	8%	7%	13%	20%	0%	100%
	20	695	395	172	289	340	93	0	3062	24%	19%	10%	17%	23%	6%	0%	100%
	23	651	128	105	228	129	31	0	1822	38%	11%	10%	23%	14%	3%	0%	100%
	28	552	165	88	113	116	133	0	1714	34%	15%	9%	12%	14%	16%	0%	100%
1	30	895	228	175	207	398	336	0	3495	27%	10%	9%	11%	23%	20%	0%	100%
	34	1163	657	265	299	602	61	0	4615	27%	21%	10%	12%	27%	3%	0%	100%
	36	1108	515	237	301	529	472	0	4984	24%	16%	9%	11%	22%	19%	0%	100%
	42	661	223	117	183	269	17	0	2173	33%	15%	10%	15%	25%	2%	0%	100%
	44	1086	369	204	233	458	44	0	3539	33%	16%	10%	12%	26%	3%	0%	100%
	49	1167	269	199	291	417	47	0	3493	36%	12%	10%	15%	24%	3%	0%	100%
	51	1046	215	188	257	426	44	0	3213	35%	10%	11%	15%	27%	3%	0%	100%
	56	1026	150	176	273	392	330	0	3614	30%	6%	9%	14%	22%	19%	0%	100%
	58	1108	256	202	282	432	367	0	4083	29%	9%	9%	13%	22%	18%	0%	100%

	CSTR 1 (CAS Effluent)															
	C2	C3	i-C4	C4	i-C5	C5	C6	Tot VFA	C2	C3	i-C4	C4	i-C5	C5	C6	check
	mg/L	mg/L	mg/L	mg/L	mg/L	mg/L	mg/L	^a mg COD/L	^b 1.07 %	1.51 %	1.82 %	1.82 %	2.04 %	2.04 %	2.20 %	%
64	1361	191	245	336	586	298	0	4605	32%	6%	10%	13%	26%	13%	0%	100%
70	1686	119	233	485	537	442	13	5316	34%	3%	8%	17%	21%	17%	1%	100%
72	1506	123	231	373	513	452	13	4894	33%	4%	9%	14%	21%	19%	1%	100%
84	1435	161	219	419	591	512	0	5190	30%	5%	8%	15%	23%	20%	0%	100%
90	1316	94	34	183	67	71	0	2227	63%	6%	3%	15%	6%	6%	0%	100%
91	1243	138	27	241	55	73	7	2300	58%	9%	2%	19%	5%	6%	1%	100%
93	1193	461	27	302	52	98	8	2895	44%	24%	2%	19%	4%	7%	1%	100%
97	1808	216	91	617	194	203	17	4399	44%	7%	4%	26%	9%	9%	1%	100%
100	1294	228	72	638	151	162	14	3686	38%	9%	4%	31%	8%	9%	1%	100%
105	1155	471	62	443	136	164	12	3506	35%	20%	3%	23%	8%	10%	1%	100%
107	1071	203	47	583	98	126	12	3082	37%	10%	3%	34%	7%	8%	1%	100%
2 112	1339	322	77	571	168	210	23	3918	37%	12%	4%	27%	9%	11%	1%	100%
114	1149	227	61	658	132	193	22	3592	34%	10%	3%	33%	7%	11%	1%	100%
119	953	452	100	453	216	357	126	4154	25%	16%	4%	20%	11%	18%	7%	100%
121	1067	254	79	576	169	269	82	3791	30%	10%	4%	28%	9%	14%	5%	100%
125	1900	146	101	448	218	223	31	4222	48%	5%	4%	19%	11%	11%	2%	100%
126	2135	139	91	386	196	194	21	4203	54%	5%	4%	17%	9%	9%	1%	100%
128	1833	314	83	456	179	183	13	4184	47%	11%	4%	20%	9%	9%	1%	100%
132	1994	244	95	355	203	197	16	4171	51%	9%	4%	15%	10%	10%	1%	100%

^aTotal VFA is the sum of measured VFA concentrations in mg COD/L, the mass concentration of VFAs were converted to COD concentration by multiplying the ^b conversion factors.

Table S1 - VFA concentration in CAS and LAC effluent (part 2 – LAC)

Stage	Day	CSTR 2 (LAC Effluent)															
		C2	C3	i-C4	C4	i-C5	C5	C6	Tot VFA	C2	C3	i-C4	C4	i-C5	C5	C6	check
		mg/L	mg/L	mg/L	mg/L	mg/L	mg/L	mg/L	mg COD/L	1.07	1.51	1.82	1.82	2.04	2.04	2.2	%
	7	365	125	6	535	0	18	100	1821	21%	10%	1%	53%	0%	2%	12%	100%
	8	420	23	0	325	0	18	95	1321	34%	3%	0%	45%	0%	3%	16%	100%
	9	580	130	0	490	0	27	126	2041	30%	10%	0%	44%	0%	3%	14%	100%
	14	511	104	0	253	0	9	18	1222	45%	13%	0%	38%	0%	2%	3%	100%
	16	556	93	0	216	0	0	0	1128	53%	12%	0%	35%	0%	0%	0%	100%
	20	600	34	0	75	0	0	0	830	77%	6%	0%	16%	0%	0%	0%	100%
	23	710	53	5	126	0	0	0	1078	70%	7%	1%	21%	0%	0%	0%	100%
	28	513	78	0	111	0	0	0	869	63%	14%	0%	23%	0%	0%	0%	100%
	30	665	145	0	135	0	0	0	1176	60%	19%	0%	21%	0%	0%	0%	100%
1	34	600	97	0	400	0	0	0	1516	42%	10%	0%	48%	0%	0%	0%	100%
	36	710	86	0	225	0	0	0	1299	58%	10%	0%	32%	0%	0%	0%	100%
	42	695	145	0	290	0	0	0	1490	50%	15%	0%	35%	0%	0%	0%	100%
	44	670	40	0	275	0	0	0	1278	56%	5%	0%	39%	0%	0%	0%	100%
	49	795	155	0	255	0	0	0	1548	55%	15%	0%	30%	0%	0%	0%	100%
	51	590	99	0	230	0	0	0	1199	53%	12%	0%	35%	0%	0%	0%	100%
	56	585	97	0	420	0	0	0	1537	41%	10%	0%	50%	0%	0%	0%	100%
	58	1035	165	0	515	0	0	0	2294	48%	11%	0%	41%	0%	0%	0%	100%
	64	680	195	0	355	0	0	0	1668	44%	18%	0%	39%	0%	0%	0%	100%
	70	700	155	0	385	0	6	0	1696	44%	14%	0%	41%	0%	1%	0%	100%
	72	800	170	0	520	0	0	0	2059	42%	12%	0%	46%	0%	0%	0%	100%

		CSTR 2 (LAC Effluent)															
	C2	C3	i-C4	C4	i-C5	C5	C6	Tot VFA	C2	C3	i-C4	C4	i-C5	C5	C6	check	
	mg COD/L							1.07	1.51	1.82	1.82	2.04	2.04	2.2			
	mg/L	mg/L	mg/L	mg/L	mg/L	mg/L	mg/L	mg COD/L	%	%	%	%	%	%	%	%	
	84	540	99	0	375	0	0	0	1410	41%	11%	0%	48%	0%	0%	0%	100%
	90	1055	134	16	406	32	16	0	2197	51%	9%	1%	34%	3%	2%	0%	100%
	91	1021	116	14	544	29	18	10	2403	45%	7%	1%	41%	2%	2%	1%	100%
	93	990	92	16	588	33	20	53	2522	42%	6%	1%	42%	3%	2%	5%	100%
	97	1249	124	61	656	126	50	131	3482	38%	5%	3%	34%	7%	3%	8%	100%
	100	1195	117	52	530	107	109	141	3267	39%	5%	3%	30%	7%	7%	9%	100%
	105	958	321	84	669	185	204	126	3951	26%	12%	4%	31%	10%	11%	7%	100%
	107	945	285	72	733	158	191	115	3870	26%	11%	3%	34%	8%	10%	7%	100%
2	112	1213	165	100	807	216	187	155	4362	30%	6%	4%	34%	10%	9%	8%	100%
	114	1266	181	99	794	215	188	154	4414	31%	6%	4%	33%	10%	9%	8%	100%
	119	1002	477	105	623	222	237	114	4302	25%	17%	4%	26%	11%	11%	6%	100%
	121	1004	430	100	729	215	237	94	4361	25%	15%	4%	30%	10%	11%	5%	100%
	125	1384	181	82	604	176	167	119	3964	37%	7%	4%	28%	9%	9%	7%	100%
	126	1441	149	66	641	140	135	98	3831	40%	6%	3%	30%	7%	7%	6%	100%
	128	1354	110	52	630	108	109	85	3488	42%	5%	3%	33%	6%	6%	5%	100%
	132	1620	126	73	426	154	145	61	3575	48%	5%	4%	22%	9%	8%	4%	100%

^ATotal VFA is the sum of measured VFA concentrations in mg COD/L, the mass concentration of VFAs were converted to COD concentration by multiplying the ^Bconversion factors.

CHAPTER 5

IDENTIFICATION OF PROTEIN-DEGRADERS IN AN ANAEROBIC DIGESTER BY PROTEIN ISOTOPE PROBING COMBINED WITH METAGENOMICS

This Chapter is based on: Deng, Z., Poulsen, J.S., Nielsen, J.L., Weissbrodt, D.G., Spanjers, H., & van Lier, J.B. (2023). Identification of protein-degraders in an anaerobic digester by protein stable isotope probing combined with metagenomics. Under Review.

Abstract

Presence of carbohydrates hampers the degradation of proteins in anaerobic digesters. To understand this phenomenon, we used proteogenomics to identify the active protein-degraders in the presence of low and high concentrations of carbohydrates. Active metabolic pathways of the identified protein-degraders were investigated through the application of proteomics with ^{13}C -protein substrates (protein stable isotope probing). Taxonomic annotation of the labelled proteins helped to identify populations of the genus *Acinetobacter* as the active protein-degraders under both protein-fed and protein-glucose mixture-fed conditions. Results showed that the outer membrane-bound proteins and porin proteins were the most frequently labelled by incorporation of the ^{13}C -protein substrate. These labelled proteins are associated with the proteinases or the amino acids transportation channel across the cell wall. Based on the metabolic model built with the extracted *Acinetobacter* genome and the incubation conditions, it was inferred that glucose and proteins were degraded through anaerobic respiration. The unfavourable effect of the presence of carbohydrates on protein biodegradation was attributed to the substrate preference of *Acinetobacter*, since one mole of glucose provides more energy than one mole of amino acids in the respiration pathway. This work highlights that efficient degradation of protein and carbohydrate mixtures in anaerobic digesters requires a staged or time-phased approach.

1 Introduction

Microorganisms are central for the biological treatment of waste and wastewater. A better understanding of the underlying microbial ecology provides important insights into phenomena observed in the degradation processes (Cerruti et al. 2021). Anaerobic digestion (AD) is a consolidated technology, but still many fundamental questions remain to be addressed. One specific challenge relates to why the presence of carbohydrates negatively affects the anaerobic protein degradation, especially in continuously fed reactors.

Anaerobic protein degradation generally involves three steps, hydrolysis of proteins to amino acids, acidification or deamination of amino acids to ammonium (NH_4^+) and volatile fatty acids (VFA), and finally methanogenesis of VFAs (Deng et al. 2021). The presence of carbohydrates retards the anaerobic degradation of proteins as observed in mixed cultures acclimated to proteins and exposed to carbohydrates (Breure et al. 1986a, Yu and Fang 2001). In chapter 4, a decrease of 75 % in protease activity and of 90 % in deamination activity was observed when lactose was added to the substrate of an acidification reactor after 84 days of feeding with only casein (Deng et al. 2022). Concomitantly, a community shift was observed; 50% of all the identified dominating genera before and after the shift has been described with metabolic traits to degrade carbohydrates and proteins (or amino acids) in the MiDAS field guide (Dueholm et al. 2021). It was concluded that the competition between substrate utilization by active species, rather than the competition between microbial populations, impairs the anaerobic degradation of proteins (Deng et al. 2022).

In a microbial community, the predominant microorganisms do not always harbour the required metabolic function (Hooper et al. 2005). Regarding protein-degraders, the identity of the active species in a mixed culture from a digester ecosystem remains unsolved. Moreover, the metabolic activity of these protein-degraders, and their impairment by the presence of carbohydrates, are yet to be unveiled.

Ecophysiological responses to different perturbations can be addressed through methods involving stable isotope probing (SIP) such as DNA-SIP or RNA-SIP (Friedrich 2006, Whiteley et al. 2006), lipid-SIP (Webster et al. 2006), and protein-SIP (de Jonge et al. 2022, Mosbæk et al. 2016). SIP methods are based on the labelling of various macromolecules of the metabolically active species through assimilation of typically ^{13}C - or ^{15}N -labelled

substrates. The nucleic acids, lipids, and proteins of these active species subsequently can be used to identify the organisms actively incorporating these molecules. DNA-SIP and RNA-SIP can provide phylogenetic identities of the active assimilating microorganisms. However, it is challenged by 1) the low mass fraction of DNA (~1%) and RNA (~5-15%) in cells compared to other cellular constituents such as proteins (~30-60%), and 2) the fractionation of partially labelled nucleic acids (Friedrich 2006, Jehmlich et al. 2008, Webster et al. 2006). Lipid-SIP can identify the microbial populations of interest (e.g., methane-oxidizing), but only provides a low taxonomic resolution (Jehmlich et al. 2008). For the above reasons, in this chapter, we focused on the use of protein-SIP to identify the active microbiome. In fact, Mosbæk et al. (2016) show that the combination of protein-SIP with genome-centric metagenomics is a powerful approach to link phylogenetic and functional information of active microorganisms. Since enzymes catalyse biochemical reactions, the identification of actively labelled proteins can provide important information of metabolic processes within the active microorganisms (Jehmlich et al. 2008).

Here, we combined SIP and proteogenomics to identify the actual protein degraders in a mixed culture of an anaerobic sequencing batch reactor treating slaughterhouse wastewater. We compared the identified protein degraders when exposed to regimes with low and high concentrations of carbohydrates. Finally, the metabolic pathways of the active protein-degraders were investigated. Our results provide important information on the functional ecosystem of the anaerobic mixed culture, elucidating protein biodegradation in this complex ecosystem. Results will guide future strategies for microbial resource management for efficient reactor operation.

2 Materials and Methods

2.1 Inoculum and substrate

The inoculum was taken from an anaerobic sequencing batch reactor (AnSBR) fed with real slaughterhouse wastewater; the operation of the AnSBR is explained in Deng et al. (2023b). The inoculum was composed of total suspended solids (TSS) at $13.7 \text{ g}\cdot\text{L}^{-1}$, volatile suspended solids (VSS) at $12.4 \text{ g}\cdot\text{L}^{-1}$, and ammonium ($\text{NH}_4^+\text{-N}$) at $0.1 \text{ g}\cdot\text{L}^{-1}$. On average, $52.5 \pm 1.0 \text{ mL}$ of inoculum was added to each incubation bottle, to obtain an initial biomass concentration

of about $2.0 \text{ g VSS} \cdot \text{L}^{-1}$. The VSS and $\text{NH}_4^+\text{-N}$ concentration of the biomass in the incubation bottles are listed in **Table 1**.

Table 1 - Composition and characteristics of the three types of substrate media and characteristics of inoculum used in the UP (unlabelled protein), LP (labelled protein), and LPG (labelled protein and glucose) incubations batches.

Incubations	Substrate medium composition	Substrate Characteristics				Inoculum Characteristics	
		Added in 1 L demineralised water (mL)	Initial concentration in the incubation bottles			VSS ($\text{g} \cdot \text{L}^{-1}$)	$\text{NH}_4^+\text{-N}$ ($\text{mg} \cdot \text{L}^{-1}$)
			COD ($\text{mg} \cdot \text{L}^{-1}$)	TN ($\text{mg} \cdot \text{L}^{-1}$)	$\text{NH}_4^+\text{-N}$ ($\text{mg} \cdot \text{L}^{-1}$)		
UP	unlabelled proteins	^a 120.0 ± 0.0	717 ± 0.1	72 ± 0.0	13 ± 0.0	2.2 ± 0.07	18 ± 0.5
LP	¹³ C proteins	^b 190.0 ± 0.0	717 ± 0.0	72 ± 0.0	9 ± 0.0	2.1 ± 0.0	17 ± 0.0
LPG	¹³ C proteins and glucose	^{b,c} 190.0 ± 0.1	1330 ± 0.0	133 ± 0.1	75 ± 0.0	2.1 ± 0.0	17 ± 0.0

^aUnlabelled High Performance OD2 Media solution; ^b¹³C High Performance OD2 Media solution; ^c280 $\text{mg} \cdot \text{L}^{-1}$ NH_4Cl was added to adjust the COD/N (chemical oxygen demand/nitrogen) ratio to 10; 250 mg NaHCO_3 was added into UP and LP substrate media, 700 mg was added into the LPG medium.

Incubations were performed using a medium rich in proteins, either Unlabelled High Performance OD2 Media solution for *E. coli* (111001402, Silantes, Germany) or labelled ¹³C High Performance OD2 Media solution for *E. coli* (110201402, Silantes, Germany), as well as glucose (G8270, Sigma Aldrich, the Netherlands) for protein-glucose mixtures. Both OD2 Media were based on a bacterial hydrolysate of *Ralstonia eutropha*. More than 98% carbon in the ¹³C High Performance OD2 Media solution for *E. coli* is ¹³C-labelled. The details of chemical compositions can be found in the supplementary material **Table S1**. The composition and characteristics of the three substrate media, unlabelled protein, ¹³C-protein, and mixture of ¹³C-protein and glucose, are listed in **Table 1**. The three substrate media were used in the UP (unlabelled protein), LP (labelled protein), and LPG (labelled protein and glucose) incubation batches, respectively. The content of glucose was less than 30 mg in 1000 mL substrate media. Before starting the experiment, the pH of the substrate media was adjusted to 6.0 ± 0.1 by adding drops of NaOH or HCl at $0.1 \text{ mol} \cdot \text{L}^{-1}$, and buffered by adding NaHCO_3 (144-55-8, Sigma Aldrich, the Netherlands) and flushing N_2/CO_2 gas ($\text{N}_2 : \text{CO}_2 = 70\%:30\%$) into the liquid for 2 min.

2.2 Anaerobic incubations

The incubation was carried out in triplicates with 500 mL glass bottles (Z674400, Duran®, the Netherlands) with a working volume of 300 mL and a headspace of 200 mL. Inoculum was first added into the bottles, followed by the substrate medium, and then the bottles were closed with a lid GL 45 with twin connectors (01-0206-02, BPC Instruments AB, Sweden). A tube (6.4/3.2 mm, Tygon® Tubing, BPC Instruments AB, Sweden) connected to the inlet was submerged in the liquid and used for sampling of the liquid phase of the batch, a tube connecting to the outlet was used for gas collection. A photo of the setup and the schematic diagram of each incubation bottle are given in the supplementary material **Figure S1**. Before incubation, N₂/CO₂ gas was used to flush the bottles to establish anaerobic conditions through the tube connecting to the inlet. The bottles were then incubated over 96 h in a water bath at 25 °C and continuously stirred at 100 rpm. The zero-time instant (0 h) was set when the temperature in the reactor reached 25 °C, which was about 30 min after incubation bottles were placed into the water bath.

Mixed liquor samples of 2.5 mL were collected from the batches with a syringe (307731, BD, USA) at 0, 1, 2, 4, 6, 9, 24, 30, 48, 72, and 96 h, to analyse the pH, total nitrogen (TN), NH₄⁺-N, VFAs, and the total (TCOD) and soluble (SCOD) concentrations of chemical oxygen demand (COD). The pH was measured with a pH electrode Multi 9420, WTW inoLab®, Germany). Mixed liquor samples (1 mL and 0.5 mL) were stored at -20 °C pending proteins and DNA extraction, respectively. An additional 1 mL of each mixed liquor sample was stored at 4 °C and analysed for the aforementioned chemical constituents on the same day as when the samples were collected. The sample conditioning and preparation of the analyses for chemical analyses are described hereafter.

2.3 Basic performance parameters

The TCOD of the samples was measured with Hach kits (LCK214 and LCK514, Merck, Germany) without any pre-treatment. For the measurement of TN, NH₄⁺-N and SCOD with Hach kits (LCK338, LCK303, and LCK214, Merck, Germany), the samples were first centrifuged at 13,000 × g for 5 min, and then filtered through a 0.45-µm polypropylene membrane filter (WHA68782504, Whatman®, UK). The same pre-treatment steps were also done before measuring VFAs. The composition of VFAs, including C2 (acetic acid), C3

(propionic acid), C4 (butyric acid), iC4 (iso-butyric acid), C5 (valeric acid), iC5 (iso-valeric acid), iC6 (iso-caproic acid), was analysed using a gas chromatograph (GC, 7820A, Agilent Technologies, the Netherlands) equipped with a flame ionization detector using a CP 7614 column (WCOT fused Silica 25 m × 0.55 mm, CP-wax 58 FFAP capillary, Agilent Technologies, the Netherlands). The temperature of the injector was 250°C. Dinitrogen carrier gas was supplied at 28.5 mL·min⁻¹ with a split ratio of 10. The GC temperature gradient was started at 100 °C held for 2 min and increased to 140 °C at 7 °C·min⁻¹ and held for 6 min at this temperature.

2.4 V3-V4 16S rRNA gene amplicon sequencing

The 0.5 mL mixed liquor samples taken at the beginning (0 h) and end (96 h) of the incubations were used for amplicon sequencing to characterise their bacterial community compositions. DNA was extracted with FastDNA™ Spin Kits for Soil (MP BIOMEDICALS, USA). The concentrations of the DNA extracts were measured using a Qubit 3 Fluorometer (Thermo Fisher Scientific, USA). The DNA extracts with a concentration higher than 20 ng·μL⁻¹ were then sent for V3-V4 16S rRNA gene amplicon sequencing on an Illumina NovaSeq 6000 platform (Novogene, UK). The amplicon libraries were generated using the forward and reverse primers 341F [(5′-3′) CCTAYGGGRBGCASCAG] and 806R [(5′-3′) GGACTACNNGGGTATCTAAT] for bacteria/archaea in the V3–V4 hypervariable regions of the 16S rRNA gene (Novogene, UK). Paired-end reads (2 × 250 bp) were assigned to samples based on their unique barcodes and truncated by cutting off the barcode and primer sequences. Paired-end reads were merged using FLASH (V1.2.7) (Magoč and Salzberg 2011), and the splicing sequences were filtered using QIIME (V1.7.0) (Caporaso et al. 2010) to obtain high-quality clean tags (Bokulich et al. 2013). The effective tags were obtained by using the UCHIME algorithm (Edgar et al. 2011) to detect and remove chimeric sequences (Haas et al. 2011). The sequences of the effective tags were analysed with Uparse (V7.0.1001) (Edgar 2013). Sequences with ≥ 97% similarity were assigned to the same Operational Taxonomic Unit (OTU) and screened for further annotation by the Mothur software against the SSUrRNA database of the SILVA Database (Wang et al. 2007). Phylogenetic relationship of all OTUs were obtained using MUSCLE (Version 3.8.31) (Edgar, 2004). OTUs abundance information were normalised using a standard of sequence number corresponding to the sample with the least sequences. The amplicon sequencing were visualised using the ampvis2

(Andersen et al. 2018) and ggplot2 (Wickham et al. 2016) packages in the R software (V 2.15.3). The sequences were deposited at DDBJ/EMBL/GenBank under the accession numbers OP474180-OP476210.

2.5 Metagenomics and bioinformatics

Three metagenomes were prepared from the inoculum, as references for the mapping of the metaproteomes. DNA was extracted using the FastDNA™ Spin Kit for Soil (MP Biomedicals, USA), following the manufacturer's recommendations. The DNA extracts were commercially sequenced by Novogene (UK) on an Illumina HiSeq platform. Pair-end reads with a length of 250 bp were generated, the sequencing depth was at least 40 million read pairs per sample. The pre-processing, trimming, filtering, and assembling of the metagenome was conducted as previously described (Poulsen et al. 2022). Briefly, the raw reads were pre-processed by PhiX sequence control, trimmed for adaptors, and quality filtered for a minimum Phred score of 20. The trimmed reads were assembled applying k-mers of 21, 33, 55, and 77, and contigs shorter than 1000 bp were removed. The mmgenome2 package (<https://kasperskytte.github.io/mmgenome2/>) was used in R to generate a prediction of open reading frames in the metagenome, identify the essential genes, taxonomically classify the contigs, and locate the labelled bins and the known protein-degraders, resulting in the obtaining of their metagenome-assembled genomes (MAGs). The three obtained MAGs were deposited DDBJ/EMBL/GenBank under the accession number SAMN32366555. Known protein-degraders within bacteria and archaea containing protease coding genes were identified according to the UniprotKB database (Zaru et al. 2020) and literature.

2.6 Protein extraction and protein-SIP analysis

Proteins were extracted using phenol liquid-liquid extraction as previously described (Poulsen et al. 2022), followed by in-gel digestion (Mosbæk et al 2016). The desalting and analysis of tryptic peptides by automated liquid chromatograph-electrospray ionisation tandem mass spectrometry (LC-ESI-MS/MS) were performed as previously described (Poulsen et al. 2021). The MetaProSIP tool was used to analyse the proteomic data in an OpenMS pipeline, and the search database metaproteome was generated from the metagenome and annotated using Prokka (v.1.14), as previously described (Mosbæk et al. 2016, Poulsen et al. 2022).

2.7 Metabolic pathway analysis of predominant degraders of proteins

Among the identified active degraders of proteins, the metabolic pathway of *Acinetobacter* was analysed from its MAG. A narrative was built in KBase to this end (Arkin et al. 2018). The DNA contigs related to *Acinetobacter* were extracted from one of the sequenced MAGs. The extracted *Acinetobacter* contigs were then binned to produce an *Acinetobacter* MAG, using the algorithm “Extract Bins as Assemblies from BinnedContigs” (v1.1.1). The *Acinetobacter* MAG was checked by using “Assess Genome Quality with CheckM” (v1.0.18), and then annotated using “Annotate Microbial Assembly with RASTtk” (v1.073). The *Acinetobacter* MAG was compared with complete reference genome of 30 *Acinetobacter* species (NCBI database) using “Insert Set of Genomes Into SpeciesTree” (v2.2.0). The function profile of *Acinetobacter* MAG was further visualised using “View Function Profile for Genomes” (v1.4.0). The metabolic pathway was analysed by building a metabolic model using “Gapfill Metabolic Model”.

3 Results and discussion

3.1 Comparison of the protein degradation performance and the microbial community compositions in the incubation batches

3.1.1 Protein degradation in the presence of low and high concentrations of glucose

Figure 1 shows the concentrations of total (TCOD) and soluble (SCOD) COD normalised by their initial concentrations, the concentrations of the ammonium ($\text{NH}_4^+\text{-N}$) produced as percentage of the initial total nitrogen (TN) (i.e., $\text{NH}_4^+\text{-N}/\text{TN}$ ratio), and the pH during the anaerobic incubation performed with unlabelled proteins (UP), labelled proteins (LP) and a mixture of labelled proteins and glucose (LPG).

On the average, the normalised TCOD in the three incubations with UP, LP, and LPG was removed by a percentage of $20\% \pm 7\%$ (**Figure 1A**). The normalised SCOD decreased by $70\% \pm 12\%$ (**Figure 1B**). In concentration terms, the decrease of TCOD ($1100 \pm 300 \text{ mg}\cdot\text{L}^{-1}$) was similar to that of SCOD ($1050 \pm 75 \text{ mg}\cdot\text{L}^{-1}$) in LPG. In UP and LP, the decrease in SCOD ($450 \pm 60 \text{ mg}\cdot\text{L}^{-1}$ and $530 \pm 50 \text{ mg}\cdot\text{L}^{-1}$, respectively) was about 50% of the decrease in TCOD ($890 \pm 150 \text{ mg}\cdot\text{L}^{-1}$ and $1030 \pm 200 \text{ mg}\cdot\text{L}^{-1}$, respectively). The ignorable

concentration of volatile fatty acids (VFAs) (**Figure S2** in supplementary information) suggested that the residual SCOD might be soluble peptides or amino acids.

However, the $\text{NH}_4^+\text{-N/TN}$ ratio in the UP and LP incubations increased to as high as $90 \pm 6\%$ after 96 h (**Figure 1C**). This suggests that the proteins supplied in the UP and LP media were efficiently converted and deaminated. Whereas with LPG, the $\text{NH}_4^+\text{-N/TN}$ reached only a partial conversion ratio of $75 \pm 1\%$ after 96 h (**Figure 1C**).

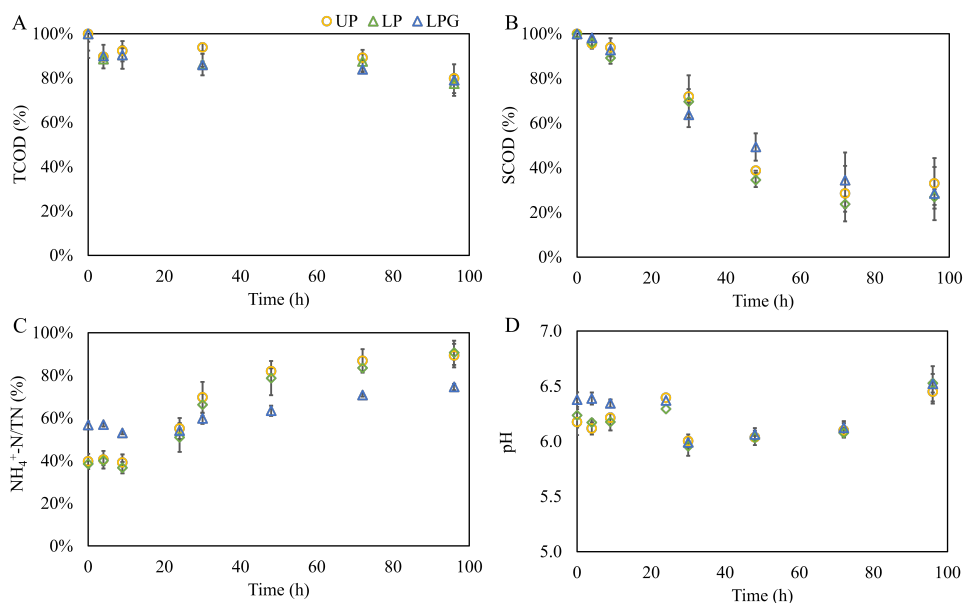


Figure 1 - Substrate concentrations and pH during the 96-h incubation period. A) Total COD (% of initial TCOD concentration); B) Soluble COD (% of the initial SCOD concentration); C) Conversion ratio of ammonium from total nitrogen ($\text{NH}_4^+\text{-N/TN}$) indicating the $\text{NH}_4^+\text{-N}$ production as % of the added TN; D) pH evolutions. All data points are presented as averages and standard deviations from triplicate incubations. Legends of incubations: yellow dot – unlabelled proteins (UP), green diamond – ^{13}C -labelled proteins (LP), blue triangle – mixture of ^{13}C -labelled proteins and glucose (LPG).

Assuming a COD consumption of 5% in bacterial growth under anaerobic conditions (van Lier et al. 2020) and a COD:N molar ratio of 5 needed to form bacterial biomass (Münch and Pollard 1997), a mass of 3 mg of nitrogen was theoretically assimilated by microorganisms in the LPG incubation. Based on this assumption, there was still a gap of 9 mg N between

the amount of produced $\text{NH}_4^+\text{-N}$ and the added TN in the LPG. This gap indicated that the added protein was not fully converted in the presence of glucose.

The pH was maintained between 6.0 and 6.5 during the incubations, and due to the increasing NH_4^+ concentration, it increased to 7.0 at the end of the incubations (**Figure 1D**).

3.1.2 Bacterial community composition

The effect of the substrate compositions on the bacterial community composition was investigated by V3-V4 16S rRNA gene amplicon sequencing for the three incubations batches (UP, LP, LPG). In total, 1,271,436 reads were obtained from 18 samples. The minimum count of sequences obtained per sample was 61,187, the maximum count obtained was 77,097, and the median was 72,416. The community profile of sample taken at 0 h, which was 30 min after the incubation bottles were placed into the water batch, was comparable at both phylum and genus levels in all incubation bottles and did neither vary significantly between the different treatments nor during the incubation periods of 96 h (**Figure 2**).

The phyla of *Proteobacteria* (relative abundance of 26-29 % of OTUs) and *Cloacimonetes* (16-21%) were predominant in the microbiomes of all incubation batches, regardless of the substrates supplied (**Figure 2A**). Flanking populations of *Firmicutes*, *Bacteroidetes*, *Chloroflexi*, *Euryarchaeota*, *Thermotogae*, *Spirochaetes* and *Campylobacteriota* were present at a relative abundance above 1%. The results matched with previous studies: *Chloroflexi*, *Proteobacteria*, and *Bacteroidetes* were reported dominant in a casein-fed reactor (Deng et al. 2022); *Firmicutes* in a reactor fed with bovine serum albumin (Tang et al. 2005); and *Firmicutes*, *Proteobacteria*, and *Bacteroidetes* in an anaerobic reactor treating slaughterhouse wastewater (Jabari et al. 2016).

A Phylum		0h			96h		
<i>Proteobacteria</i> -		28.6	28.5	26.7	29.3	26.4	27.1
<i>Cloacimonetes</i> -		19	21.3	20.1	16.1	20	17.7
<i>Firmicutes</i> -		11	11.7	11.6	15.4	13.3	15.5
<i>Bacteroidetes</i> -		13.2	13.1	12.9	11.8	11.5	12.1
<i>Chloroflexi</i> -		10.8	8.9	10.4	10.8	10.3	10.7
<i>Euryarchaeota</i> -		9.8	8.4	10.7	8.9	9.3	9.5
<i>Thermotogae</i> -		1.4	1.3	1.5	1.5	2.3	1.5
<i>Spirochaetes</i> -		1.5	1.4	1.3	1.1	1	1
<i>Campylobacterota</i> -		0.7	1.5	1.1	0.8	2	1.2
<i>Synergistetes</i> -		0.7	0.7	0.7	0.9	0.9	0.9
<i>Verrucomicrobia</i> -		0.6	0.6	0.5	0.6	0.5	0.5
<i>Atribacteria</i> -		0.3	0.3	0.3	0.3	0.3	0.3
<i>Kiritimatiellaeota</i> -		0.2	0.3	0.2	0.2	0.2	0.2
<i>Planctomycetes</i> -		0.2	0.2	0.2	0.2	0.2	0.1
<i>Calditrichaeota</i> -		0.2	0.2	0.2	0.2	0.2	0.2
		UP [†]	LP [†]	LPG [†]	UP [†]	LP [†]	LPG [†]

B Genus		0h			96h		
<i>Candidatus_Cloacimonas</i> -		18	20.1	19	15.2	18.9	16.8
<i>unidentified_Anaerolineaceae</i> -		8	6.5	7.7	8.1	7.7	8.1
<i>Acinetobacter</i> -		5.5	5.9	4.8	7.2	6.4	5.9
<i>Smithella</i> -		5.3	5.3	5.4	4.7	4.8	4.8
<i>Methanosaeta</i> -		5.2	4.4	5.8	4.6	4.6	5.1
<i>Methanobacterium</i> -		3.7	3.3	4	3.5	3.8	3.6
<i>unidentified_Clostridiales</i> -		2.8	2.9	2.8	4.8	3.6	4.7
<i>o_Bacteroidales_OTU_6</i> -		2.4	2.5	2.4	2.4	2.3	2.5
<i>o_Bacteroidales_OTU_7</i> -		2.4	2.3	2.3	1.9	1.9	2
<i>Syntrophorhabdus</i> -		1.9	1.8	1.8	1.8	1.7	1.6
<i>Mesotoga</i> -		1.4	1.3	1.5	1.5	2.3	1.5
<i>f_Syntrophaceae_OTU_16</i> -		1.5	1.5	1.5	1.3	1.2	1.2
<i>Denitratisoma</i> -		1.5	1.5	1.4	1.3	1.2	1.2
<i>f_Lentimicrobiaceae_OTU_9</i> -		1.4	1.4	1.4	1.3	1.3	1.3
<i>f_Prolixibacteraceae_OTU_10</i> -		1.4	1.4	1.4	1.1	1.2	1.3
		UP [†]	LP [†]	LPG [†]	UP [†]	LP [†]	LPG [†]

Figure 2 - Evolutions of the bacterial community compositions over the incubation period of 96 h. A) top 15 phyla and B) top 15 genera in UP, LP, and LPG incubation batches. V3-V4 amplicon sequencing profiles were analysed at 0 h and 96 h of the incubations. The relative abundances of operational taxonomic units (OTUs) displayed on the heatmaps are averages calculated on triplicate incubations.

Figure 2B displays the top 15 genera in each incubation batch, whereas the relative abundance of the top 15 genera in each incubation bottle are shown in supplementary material **Figure S3**. *Acinetobacter* increased by 0.5 – 1.7 %, an unidentified *Clostridiales* by 0.7 – 2 %, whereas “*Candidatus Cloacimonas*” decreased by 1.2 - 2.8 % over the incubation period of 96 h. Populations of the order *Clostridiales* are reported degraders of amino acids (McInerney 1988). Although “*Ca. Cloacimonas acidaminovorans*” is known to degrade amino acids, this population has been out-selected from 2% to below detection limit in an anaerobic fed-batch reactor supplied with casein; the decrease has been related to a low C/N (carbon to nitrogen mass) ratio of 3 (Kovács et al. 2013). Notably, these averaged variations do not necessarily indicate the change of genera populations, but a potential predominancy of active protein-degraders.

3.2 Metagenome analysis

The total number of paired-end sequences used to build the metagenome was 172,172,549 bp. When assembled, it resulted in a *de novo* metagenome assembly of 1,242,870,255 bp divided in 368,064 contigs. Half of the metagenome assembly was covered by contigs larger than or equal to 5,650 bp (N50 value). The metagenome assembly consisted of 82.6 % of *Bacteria* and 17.3 % of *Archaea*, eukaryotic and viral sequences were removed from the dataset. Among the 36 identified phyla, *Proteobacteria* were the most abundant representatives with 51 % of all identified scaffolds. The microbial composition of the metagenome was in accordance with the 16S rRNA gene amplicon sequencing profiles. A comparison of the metagenome profile and amplicon sequencing profile is provided in the supplementary material **Figure S4**.

3.3 Identification of protein degraders

3.3.1 Protein degraders identified in the LP incubation batch

The protein pools extracted from biomass samples, collected after 0, 6, 24 and 48 h of LP incubation batch involving ^{13}C -labelled proteins as substrate, were analysed for protein-SIP by MetaProSIP. The ^{13}C -labelled proteins as substrate was a hydrolysate of *Ralstonia eutropha*, containing mainly proteins and amino acids, and less than $30 \text{ mg}\cdot\text{L}^{-1}$ glucose. A detailed composition of the substrate can be found in **Table 1** and supplementary materials **Table S1**. **Table 2** lists the number of identified proteins that incorporated the ^{13}C -label at the

different time instants, in the column labelled protein ID. The number of reference proteins (NCBI database) that have an almost identical match (> 99%) to the detected proteins are given in the column Hits, and the functional and phylogenetic annotation of the reference proteins are provided as well. The ^{13}C -labelled substrate was found to be incorporated into biomass proteins after 6 h, and the number of labelled proteins increased over time. After 6 h, three labelled proteins were detected: all were assigned to the phylum *Proteobacteria*, of which two affiliated with the genus *Acinetobacter* and one to *Klebsiella*. After 24 h, ten labelled proteins were detected; of which nine could be assigned to the genus *Acinetobacter*. After 48 h, fifteen labelled proteins were detected; two could not be annotated and all others were assigned to the genus *Acinetobacter*. This highlighted the preponderance of populations of *Acinetobacter* as proteins-degraders.

Most of the labelled proteins were identified as outer membrane proteins or porin proteins; their function has generally been considered for the transportation or diffusion of molecules (Welte et al. 1995). One protein was identified as an elongation factor Ts. It associates with the EF-TuGDP complex and induces the exchange of guanosine diphosphate to guanosine triphosphate (Xin et al. 1995). The time-resolved protein-SIP confirmed the uptake of the ^{13}C -labelled protein substrate in the identified microorganisms.

Table 3 summarises the substrate utilization properties that have been reported in literature for the labelled genera detected in this chapter. The genus *Acinetobacter* was the most frequently identified.

Table 2 - Identified proteins that incorporated the ¹³C-label supplied by the proteinaceous substrate in LP incubation batch. Samples were measured for protein-SIP after 0, 6, 24 and 48 h. The number of reference proteins with over 99% matching identity (Hits) are given, together with their functional and phylogenetic annotations (at phylum and genus level).

Sample Time	Labelled protein ID	Hits	Protein	Phylum	Genus	
6 h	1	1	Elongation factor Ts	<i>Proteobacteria</i>	<i>Acinetobacter</i>	
		1	outer membrane protein			
	2	1	outer membrane protein Omp38	<i>Proteobacteria</i>	<i>Acinetobacter</i>	
		7	OmpA family protein			
3	2	OmpK36	<i>Proteobacteria</i>	<i>Klebsiella</i>		
24 h	1	1	hypothetical protein	<i>Proteobacteria</i>	<i>Acinetobacter</i>	
		1	choice-of-anchor F family protein			
	2	1	fimbrial protein	<i>Proteobacteria</i>	<i>Klebsiella</i>	
	3	1	hypothetical protein	<i>Proteobacteria</i>		
	4	1	Elongation factor Ts	<i>Proteobacteria</i>	<i>Acinetobacter</i>	
	5	1	outer membrane protein HMP			
		1	hypothetical protein			
		1	outer membrane protein Omp38	<i>Proteobacteria</i>	<i>Acinetobacter</i>	
	6	11	1	OmpA family protein		
			1	outer membrane protein		
			1	hypothetical protein	<i>Proteobacteria</i>	<i>Acinetobacter</i>
	7	7	1	outer membrane protein Omp38		
			1	outer membrane protein Omp38	<i>Proteobacteria</i>	<i>Acinetobacter</i>
7			OmpA family protein			
7	5	1	hypothetical protein			
		1	outer membrane protein Omp38	<i>Proteobacteria</i>	<i>Acinetobacter</i>	
		5	OmpA family protein			

Sample Time	Labelled protein ID	Hits	Protein	Phylum	Genus
24 h	8	1	OmpA family protein	<i>Proteobacteria</i>	<i>Acinetobacter</i>
	9	1	OmpA family protein	<i>Proteobacteria</i>	<i>Acinetobacter</i>
	10	1	hypothetical protein	<i>Proteobacteria</i>	<i>Acinetobacter</i>
48 h		1	outer membrane protein A		<i>Salmonella</i>
		1	outer membrane protein A		<i>Shigella</i>
		2	outer membrane protein A	<i>Proteobacteria</i>	<i>Escherichia</i>
		1	OmpA/MotB domain protein		<i>Pluralibacter</i>
	1	1	porin OmpA		<i>Mangrovibacter</i>
		1	porin OmpA	<i>Firmicutes</i>	<i>Staphylococcus</i>
		2	porin OmpA		<i>Escherichia</i>
		1	porin OmpA	<i>Proteobacteria</i>	<i>Klebsiella</i>
		1	porin OmpA		<i>Enterobacter</i>
		2	hypothetical protein	<i>Proteobacteria</i>	<i>Syntrophus</i>
		3	1 hypothetical protein	<i>Proteobacteria</i>	<i>Acinetobacter</i>
		4	1 choice-of-anchor F family protein	<i>Proteobacteria</i>	<i>Klebsiella</i>
		5	1 fimbrial protein	<i>Proteobacteria</i>	<i>Klebsiella</i>
	6	1 hypothetical protein	<i>Proteobacteria</i>	<i>Acinetobacter</i>	
		1	outer membrane protein HMP		
	7	1	hypothetical protein		<i>Acinetobacter</i>
		1	outer membrane protein Omp38		
		11	OmpA family protein		

Sample Time	Labelled protein ID	Hits	Protein	Phylum	Genus	
48 h	8	1	outer membrane protein	<i>Proteobacteria</i>	<i>Acinetobacter</i>	
		1	hypothetical protein			
		1	outer membrane protein Omp38			
		7	OmpA family protein			
	9	1	hypothetical protein	<i>Proteobacteria</i>	<i>Acinetobacter</i>	
	10	1	hypothetical protein	<i>Proteobacteria</i>	<i>Acinetobacter</i>	
		1	choice-of-anchor F family protein			
	11	1	hypothetical protein	<i>Proteobacteria</i>	<i>Acinetobacter</i>	
		1	outer membrane protein Omp38			
		5	OmpA family protein			
		12	1			OmpA family protein
		13	1			OmpA family protein
		14	1			hypothetical protein
		15	1			hypothetical protein
			1	hypothetical protein	<i>Proteobacteria</i>	<i>Pulveribacter</i>
		1	hypothetical protein	<i>Proteobacteria</i>	<i>Polaromonas</i>	

Proteins that incorporated ^{13}C -label was not detected at 0 h.

Table 3 – Substrate utilization properties of the identified protein-degraders in the LP incubation batch. Annotation of the labelled proteins at genus level, number of hits, and metabolic information retrieved from literature are listed.

Genus	Hit counts	Ability to degrade		
		Protein or amino acids	Sugars	Reference
<i>Acinetobacter</i>	87	YES	YES	(Dueholm et al. 2021)
<i>Klebsiella</i>	5	n.a	YES	(Pishchik et al. 1997)
<i>Escherichia</i>	4	YES	YES	(Ud-Din and Wahid 2015)
<i>Enterobacter</i>	1	YES	YES	(Grimont and Grimont 2006)
<i>Syntrophus</i>	1	NO	NO	(Dueholm et al. 2021)
<i>Salmonella</i>	1	YES	YES	(Grimont et al. 2000)
<i>Pulveribacter</i>	1	YES	YES	(Heo et al. 2019)
<i>Shigella</i>	1	NO	NO	(Ud-Din and Wahid 2015)
<i>Staphylococcus</i>	1	YES	YES	(Sivakanesan and Dawes 1980)
<i>Mangrovibacter</i>	1	YES	YES	(Zhang et al. 2015)
<i>Pluralibacter</i>	1	YES	NO	(Brady et al. 2013)
<i>Polaromonas</i>	1	YES	YES	(Dueholm et al. 2021)
Total of assigned proteins	105			

n.a. not available

3.3.2 Protein degraders identified in the LPG incubation batch

Table 4 lists the identified proteins having incorporated ^{13}C -label from the proteinaceous substrate in presence of glucose (LPG). In the LPG incubation batch, the ^{13}C -labelled substrate was found to be incorporated into microorganisms as early as at time 0 h, i.e., 30 min after the incubation bottles were placed into the 25 °C water bath. Three labelled proteins were identified at 0 h and assigned to the genus *Acinetobacter* (**Table 4**). Compared to the LP incubation batch, the incorporation of ^{13}C -labelled substrate into microorganisms occurred earlier in the LPG incubation batch. According to the kinetic study of Deng et al. (2023a), the presence of glucose increased the protein hydrolysis rate by 1.6 - 1.7 times. Glucose might provide energy for the facultative protein-degraders to produce protease, and lead to a faster incorporation of ^{13}C in the LPG incubation batch.

After 6 h, only one protein was labelled; its sequence could not be annotated (hypothetical protein). The number of labelled proteins peaked after 24 h, with seven proteins having incorporated ^{13}C . Most of the labelled proteins were assigned to the proteobacterial genera *Acinetobacter*, *Escherichia*, *Pluralibacter* or *Lysobacter*. The genus level annotation of some

labelled proteins was difficult due to the close genetic relationships among genera *Escherichia*, *Salmonella* and *Shigella* (Silverman et al. 2006). One protein was assigned to the phylum of *Firmicutes*, further related to either the genus *Christensenella* or *Clostridium*. *Clostridia* are known to degrade amino acids and have reported to dominate the microbiome of an anaerobic reactor fed with bovine serum albumin (Tang et al. 2005). After 48 h, only two labelled proteins were detected and were assigned to the proteobacterial genera *Escherichia* or *Lysobacter* and *Xanthomonas*. Similar to the LP incubation batch, most of the labelled proteins in the LPG batch were identified as outer membrane proteins or porin proteins.

In addition, **Table 5** shows the substrate utilization of the labelled protein-degraders in the LPG incubation batch. *Acinetobacter* and *Escherichia* were the most frequently identified genera that metabolised the ^{13}C -labelled protein substrate. Both populations are capable of degrading proteins and sugars, through respiration and fermentation, respectively (Dueholm et al. 2021, Ud-Din and Wahid 2015).

Table 4 - Identified protein that incorporated the ^{13}C -label supplied by the proteinaceous substrate in the LPG incubation batch. Samples were measured for protein-SIP after 0, 6, 24 and 48 h. The number of reference proteins with over 99% matching identity (Hits) are given, together with their functional and phylogenetic annotations (at phylum and genus level).

Sample Time	Labelled protein ID	Hits	Protein	Phylum	Genus
0 h	1	1	outer membrane protein		
		2	Outer membrane protein Omp38	<i>Proteobacteria</i>	<i>Acinetobacter</i>
		7	OmpA family protein		
	2	2	Outer membrane protein Omp38	<i>Proteobacteria</i>	<i>Acinetobacter</i>
		5	OmpA family protein		
		3	Outer membrane protein Omp38	<i>Proteobacteria</i>	<i>Acinetobacter</i>
6 h	1	10	OmpA family protein		
		1	hypothetical protein		
24 h	1	1	outer membrane protein II		
		1	outer membrane protein A precursor		<i>Escherichia</i>
		1	outer membrane protein A	<i>Proteobacteria</i>	
		1	Unclassified		<i>Lysobacter</i>
		2	porin OmpA		<i>Escherichia</i>
	2	1	outer membrane protein II		
		1	outer membrane protein A precursor		<i>Escherichia</i>
		1	outer membrane protein A	<i>Proteobacteria</i>	
		2	OmpA/MotB domain protein		<i>Pluralibacter</i>
		1	porin OmpA		<i>Escherichia</i>
	3	1	Unclassified	<i>Firmicutes</i>	<i>Christensenella</i>
		1	Unclassified		<i>Clostridium</i>
	4	1	outer membrane protein II		
		1	outer membrane protein A	<i>Proteobacteria</i>	<i>Escherichia</i>

		2	porin OmpA		
		1	porin OmpA		<i>Escherichia</i>
	5	1	Unclassified	<i>Proteobacteria</i>	
		1	outer membrane protein Omp38		<i>Acinetobacter</i>
		6	OmpA family protein		
	6	1	outer membrane protein II		<i>Escherichia</i>
		2	outer membrane protein A	<i>Proteobacteria</i>	
		2	porin OmpA		<i>Escherichia</i>
		1	Unclassified		<i>Lysobacter</i>
		1	outer membrane protein II		<i>Escherichia</i>
		1	outer membrane protein II		<i>Shimwellia</i>
		1	outer membrane protein II		<i>Citrobacter</i>
		1	outer membrane protein A		<i>Salmonella</i>
		1	outer membrane protein A		<i>Shigella</i>
	7	2	outer membrane protein A	<i>Proteobacteria</i>	<i>Escherichia</i>
		1	outer membrane protein A		<i>Serratia</i>
		1	membrane protein		<i>Serratia</i>
		1	porin OmpA		<i>Escherichia</i>
		1	porin OmpA		<i>Klebsiella</i>
		1	porin OmpA		<i>Enterobacter</i>
		1	outer membrane protein II		<i>Escherichia</i>
48 h	1	2	outer membrane protein A	<i>Proteobacteria</i>	
		1	Unclassified		<i>Lysobacter</i>
		2	porin OmpA		<i>Escherichia</i>
	2	1	Unclassified	<i>Proteobacteria</i>	<i>Xanthomonas</i>

Table 5 - Annotation of the labelled proteins at genus level and metabolic information retrieved from literature on the substrate utilization properties of the identified protein degraders in the LPG incubation batch.

Genus	Hit counts	Ability to degrade		
		Proteins or amino acids	Sugars	Reference
<i>Acinetobacter</i>	35	YES	YES	(Dueholm et al. 2021)
<i>Christensenella</i>	1	n.a.	YES	(Morotomi et al. 2012)
<i>Citrobacter</i>	1	YES	YES	(Brenner et al. 1999)
<i>Clostridium</i>	1	YES	YES	(Dueholm et al. 2021) (Grimont and Grimont 2006)
<i>Enterobacter</i>	1	YES	YES	
<i>Escherichia</i>	28	YES	YES	(Ud-Din and Wahid 2015)
<i>Klebsiella</i>	1	n.a.	YES	(Pishchik et al. 1997)
<i>Lysobacter</i>	3	YES	YES	(Dueholm et al. 2021)
<i>Pluralibacter</i>	2	YES	YES	(Heo et al. 2019)
<i>Salmonella</i>	1	YES	YES	(Grimont et al. 2000)
<i>Serratia</i>	2	YES	YES	(Dueholm et al. 2021)
<i>Shigella</i>	1	NO	NO	(Ud-Din and Wahid 2015)
<i>Shimwellia</i>	1	n.a.	n.a.	
<i>Xanthomonas</i>	1	n.a.	n.a.	
Total of assigned proteins	79			

n.a. not available.

3.3.3 *Acinetobacter* as the main protein-degraders

Figure 3A displays the scaffold coverage and GC content of the metagenome of the microbial community, overlaid by the protein-SIP data. The eight scaffolds holding the labelled protein detected in the LP incubation batch are highlighted in yellow, whereas the fourteen scaffolds holding the labelled protein detected in the LPG incubation batch are highlighted in red. The phyla *Firmicutes* and *Proteobacteria*, to which the scaffolds are affiliated, are coloured. The results indicate that *Acinetobacter* was the active protein degrader in the communities of the incubations conducted in both absence and presence of glucose. According to the community profiles, *Acinetobacter* and an unclassified *Clostridiales* were selected over the 96 h of incubation (**Figure 2B**), supporting the preponderance of these organisms.

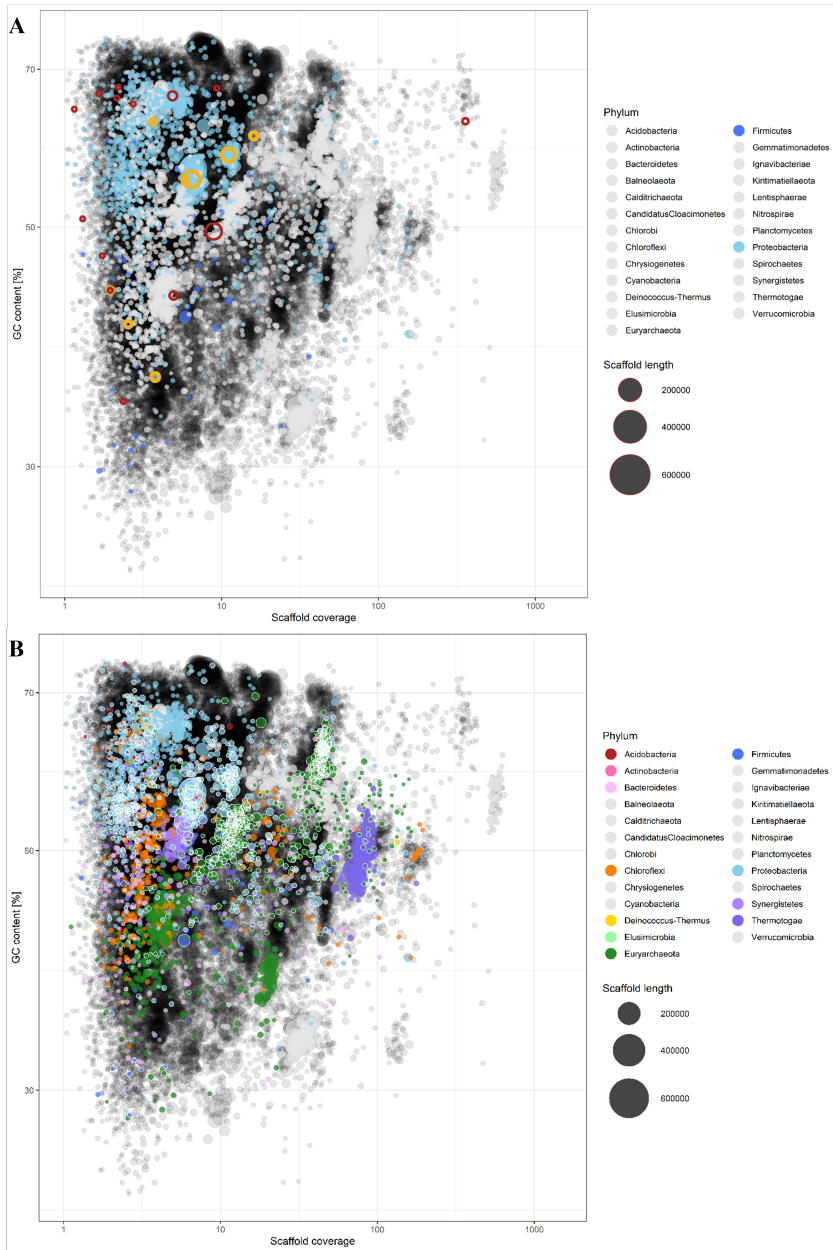


Figure 3 - Identification of protein-degraders in the bacterial community. The scaffold coverage from the generated metagenome with a minimum length of 5000 bp is plotted against the GC content, the dot sizes indicate the length of the scaffold. A) The scaffolds holding labelled proteins identified by stable isotope probing (SIP) and proteogenomics are highlighted in yellow (LP incubation batch) and red (LPG incubation batch), and the affiliated phyla are coloured. B) The phyla holding protease are coloured and the genera are highlighted in white.

Acinetobacter is generally regarded as obligate aerobic, often present in anaerobic-aerobic sequencing batch reactors (SBR) operated for biological removal of organic matter, phosphorus and nitrogen from wastewater (Lang et al. 2020, Shelly et al. 2021). This genus has been selected when the readily biodegradable substrate was leaking from the anaerobic to the aerobic phase of a granular sludge SBR (Weissbrodt et al. 2012). The species *Acinetobacter baumannii* DT and *Acinetobacter H12* can survive under conditions without air supply (Ali et al. 2021, Oanh et al. 2020). *Acinetobacter* can remove phosphorus (van Groenestijn et al. 1987), but is not the main phosphorus-accumulating organism (PAO) in WWTPs (Nielsen et al. 2012).

In previous studies, the genera *Clostridium* (McInerney 1988), *Peptostrptococcus* (Dürre et al. 1983), *Acidaminobacter* (Stams and Hansen 1984), *Aminomonas* (Baena et al. 1999), *Thermanaerovibrio* (Nanninga et al. 1987), *Sporanaerobacter* (Hernandez-Eugenio et al. 2002), *Sedimentibacter* (Breitenstein et al. 2002), *Aminobacterium* (Baena et al. 2000), *Tissierella* and *Lutispora* (Chen et al. 2018) have been able to ferment amino acids or proteins. Most of the known anaerobic degraders of amino acids belong to the phylum *Firmicutes*. In addition, the genus *Bacteroides* (phylum of *Bacteroidetes*), and the genera *Streptococcus*, *Clostridium*, *Bacillus* and *Staphylococcus* (phylum of *Firmicutes*) are protein-degraders in the human gut (Macfarlane et al. 1986), whereas ruminal protozoa are important protein degraders in cow rumen (McInerney 1988). According to the UniProt database and literature, the known protein-degraders that hold a protease were identified from the metagenome of the incubated biomass (**Figure 3B**). A detailed list of the genera is given in **Table S2** in supplementary information.

Although *Acinetobacter* is one of the genera that harbour proteases (**Table S2**), it has been seldom reported as the main protein degrader in anaerobic digestion. The identification of *Acinetobacter* as the main protein degrader in this chapter is therefore interesting and intriguing. According to Sadat-Mekmene et al. (2011), the function of the outer membrane protein and porin membrane can possess a cell envelope-associated protease, which hydrolyse proteinaceous substrates on the surface of the cell and facilitate transport of the formed peptides into the cell. The cell envelope-bounding protease activity has been reported in *Acinetobacter calcoaceticus* under aerobic conditions (Fricke et al. 1987); and the growth and respiratory efficiency of *Acinetobacter calcoaceticus* is reported to be unaffected by

oxygen concentration in the range of 0.0 – 0.8 mg·L⁻¹ (Hardy and Dawes 1985). However, according to Pulami et al. (2021), the *Acinetobacter* can survive under anaerobic conditions, but thus far, no growth of the population was observed. The metabolism of protein degradation by *Acinetobacter*, whether via fermentation or anaerobic respiration is still unclear.

3.3.4 Possible metabolic pathway of *Acinetobacter* under anaerobic conditions

To investigate the metabolic pathway coded in the genome of *Acinetobacter* for the biodegradation of proteins, a metabolic model was built using the MAG of *Acinetobacter* that was extracted from the sequenced metagenome. The *Acinetobacter* MAG had a 14.5 % completeness and 0.0 % contamination. We re-annotated the *Acinetobacter* MAG and compared it with 30 complete reference genomes of *Acinetobacter* species downloaded from NCBI database (supplementary **Figure S5**).

As shown in **Figure 4**, the valine (Val), leucine (Leu), and isoleucine (Ile) can be degraded by *Acinetobacter* through the TCA cycle. The pathway for fermentation of VFAs was not found in the built *Acinetobacter* metabolic model. The metabolism of fatty acids leads to the production of acetyl-CoA instead of VFAs, which may explain the low VFA concentration during the incubations (supplementary **Figure S2**). The TCA cycle provides energy to organisms through oxidation of acetyl-CoA derived from carbohydrates, proteins, and fatty acids. The TCA cycle is involved through respiration (Thauer 1988).

Known terminal acceptors involved in anaerobic respiration include organic compounds, i.e., fumarate, dimethyl sulfoxide, and trimethylamine N-oxide, or inorganic compounds, i.e., nitrate (NO₃⁻), nitrite (NO₂⁻), nitrous oxide (N₂O), chlorate (ClO₃⁻), perchlorate, oxidised manganese ions, ferric iron (Fe³⁺), gold (Au), selenate, arsenate, sulfate (SO₄²⁻) and elemental sulfur (S⁰) (Caspi et al., 2018). Possibly, the labelled *Acinetobacter* in the LP and LPG incubation batches degraded protein through anaerobic respiration, using terminal electron acceptors such as SO₄²⁻, phosphate (PO₄³⁻) and Fe³⁺ that are supposed to be present in slaughterhouse wastewaters.

Another possible e-acceptor is oxygen (O₂) that might have been present in the gas collection tube that was connected to the outlet of the lid. However, the total volume of liquid samples taken was 25 mL during the 96 h incubation. Based on this and ignoring the gas production

from substrate degradation, a maximum total volume of 5 mL of O₂ (i.e., 7.1 mg COD) could have diffused back from the tube into the incubation bottles due to pressure change. Considering the reduced TCOD of $1000 \pm 100 \text{ mg} \cdot \text{L}^{-1}$ in the LP and LPG incubation batches, the amount of O₂ was too low to serve as the terminal electron acceptor.

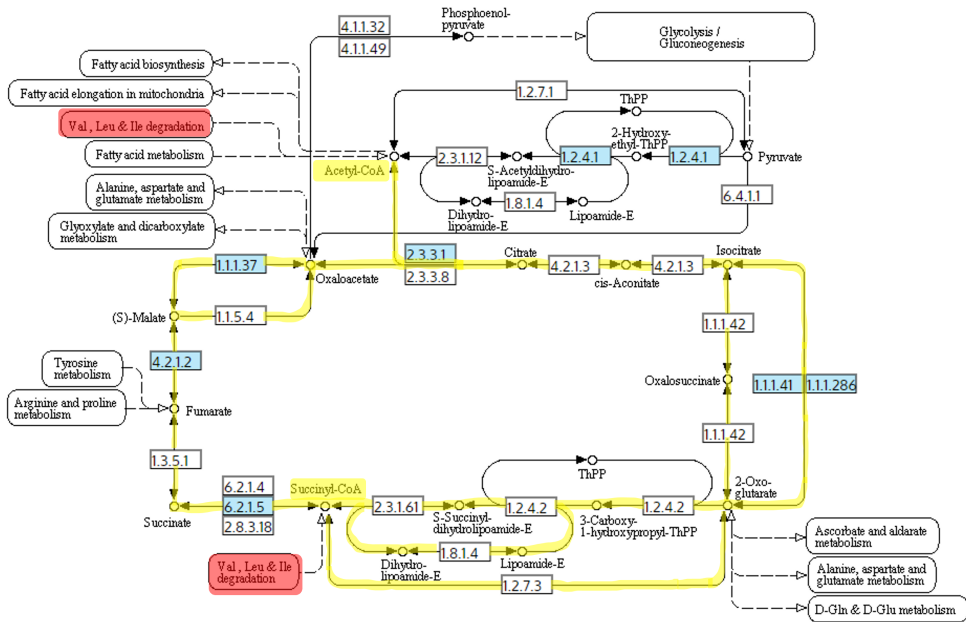


Figure 4 - Model of the TCA cycle constructed based on the extracted *Acinetobacter* MAG by using the “Gapfill Metabolic model” in KBase, the presence of metabolic reactions are highlighted in blue.

3.3.5 Discussion on anaerobic digestion of proteins

Based on the built metabolic model and the estimated maximum available volume of O₂, *Acinetobacter* seemed to primarily metabolise proteins and glucose through anaerobic respiration during the incubation. Anaerobic respiration of glucose is more energy-efficient than amino acids, i.e., the glycolysis of 1 mole glucose to pyruvate provides 2 moles ATP (Melkonian and Schury 2019), whereas the conversion of 1 mole alanine or serine to pyruvate provides 0 mole ATP (Jakubowski et al. 2022). The reason for the lower NH₄⁺-N /TN conversion ratio measured in the LPG incubation batch conducted with a mixture of proteins and glucose can be attributed to a higher energy efficiency in the anaerobic respiration of glucose than amino acids, thus resulting in less proteins degraded and less NH₄⁺ produced.

Due to a lack of quantification of the potential terminal electron acceptors, the actual metabolic pathway for anaerobic protein degradation by *Acinetobacter* could not be concluded. It is recommended to examine the anaerobic metabolism of glucose and protein by *Acinetobacter* experimentally in future research.

A feast-famine scheme can allow the depletion of compounds that are rapidly metabolised during the feast phase and the degradation of the slower-biodegradable compounds in the famine phase. Protein has been observed to accumulate to a lower extent in an AnSBR than in a continuously-fed reactor (Tan et al. 2021). The feast-famine regime is deemed advantageous for protein-degraders, which can facilitate the sequential consumption of carbohydrates and proteins. Therefore, the approach is recommended for AD of protein-rich streams.

Additionally, the relative abundance of *Acinetobacter* in the LPG incubation batch was 0.5 – 1.0 % lower than in the LP incubation batch (**Figure 2B**), which might also contribute to the lower protein degradation. The observed phenomenon aligns with the findings of Chen et al. (2018), who demonstrated that the enrichment of protein-utilizing bacteria enhances biogas production from protein-rich sludge. Consequently, to enhance the AD of protein-rich streams, it is recommended to increase the population of active protein-degraders.

4 Conclusions

This chapter aimed for the identification of the main bacterial populations that degrade proteins in the environment of an anaerobic digester. From incubations with a ^{13}C -labelled proteinaceous substrate followed by protein-SIP and proteogenomics analyses, we conclude that:

- *Acinetobacter* was identified as one predominant active degrader of proteins in both the absence and presence of glucose in the medium. It is the first time that *Acinetobacter* is reported to consume both proteins and carbohydrates under anaerobic conditions.
- Outer membrane-bound proteins and porin proteins were the most frequently labelled by ^{13}C in the biomass. These proteins can act as cell envelope-bound proteases and peptide transporters.
- The anaerobic metabolism of glucose and proteins by *Acinetobacter* remains to be elucidated experimentally in future research. Metabolic pathway analysis conducted on its MAG highlighted that amino acids can be anaerobically respired in the presence of alternative electron acceptors, e.g., sulphate and ferric iron, that are likely present in slaughterhouse wastewater.

Supporting information

Table S1 - Composition of Silantes OD2 growth media.

Component	Composition (g/g DCW)
protein	0.68
Phospholipid	0.05
Cofactors and vitamins	0.03
Cell wall	0.15
Peptidoglycan	0.09
Ash	0.00

Table S₂ - List of known protein degraders that holding protease according to literature and UniProt database.

Kingdom	Phylum	Genus	Reference
Bacteria	<i>Acidobacteria</i>	<i>Candidatus Koribacter</i>	UniProt
Bacteria	<i>Acidobacteria</i>	<i>Candidatus Solibacter</i>	UniProt
Bacteria	<i>Actinobacteria</i>	<i>Acidimicrobium</i>	UniProt
Bacteria	<i>Actinobacteria</i>	<i>Acidothermus</i>	UniProt
Bacteria	<i>Actinobacteria</i>	<i>Actinosynnema</i>	UniProt
Bacteria	<i>Actinobacteria</i>	<i>Arthrobacter</i>	UniProt
Bacteria	<i>Actinobacteria</i>	<i>Beutenbergia</i>	UniProt
Bacteria	<i>Actinobacteria</i>	<i>Catenulispora</i>	UniProt
Bacteria	<i>Actinobacteria</i>	<i>Frankia</i>	UniProt
Bacteria	<i>Actinobacteria</i>	<i>Geodermatophilus</i>	UniProt
Bacteria	<i>Actinobacteria</i>	<i>Gordonia</i>	UniProt
Bacteria	<i>Actinobacteria</i>	<i>Jonesia</i>	UniProt
Bacteria	<i>Actinobacteria</i>	<i>Kineococcus</i>	UniProt
Bacteria	<i>Actinobacteria</i>	<i>Kribbella</i>	UniProt
Bacteria	<i>Actinobacteria</i>	<i>Mycobacterium</i>	UniProt
Bacteria	<i>Actinobacteria</i>	<i>Mycobacteroides</i>	UniProt
Bacteria	<i>Actinobacteria</i>	<i>Mycolicibacterium</i>	UniProt
Bacteria	<i>Actinobacteria</i>	<i>Nakamurella</i>	UniProt
Bacteria	<i>Actinobacteria</i>	<i>Nocardia</i>	UniProt
Bacteria	<i>Actinobacteria</i>	<i>Nocardioides</i>	UniProt
Bacteria	<i>Actinobacteria</i>	<i>Paenarthrobacter</i>	UniProt
Bacteria	<i>Actinobacteria</i>	<i>Pseudarthrobacter</i>	UniProt
Bacteria	<i>Actinobacteria</i>	<i>Renibacterium</i>	UniProt
Bacteria	<i>Actinobacteria</i>	<i>Rhodococcus</i>	UniProt
Bacteria	<i>Actinobacteria</i>	<i>Saccharomonospora</i>	UniProt
Bacteria	<i>Actinobacteria</i>	<i>Saccharopolyspora</i>	UniProt
Bacteria	<i>Actinobacteria</i>	<i>Salinispora</i>	UniProt

Kingdom	Phylum	Genus	Reference
Bacteria	<i>Actinobacteria</i>	<i>Sanguibacter</i>	UniProt
Bacteria	<i>Actinobacteria</i>	<i>Stackebrandtia</i>	UniProt
Bacteria	<i>Actinobacteria</i>	<i>Streptomyces</i>	UniProt
Bacteria	<i>Actinobacteria</i>	<i>Streptosporangium</i>	UniProt
Bacteria	<i>Actinobacteria</i>	<i>Thermobifida</i>	UniProt
Bacteria	<i>Actinobacteria</i>	<i>Thermomonospora</i>	UniProt
Bacteria	<i>Actinobacteria</i>	<i>Xylanimonas</i>	UniProt
Bacteria	<i>Aquificae</i>	<i>Aquifex</i>	UniProt
Bacteria	<i>Aquificae</i>	<i>Sulfurihydrogenibium</i>	UniProt
Bacteria	<i>Bacteroidetes</i>	<i>Candidatus Amoebophilus</i>	UniProt
Bacteria	<i>Bacteroidetes</i>	<i>Candidatus Sulcia</i>	UniProt
Bacteria	<i>Bacteroidetes</i>	<i>Chloroherpeton</i>	UniProt
Bacteria	<i>Bacteroidetes</i>	<i>Cytophaga</i>	UniProt
Bacteria	<i>Bacteroidetes</i>	<i>Flavobacterium</i>	UniProt
Bacteria	<i>Bacteroidetes</i>	<i>Parabacteroides</i>	UniProt
Bacteria	<i>Bacteroidetes</i>	<i>Porphyromonas</i>	UniProt
Bacteria	<i>Bacteroidota</i>	<i>Acetobacteroides</i>	(Dueholm et al., 2021)
Bacteria	<i>Bacteroidota</i>	<i>Bacteroides (or Prevotella)</i>	(Macfarlane et al., 1986)
Bacteria	<i>Chlamydiae</i>	<i>Candidatus Protochlamydia</i>	UniProt
Bacteria	<i>Chlamydiae</i>	<i>Chlamydia</i>	UniProt
Bacteria	<i>Chloroflexi</i>	<i>Chloroflexus</i>	UniProt
Bacteria	<i>Chloroflexi</i>	<i>Herpetosiphon</i>	UniProt
Bacteria	<i>Chloroflexi</i>	<i>Roseiflexus</i>	UniProt
Bacteria	<i>Coprothermobacterota</i>	<i>Coprothermobacter</i>	UniProt
Bacteria	<i>Deinococcus-Thermus</i>	<i>Deinococcus</i>	UniProt
Bacteria	<i>Deinococcus-Thermus</i>	<i>Thermus</i>	UniProt
Bacteria	<i>Dictyoglomi</i>	<i>Dictyoglomus</i>	UniProt
Bacteria	<i>Elusimicrobia</i>	<i>Endomicrobium</i>	UniProt

Kingdom	Phylum	Genus	Reference
Bacteria	<i>Firmicutes</i>	<i>Acidaminobacter</i>	(Stams and Hansen, 1984)
Bacteria	<i>Firmicutes</i>	<i>Alicyclobacillus</i>	UniProt
Bacteria	<i>Firmicutes</i>	<i>Alkalihalobacillus</i>	UniProt
Bacteria	<i>Firmicutes</i>	<i>Bacillus</i>	UniProt
Bacteria	<i>Firmicutes</i>	<i>Brevibacillus</i>	UniProt
Bacteria	<i>Firmicutes</i>	<i>Caldanaerobacter</i>	UniProt
Bacteria	<i>Firmicutes</i>	<i>Caldicellulosiruptor</i>	UniProt
Bacteria	<i>Firmicutes</i>	<i>Clostridioides</i>	UniProt
Bacteria	<i>Firmicutes</i>	<i>Clostridium</i>	UniProt
Bacteria	<i>Firmicutes</i>	<i>Desulforamulus</i>	UniProt
Bacteria	<i>Firmicutes</i>	<i>Enterococcus</i>	UniProt
Bacteria	<i>Firmicutes</i>	<i>Finegoldia</i>	UniProt
Bacteria	<i>Firmicutes</i>	<i>Geobacillus</i>	UniProt
Bacteria	<i>Firmicutes</i>	<i>Halothermothrix</i>	UniProt
Bacteria	<i>Firmicutes</i>	<i>Heliomicrobium</i>	UniProt
Bacteria	<i>Firmicutes</i>	<i>Lachnoclostridium</i>	UniProt
Bacteria	<i>Firmicutes</i>	<i>Lacticaseibacillus</i>	UniProt
Bacteria	<i>Firmicutes</i>	<i>Lactobacillus</i>	(Dueholm et al., 2021)
Bacteria	<i>Firmicutes</i>	<i>Lactococcus</i>	UniProt
Bacteria	<i>Firmicutes</i>	<i>Oceanobacillus</i>	UniProt
Bacteria	<i>Firmicutes</i>	<i>Paenibacillus</i>	UniProt
Bacteria	<i>Firmicutes</i>	<i>Paraclostridium</i>	(Dueholm et al., 2021)
Bacteria	<i>Firmicutes</i>	<i>Priestia</i>	UniProt
Bacteria	<i>Firmicutes</i>	<i>Proteiniclasticum</i>	(Li et al., 2015a)
Bacteria	<i>Firmicutes</i>	<i>Sedimentibacter</i>	(Breitenstein et al., 2002)
Bacteria	<i>Firmicutes</i>	<i>Sporanaerobacter</i>	(Hernandez-Eugenio et al., 2002)
Bacteria	<i>Firmicutes</i>	<i>Staphylococcus</i>	UniProt
Bacteria	<i>Firmicutes</i>	<i>Streptococcus (Lactococcus)</i>	(Macfarlane et al., 1986)

Kingdom	Phylum	Genus	Reference
Bacteria	<i>Firmicutes</i>	<i>Syntrophomonas</i>	UniProt
Bacteria	<i>Firmicutes</i>	<i>Tissierella</i>	(Chen et al., 2018)
Bacteria	<i>Fusobacteria</i>	<i>Fusobacterium</i>	UniProt
Bacteria	<i>Proteobacteria</i>	<i>Achromobacter</i>	UniProt
Bacteria	<i>Proteobacteria</i>	<i>Acinetobacter</i>	UniProt
Bacteria	<i>Proteobacteria</i>	<i>Anaeromyxobacter</i>	UniProt
Bacteria	<i>Proteobacteria</i>	<i>Azorhizobium</i>	UniProt
Bacteria	<i>Proteobacteria</i>	<i>Azospirillum</i>	UniProt
Bacteria	<i>Proteobacteria</i>	<i>Bdellovibrio</i>	UniProt
Bacteria	<i>Proteobacteria</i>	<i>Brucella</i>	UniProt
Bacteria	<i>Proteobacteria</i>	<i>Buchnera</i>	UniProt
Bacteria	<i>Proteobacteria</i>	<i>Campylobacter</i>	UniProt
Bacteria	<i>Proteobacteria</i>	<i>Campylobacter</i>	UniProt
Bacteria	<i>Proteobacteria</i>	<i>Caulobacter</i>	UniProt
Bacteria	<i>Proteobacteria</i>	<i>Citri fermentans</i>	UniProt
Bacteria	<i>Proteobacteria</i>	<i>Desulfatibacillum</i>	UniProt
Bacteria	<i>Proteobacteria</i>	<i>Desulfosudis</i>	UniProt
Bacteria	<i>Proteobacteria</i>	<i>Desulfotalea</i>	UniProt
Bacteria	<i>Proteobacteria</i>	<i>Desulfovibrio</i>	UniProt
Bacteria	<i>Proteobacteria</i>	<i>Dichelobacter</i>	UniProt
Bacteria	<i>Proteobacteria</i>	<i>Dickeya</i>	UniProt
Bacteria	<i>Proteobacteria</i>	<i>Erwinia</i>	UniProt
Bacteria	<i>Proteobacteria</i>	<i>Escherichia</i>	UniProt
Bacteria	<i>Proteobacteria</i>	<i>Francisella</i>	UniProt
Bacteria	<i>Proteobacteria</i>	<i>Geobacter</i>	UniProt
Bacteria	<i>Proteobacteria</i>	<i>Haemophilus</i>	UniProt
Bacteria	<i>Proteobacteria</i>	<i>Helicobacter</i>	UniProt
Bacteria	<i>Proteobacteria</i>	<i>Hydrogenovibrio</i>	UniProt

Kingdom	Phylum	Genus	Reference
Bacteria	<i>Proteobacteria</i>	<i>Lawsonia</i>	UniProt
Bacteria	<i>Proteobacteria</i>	<i>Lysobacter</i>	UniProt
Bacteria	<i>Proteobacteria</i>	<i>Magnetococcus</i>	UniProt
Bacteria	<i>Proteobacteria</i>	<i>Methylocella</i>	UniProt
Bacteria	<i>Proteobacteria</i>	<i>Myxococcus</i>	UniProt
Bacteria	<i>Proteobacteria</i>	<i>Neorickettsia</i>	UniProt
Bacteria	<i>Proteobacteria</i>	<i>Nitrosococcus</i>	UniProt
Bacteria	<i>Proteobacteria</i>	<i>Orientia</i>	UniProt
Bacteria	<i>Proteobacteria</i>	<i>Paraburkholderia</i>	UniProt
Bacteria	<i>Proteobacteria</i>	<i>Phenylobacterium</i>	UniProt
Bacteria	<i>Proteobacteria</i>	<i>Photorhabdus</i>	UniProt
Bacteria	<i>Proteobacteria</i>	<i>Proteus</i>	UniProt
Bacteria	<i>Proteobacteria</i>	<i>Pseudomonas</i>	UniProt
Bacteria	<i>Proteobacteria</i>	<i>Rickettsia</i>	UniProt
Bacteria	<i>Proteobacteria</i>	<i>Serratia</i>	UniProt
Bacteria	<i>Proteobacteria</i>	<i>Shigella</i>	UniProt
Bacteria	<i>Proteobacteria</i>	<i>Sinorhizobium</i>	UniProt
Bacteria	<i>Proteobacteria</i>	<i>Sorangium</i>	UniProt
Bacteria	<i>Proteobacteria</i>	<i>Stenotrophomonas</i>	UniProt
Bacteria	<i>Proteobacteria</i>	<i>Syntrophobacter</i>	UniProt
Bacteria	<i>Proteobacteria</i>	<i>Syntrophotalea</i>	UniProt
Bacteria	<i>Proteobacteria</i>	<i>Syntrophus</i>	UniProt
Bacteria	<i>Proteobacteria</i>	<i>Trichlorobacter</i>	UniProt
Bacteria	<i>Proteobacteria</i>	<i>Vibrio</i>	UniProt
Bacteria	<i>Proteobacteria</i>	<i>Wolbachia</i>	UniProt
Bacteria	<i>Proteobacteria</i>	<i>Xanthomonas</i>	UniProt
Bacteria	<i>Spirochaetes</i>	<i>Borrelia</i>	UniProt
Bacteria	<i>Spirochaetes</i>	<i>Borreliella</i>	UniProt

Kingdom	Phylum	Genus	Reference
Bacteria	<i>Spirochaetes</i>	<i>Leptospira</i>	UniProt
Bacteria	<i>Spirochaetes</i>	<i>Treponema</i>	UniProt
Bacteria	<i>Synergistota</i>	<i>Aminobacterium</i>	(Baena et al., 2000)
Bacteria	<i>Synergistota</i>	<i>Thermanaerovibrio</i>	(Nanninga et al., 1987)
Bacteria	<i>Tenericutes</i>	<i>Candidatus Phytoplasma</i>	UniProt
Bacteria	<i>Tenericutes</i>	<i>Malacoplasma</i>	UniProt
Bacteria	<i>Tenericutes</i>	<i>Metamycoplasma</i>	UniProt
Bacteria	<i>Tenericutes</i>	<i>Ureaplasma</i>	UniProt
Bacteria	<i>Tenericutes</i>	<i>Mesomycoplasma</i>	UniProt
Bacteria	<i>Tenericutes</i>	<i>Mycoplasma</i>	UniProt
Bacteria	<i>Tenericutes</i>	<i>Mycoplasma</i>	UniProt
Bacteria	<i>Thermotogae</i>	<i>Fervidobacterium</i>	UniProt
Bacteria	<i>Thermotogae</i>	<i>Pseudoothermotoga</i>	UniProt
Bacteria	/	<i>Aminomonas</i>	(Baena et al., 1999)
Bacteria	/	<i>Lutispora</i>	(Chen et al., 2018)
Bacteria	/	<i>Peptostreptococcus</i>	(Dürre et al., 1983)
Archaea	<i>Candidatus Thermoplasmatota</i>	<i>Aciduliprofundum</i>	UniProt
Archaea	<i>Candidatus Thermoplasmatota</i>	<i>Picrophilus</i>	UniProt
Archaea	<i>Candidatus Thermoplasmatota</i>	<i>Thermoplasma</i>	UniProt
Archaea	<i>Crenarchaeota</i>	<i>Aeropyrum</i>	UniProt
Archaea	<i>Crenarchaeota</i>	<i>Caldivirga</i>	UniProt
Archaea	<i>Crenarchaeota</i>	<i>Desulfurococcus</i>	UniProt
Archaea	<i>Crenarchaeota</i>	<i>Hyperthermus</i>	UniProt
Archaea	<i>Crenarchaeota</i>	<i>Ignicoccus</i>	UniProt
Archaea	<i>Crenarchaeota</i>	<i>Metallosphaera</i>	UniProt
Archaea	<i>Crenarchaeota</i>	<i>Pyrobaculum</i>	UniProt
Archaea	<i>Crenarchaeota</i>	<i>Saccharolobus</i>	UniProt
Archaea	<i>Crenarchaeota</i>	<i>Staphylothermus</i>	UniProt

Kingdom	Phylum	Genus	Reference
Archaea	<i>Crenarchaeota</i>	<i>Sulfolobus</i>	UniProt
Archaea	<i>Crenarchaeota</i>	<i>Sulfurisphaera</i>	UniProt
Archaea	<i>Crenarchaeota</i>	<i>Thermofilum</i>	UniProt
Archaea	<i>Euryarchaeota</i>	<i>Archaeoglobus</i>	UniProt
Archaea	<i>Euryarchaeota</i>	<i>Archaeoglobus</i>	UniProt
Archaea	<i>Euryarchaeota</i>	<i>Ferroglobus</i>	UniProt
Archaea	<i>Euryarchaeota</i>	<i>Haloarcula</i>	UniProt
Archaea	<i>Euryarchaeota</i>	<i>Halobacterium</i>	UniProt
Archaea	<i>Euryarchaeota</i>	<i>Haloferax</i>	UniProt
Archaea	<i>Euryarchaeota</i>	<i>Halomicrobium</i>	UniProt
Archaea	<i>Euryarchaeota</i>	<i>Haloquadratum</i>	UniProt
Archaea	<i>Euryarchaeota</i>	<i>Halorhabdus</i>	UniProt
Archaea	<i>Euryarchaeota</i>	<i>Halorubrum</i>	UniProt
Archaea	<i>Euryarchaeota</i>	<i>Haloterrigena</i>	UniProt
Archaea	<i>Euryarchaeota</i>	<i>Methanobrevibacter</i>	UniProt
Archaea	<i>Euryarchaeota</i>	<i>Methanocaldococcus</i>	UniProt
Archaea	<i>Euryarchaeota</i>	<i>Methanocella</i>	UniProt
Archaea	<i>Euryarchaeota</i>	<i>Methanococcoides</i>	UniProt
Archaea	<i>Euryarchaeota</i>	<i>Methanococcus</i>	UniProt
Archaea	<i>Euryarchaeota</i>	<i>Methanocorpusculum</i>	UniProt
Archaea	<i>Euryarchaeota</i>	<i>Methanoculleus</i>	UniProt
Archaea	<i>Euryarchaeota</i>	<i>Methanohalophilus</i>	UniProt
Archaea	<i>Euryarchaeota</i>	<i>Methanopyrus</i>	UniProt
Archaea	<i>Euryarchaeota</i>	<i>Methanoregula</i>	UniProt
Archaea	<i>Euryarchaeota</i>	<i>Methanosarcina</i>	UniProt
Archaea	<i>Euryarchaeota</i>	<i>Methanosphaera</i>	UniProt
Archaea	<i>Euryarchaeota</i>	<i>Methanosphaerula</i>	UniProt
Archaea	<i>Euryarchaeota</i>	<i>Methanospirillum</i>	UniProt

Kingdom	Phylum	Genus	Reference
Archaea	<i>Euryarchaeota</i>	<i>Methanothermobacter</i>	UniProt
Archaea	<i>Euryarchaeota</i>	<i>Methanotherrix</i>	UniProt
Archaea	<i>Euryarchaeota</i>	<i>Natrialba</i>	UniProt
Archaea	<i>Euryarchaeota</i>	<i>Natronomonas</i>	UniProt
Archaea	<i>Euryarchaeota</i>	<i>Pyrococcus</i>	UniProt
Archaea	<i>Euryarchaeota</i>	<i>Thermococcus</i>	UniProt
Archaea	<i>Nanoarchaeota</i>	<i>Nanoarchaeum</i>	UniProt
Archaea	<i>TACK group</i>	<i>Candidatus Korarchaeum</i>	UniProt
Archaea	<i>TACK group</i>	<i>Cenarchaeum</i>	UniProt
Archaea	<i>TACK group</i>	<i>Nitrosopumilus</i>	UniProt

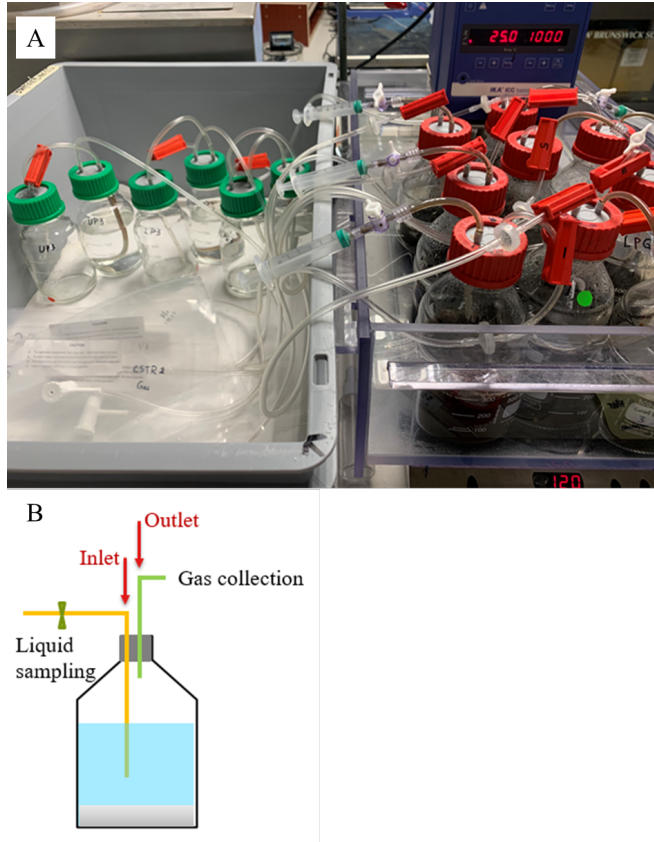


Figure S1 - A) Photo of batch incubation setup and B) schematic diagram of each incubation bottle.

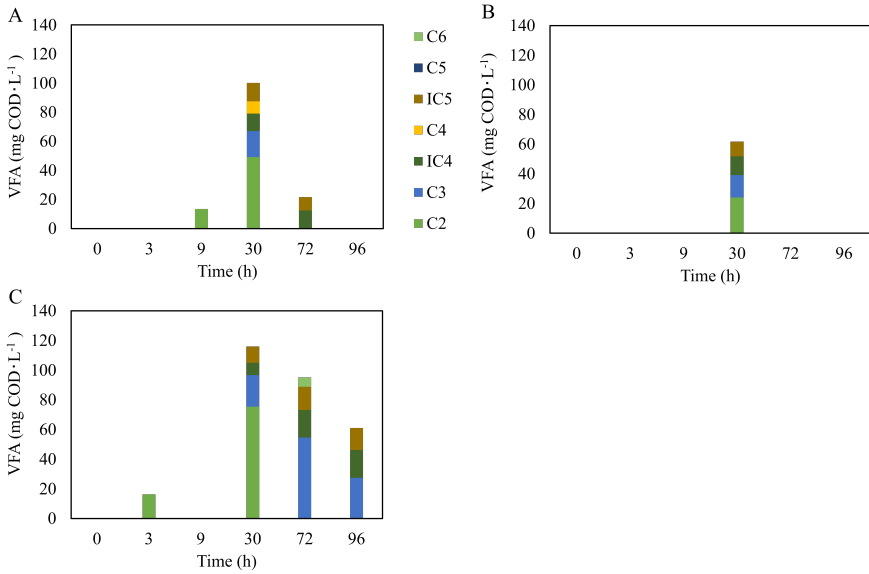


Figure S2 - Concentration and composition of VFAs in the A) UP, B) LP and C) LPG incubation batches. VFAs concentrations of C2-C6 were measured and averaged results were plot in bar chart against sampling time.

Genus	0h									96h								
	UP	LP	LPG	UP	LP	LPG	UP	LP	LPG	UP	LP	LPG	UP	LP	LPG			
<i>Candidatus_Cloacimonas</i>	19.3	16.6	18.2	18.7	18.8	22.8	20.3	18.1	18.7	15	17.1	13.6	18.3	18.6	19.6	16.2	18.3	15.9
<i>unidentified_Anaerolineaceae</i>	7.4	8.1	8.6	7	6.7	5.8	7.3	7.4	8.5	8.8	8.2	7.3	7.8	7.2	8	8.8	7.8	7.6
<i>Acinetobacter</i>	4.2	7	5.3	6.7	5.7	5.2	3.6	6	4.7	5.7	4.7	11.2	5.6	8.8	4.7	4.5	3.8	9.5
<i>Smithella</i>	5.1	5.6	5	5.4	5.3	5.1	5.5	5.3	5.3	4.4	4.7	4.9	4.3	4.6	5.4	4.7	4.9	4.8
<i>Methanosaeta</i>	5.7	3.8	6.2	3.7	4.7	4.7	6.7	4.4	6.2	5.5	4.6	3.8	6.6	4.7	2.4	5.8	5.3	4
<i>Methanobacterium</i>	4.2	3.2	3.5	3.5	3.4	3	4.9	3.2	4	3.5	3.5	3.5	4.5	3.7	3.2	3.7	3.5	3.6
<i>unidentified_Clostridiales</i>	2.9	2.9	2.7	3.2	2.9	2.7	2.7	2.9	2.9	4.6	4.7	5.3	3.9	3.1	3.9	4.5	4.5	5
<i>o_Bacteroidales_OTU_6</i>	2.6	2.3	2.3	2.5	2.6	2.3	2.4	2.5	2.1	2.6	2.5	2.2	2.2	2.4	2.4	2.6	2.6	2.3
<i>o_Bacteroidales_OTU_7</i>	2.5	2.3	2.3	2.2	2.4	2.2	2.3	2.4	2.3	1.9	2	1.7	1.7	2	2	2	2.2	1.7
<i>Syntrophorhabdus</i>	1.9	1.8	2	1.9	1.8	1.7	1.7	1.8	1.7	1.7	1.7	1.9	1.6	1.7	1.8	1.6	1.6	1.6
<i>Mesotoga</i>	0.6	1.7	2	1.4	1.4	1.1	0.6	2	2	1.8	1.4	1.3	3.9	1.5	1.6	1.9	1.3	1.5
<i>f_Syntrophaceae_OTU_16</i>	1.7	1.6	1.3	1.6	1.4	1.4	1.5	1.6	1.3	1.4	1.4	1.3	1.2	1.1	1.4	1.1	1.4	1.2
<i>Denitratisoma</i>	1.6	1.6	1.4	1.7	1.3	1.5	1.3	1.5	1.5	1.1	1.3	1.4	1.1	1.1	1.3	1.2	1.2	1.2
<i>f_Lentimicrobiaceae_OTU_9</i>	1.4	1.4	1.4	1.4	1.4	1.4	1.3	1.2	1.5	1.3	1.2	1.3	1.2	1.1	1.5	1.2	1.3	1.3
<i>f_Prolixibacteraceae_OTU_10</i>	1.5	1.4	1.3	1.3	1.4	1.3	1.4	1.4	1.4	1	1.2	1.1	1.1	1.1	1.3	1.2	1.3	1.3

Figure S3 - Evolutions of top 15 genera in UP, LP, and LPG incubation bottles over the 96 h incubation period. V3-V4 amplicon sequencing profiles were analysed.

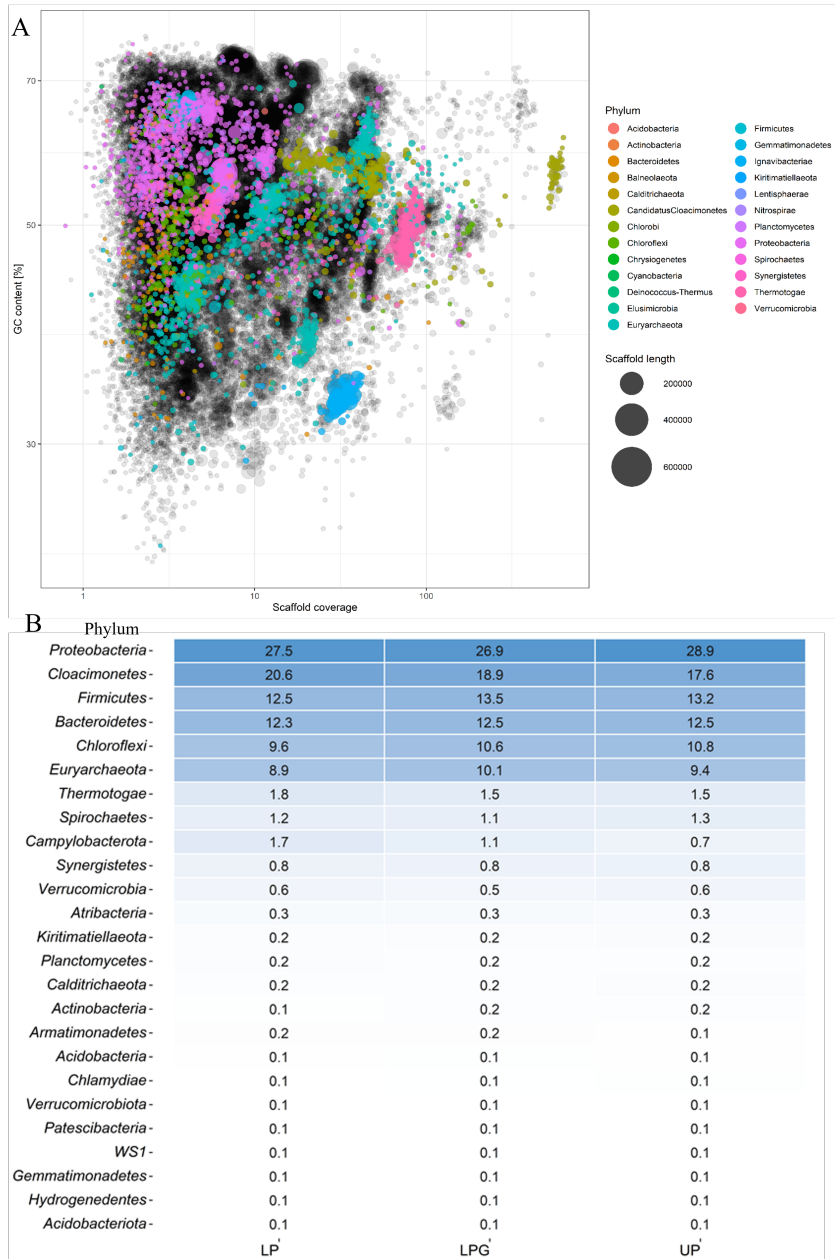


Figure S4 - Comparison of phyla relative abundance in MAG and amplicon sequencing results. A) The scaffold coverage of the metagenome is plotted against the GC content, and the scaffolds are coloured by phylum and have a minimum length of 5000 bp, the length of the scaffolds are indicated by the sizes of the dot. B) The averaged relative abundance of the top 25 phyla in the UP, LP, and LPG incubation batches.

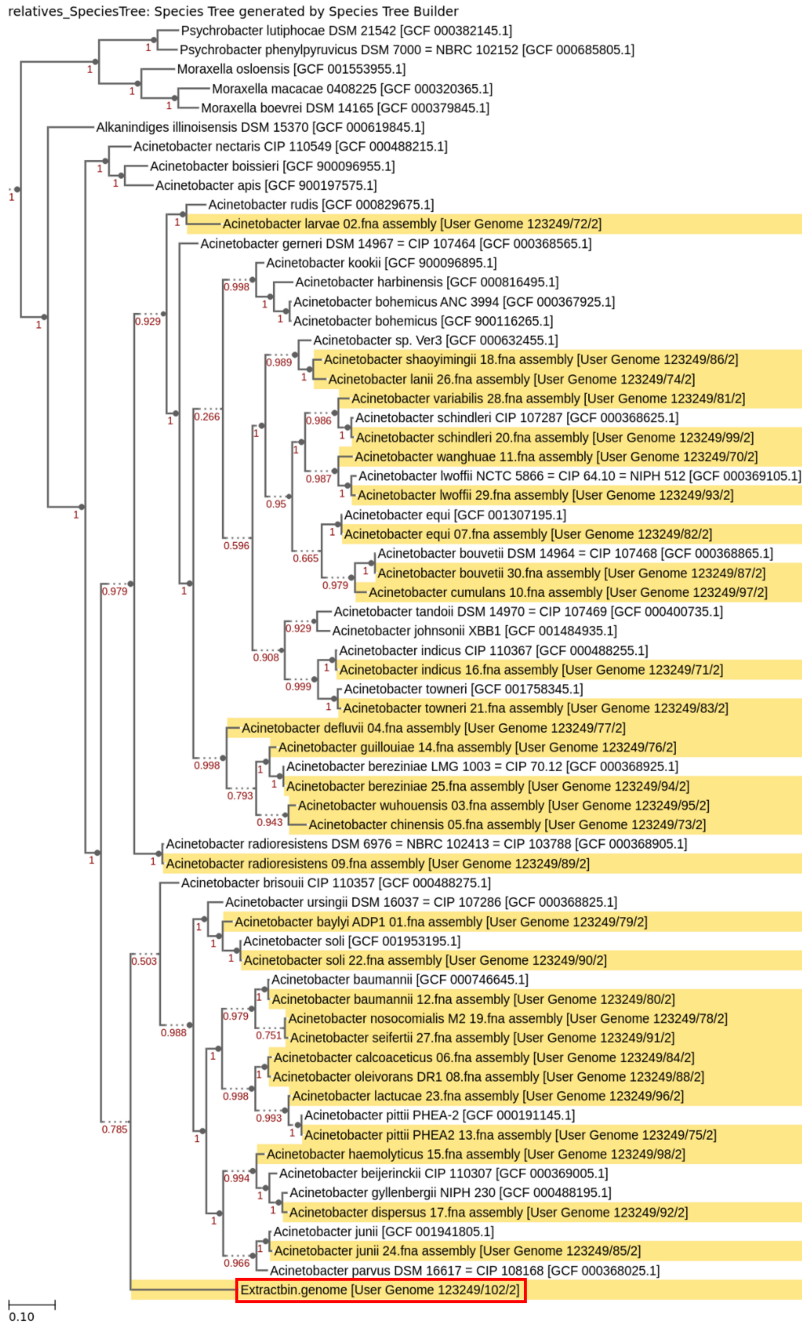


Figure S5 - Phylogenetic analysis of the *Acinetobacter* genome bin extracted from the generated metagenome. Thirty complete *Acinetobacter* reference genomes were downloaded from the NCBI database and highlighted in yellow, and the extracted *Acinetobacter* genome was highlighted in red rectangle.

CHAPTER 6

EFFECT OF OPERATIONAL PARAMETERS ON THE PERFORMANCE OF AN ANEROBIC SEQUENCING BATCH REACTOR TREATING PROTEIN-RICH WASTEWATER

This Chapter is based on: Deng, Z., Muñoz Sierra, J., Ferreira, A.L.M., Cerqueda-Garcia, D., Spanjers, H., & van Lier, J.B. (2023). Effect of operational parameters on the performance of an anaerobic sequencing batch reactor (AnSBR) treating protein-rich wastewater. *Environmental Science and Ecotechnology* 17 (2024): 100296.

Abstract

Treating protein-rich wastewater using cost-effective and simple-structured single-stage reactors presents several challenges. In this chapter, we applied an anaerobic sequencing batch reactor (AnSBR) to treat protein-rich slaughterhouse wastewater. We focused on identifying the key factors influencing the removal of chemical oxygen demand (COD) and the settling performance of the sludge. The AnSBR achieved a maximum total COD of 90%, a protein degradation efficiency exceeding 80%, and a COD to methane conversion efficiency of over 70% at organic loading rates (OLR) up to $6.2 \text{ g COD}\cdot\text{L}^{-1}\cdot\text{d}^{-1}$. We found that the variations in both the organic loading rate within the reactor and the hydraulic retention time in the buffer tank had a significant effect on COD removal. The hydraulic retention time in the buffer tank and the reactor, which determined the ammonification efficiencies and the residual carbohydrates concentrations, affected the sludge settleability. Furthermore, the genus *Clostridium sensu stricto 1*, known as protein- and lipids-degraders, was dominant in the reactor. Statistical analysis showed a significant correlation between the core microbiome and ammonification efficiency, highlighting the importance of protein degradation as the governing process in the treatment. Our results will provide valuable insights to optimise the design and operation of AnSBR for efficient treatment of protein-rich wastewater.

1 Introduction

The wastewaters from several industries, such as the production of specific beverages and fish, dairy, and meat processing, contains large quantities of proteins that can account for up to 90% of the chemical oxygen demand (COD) (Duong et al. 2019). Continuous increase in meat and meat alternative products to meet the growing populations' protein needs have resulted in pollution issues (Rajab et al. 2017, Wang and Serventi 2019). For example, slaughterhouse wastewater (SWW) is characterised by high concentrations of organic compounds, such as proteins as well as fats, oil & grease (FOG), and high nutrients load (Musa and Idrus 2021, Palatsi et al. 2011). Direct discharge of SWW to surface water severely affects the environment and public health.

Current treatments include physiochemical and biological technologies (Aziz et al. 2019, Hilares et al. 2021). Although anaerobic digestion (AD) is generally preferred for treating wastewater with a high organic load, a treatment chain, including an anaerobic high-rate reactor, typically starts with pre-treatment to decrease the high concentrations of solids and fats (Musa and Idrus 2021). The major challenge in the treatment of SWW is the presence of high contents of proteins and FOG, which commonly accumulate in single-stage reactors (Hilares et al. 2021). Additionally, various undesirable effects, such as foaming, sludge flotation, sludge washout, and inhibition caused by the accumulation of long-chain fatty acids (LCFA) from lipids degradation, can occur during the treatment (Rodríguez-Méndez et al. 2017, Silva et al. 2014). These obstacles make it difficult to treat high-strength SWW efficiently. Development of a simple single-stage method for effectively treating SWW at acceptable costs is still challenging (Crini and Lichtfouse 2019, Ripoll et al. 2022). In Chapter 4, we found that carbohydrates were degraded before protein and that the constant presence of carbohydrates retard the degradation of proteins (Deng et al. 2023a).

Under anaerobic conditions, proteins are firstly hydrolysed to peptides and amino acids, then deaminated to ammonium (NH_4^+) and volatile fatty acids (VFAs). The process is also known as ammonification. Accumulating ammonium concentrations exceeding $1500 \text{ mg}\cdot\text{L}^{-1}$ can cause inhibition, especially to the methanogens, at the commonly applied reactor pH and temperature (Rajagopal et al. 2013). Breure et al. (1986a) suggested that the degradation of proteins and carbohydrates should be separated in space or time. Such separation can be

accomplished using the feast-and-famine operation of an anaerobic sequencing batch reactor (AnSBR), allowing for the depletion of more rapidly degradable compounds and using intervals for the degradation of more slowly degradable compounds. Tan et al. (2021) compared the effect of different feeding regimes on the performance of anaerobic membrane bio-reactors and found that the accumulation of proteins and carbohydrates was 30% - 50% higher in a continuously-fed reactor than in a batch-fed reactor.

AnSBRs combine the feeding, bioconversion, settling, and decanting processes within a single reactor, and are beneficial for SWW treatment because of its low capital costs and low energy and manpower requirements (Massé and Massé 2000). The AnSBR is considered an alternative to continuous-flow single-stage reactors, such as anaerobic filter and upflow anaerobic sludge blanket reactor, which experience clogging, biomass adhesion issues, granules breakage and loss of density, scum formation, and sludge flotation and washout (Holohan et al. 2022). Various combinations of pre-treatment and post-treatment, different cycle sequences, organic loading rates (OLR), hydraulic retention times (HRT) have been designed and tested (Ripoll et al. 2022). According to Shende and Pophali (2021), an OLR range between 1.1 and 12.8 g COD·L⁻¹·d⁻¹ can be applied in conventional AnSBRs with a total cycle sequence duration of 24 – 42 h and a reaction time longer than 16 h. An AnSBR can achieve a total COD removal efficiency between 78 and 97%. However, to achieve high COD removal efficiencies, the HRT, which is usually coupled with the reaction time, needs to be long compared with other high-rate anaerobic technologies, such as upflow anaerobic sludge blanket reactors and anaerobic baffled reactor. Additionally, because of the batch-wise feeding, a parallel reactor is required for continuous flow operation (Shende and Pophali 2021). Moreover, poor sludge settling performance leads to deteriorating in the effluent quality, while the settling of the resulting flocculent sludge often takes considerable time, thereby reducing the reaction time (Singh and Srivastava 2011).

The anaerobic bioconversion process largely depends on the activity and balanced metabolic cooperation of the microbiome in the reactor. The presence of specific microbiota is determined by the operational parameters, such as the pH, OLR, and HRT, and may ultimately affect the performance of the reactor (Pasarari et al. 2021). According to Ziels et al. (2017), the feeding frequency and OLR are the two main parameters that exert a selective

pressure and influences the microbial community structure and biokinetic conversion of complex substrates in AnSBRs.

Given the theoretical advantage of the AnSBR for protein-rich wastewater treatment, the aim of this chapter was to evaluate the treatment performance of a novel AnSBR to treat SWW regarding COD removal, protein degradation, overall conversion of COD to methane (CH_4), and sludge settling. The applied AnSBR consisted of a main reactor followed by a settling tank. Consequently, the reaction time in the reactor was not limited by the required settling time for the cultivated sludge. In fact, owing to the applied set-up, the reaction time lasted for the entire batch cycle period. The SWW was fed to the AnSBR without additional physiochemical pre-treatment. Three operation phases with various OLRs and HRTs were applied to assess the process performance under different conditions. Correlation analysis between the operational parameters and performance indicators was performed to identify the processes determining the operational parameters. Moreover, we investigated the microbial community dynamics and diversity while paying particular attention to the microbiome of protein-degrading amplicon sequence variants (ASVs) and their correlation with performance and operational parameters. The results will provide valuable insights to optimise the design and operation of AnSBR, ensuring efficient treatment of protein-rich wastewater.

2 Materials and methods

2.1 Inoculum and wastewater characteristics

The inoculum sludge was taken from an anaerobic high-rate granular sludge bed reactor of a biochemical company producing pharmaceuticals in the Netherlands. The sludge had a total suspended solids (TSS) content of $9.2 \text{ g}\cdot\text{L}^{-1}$ and a volatile suspended solids (VSS) content of $8.4 \text{ g}\cdot\text{L}^{-1}$. An initial sludge concentration of $10 \text{ gVSS}\cdot\text{L}^{-1}$ in the reactor was obtained by filtering 36 L inoculum.

The protein-rich feed to the AnSBR was raw wastewater collected from the inlet of an SWW treatment plant (HydroBusiness B.V., The Netherlands). The main characteristics of the wastewater and inoculum are shown in **Table 1**.

Table 1 - Characteristics of protein-rich SWW and inoculum.

	Units	SWW	Inoculum
pH	-	6.8-7.8	-
TSS	mg·L ⁻¹	1,100 – 3,700	9,200
VSS	mg·L ⁻¹	1,100 – 3,500	8,400
TCOD	mg·L ⁻¹	4,700 – 6,500	-
SCOD	mg·L ⁻¹	1,500 – 3,800	-
NH ₄ ⁺ -N	mg·L ⁻¹	175 - 420	-
^a Proteins	mg·L ⁻¹	500 –1,150	-
^b Carbohydrates	mg·L ⁻¹	100 - 250	-
FOG	mg·L ⁻¹	100 – 600	-

^a The protein concentration was measured as mg BSA·L⁻¹, which has a conversion factor of 1.5 g COD·g⁻¹ BSA; ^b The carbohydrate concentration was measured as mg glucose·L⁻¹, which has a conversion factor of 1.1 g COD·g⁻¹ glucose.

2.2 Reactor setup and operational conditions

The AnSBR set-up consisted of a 10 L buffer tank (BT), a 30 L reactor and a 12 L settling tank (**Figure 1**). The treated effluent was collected in an effluent tank. Four cycles were performed each day, and each cycle lasted for 6 h. At the start of each cycle, the effluent of the BT was fed to the reactor, after which the BT was replenished with raw SWW. Two hours after the feeding sequence, 10 L of the reactor content was transferred to the settling tank for degassing (2 h) and settling (2 h). At the end of the 2 h settling phase, the liquid in the settling tank was discharged to the effluent tank, and the settled sludge was returned to the reactor.

The OLR was calculated as the daily COD load of the four cycles by multiplying the influent total COD (TCOD) concentration by the added volume and dividing it by the reactor working volume. The reactor OLR was gradually increased from 2.0 g COD ·L⁻¹·d⁻¹ to the design threshold of 6.2 g COD ·L⁻¹·d⁻¹ over three different operational phases. During the startup phase (phase I, 0 – 55 days), the biomass was acclimated to the SWW. In phase II (days 56 – 196), the reactor was operated with an average OLR of 2.0 ± 0.6 g COD·L⁻¹·d⁻¹ and an average solid loading rate (SLR) of 0.2 ± 0.1 g COD·g VSS⁻¹·d⁻¹. In phase III (Days 197 – 260), the OLR was gradually increased to 6.2 g COD·L⁻¹·d⁻¹ to investigate the maximum treatment capacity of the reactor.

The pH in the BT and the reactor was kept in the range of 6.8 and 7.5 using a controller (SC200 Universal Controller, Hach, USA) equipped with pH sensors (K8, Hamilton, Denmark). The temperature of the reactor was controlled at 36 ± 0.5 °C with a recirculating water bath (MX06S135, VWR International, USA). The BT and the settling reactor were operated at ambient temperature (20 ± 5 °C). The operational parameters of the reactor, including the average HRT and solid retention time (SRT), are summarised in **Table 2**. The HRT was calculated by dividing the reactor volume by the average daily flow rate, which was the total added volume divided by 24 h. The SRT was calculated by the total sludge (g) in the reactor divided by the daily wasted sludge ($\text{g} \cdot \text{d}^{-1}$).

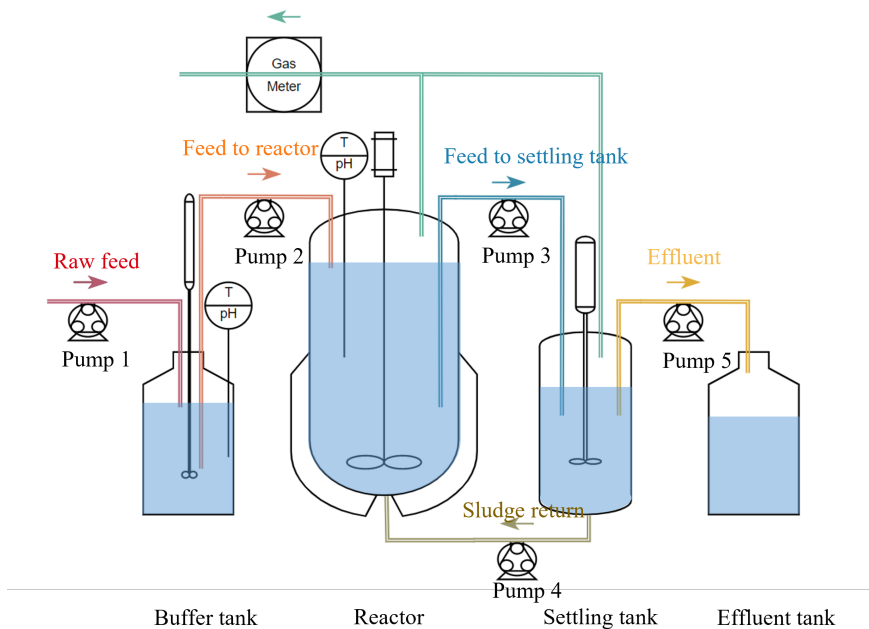


Figure 1 - Schematic representation of the AnSBR experimental setup.

2.3 Sampling and Analysis

2.3.1 Basic analytical parameters

Samples were taken from the raw feed, BT, reactor, and effluent tank. TCOD and soluble COD (SCOD) were analysed twice a week. The TCOD and SCOD measurement were carried using HACH-Lange kits (LCK014, Merck Life Science NV., the Netherlands). Samples were

filtered through a 0.45 μm membrane filter (WHA10463513, Whatman, the Netherlands) before SCOD measurement. TSS, VSS, total Kjeldahl nitrogen (TKN), soluble Kjeldahl nitrogen (SKN), NH_4^+ , and VFAs were analysed once a week. The solids content and nitrogen concentrations were analysed following standard methods (APHA, 1998). Samples for VFA analysis were first centrifuged at $13,500 \times g$ for 5 min and then filtered through 0.45 μm membrane filters (WHA10463513, Whatman). The VFAs composition was analysed as described previously by Tan et al. (2021).

Table 2 - Loading rate, retention time, solids content and cycle length in the Buffer tank (BT), Reactor (R), and settling tank.

AnSBR	^a OLR	SLR	HRT	SRT	TSS	VSS	^b Cycle Time
	$\text{gTCOD} \cdot \text{L}^{-1} \cdot \text{d}^{-1}$	$\text{gTCOD} \cdot \text{gVSS}^{-1} \cdot \text{d}^{-1}$	d	d	$\text{g} \cdot \text{L}^{-1}$	$\text{g} \cdot \text{L}^{-1}$	h
Buffer Tank	2.0 - 6.2	-	0.7 \pm 0.5	-	-	-	6
^c Reactor	I: 1.8 \pm 1.0	0.25 \pm 0.13	2.9 \pm 1.6	55 \pm 15	7.0 \pm 1.0	6.0 \pm 1.0	4
	II: 2.0 \pm 0.6	0.17 \pm 0.07	2.4 \pm 1.3	115 \pm 35	8.8 \pm 1.1	7.9 \pm 1.1	4
	III: 3.2 \pm 1.0	0.23 \pm 0.06	1.5 \pm 0.7	60 \pm 10	10.6 \pm 2.0	9.9 \pm 2.0	4
Settling Tank	-	-	-	-	-	-	2

^a the OLR was calculated as the daily organic load of the four cycles, i.e., influent TCOD concentration times added volume, divided by the reactor working volume.

^b Four cycles a day.

^c Averaged values of each stage with standard deviation are presented, the temperature was maintained at 20 ± 5 °C in the Buffer Tank and 36 ± 0.5 °C in the Reactor, pH was regulated in the range of 6.8-7.5.

The COD removal efficiencies (%) were calculated as the differences in COD concentration between the influent and effluent, divided by the COD concentration in the influent. The acidification degree (%) in the BT was calculated as the percentage of VFA production, expressed in g COD, from the influent TCOD or SCOD. The ammonification efficiency (%) was calculated as the NH_4^+ concentration ($\text{mg N} \cdot \text{L}^{-1}$) divided by the TKN concentration ($\text{mg N} \cdot \text{L}^{-1}$) in the BT and reactor, multiplied by 100%.

Protein and carbohydrate concentrations were analysed once a week. Samples from the BT and the reactor were centrifuged at $6,500 \times g$ for 10 min and subsequently filtered with 1 μm or 0.45 μm mesh membrane filters (WHA10463523 and WHA10463513, Whatman), after which the protein and carbohydrate contents were measured. The protein concentrations were

assessed following the manufacturer's protocol with the Bicinchoninic acid kit (BCA1-1KT, Merk Life Science NV.). The absorption was measured by a spectrometer at 562 nm. Bovine Serum Albumin was used as standard. Carbohydrates were analysed following the Dubois method (Dubois et al. 1956).

Biogas production was monitored by a drum-type gas meter (TG05/5, Ritter, Germany), and the biogas composition, including the percentages of CH₄, CO₂, and O₂, was analysed using a BIOGAS 5000 Analyzer (Scantec Industries NV, Belgium). The COD to CH₄ (COD_{CH₄}) conversion efficiency (in %) was calculated as the CH₄ production (in g COD·d⁻¹) relative to the COD fed to the reactor (in g COD·d⁻¹) using the following equation:

$$COD_{CH_4} \text{ conversion efficiency (\%)} = \frac{CH_4-COD \text{ production rate}}{COD \text{ fed to reactor}}, \quad (1)$$

Where the CH₄-COD production rate is the daily CH₄ production (g COD·d⁻¹), and the COD fed to reactor is the daily organic matter fed to the reactor (g COD·d⁻¹).

The sludge's particle size distribution (PSD) in the 0.01 - 2000 μm range was measured using a Microtrac Bluewave light scattering instrument (Retsch Technology GmbH, Germany) with Microtrac FLEX 11.1.0.2 software. The flow rate of 25%.

2.3.2 Settling distance and zone settling velocity

The settling distance of the sludge was assessed by measuring the distance from the surface of the liquid to the liquid-solid interface at 15 min, 30 min, 45 min, 1.5 h and 2 h. The zone settling velocity (ZSV) was used to characterise the sludge settleability. The unhindered settling velocity v_0 (m·h⁻¹) and the compressibility factor k (L·g⁻¹TSS) were measured with a transparent vertical cylinder according to an established method of White (1975). The ZSV was calculated using the Vesilind equation (Vesilind 1968) as follows:

$$v = v_0 \times e^{(-kX)}, \quad (2)$$

Where v is the ZSV (m·h⁻¹), X is sludge concentration (g TSS·L⁻¹) in the reactor, k is the compressibility factor (L·g⁻¹TSS), and v_0 is the unhindered settling velocity (m·h⁻¹).

2.3.3 AnSBR cycle analysis

Cycle analysis was performed by taking samples from the BT and the reactor every hour throughout one entire cycle (6 hours). The samples were used for size fractionation analysis of COD, proteins, and carbohydrates, and the results were used to track the degradation of organic matters during the operation.

2.3.4 Microbial community analysis

Sludge samples (10 mL) were taken regularly from the BT and the reactor and centrifuged at 13,500 x g for 5 min. The supernatant was discarded and the biomass pellets were stored at - 20 °C in Eppendorf tubes (Eppendorf, Germany). The sludge samples were then sent for DNA extraction and amplicon sequencing (Novogene, UK).

Before the DNA extraction, the biomass pellets were thawed, and biomass of duplicate samples were combined, weighed to 250 mg, and then transferred to PowerBead Pro tubes. DNA was extracted with the DNeasy PowerSoil Pro Kit (Qiagen, Germany), and the DNA quality and quantity were verified by agarose gel electrophoresis and using a 5400 Fragment Analyzer System (Agilent, USA). DNA (16S rRNA gene) amplification was carried out by the Illumina Novaseq 6000 platform. The primers were 341F [(5'-3') CCTAYGGGRBGCASCAG] and 806R [(5'-3') GGACTACNNGGGTATCTAAT] for bacteria/archaea in the V3-V4 regions.

The Illumina paired-end raw reads were processed using the QIIME2 platform (Bolyen et al. 2019). The raw reads were inspected for their Phred quality scores to prune and trim low-quality positions. With the DADA2 plugin (Callahan et al. 2016), raw reads were trimmed to position 20 in the 3' end and truncated to position 240 in both forward and reverse reads. The amplicon sequence variants (ASVs) were resolved, and chimeric sequences were removed with the consensus method. The representative sequences of ASVs were taxonomically assigned with the "classify-consensus-vsearch" plugin (Rognes et al. 2016), using the SILVA 138 database (Quast et al. 2012) as a reference. A phylogeny was built with the "align-to-tree-mafft-fasttree" plugin. Briefly, this plugin aligned the sequences with the MAFFT algorithm (Nakamura et al. 2018), then ambiguous positions were masked, and a tree was constructed with the FastTree2 algorithm (Price et al. 2010). The resulting abundance table and phylogeny were exported to the R environment.

Samples were normalised by rarefaction to 50,000 counts. Alpha and beta diversities were calculated with the phyloseq library (McMurdie and Holmes 2013) in R. Taxonomic abundance was scaled to relative abundance (%) and visualised with the ggplot2 library (Wickham 2011). A principal coordinate analysis was plotted to visualise the beta diversity differences between samples using the unweighted UniFrac distance metric.

To determine the shared ASVs in samples, 1000 random resamples were performed with replacing. In each resample, the ASVs that prevailed in all samples were detected. Only the ASVs that prevailed in 95% of all resamples were considered as the core microbiota. Core members within the operational phases were analysed with BLAST against the Refseq RNA database to identify the closest related species. The sequences were deposited in the SRA (NCBI) database under the accession number PRJNA847614.

2.3.5 Statistical correlation analysis

Correlation analysis of different operational parameters was performed to identify the most relevant parameters affecting the performance of the reactor. T output variables were the TCOD and SCOD removal efficiencies and ZSV. Pearson correlation coefficient was calculated to assess the correlations between two parameters, and $p < 0.05$ indicating a significant correlation. The correlations were categorised into four levels according to the p-values and the absolute values of the correlation coefficients. A p-value higher than 0.05 indicated that there was not a significant correlation between the two parameters. A p-value lower than 0.05 and an absolute coefficient value of 0.00 - 0.30 indicated that there was a low correlation between the two parameters, an absolute coefficient of 0.31 - 0.60 indicated a moderate correlation and an absolute coefficient of 0.61 - 1.00 indicated a high correlation.

A Permutational Multivariate Analysis of Variance (PERMANOVA) was calculated with the vegan library (Oksanen et al. 2007) to correlate the changes in the microbial community composition (distances) in samples of the AnSBR with the operational parameters and performance indicators. The datasets were considered statistically different when a p-value ≤ 0.05 was obtained.

3 Results and discussion

3.1 AnSBR performance

3.1.1 Treatment efficiencies under varied operational conditions

COD removal efficiencies and conversion efficiencies

The AnSBR was operated for 260 days. During the start-up phase (phase I) with an OLR of $1.8 \pm 1.0 \text{ gTCOD}\cdot\text{L}^{-1}\cdot\text{d}^{-1}$, the TCOD removal efficiency gradually increased and achieved an average of $78 \pm 10 \%$ (**Figure 2A**). In the stable operation phase (phase II), an OLR of $2.0 \pm 0.6 \text{ g TCOD}\cdot\text{L}^{-1}\cdot\text{d}^{-1}$ was applied, and the average TOCD removal efficiency was of $81 \pm 5\%$. In the last operational phase (phase III) with an OLR of up to $6.2 \text{ g TCOD}\cdot\text{L}^{-1}\cdot\text{d}^{-1}$, the TCOD removal reached an average of $83 \pm 6\%$. A maximum removal efficiency of 90% was achieved at the highest OLR. The SCOD removal efficiency (**Figure 2B**) was $87 \pm 5\%$ during phase I, then decreased to $82 \pm 8\%$ during phase II and $83 \pm 6\%$ during phases III as the OLR increased.

The SRT and HRT during the operational periods are shown in **Figure 2C**. During phases I and II, the SRT was 55 ± 15 and 115 ± 35 days, respectively. During phase III, the SRT was gradually decreased to 60 ± 10 days. During phases I and II, the average HRTs were 2.9 ± 1.7 days and 2.4 ± 1.3 days, respectively. In phase III, the HRT was 1.5 ± 0.7 days.

Hai et al. (2015) reported a maximum removal efficiency of 98% at an OLR of $2.0 - 6.8 \text{ g COD}\cdot\text{L}^{-1}\cdot\text{d}^{-1}$ and an HRT of 24 h in an anaerobic/aerobic intermittent sequencing batch biofilm reactor treating SWW. Similarly, Rajab et al. (2017) reported a maximum removal efficiency of 97% at an OLR of $0.5 - 4.5 \text{ g COD}\cdot\text{L}^{-1}\cdot\text{d}^{-1}$ and an HRT of 72 h in a two-stage anaerobic/aerobic sequencing batch reactor. For an AnSBR without pre-treatment, the recommended OLRs for treating diluted and concentrated SWW are $4.5 \text{ g COD}\cdot\text{L}^{-1}\cdot\text{d}^{-1}$ and $6.0 \text{ g COD}\cdot\text{L}^{-1}\cdot\text{d}^{-1}$, respectively (Ruiz et al. 2001). The applied operational cycle in this chapter, including feeding, reaction, settling and decanting, took 6 h. Compared with single- and two-stage anaerobic/aerobic sequencing batch reactor with similar OLRs reported by Hai et al. (2015) and Rajab et al. (2017), our AnSBR set-up is considered compact and energy-efficient for treating SWW.

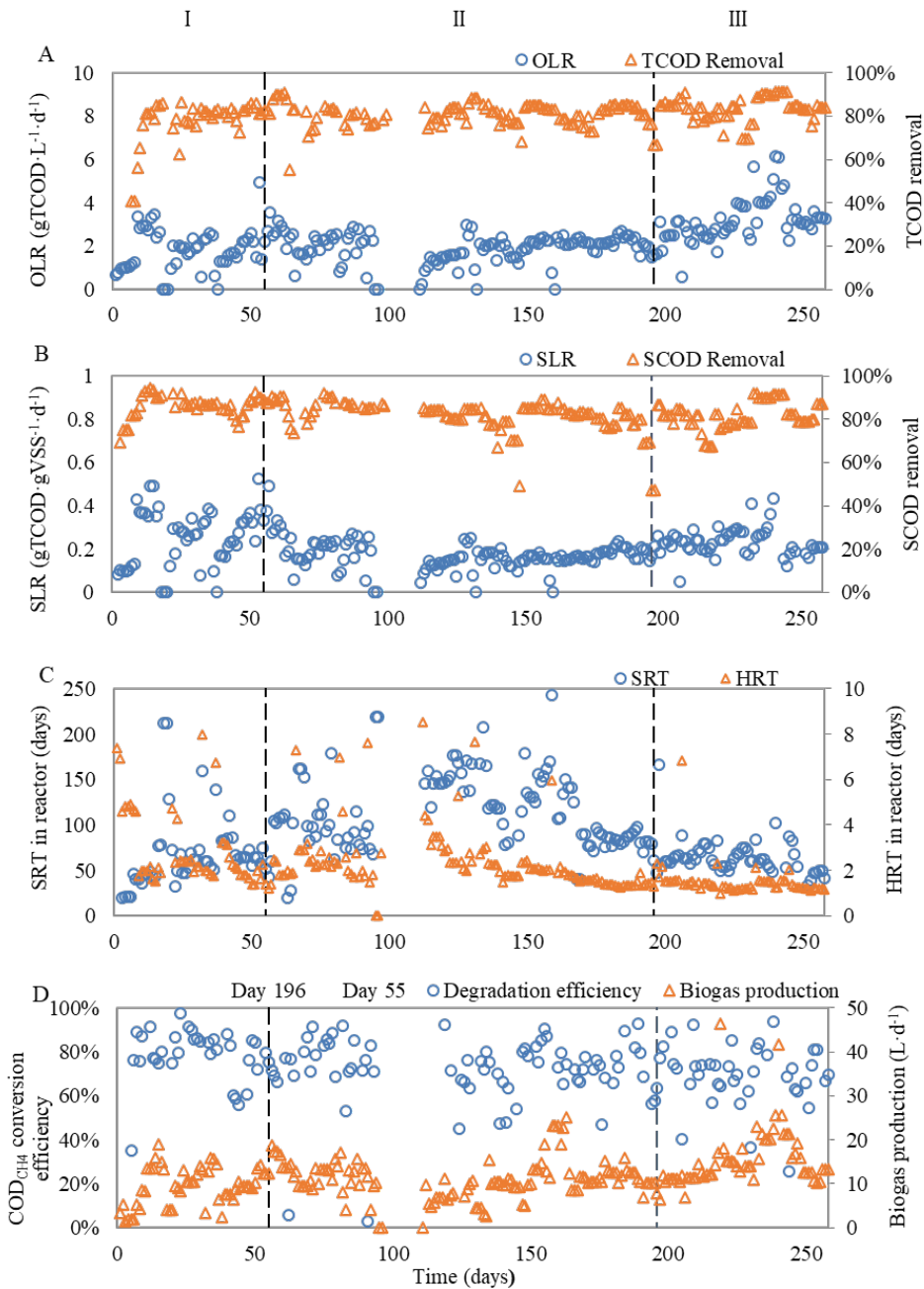


Figure 2 – Operational and performance of the AnSBR set-up. A) OLR and TCOD removal efficiency, B) SLR and SCOD removal efficiency, C) SRT and HRT in the reactor during the operation period of 260 days, and D) COD_{CH4} (COD to CH₄) conversion efficiency of organic compounds to CH₄ and daily biogas production.

The daily biogas production ($L \cdot d^{-1}$) and COD to CH_4 (COD_{CH_4}) conversion efficiency (%) are shown in **Figure 2D**. The COD_{CH_4} conversion efficiency was defined as the conversion of organic compounds to CH_4 relative to the amount fed to the AnSBR. During phase I, the average COD_{CH_4} conversion efficiency was $79 \pm 12\%$. As the OLR increased, the conversion efficiency decreased to $72 \pm 15\%$ during phase II, and slightly decreased again to $70 \pm 14\%$ in phase III.

Although the average OLRs were similar during phase I and II, there was less variation in the OLR, particularly in the final part of phase II (**Figure 2A**). With a more stable OLR, there were fewer feed interruptions during the operation, which resulted in a higher total volumetric loading in phase II than in phase I. Consequently, the HRT, particularly in the later part of phase II, was shorter than in phase I (**Figure 2C**). Apparently, the methanogen biomass was negatively affected by the shortened HRT, which led to a decrease in the COD_{CH_4} conversion efficiency.

Degree of acidification of TCOD and SCOD in the BT

Irrespective of the types of influent and the applied pre-treatment technology, an increase in SCOD is reported to improve the biogas production by a factor of 1.2 - 1.5 and the COD removal efficiency by a factor of 1.2 – 1.8 (Harris and McCabe 2015). In this chapter, a BT was applied to pre-acidify the raw SWW with the aim of enhancing hydrolysis and the availability of soluble substrates to the microorganisms in the reactor. The acidification degree (%) was used to indicate the VFA production as a percentage of TCOD and SCOD in the BT. This was measured to evaluate the effect of pre-acidification on COD removal and COD_{CH_4} conversion efficiency. **Figure 3A** shows the VFA production in the BT during the operational period. The acidification degree of TCOD was below 40%, which was likely because of the high solids content of the influent. The acidification degree of SCOD was generally higher than 60% after phase I. During phase III (days 196 – 260), the degree of pre-acidification was varied by adjusting the HRT in the BT, aiming for a high degree of pre-acidification in the BT.

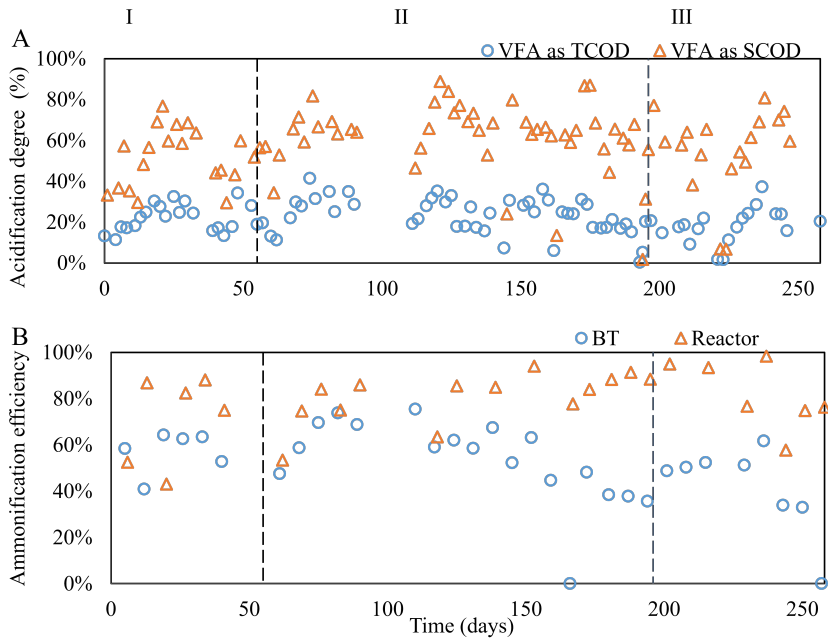


Figure 3 Acidification degree and ammonification efficiency. A) VFA production as percentages of TCOD and SCOD in the buffer tank (BT), B) Ammonification efficiency ($\text{NH}_4^+\text{-N/TKN}$) in the BT and reactor.

Ammonification efficiency in the BT and reactor

The ammonification efficiency was calculated as the measured ammonium concentration ($\text{mg N}\cdot\text{L}^{-1}$) divided by the measured TKN concentration ($\text{mg N}\cdot\text{L}^{-1}$) (**Figure 3B**). During phase I, the average ammonification efficiency in the BT was $57 \pm 9\%$. In the reactor, the ammonification efficiency increased from 50 to 85%, which indicated that the microbes were acclimated to the SWW, which was likely caused by the recirculation of the settled biomass. During phase II, the ammonification efficiency decreased an average of $53 \pm 18\%$ with increases in the OLR in the BT. In the reactor, the ammonification efficiency increased to an average of $82 \pm 12\%$. Between days 125 – 200, the ammonification efficiency increased to $92 \pm 12\%$. During phase III, the ammonification efficiency in the BT decreased to an average of $47 \pm 10\%$. In the reactor, the ammonification efficiency decreased from $> 90\%$ to $< 80\%$ as the OLR increased from 3.5 to $6.2 \text{ g COD}\cdot\text{L}^{-1}\cdot\text{d}^{-1}$. The average ammonification efficiency during phase III was $87 \pm 20\%$. Other research has shown that protein degradation is greatly retarded under a high OLR (e.g., 20–25% ammonification with $> 100 \text{ g COD}\cdot\text{L}^{-1}\cdot\text{d}^{-1}$) in the

study of Handous et al. (2019). According to our results, a moderate OLR between 2.0 and 3.5 g COD·L⁻¹·d⁻¹ is recommended for maintaining a high ammonification efficiency (≥85%). The NH₄⁺-N/TKN ratios were similar in the raw SWW and the BT, which indicated that proteins were mainly degraded in the reactor.

Proteins and carbohydrates in the BT and reactor liquid

Cycle analysis was performed once a week. Samples of the BT and reactor liquid were collected every hour during one cycle to investigate the system performance. **Figure 4** shows three size fractions of carbohydrates and proteins (> 1 μm, 1 - 0.45 μm, and < 0.45 μm), including suspended, colloidal, and soluble matter. The results were averaged and compared between the BT and reactor liquid.

Generally, carbohydrates and proteins that are smaller than 1 μm were dominant in the BT and reactor liquid, contributing to 40 – 90% of the total concentrations. The carbohydrate concentration decreased from an average of 40 mg·L⁻¹ in the BT liquid to an average of < 20 mg·L⁻¹ in the reactor liquid (**Figure 4A** and **4B**). In phase III, the carbohydrate concentration in the reactor remained below 15 mg·L⁻¹ despite the higher OLR, which indicated that there was an active removal of carbohydrates in the reactor.

The protein concentration in the BT varied between 200 and 750 mg·L⁻¹ (**Figure 4C**). From day 22 to 109, the protein concentration decreased to below 200 mg·L⁻¹ in the reactor (**Figure 4D**). It then further decreased to < 100 mg·L⁻¹ in the second half of phase II. Decreases in the concentrations of the three size fractions of proteins was observed throughout the operational period. The observed decreases were attributed to the ongoing acclimatisation of the microbes to the feed wastewater, which would also explain the increase in ammonification efficiency. The protein concentration remained at approximately 100 mg·L⁻¹ regardless of the increasing OLR during phase III.

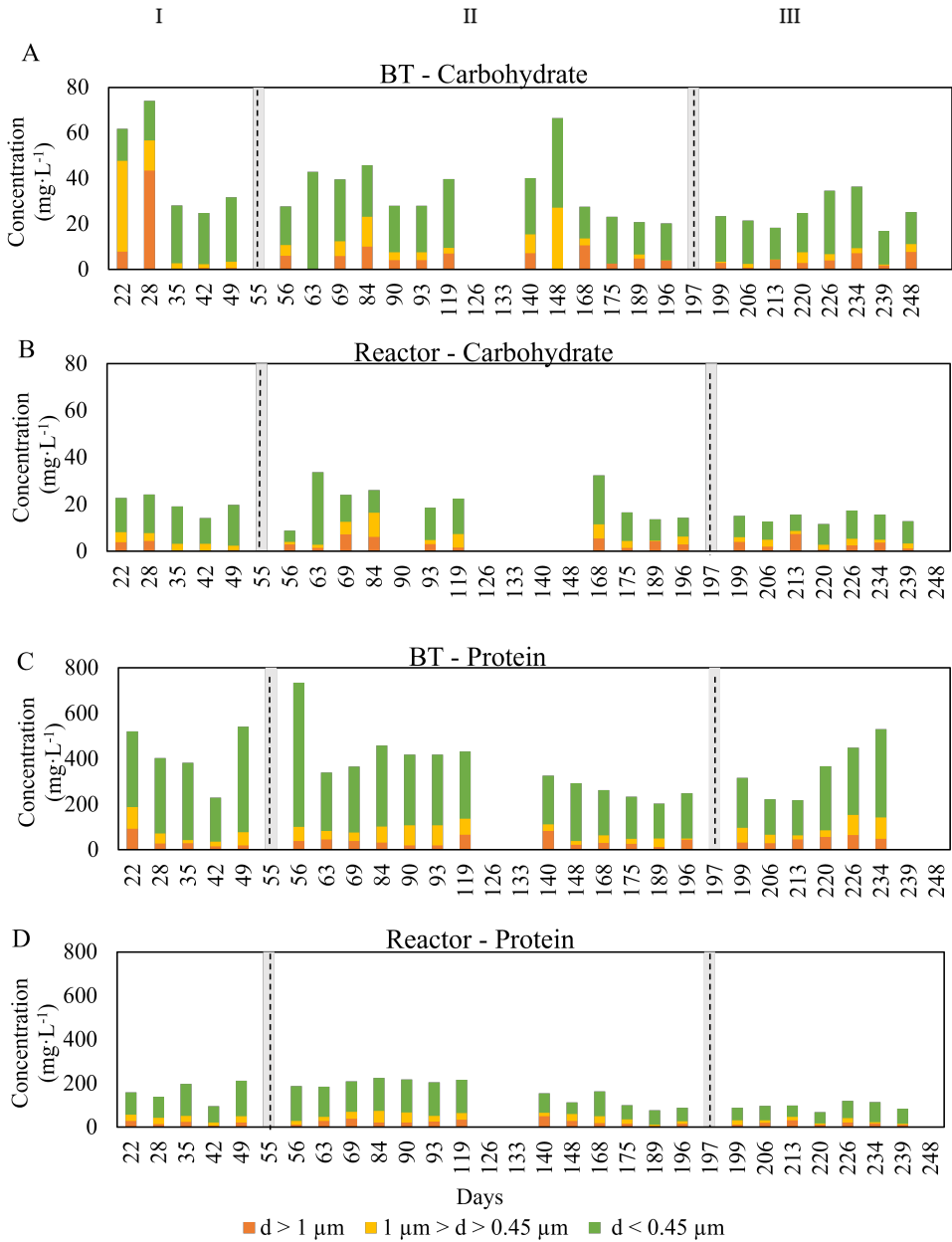


Figure 4 – Concentration of carbohydrates and proteins. A) Three size fractions of carbohydrates concentrations in A) buffer tank and B) reactor (R) liquid, three size fractions of proteins concentrations in C) buffer tank and D) R liquid. Averaged results of hourly samples in one cycle were shown, and the different size fractions were indicated by different diameters (d), x-axis indicates the operational days.

The applied AnSBR showed an efficient degradation of proteins treating real SWW. The anaerobic protein degradation is reportedly often to be in the range of 17 – 77% (Bareha et al. 2018). Additionally, the concentration of proteins accumulated in an AnSBR reactor liquid may increase from 250 mg·L⁻¹ to 1500 mg·L⁻¹ after an increase in OLR from 3.1 to 5.5 g COD·L⁻¹·d⁻¹ (Tan et al. 2021). In this chapter, the AnSBR achieved an average protein degradation efficiency of 81 ± 10% at an OLR of 2.0 - 6.2 g COD·L⁻¹·d⁻¹, and the protein concentration was kept below 100 mg·L⁻¹ in the reactor. To further improve the protein degradation efficiency, granular sludge with a higher conversion capacity could be used, which would reduce the concentration of all organic residues (Shende and Pophali 2021).

3.1.2 Sludge settling performance

The settling distances of the sludge in the first 15 min, 30 min, 45 min, 1.5 h and 2 h as 100% stacked bar are plotted in **Figure 5A**. During phase I, about 50% of the sludge settling distance was achieved within the first 15 min, and 75% was reached within the first 30 min. The settling was improved during the more stable AnSBR operation of phase II, with 80% of the settled distance achieved within the first 15 min. A settling time of 45 min or longer only led to an increase of approximately 20% in the settled distance. The sludge settling was further improved during phase III, with more than 90% of the sludge settled within the first 15 min. However, the total settling distance decreased from 55% of the settling tank height during phase I to 45% during the stable operation phase (phase II), and further decreased to 35% during the high-loading phase (phase III).

The settling behaviour of sludge is considered to be an essential performance indicator for reactors that use gravitational separation of solids from liquid (Tassew et al. 2019). In this chapter, the settling distance within the first 15 min clearly connected to the ZSV. The lowest ZSVs occurred on days 26, 70, 119, 169 and 232, and also when a short settling distances within the first 15 min was observed (**Figure 5A** and **5B**). The settling distance analysis could be used to set a required settling time during an operational cycle, with the ZSV being indicative of the sludge settling performance. Ex-situ assessment of the ZSV is particularly useful when the settling distance in full-scale reactors cannot be measured.

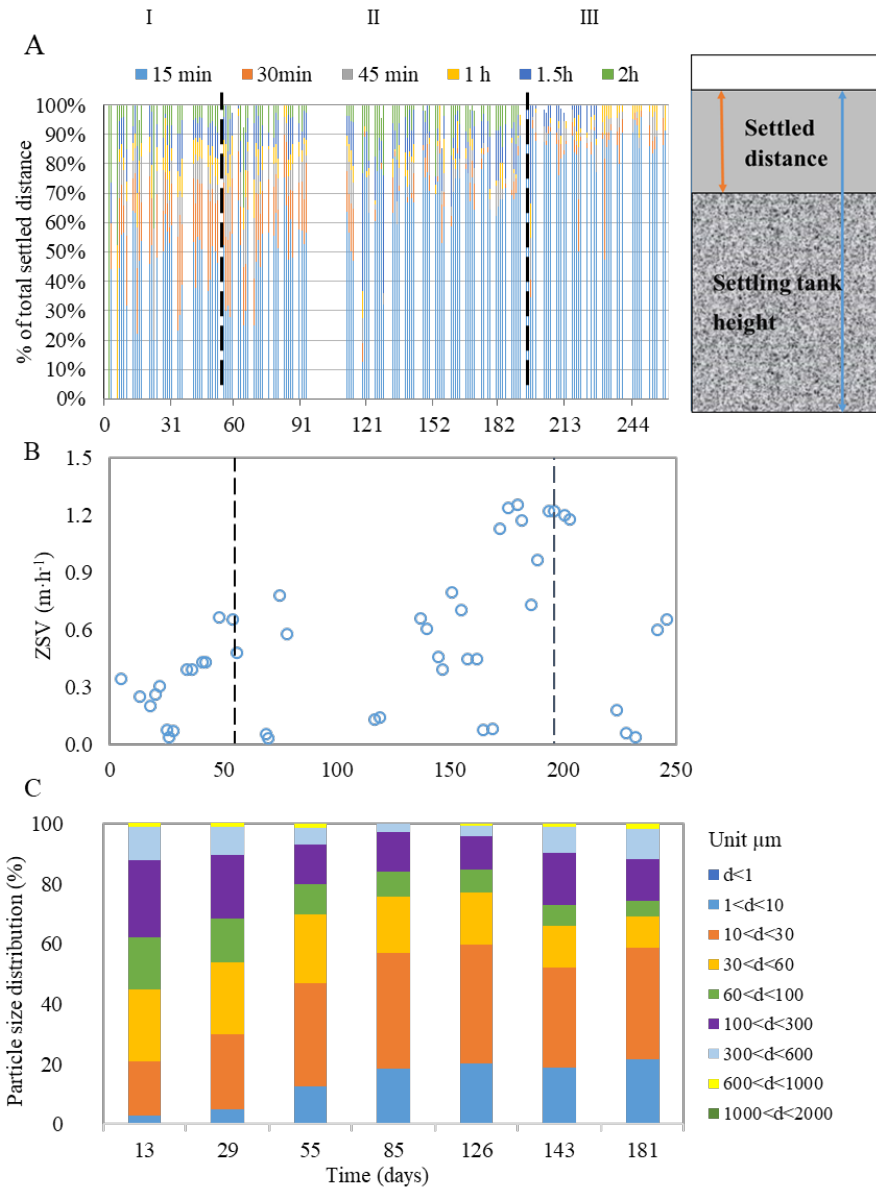


Figure 5 - A) Settled sludge distance in different time periods, B) Zone settling velocity (ZSV) of the sludge, C) Particle size distribution (PSD) of the sludge in reactor during the start-up phase and stable operation phase, d is mean diameter of the particle (μm), the averaged results of three samples are presented in one column.

In addition to the sludge settleability, also the particle size distribution (PSD) and the mean particle size may affect sludge sedimentation, thickening, digestion, and subsequent

dewatering (Li and Stenstrom 2018). Therefore, we collected samples to monitor the PSD in the reactor and investigate the correlation between PSD and sludge settleability. The PSD results showed the following: 1) a steady increase in the fraction small particles ($1 \mu\text{m} < \text{diameter} < 30 \mu\text{m}$); 2) a steady decrease in the fraction particles between 30 and $300 \mu\text{m}$; and 3) an initial decrease in the fraction large particles ($300 \mu\text{m} < \text{diameter} < 600 \mu\text{m}$) with increases in the SRT, followed by an increase in this fraction with the decreases in the SRT (**Figure 2C** and **5C**).

An average SRT exceeding 50 days in phase I and II decreased the fraction $300 - 600 \mu\text{m}$ particles and increased the fraction of $1 - 30 \mu\text{m}$ particles. However, the increase in the fraction of $1 - 30 \mu\text{m}$ particles did not negatively affect the sludge settling or ZSV. In phase I, 55% of the sludge was settled within 15 min, and the fraction of small particles increased from 20% to 45% (**Figure 5A**). The ZSV increased during phase I, and when the reactor was restarted on day 111, the ZSV increased from $< 0.3 \text{ m}\cdot\text{h}^{-1}$ to $1.2 \text{ m}\cdot\text{h}^{-1}$, while the fraction of small particles remained 50% (**Figure 5B**). Hence, the variation in PSD was not correlated with the sludge settling performance during the operational period.

3.2 Microbial community dynamics and diversity

The structure and dynamics of the microbial community in the BT and the reactor biomass were analysed (**Figure 6**) and possible correlation with protein degradation in the reactor were assessed. The dominant bacteria in the BT belonged to the phylum *Firmicutes*, followed by *Proteobacteria* and *Bacteroidota* (**Figure 6A**). The relative abundance of *Firmicutes* decreased from $76 \pm 3 \%$ in phase I, to $52 \pm 12 \%$ in phase II and $47 \pm 11 \%$ in phase III. For *Proteobacteria*, the relative abundance increased from $8 \pm 1 \%$ in phase I to $38 \pm 11 \%$ in phase III. The relative abundance of *Bacteroidota* remained at approximately $5 \pm 1 \%$ throughout the operation period, and all belonged to the class *Bacteroidia* (**Figure S1**). *Bacteroidia* play a crucial role in the degradation of complex polymers and are proteolytic bacteria involved in converting proteins to VFAs and ammonium (Yi et al. 2014). The most abundant genera were *Clostridium sensu stricto 1* ($21 \pm 7 \%$) and *T34* ($19 \pm 13 \%$), and especially in phase III, *Brachymonas* ($9 \pm 7 \%$), *Proteiniclasticum* ($6 \pm 2 \%$), *Terrisporobacter* ($5 \pm 2 \%$), *Lactobacillus* ($4 \pm 3 \%$), *Methanosaeta* ($3 \pm 4 \%$), *Streptococcus* ($3 \pm 1 \%$), *Bacteroidetes vadinHA17* ($2 \pm 1 \%$), and *Romboutsia* ($2 \pm 1 \%$) (**Figure 6B**).

Clostridium sensu stricto 1 metabolises diverse compounds present in SWW, such as proteins/amino acids, carbohydrates, short chain fatty-acids (Wiegel et al. 2006), and has a major role in lipids/LCFAs degradation and a syntrophic relationship with methanogens (Usman et al. 2022). A high protein content combined with low fatty acid content favours the abundance of *Proteiniclasticum* (Liu et al. 2016b), which can also degrade amino acids and proteins (Li et al. 2015). *Terrisporobacter* has high hydrolytic capabilities (Deng et al. 2015). *Romboutsia* species are anaerobes adapted to a nutrient-rich environment, in which carbohydrates and sources of amino acids and vitamins are abundant (Gerritsen et al. 2014).

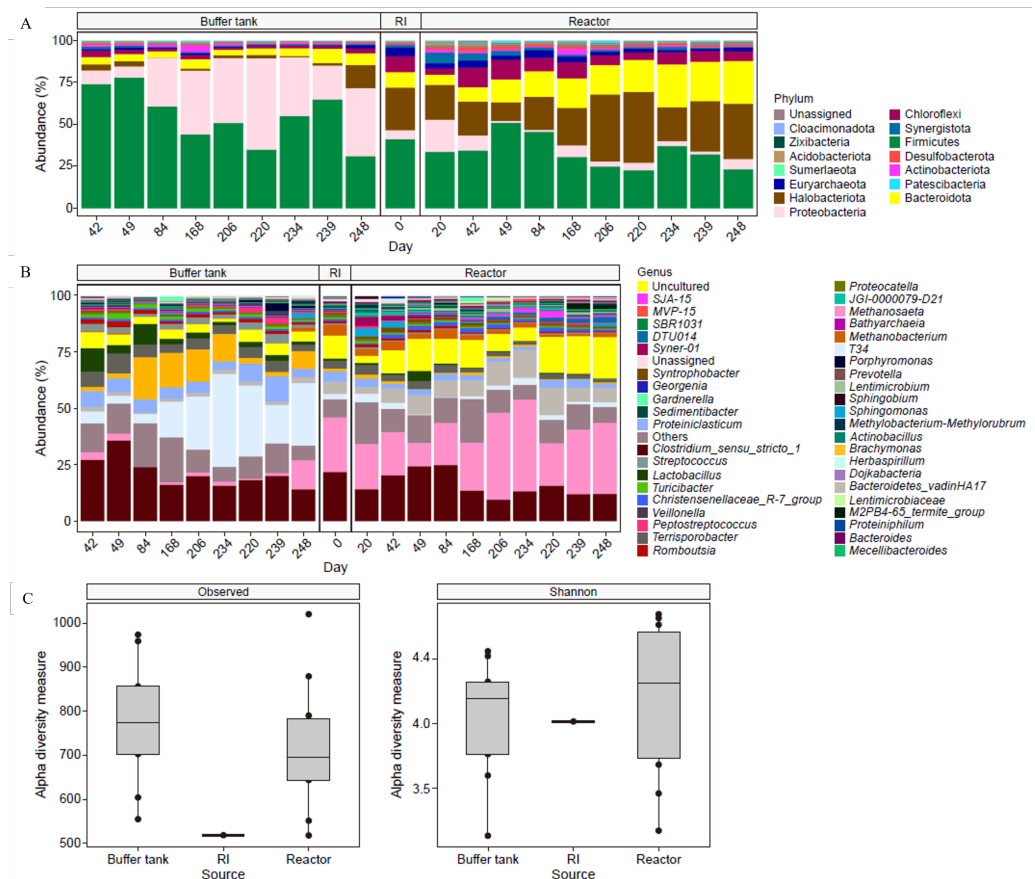


Figure 6 - Microbial community dynamics in the buffer tank, inoculum (RI), and reactor at the A) Phylum level and B) Genus level. Phase I: up to day 55, phase II: up to day 197, and phase III: up to day 260. C) Alpha diversity plots for the microbial community in the buffer tank, RI, and reactor. Left: observed ASVs numbers, Right: Shannon's index.

During the entire operation, the most dominant bacteria in the reactor belonged to phyla *Firmicutes* ($34 \pm 9\%$), *Bacteroidota* ($17 \pm 7\%$), *Chloroflexi* ($8 \pm 3\%$), and *Proteobacteria* ($6 \pm 5\%$), while the dominant archaea were *Halobacterota* ($26 \pm 10\%$) and *Euryarchaeota* ($3 \pm 1\%$) (**Figure 6A**). Jabari et al. (2016) also reported that the most frequently detected bacteria in an anaerobic reactor treating protein-rich SWW belonged to *Firmicutes*, specifically to the class *Clostridia* (**Figure S1**), and *Bacteroidota*. As in the BT, *Clostridium sensu stricto 1* was also prevalent in the reactor but decreased in relative abundance from $18 \pm 4\%$ in phase I to $13 \pm 2\%$ in phase III as the OLR increased. By contrast, the abundance of the archaea *Methanosaeta* increased from $22 \pm 3\%$ to $30 \pm 9\%$ during phase III (**Figure 6B**), which indicated that enrichment of methanogens occurred in the reactor. The enriched species were identified as *Methanotherx harundinacea strain 8Ac* and *Methanotherx soehngeni GP6* (**Table S1**).

It should be noted that the identified core microbiome contained mainly protein/amino acids degraders such as *Turicibacter sp.*, *Turicibacter sanguinis strain MOL361*, *Romboustia sp.*, *Romboustia timonensis strain DR1*, *Proteiniclasticum*, *Clostridium sensu stricto 1 sp.*, and *Clostridium disporicum strain DS1* in the BT, and *Proteiniclasticum* and *Clostridium sensu stricto 1* in the reactor (**Figure S2**). Other protein- and amino acids-degrading genera such as *Proteocatella* and *Proteiniphilum* were also present but in lower relative abundances (**Figure 6B**). The dominance of protein degraders indicated that the AnSBR was favoured for selection of this microbiota.

Alpha diversity indices were used to compare the evenness and richness of the microbial population of the inoculum and in the BT and reactor throughout the entire operation period (**Figure 6C**). The median alpha diversity metrics from the observed ASVs were 775 for the BT, 696 for the reactor, and 525 for the inoculum. Even though the BT had the highest microbial richness, the variation among the scores indicated no substantial difference among the samples. By contrast, the Shannon index showed a higher score in the reactor (4.27) than in the BT (4.16) or inoculum (4.02) (**Figure 6C**). Because the Shannon index score considers the richness and evenness of the microbial population, the highest value observed in the reactor indicated a more even microbial population than in the BT. The differences in the diversity among samples was attributed to the changes in OLR over 260 days. These changes could promote higher diversity but could also lead to variable microbial community functions

(Santillan et al. 2019), i.e., a high alpha diversity may indicate a relatively stable COD conversion in the reactor. Still, a decreasing COD to CH₄ conversion was observed even though enrichment of methanogens occurred. Apparently, there was no increased in the methanogenic activity, which might also be attributed to reasons other than microbial diversity and species richness. Moreover, beta diversity analysis of the principal coordinates indicated that the reactor's microbial community matched with the inoculum sample and differed from that in the BT (**Figure S3**).

3.3 Correlation analysis

3.3.1 Parameter affecting COD removal

The Pearson correlation analysis showed that SLR, HRT, SRT, and acidification degree of TCOD had low correlations (< 0.30) with the TCOD removal efficiency (**Table 3**). Therefore, variations in these parameters would have a minor effect on TCOD removal. At the same time, the OLR, acidification degree of SCOD, and ammonification efficiency in the reactor had moderate correlation ($0.31 - 0.60$) with the TCOD removal efficiency. Among the identified indicators, the ammonification efficiency in the reactor had the highest correlation coefficient (0.56) with TCOD removal. The results showed that protein degradation had a statistically significant contribution to TCOD removal, and the ammonification efficiency was a good indicator of protein degradation.

SLR, acidification and protein concentration in the reactor liquid showed moderate correlations ($0.31 - 0.60$) with the SCOD removal efficiency. SLR had a correlation coefficient of 0.41 , and OLR had a correlation coefficient of 0.30 with SCOD removal. Acidification of TCOD had a correlation coefficient of 0.60 with SCOD removal, which meant that hydrolysis and/or acidification of TCOD was limiting SCOD removal. The protein concentration in the reactor liquid had a correlation coefficient of 0.51 with SCOD removal, which indicated that residual protein in the reactor was limiting the SCOD removal.

Our results indicate that the OLR in the reactor and HRT in the BT, which determines the acidification degree, shall be prioritised as control parameters when treating SWW with a high solids content. However, when treating wastewater containing mainly SCOD, the SLR in the reactor and HRT in the BT shall be prioritised as control parameters.

Overall, both the loading rate and attained acidification degree in the BT are important for COD removal. Additionally, ammonification efficiency in the reactor was closely related to TCOD removal, and protein residues in the reactor liquid affected SCOD removal. The applied ranges of HRT and SRT in the reactor do not significantly affect TCOD and SCOD removal, indicating that the applied retention times are sufficiently long. Therefore, further investigations are required to determine the correlation between COD removal efficiency and applied retention time and to optimise the required reactor volume.

3.3.2 Parameters affecting the sludge ZSV

There were high correlations between sludge ZSV and ammonification efficiency in the BT (- 0.71) and reactor (0.70), and between the ZSV and the carbohydrate concentration in the reactor liquid (- 0.81) (Table 3). These results indicated that the degradation of proteins and carbohydrates had a significant effect on the sludge settling performance. The high negative correlation (-0.71) between ammonification efficiency in the BT and ZSV illustrates that a shorter HRT in the BT is preferred for better settling.

Table 3 - Correlation analysis of TCOD, SCOD, ZSV and reactor operational and performance parameters.

Output variables	Pearson correlation	Loading rate		HRT SRT		Acidification		Ammonification		Protein concentration	Carbohydrate concentration
		OLR	SLR	TCOD	SCOD	BT	Reactor	Reactor liquid	Reactor liquid		
TCOD removal	Correlation coefficient	0.37	0.25	-0.17	0.17	0.27	0.31	0.08	0.56	0.10	0.02
	<i>p</i> value	0.00	0.00	0.01	0.01	0.01	0.00	0.68	0.00	0.64	0.93
SCOD removal	Correlation coefficient	0.30	0.41	0.08	0.00	0.60	0.38	0.20	-0.20	0.51	0.03
	<i>p</i> value	0.00	0.00	0.21	0.98	0.00	0.00	0.29	0.30	0.01	0.90
ZSV	Correlation coefficient	0.15	0.01	-0.40	-0.05	-0.36	-0.03	-0.71	0.7	-0.39	-0.81
	<i>p</i> value	0.32	0.93	0.01	0.76	0.08	0.88	0.03	0.05	0.39	0.03

$P > 0.05$ No correlation,

0.00 - 0.30 Low correlation,

0.31 - 0.60 Medium correlation,

0.61- 1.0 High correlation.

The HRT in the reactor had a moderate correlation with the ZSV, and the negative value indicated a higher HRT in the reactor led to a lower ZSV. Possibly, an increase in the fraction of small size particles in the sludge at a high HRT will gradually contribute to a reduction in the ZSV over long-term operation.

The correlation analysis statistically identified the HRT in the BT and the reactor as the key parameters affecting sludge settling, and a relatively short HRT in the BT and reactor is recommended to achieve higher ZSV. However, HRT in the BT also controls the acidification of TCOD and SCOD, which had a low-medium correlation with TCOD and SCOD removal. Further studies are needed to optimise the HRT in the BT and the reactor to achieve both high COD removal and good sludge settling.

3.3.3 Microbial community correlation

A PERMANOVA statistical test (**Table 4**) was carried out to analyse the correlation between the core microbial community structure, the AnSBR performance indicators, and the operational parameters. A statistically significant correlation ($p < 0.05$) was identified between the core microbial community and the attained ammonification efficiency ($R^2 = 0.14$). The R^2 of PERMANOVA represents the correlation of the distance matrix with a given variable. The results indicated that the change in the core microbial community structure, specifically the variation in the relative abundance of the protein-degrading *Clostridium sensu stricto 1* (**Figure S2B**), affected the ammonification efficiency. Even though the coefficient of determination was low, it inferred that protein ammonification was the key process governing the AnSBR treatment performance. Similarly, Li et al. (2015) found that *Clostridium sensu stricto*, the dominant microbiome genus from 20 full-scale anaerobic reactors treating manure, was positively correlated with increasing ammonium concentrations in the reactors. Moreover, Duong et al. (2019) concluded that degradation of amino acids to $\text{NH}_4^+\text{-N}$, VFAs, H_2 and CO_2 , instead of hydrolysis of proteins to amino acids, governed the optimisation of the design for anaerobic reactors treating protein-rich wastewaters.

Table 4 - Statistical significance between the microbial community and ammonification efficiency in reactor by PERMANOVA ($p < 0.05$) analysis (using unweighted unifrac distance).

Factor	R ²	<i>p</i> value
TCOD removal (%)	0.12	0.29
SCOD removal (%)	0.11	0.48
OLR (gCOD·L ⁻¹ ·d ⁻¹)	0.12	0.29
SLR (gCOD·gVSS ⁻¹ ·d ⁻¹)	0.10	0.76
HRT (d)	0.09	0.80
SRT (d)	0.14	0.05
Acidification (VFAs) TCOD (%)	0.10	0.75
Acidification (VFAs) SCOD (%)	0.11	0.44
Ammonification efficiency (%)	0.14	0.01

R²: coefficient of determination, *p* value: probability value.

4 Conclusions

- Without pre-removal of FOG or solids, the present AnSBR set-up achieved a maximum TCOD removal of 90%, a protein degradation efficiency exceeding 80%, and a COD to CH₄ conversion efficiency of over 70% at OLRs up to 6.2 gCOD·L⁻¹·d⁻¹ when treating protein-rich SWW.
- The OLR substantially affected the COD removal efficiency of the AnSBR, concomitantly with the HRT in the BT, and the SLR.
- The HRT in the BT and the reactor, which determined the ammonification efficiencies and the residual carbohydrate concentrations in the reactor liquid, affected the sludge settleability.
- The genus *Clostridium sensu stricto 1*, involved in protein and lipids degradation, was the predominant genera in the reactor. Additionally, the core microbiome showed a low but statistically significant correlation with the ammonification efficiency in the reactor, which indicated that the degradation of proteins and amino acids was the governing process determining the overall COD removal and reactor performance.

Supporting information

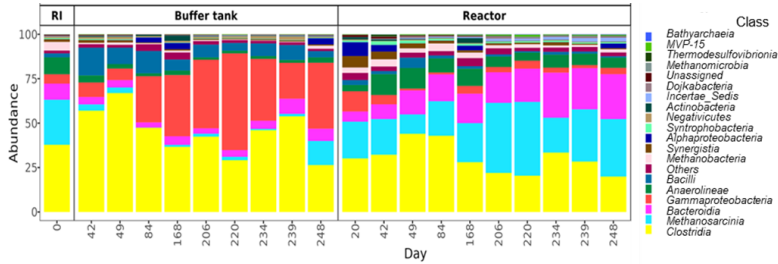


Figure S1 Microbial community dynamics in AnSBR and buffer tank at the class level.

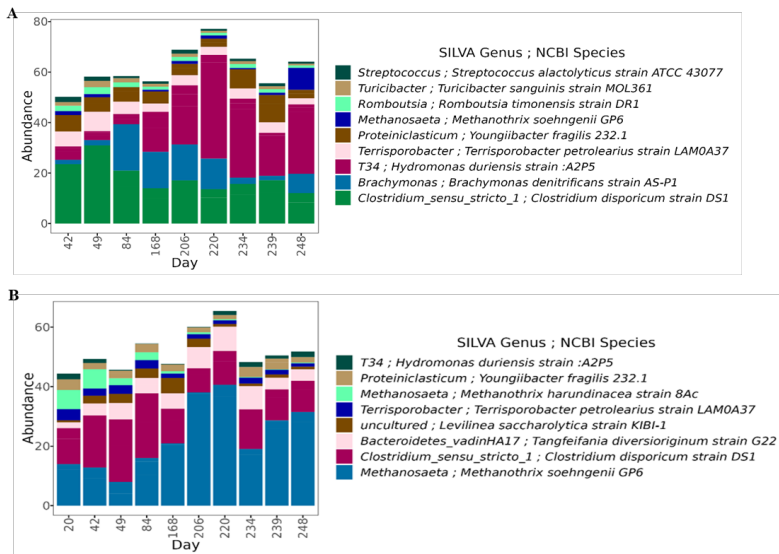


Figure S2 Core microbiome or predominant amplicon sequence variants (ASVs) with average relative abundance > 1% in A) Buffer tank and B) Reactor at the species level.

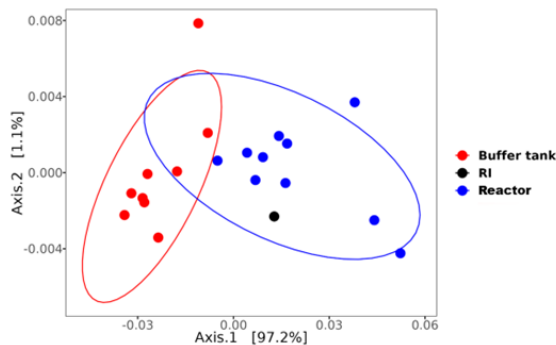


Figure S3 Beta diversity PCoA analysis of buffer tank and reactor samples.

CHAPTER 7

CONCLUSIONS AND RECOMMENDATIONS

1 Overview of the ammoniacal nitrogen recovery from nitrogen-loaded residual streams

Chapter 2 reviews the whole chain of TAN recovery from N-loaded residual streams. In this chapter, the N-loaded residual streams are identified as residual streams with a minimum TKN of $0.5 \text{ g N}\cdot\text{L}^{-1}$ and are categorised by their TAN recovery potential, which is depending on TAN/TKN ratio and TSS content, into three different groups. Based on the categorisation, currently available physical, chemical, and biological technologies can be selected or combined for TAN recovery, or directions for development of future technologies can be identified.

Typically, TAN in residual streams are released from proteins. AD is recommended for protein to TAN conversion in upstream processes prior to TAN recovery, because it converts the protein into TAN while reducing COD and TSS. However, AD has its own limitations, such as low conversion rates and limited conversion efficiencies, mainly due to incomplete hydrolysis and TAN inhibition. In order to enhance the protein to TAN conversion, it is recommended to investigate the rate-limiting step during anaerobic treatment of protein-rich wastewater and understand the factors limiting protein degradation.

Chapter 2 categorises currently available technologies into TAN concentrating technologies (i.e., TAN is not separated from the original stream) and TAN recovery technologies (i.e., TAN is separated from the original stream). Directly available TAN can be concentrated by forward osmosis, reverse osmosis, (bio-) electrochemical cells, and electrodialysis, and then recovered by precipitation and stripping. The recovered TAN is present in various forms, such as TAN solutions, NH_3 gas, solid NH_4^+ salts, etc. Difficulties were identified in comparing the energy and resource input per unit of TAN recovered by the above-mentioned technologies. For future studies on TAN recovery, it is recommended to report a normalised input, i.e., energy, costs, and chemicals, that is required when applying specific technologies.

Chapter 2 also identifies and discusses various applications of the recovered TAN, including N-fertiliser production, energy generation, industrial processes usage, and some novel ones such as microbial protein production. The amount of TAN that can be recovered and the quality of the recovered TAN are constraining the reuse of TAN. Most studies focused on

TAN recovery efficiency of specific technologies but overlooked the effect of the recovered TAN during reuse, as well as the quantity and quality demand of the end-users of the recovered TAN. It is recommended to bridge the communication between the researchers working on TAN recovery and the end-users, and to better select the available technologies based on both characteristics of the residual stream and the actual demand of the end-users.

2 Rate-limiting step in anaerobic protein degradation and effect of the presence of carbohydrates and intermediates

Chapter 3 identifies deamination as the rate-limiting step in anaerobic protein degradation. Compared to CAS with a simpler structure, BSA showed lower hydrolysis and deamination rates, which was identified as a negative effect of higher structural complexity. According to the reaction rates obtained from the applied Gompertz model, presence of carbohydrates resulted in a positive effect on the protein hydrolysis and methanogenesis, but a negative effect on deamination. A high initial VFA concentration negatively affected the protein hydrolysis and deamination rates. Therefore, it is recommended to design the anaerobic reactors based on the attainable deamination rate when treating protein-rich wastewaters, and to avoid high VFA concentrations.

3 Mechanism of retardation of anaerobic protein degradation by the presence of carbohydrates

Chapter 4 correlates the shift in microbial community composition with the retardation of anaerobic protein degradation and concludes that the retardation of casein degradation by the presence of lactose was due to 1) the substrate-preference of the dominant bacteria, including the facultative bacteria and the sugar fermenters, and 2) the higher growth rate and yield of the dominant bacteria.

Chapter 5 applies the novel proteogenomic technology and directly identifies *Acinetobacter* as the active anaerobic protein degraders. The results from this chapter confirmed that the retardation of anaerobic protein degradation in the presence of carbohydrates was caused by the substrate preference of the active protein degraders, which were able to ferment both

proteins and carbohydrates. Additionally, both the hydrolysis and deamination were found to be carried out by the active protein degraders. The presence of glucose was hypothesised to provide energy for hydrolysing proteins, which explains the higher hydrolysis rate in the presence of carbohydrates.

Overall, **Chapter 4** and **5** offer a better understanding of the mechanisms behind the retardation of protein degradation in the presence of carbohydrates. To relieve the retardation of protein degradation, specifically deamination, separation of proteins and carbohydrates degradation is recommended, e.g., by feast and famine feeding regime, to allow completion of carbohydrate first and degrade protein in the absence of carbohydrate.

4 Application of anaerobic sequencing batch reactor to reduce the retardation of anaerobic protein degradation by the presence of carbohydrates

Chapter 6 describes the performance of a novel AnSBR system treating protein-rich SWW. The AnSBR achieved maximum 90% TCOD removal, 85% protein degradation efficiency, and over 70% COD to CH₄ conversion efficiency without pre-treatment at an OLR up to 6.2 kg COD·L⁻¹·d⁻¹. The high COD removal efficiency and protein degradation efficiency suggested that the AnSBR is suitable for protein-rich wastewater treatment. This chapter also identifies the OLR, HRT and SLR as the key operational parameters, which affected COD removal efficiency and sludge settleability. Furthermore, the low but statistically significant correlation between *Clostridium sensu stricto 1*, i.e., involved in protein degradation, and the ammonification efficiency, indicated that protein degradation to ammonium is the governing process in overall TCOD removal and reactor performance.

Therefore, it is recommended to apply AnSBR for the treatment of complex protein-rich industrial wastewater. To achieve high COD removal and conversion efficiencies, the HRT in the BT and the OLR and SLR in the reactor shall be optimised. Besides, a good sludge settleability in the reactor can be obtained by properly regulating the HRT in the BT. Additionally, bioaugmentation of protein-degraders can be applied to increase the protein degradation capacity and further improve protein degradation.

BIBLIOGRAPHY

- Adhikari, B.B., Chae, M. and Bressler, D.C. (2018) Utilization of Slaughterhouse Waste in Value-Added Applications: Recent Advances in the Development of Wood Adhesives. *Polymers* 10(2), 176.
- Afif, A., Radenahmad, N., Cheok, Q., Shams, S., Kim, J.H. and Azad, A.K. (2016) Ammonia-fed fuel cells: A comprehensive review. *Renew. Sust. Energ. Rev.* 60, 822-835.
- Ahmad, F., Silva, E.L. and Varesche, M.B.A. (2018) Hydrothermal processing of biomass for anaerobic digestion – A review. *Renew. Sust. Energ. Rev.* 98, 108-124.
- Ahn, J.H., Do, T.H., Kim, S.D. and Hwang, S. (2006) The effect of calcium on the anaerobic digestion treating swine wastewater. *Biochem. Eng. J.* 30(1), 33-38.
- Ali, A., Wu, Z., Li, M. and Su, J. (2021) Carbon to nitrogen ratios influence the removal performance of calcium, fluoride, and nitrate by *Acinetobacter* H12 in a quartz sand-filled biofilm reactor. *Bioresour. Technol.* 333, 125154.
- Andersen, K.S., Kirkegaard, R.H., Karst, S.M. and Albertsen, M. (2018) ampvis2: an R package to analyse and visualise 16S rRNA amplicon data. *bioRxiv*, 299537.
- André, L., Pauss, A. and Ribeiro, T. (2017) A modified method for COD determination of solid waste, using a commercial COD kit and an adapted disposable weighing support. *Bioproc. Biosyst. Eng.* 40(3), 473-478.
- Angelidaki, I. and Ahring, B.K. (1993) Thermophilic anaerobic digestion of livestock waste: the effect of ammonia. *Appl. Microbiol. Biotechnol.* 38(1993), 560-564.
- Aoki, Y., Yamaguchi, T., Kobayashi, S., Kowalski, D., Zhu, C. and Habazaki, H. (2018) High-Efficiency Direct Ammonia Fuel Cells Based on BaZr_{0.1}Ce_{0.7}Y_{0.2}O_{3-δ}/Pd Oxide-Metal Junctions. *Global Challenges* 2(1), 1700088.
- Arkin, A.P., Cottingham, R.W., Henry, C.S., Harris, N.L., Stevens, R.L., Maslov, S., Dehal, P., Ware, D., Perez, F. and Canon, S. (2018) KBase: the United States department of energy systems biology knowledgebase. *Nat. Biotechnol.* 36(7), 566-569.
- Atamer, Z., Post, A.E., Schubert, T., Holder, A., Boom, R.M. and Hinrichs, J. (2017) Bovine β -casein: Isolation, properties and functionality. A review. *Int. Dairy J.* 66, 115-125.
- Aziz, A., Basheer, F., Sengar, A., Khan, S.U. and Farooqi, I.H. (2019) Biological wastewater treatment (anaerobic-aerobic) technologies for safe discharge of treated slaughterhouse and meat processing wastewater. *Sci. Total Environ.* 686, 681-708.
- Bäckhed, F., Ding, H., Wang, T., Hooper, L.V., Koh, G.Y., Nagy, A., Semenkovich, C.F. and Gordon, J.I. (2004) The gut microbiota as an environmental factor that regulates fat storage. *PNAS.* 101(44), 15718-15723.
- Baena, S., Fardeau, M.L., Labat, M., Ollivier, B., Garcia, J.L. and Patel, B. (2000) *Aminobacterium mobile* sp. nov., a new anaerobic amino-acid-degrading bacterium. *Int. J. Syst. Evol. Microbiol.* 50(1), 259-264.

- Baena, S., Fardeau, M.L., Ollivier, B., Labat, M., Thomas, P., Garcia, J.L. and Patel, B. (1999) *Aminomonas paucivorans* gen. nov., sp. nov., a mesophilic, anaerobic, amino-acid-utilizing bacterium. *Int. J. Syst. Evol. Microbiol.* 49(3), 975-982.
- Baker, B.R., Mohamed, R., Al-Gheethi, A. and Aziz, H.A. (2021) Advanced technologies for poultry slaughterhouse wastewater treatment: A systematic review. *J. Dispers. Sci. Technol.* 42(6), 880-899.
- Bareha, Y., Girault, R., Guezal, S., Chaker, J. and Tremier, A. (2019) Modeling the fate of organic nitrogen during anaerobic digestion : Development of a bioaccessibility based ADM1. *Water Res.* 154, 298-315.
- Bareha, Y., Girault, R., Jimenez, J. and Trémier, A. (2018) Characterization and prediction of organic nitrogen biodegradability during anaerobic digestion: A bioaccessibility approach. *Bioresour. Technol.* 263, 425-436.
- Barker, H.A. (1961) Chapter 3 - Fermentations of nitrogenous organic compounds. *Metab. Clin. Exp.*, 151-207.
- Barker, H.A. (1981) Amino Acid Degradation By Anaerobic Bacteria. *Ann. Rev. Biochem.* 1981(50), 23-40.
- Batstone, D.J., Keller, J., Angelidaki, I., Kalyuzhnyi, S.V., Pavlostathis, S.G., Rozzi, A., Sanders, W.T., Siegrist, H. and Vavilin, V.A. (2002) The IWA Anaerobic Digestion Model No 1 (ADM1). *Water Sci. Technol.* 45(10), 65-73.
- Bayard, R., Gonzalez-Ramirez, L., Guendouz, J., Benbelkacem, H., Buffière, P. and Gourdon, R. (2015) Statistical Analysis to Correlate Bio-physical and Chemical Characteristics of Organic Wastes and Digestates to Their Anaerobic Biodegradability. *Waste Biomass Valorization* 6(5), 759-769.
- Beckinghausen, A., Odlare, M., Thorin, E. and Schwede, S. (2020) From removal to recovery: An evaluation of nitrogen recovery techniques from wastewater. *Appl. Energy* 263, 114616.
- Bevilacqua, R., Regueira, A., Mauricio-Iglesias, M., Lema, J.M. and Carballa, M. (2020) Protein composition determines the preferential consumption of amino acids during anaerobic mixed-culture fermentation. *Water Res.* 183, 115958.
- Bhat, M.Y., Dar, T.A. and Singh, L.R. (2016) Milk proteins—from structure to biological properties and health aspects. Gigli, I. (ed), pp. 1-17, IntechOpen.
- Bilen, M., Mbogning, M.D., Cadoret, F., Dubourg, G., Daoud, Z., Fournier, P.E. and Raoult, D. (2016) “*Pygmaibacter massiliensis*” sp., nov., a new bacterium isolated from the human gut of a pygmy female. *NMNI* 10(1016).
- Bokulich, N.A., Subramanian, S., Faith, J.J., Gevers, D., Gordon, J.I., Knight, R., Mills, D.A. and Caporaso, J.G. (2013) Quality-filtering vastly improves diversity estimates from Illumina amplicon sequencing. *Nat. Methods* 10(1), 57-59.

Bolyen, E., Rideout, J.R., Dillon, M.R., Bokulich, N.A., Abnet, C.C., Al-Ghalith, G.A., Alexander, H., Alm, E.J., Arumugam, M., Asnicar, F., Bai, Y., Bisanz, J.E., Bittinger, K., Brejnrod, A., Brislawn, C.J., Brown, C.T., Callahan, B.J., Caraballo-Rodríguez, A.M., Chase, J., Cope, E.K., Da Silva, R., Diener, C., Dorrestein, P.C., Douglas, G.M., Durall, D.M., Duvallet, C., Edwardson, C.F., Ernst, M., Estaki, M., Fouquier, J., Gauglitz, J.M., Gibbons, S.M., Gibson, D.L., Gonzalez, A., Gorlick, K., Guo, J., Hillmann, B., Holmes, S., Holste, H., Huttenhower, C., Huttley, G.A., Janssen, S., Jarmusch, A.K., Jiang, L., Kaehler, B.D., Kang, K.B., Keefe, C.R., Keim, P., Kelley, S.T., Knights, D., Koester, I., Kosciulek, T., Kreps, J., Langille, M.G.I., Lee, J., Ley, R., Liu, Y.-X., Loftfield, E., Lozupone, C., Maher, M., Marotz, C., Martin, B.D., McDonald, D., McIver, L.J., Melnik, A.V., Metcalf, J.L., Morgan, S.C., Morton, J.T., Naimey, A.T., Navas-Molina, J.A., Nothias, L.F., Orchanian, S.B., Pearson, T., Peoples, S.L., Petras, D., Preuss, M.L., Pruesse, E., Rasmussen, L.B., Rivers, A., Robeson, M.S., Rosenthal, P., Segata, N., Shaffer, M., Shiffer, A., Sinha, R., Song, S.J., Spear, J.R., Swafford, A.D., Thompson, L.R., Torres, P.J., Trinh, P., Tripathi, A., Turnbaugh, P.J., Ul-Hasan, S., van der Hoof, J.J.J., Vargas, F., Vázquez-Baeza, Y., Vogtmann, E., von Hippel, M., Walters, W., Wan, Y., Wang, M., Warren, J., Weber, K.C., Williamson, C.H.D., Willis, A.D., Xu, Z.Z., Zaneveld, J.R., Zhang, Y., Zhu, Q., Knight, R. and Caporaso, J.G. (2019) Reproducible, interactive, scalable and extensible microbiome data science using QIIME 2. *Nature Biotechnology* 37(8), 852-857.

Bonmatí, A. and Flotats, X. (2003) Air stripping of ammonia from pig slurry: characterisation and feasibility as a pre- or post-treatment to mesophilic anaerobic digestion. *Waste Manage.* 23(3), 261-272.

Borowski, S., Boniecki, P., Kubacki, P. and Czyżowska, A. (2018) Food waste co-digestion with slaughterhouse waste and sewage sludge: Digestate conditioning and supernatant quality. *Waste Manage.* 74, 158-167.

Bourassa, P., Kanakis, C.D., Tarantilis, P., Pollissiou, M.G. and Tajmir-Riahi, H.A. (2010) Resveratrol, genistein, and curcumin bind bovine serum albumin. *J. Phys. Chem. B* 114(9), 3348-3354.

Bouvet, P. and Jeanjean, S. (1989) Delineation of new proteolytic genomic species in the genus *Acinetobacter*. *Res. Microbiol.* 140(4), 291-299.

Brady, C., Cleenwerck, I., Venter, S., Coutinho, T. and De Vos, P. (2013) Taxonomic evaluation of the genus *Enterobacter* based on multilocus sequence analysis (MLSA): proposal to reclassify *E. nimipressuralis* and *E. amnigenus* into *Lelliottia* gen. nov. as *Lelliottia nimipressuralis* comb. nov. and *Lelliottia amnigena* comb. nov., respectively, *E. gergoviae* and *E. pyrinus* into *Pluralibacter* gen. nov. as *Pluralibacter gergoviae* comb. nov. and *Pluralibacter pyrinus* comb. nov., respectively, *E. cowanii*, *E. radicincitans*, *E. oryzae* and *E. arachidis* into *Kosakonia* gen. nov. as *Kosakonia cowanii* comb. nov., *Kosakonia radicincitans* comb. nov., *Kosakonia oryzae* comb. nov. and *Kosakonia arachidis* comb. nov., respectively, and *E. turicensis*, *E. helveticus* and *E. pulveris* into *Cronobacter* as *Cronobacter*

zurichensis nom. nov., *Cronobacter helveticus* comb. nov. and *Cronobacter pulveris* comb. nov., respectively, and emended description of the genera *Enterobacter* and *Cronobacter*. *Syst. Appl. Microbiol.* 36(5), 309-319.

Braguglia, C.M., Gallipoli, A., Gianico, A. and Pagliaccia, P. (2018) Anaerobic bioconversion of food waste into energy: A critical review. *Bioresour. Technol.* 248, 37-56.

Braña, V., Cagide, C. and Morel, M.A. (2016) *Microbial Models: From Environmental to Industrial Sustainability*. Castro-Sowinski, S. (ed), pp. 227-247, Springer Singapore.

Breitenstein, A., Wiegel, J., Haertig, C., Weiss, N., Andreesen, J.R. and Lechner, U. (2002) Reclassification of *Clostridium hydroxybenzoicum* as *Sedimentibacter hydroxybenzoicus* gen. nov., comb. nov., and description of *Sedimentibacter saalensis* sp. nov. *Int. J. Syst. Evol. Microbiol.* 52(3), 801-807.

Brenner, D.J., O'Hara, C.M., Grimont, P.A.D., Janda, J.M., Falsen, E., Aldova, E., Ageron, E., Schindler, J., Abbott, S.L. and Steigerwalt, A.G. (1999) Biochemical identification of *Citrobacter* species defined by DNA hybridization and description of *Citrobacter gillenii* sp. nov. (formerly *Citrobacter genomospecies 10*) and *Citrobacter murlinae* sp. nov. (formerly *Citrobacter genomospecies 11*). *J. Clin. Microbiol.* 37(8), 2619-2624.

Bres, P., Beily, M.E., Young, B.J., Gasulla, J., Butti, M., Crespo, D., Candal, R. and Komilis, D. (2018) Performance of semi-continuous anaerobic co-digestion of poultry manure with fruit and vegetable waste and analysis of digestate quality: A bench scale study. *Waste Manage.* 82, 276-284.

Breure, A.M., Beeftink, H.H., Verkuijlen, J. and van An del, J.G. (1986a) Acidogenic fermentation of protein/carbohydrate mixtures by bacterial populations adapted to one of the substrates in anaerobic chemostat cultures. *Appl. Microbiol. Biotechnol.* 23, 245-249.

Breure, A.M., Mooijman, K.A. and van An del, J.G. (1986b) Protein degradation in anaerobic digestion: influence of volatile fatty acids and carbohydrates on hydrolysis and acidogenic fermentation of gelatin. *Appl. Microbiol. Biotechnol.* (24), 426-431.

Breure, A.M. and van An del, J.G. (1984) Hydrolysis and acidogenic fermentation of a protein, gelatin, in an anaerobic continuous culture. *Appl. Microbiol. Biotechnol.* 20(1984), 40-45.

Buckwell, A. and Nadeu, E. (2016) *Nutrient Recovery and Reuse (NRR) in European agriculture. A review of the issues, opportunities, and actions*. Brussels: RISE Foundation.

Bustillo-Lecompte, C.F. and Mehrvar, M. (2015) Slaughterhouse wastewater characteristics, treatment, and management in the meat processing industry: A review on trends and advances. *J. Environ. Manage.* 161, 287-302.

Callahan, B.J., McMurdie, P.J., Rosen, M.J., Han, A.W., Johnson, A.J.A. and Holmes, S.P. (2016) DADA2: High-resolution sample inference from Illumina amplicon data. *Nature Methods* 13(7), 581-583.

Caporaso, J.G., Kuczynski, J., Stombaugh, J., Bittinger, K., Bushman, F.D., Costello, E.K., Fierer, N., Peña, A.G., Goodrich, J.K. and Gordon, J.I. (2010) QIIME allows analysis of high-throughput community sequencing data. *Nat. Methods* 7(5), 335-336.

Carrere, H., Antonopoulou, G., Affes, R., Passos, F., Battimelli, A., Lyberatos, G. and Ferrer, I. (2016) Review of feedstock pretreatment strategies for improved anaerobic digestion: From lab-scale research to full-scale application. *Bioresour. Technol.* 199, 386-397.

Cerrillo, M., Oliveras, J., Viñas, M. and Bonmatí, A. (2016) Comparative assessment of raw and digested pig slurry treatment in bioelectrochemical systems. *Bioelectrochemistry* 110, 69-78.

Cerrillo, M., Viñas, M. and Bonmatí, A. (2017) Microbial fuel cells for polishing effluents of anaerobic digesters under inhibition, due to organic and nitrogen overloads. *J. Chem. Technol. Biotechnol.* 92(12), 2912-2920.

Cerruti, M., Guo, B., Delatolla, R., de Jonge, N., Hommes-de Vos van Steenwijk, A., Kadota, P., Lawson, C.E., Mao, T., Oosterkamp, M.J., Sabba, F., Stockholm-Bjerregaard, M., Watson, I., Frigon, D. and Weissbrodt, D.G. (2021) Plant-wide systems microbiology for the wastewater industry. *Environ. Sci. Water Res. Technol.* 7(10), 1687-1706.

Chen, I.-M.A., Chu, K., Palaniappan, K., Ratner, A., Huang, J., Huntemann, M., Hajek, P., Ritter, S., Varghese, N., Seshadri, R., Roux, S., Woyke, T., Eloë-Fadrosh, E.A., Ivanova, N.N. and Kypides, Nikos C. (2020) The IMG/M data management and analysis system v.6.0: new tools and advanced capabilities. *Nucleic Acids Res.* 49(D1), D751-D763.

Chen, M., Kim, J.-H., Kishida, N., Nishimura, O. and Sudo, R. (2004) Enhanced nitrogen removal using C/N load adjustment and real-time control strategy in sequencing batch reactors for swine wastewater treatment. *Water Sci. Technol.* 49(5-6), 309-314.

Chen, S., He, J., Wang, H., Dong, B., Li, N. and Dai, X. (2018) Microbial responses and metabolic pathways reveal the recovery mechanism of an anaerobic digestion system subjected to progressive inhibition by ammonia. *Chem. Eng. J.* 350, 312-323.

Cherkasov, N., Ibhaddon, A.O. and Fitzpatrick, P. (2015) A review of the existing and alternative methods for greener nitrogen fixation. *Chem. Eng. Process.* 90, 24-33.

Chien, S.H., Gearhart, M.M. and Villagarcía, S. (2011) Comparison of ammonium sulfate with other nitrogen and sulfur fertilizers in increasing crop production and minimizing environmental impact: A review. *Soil Sci.* 176(7), 327-335.

Christiaens, M.E.R., De Vrieze, J., Clinckemaillie, L., Ganigué, R. and Rabaey, K. (2019a) Anaerobic ureolysis of source-separated urine for NH₃ recovery enables direct removal of divalent ions at the toilet. *Water Res.* 148, 97-105.

Christiaens, M.E.R., Udert, K.M., Arends, J.B.A., Huysman, S., Vanhaecke, L., McAdam, E. and Rabaey, K. (2019b) Membrane stripping enables effective electrochemical ammonia

recovery from urine while retaining microorganisms and micropollutants. *Water Res.* 150, 349-357.

Chung, Y.-C., Son, D.-H. and Ahn, D.-H. (2000) Nitrogen and organics removal from industrial wastewater using natural zeolite media. *Water Sci. Technol.* 42(5-6), 127-134.

Cinti, G., Discepoli, G., Sisani, E. and Desideri, U. (2016) SOFC operating with ammonia: Stack test and system analysis. *Int. J. Hydrog. Energy* 41(31), 13583-13590.

Crini, G. and Lichtfouse, E. (2019) Advantages and disadvantages of techniques used for wastewater treatment. *Environ. Chem. Lett.* 17(1), 145-155.

Dakin, H. (1920) Amino-Acids of Gelatin. *J. Biol. Chem.* 44, 499-499.

de Jonge, N., Poulsen, J.S., Vechi, N.T., Kofoed, M.V.W. and Nielsen, J.L. (2022) Wood-Ljungdahl pathway utilisation during in situ H₂ biomethanation. *Sci. Total Environ.* 806, 151254.

De Vrieze, J. and Verstraete, W. (2016) Perspectives for microbial community composition in anaerobic digestion: from abundance and activity to connectivity. *Environ. Microbiol.* 18(9), 2797-2809.

Degn Pedersen, P., Jensen, K., Lyngsie, P. and Henrik Johansen, N. (2003) Nitrogen removal in industrial wastewater by nitrification and denitrification - 3 years of experience. *Water Sci. Technol.* 47(11), 181-188.

Dekker, N.J.J. and Rietveld, G. (2006) Highly efficient conversion of ammonia in electricity by solid oxide fuel cells. *J. Fuel Cell Sci. Technol.* 3(4), 499-502.

Deng, Y., Guo, X., Wang, Y., He, M., Ma, K., Wang, H., Chen, X., Kong, D., Yang, Z. and Ruan, Z. (2015) *Terrisporobacter petrolearius* sp. nov., isolated from an oilfield petroleum reservoir. *Int. J. Syst. Evol. Microbiol.* 65(Pt_10), 3522-3526.

Deng, Z., Ferreira, A.L.M., Spanjers, H. and van Lier, J.B. (2022) Characterization of microbial communities in anaerobic acidification reactors fed with casein and/or lactose. *Appl. Microbiol. Biotechnol.* 106(18), 6301-6316.

Deng, Z., Ferreira, A.L.M., Spanjers, H. and van Lier, J.B. (2023a) Anaerobic protein degradation: Effects of protein structure complexity, protein concentrations, carbohydrates, and volatile fatty acids. *Bioresour. Technol. Rep.* 22, 101501.

Deng, Z., Muñoz Sierra, J., Ferreira, A.L.M., Cerqueda-Garcia, D., Spanjers, H. and van Lier, J.B. (2023b) Effect of operational parameters on the performance of an anaerobic sequencing batch reactor (AnSBR) treating protein-rich wastewater. *Environ. Sci. Ecotechnology.* 100296.

Deng, Z., van Linden, N., Guillen, E., Spanjers, H. and van Lier, J.B. (2021) Recovery and applications of ammoniacal nitrogen from nitrogen-loaded residual streams: A review. *J. Environ. Manage.* 295, 113096.

- Desloover, J., Vlaeminck, S.E., Clauwaert, P., Verstraete, W. and Boon, N. (2012) Strategies to mitigate N₂O emissions from biological nitrogen removal systems. *Curr. Opin. Biotechnol.* 23(3), 474-482.
- Deusch, S., Camarinha-Silva, A., Conrad, J., Beifuss, U., Rodehutschord, M. and Seifert, J. (2017) A structural and functional elucidation of the rumen microbiome influenced by various diets and microenvironments. *Front. Microbiol.* 8, 1605.
- Dickinson, E. (2003) *Advanced dairy chemistry—1 proteins*, pp. 1229-1260, Springer.
- Dimitriou, P. and Javaid, R. (2020) A review of ammonia as a compression ignition engine fuel. *Int. J. Hydrog. Energy* 45(11), 7098-7118.
- DNV·GL (2020) *Maritime forecast to 2050 - Energy Transition outlook*, DNV GL - Maritime, Germany.
- Duan, J., Huo, X., Du, W., Liang, J., Wang, D. and Yang, S. (2016) Biodegradation of kraft lignin by a newly isolated anaerobic bacterial strain, *Acetoanaerobium* sp. WJDL - Y2. *Lett. Appl. Microbiol.* 62(1), 55-62.
- Dube, P.J., Vanotti, M.B., Szogi, A.A. and García-gonzález, M.C. (2016) Enhancing recovery of ammonia from swine manure anaerobic digester effluent using gas-permeable membrane technology. *Waste Manage.* 49, 372-377.
- Dubois, M., Gilles, K.A., Hamilton, J.K., Rebers, P.t. and Smith, F. (1956) Colorimetric method for determination of sugars and related substances. *Anal. Chem.* 28(3), 350-356.
- Dueholm, M.S., Nierychlo, M., Andersen, K.S., Rudkjøbing, V., Knutsson, S., Albertsen, M. and Nielsen, P.H. (2021) MiDAS 4: A global catalogue of full-length 16S rRNA gene sequences and taxonomy for studies of bacterial communities in wastewater treatment plants.
- Duong, T.H., Grolle, K., Nga, T.T.V., Zeeman, G., Temmink, H. and van Eekert, M. (2019) Protein hydrolysis and fermentation under methanogenic and acidifying conditions. *Biotechnol. Biofuels* 12, 254.
- Duong, T.H., van Eekert, M., Grolle, K., Tran, T.V.N., Zeeman, G. and Temmink, H. (2022) Effect of carbohydrates on protein hydrolysis in anaerobic digestion. *Water Sci Technol* 86(1), 66-79.
- Dürre, P., Spahr, R. and Andreesen, J.R. (1983) Glycine fermentation via a glycine reductase in *Peptococcus glycinophilus* and *Peptococcus magnus*. *Arch. Microbiol.* 134(2), 127-135.
- Edgar, R.C. (2004) MUSCLE: multiple sequence alignment with high accuracy and high throughput. *Nucleic Acids Res.* 32(5), 1792-1797.
- Edgar, R.C. (2013) UPARSE: highly accurate OTU sequences from microbial amplicon reads. *Nat. Methods* 10(10), 996-998.

- Edgar, R.C., Haas, B.J., Clemente, J.C., Quince, C. and Knight, R. (2011) UCHIME improves sensitivity and speed of chimera detection. *Bioinformatics* 27(16), 2194-2200.
- Ek, M., Bergström, R., Bjurhem, J.E., Björlenius, B. and Hellström, D. (2006) Concentration of nutrients from urine and reject water from anaerobically digested sludge. *Water Sci. Technol.* 54(11-12), 437-444.
- El-Bourawi, M.S., Khayet, M., Ma, R., Ding, Z., Li, Z. and Zhang, X. (2007) Application of vacuum membrane distillation for ammonia removal. *J. Membr. Sci.* 301(1-2), 200-209.
- El-Mashad, H.M., Zeeman, G., Van Loon, W.K., Bot, G.P. and Lettinga, G. (2004) Effect of temperature and temperature fluctuation on thermophilic anaerobic digestion of cattle manure. *Bioresour. Technol.* 95(2), 191-201.
- El Diwani, G., El Rafie, S., El Ibiari, N.N. and El-Aila, H.I. (2007) Recovery of ammonia nitrogen from industrial wastewater treatment as struvite slow releasing fertilizer. *Desalination* 214(1-3), 200-214.
- Elbeshbishy, E. and Nakhla, G. (2012) Batch anaerobic co-digestion of proteins and carbohydrates. *Bioresour. Technol.* 116, 170-178.
- Ellersdorfer, M. (2018) The ion-exchanger-loop-stripping process: ammonium recovery from sludge liquor using NaCl-treated clinoptilolite and simultaneous air stripping. *Water Sci. Technol.* 77(3), 695-705.
- Elliott, D.C., Hart, T.R., Schmidt, A.J., Neuenschwander, G.G., Rotness, L.J., Olarte, M.V., Zacher, A.H., Albrecht, K.O., Hallen, R.T. and Holladay, J.E. (2013) Process development for hydrothermal liquefaction of algae feedstocks in a continuous-flow reactor. *Algal Res.* 2(4), 445-454.
- Erisman, J.W., Bleeker, A., Galloway, J. and Sutton, M.S. (2007) Reduced nitrogen in ecology and the environment. *Environ. Pollut.* 150, 140-149.
- Erisman, J.W., Sutton, M.A., Galloway, J., Klimont, Z. and Winiwarter, W. (2008) How a century of ammonia synthesis changed the world. *Nat. Geosci.* 1, 636.
- Eurostats (2018) Agriculture, forestry and fishery statistics 2018 edition.
- FAO (2019) World fertilizer trends and outlook to 2022, Rome.
- FAO (2020) World Food and Agriculture - Statistical Yearbook 2020.
- Feng, S., Zhang, N., Liu, H., Du, X., Liu, Y. and Lin, H. (2012) The effect of COD/N ratio on process performance and membrane fouling in a submerged bioreactor. *Desalination* 285, 232-238.
- Forster-Carneiro, T., Pérez, M., Romero, L.I. and Sales, D. (2007) Dry-thermophilic anaerobic digestion of organic fraction of the municipal solid waste: Focusing on the inoculum sources. *Bioresour. Technol.* 98(17), 3195-3203.

- Fotidis, I.A., Wang, H., Fiedel, N.R., Luo, G., Karakashev, D.B. and Angelidaki, I. (2014) Bioaugmentation as a solution to increase methane production from an ammonia-rich substrate. *Environ. Sci. Technol.* 48(13), 7669-7676.
- Fournier, G.G.M., Cumming, I.W. and Hellgardt, K. (2006) High performance direct ammonia solid oxide fuel cell. *J. Power Sources* 162(1), 198-206.
- Fricke, B., Jahreis, G., Sorger, H. and Aurich, H. (1987) Zellhüllgebundene Proteinase-Aktivitäten in *Acinetobacter calcoaceticus* [Cell envelope-bound proteinase activities of *Acinetobacter calcoaceticus*]. *Biomed. Biochim. Acta.* 45(3), 257-264.
- Friedrich, M.W. (2006) Stable-isotope probing of DNA: insights into the function of uncultivated microorganisms from isotopically labeled metagenomes. *Curr. Opin. Biotechnol.* 17(1), 59-66.
- Fu, G., Cai, T. and Li, Y. (2011) Concentration of ammoniacal nitrogen in effluent from wet scrubbers using reverse osmosis membrane. *Biosyst. Eng.* 109(3), 235-240.
- Gain, E., Laborie, S., Viers, P., Rakib, M., Hartmann, D. and Durand, G. (2002) Ammonium nitrate wastewaters treatment by an electromembrane process. *Desalination* 149(1-3), 337-342.
- Gallert, C., Bauer, S. and Winter, J. (1998) Effect of ammonia on the anaerobic degradation of protein by a mesophilic and thermophilic biowaste population. *Appl. Microbiol. Biotechnol.* 50(4), 495-501.
- Galloway, J.N., Dentener, F.J., Capone, D.G., Boyer, E.W., Howarth, R.W., Seitzinger, S.P., Asner, G.P., Cleveland, C.C., Green, P.A., Holland, E.A., Karl, D.M., Michaels, A.F., Porter, J.H., Townsend, A.R. and Vo, C.J. (2004) Nitrogen cycles : past , present , and future. *Biogeochemistry* 70, 153-226.
- Galloway, J.N., Townsend, A.R., Erisman, J.W., Bekunda, M., Cai, Z., Freney, J.R., Martinelli, L.A., Seitzinger, S.P. and Sutton, M.A. (2008) Transformation of the Nitrogen Cycle : Recent Trends, Questions, and Potential Solutions. *Science* 320(5878), 889-893.
- Ganesh Saratale, R., Kumar, G., Banu, R., Xia, A., Periyasamy, S. and Dattatraya Saratale, G. (2018) A critical review on anaerobic digestion of microalgae and macroalgae and co-digestion of biomass for enhanced methane generation. *Bioresour. Technol.* 262, 319-332.
- Ganley, J.C. (2008) An intermediate-temperature direct ammonia fuel cell with a molten alkaline hydroxide electrolyte. *J. Power Sources* 178(1), 44-47.
- Garagounis, I., Vourros, A., Stoukides, D., Dasopoulos, D. and Stoukides, M. (2019) Electrochemical synthesis of ammonia: Recent efforts and future outlook. *Membranes* 9(9).
- Garcia-González, M.C. and Vanotti, M.B. (2015) Recovery of ammonia from swine manure using gas-permeable membranes: Effect of waste strength and pH. *Waste Manage.* 38, 455-461.

- García-González, M.C., Vanotti, M.B. and Szogi, A.A. (2015) Recovery of ammonia from swine manure using gas-permeable membranes: Effect of aeration. *J. Environ. Manage.* 152, 19-26.
- Gebreyessus, G.D. and Jenicek, P. (2016) Thermophilic versus Mesophilic Anaerobic Digestion of Sewage Sludge: A Comparative Review. *Bioengineering* 3(2), 15.
- Gerritsen, J., Fuentes, S., Grievink, W., van Niftrik, L., Tindall, B.J., Timmerman, H.M., Rijkers, G.T. and Smidt, H. (2014) Characterization of *Romboutsia ilealis* gen. nov., sp. nov., isolated from the gastro-intestinal tract of a rat, and proposal for the reclassification of five closely related members of the genus *Clostridium* into the genera *Romboutsia* gen. nov., *Intestinibacter* gen. nov., *Terrisporobacter* gen. nov. and *Asaccharospora* gen. nov. *Int. J. Syst. Evol. Microbiol.* 64(Pt_5), 1600-1616.
- Giddey, S., Badwal, S.P.S. and Kulkarni, A. (2013) Review of electrochemical ammonia production technologies and materials. *Int. J. Hydrog. Energy* 38(34), 14576-14594.
- Gil, A., Siles, J.A., Martín, M.A., Chica, A.F., Estévez-Pastor, F.S. and Toro-Baptista, E. (2018) Effect of microwave pretreatment on semi-continuous anaerobic digestion of sewage sludge. *Renew. Energy* 115, 917-925.
- Gil, K.I. and Choi, E. (2004) Nitrogen removal by recycle water nitrification as an attractive alternative for retrofit technologies in municipal wastewater treatment plants. *Water Sci. Technol.* 49(5-6), 39-46.
- Glenn, A.R. (1976) Production of extracellular proteins by bacteria. *Ann. Rev. Microbiol.* 30, 41-62.
- GMIA (2019) *Gelatine Handbook*, Gelatin Manufacturers Institute of America, US.
- Gong, H.Y., Z.: Liang, K. Q.: Jin, Z. Y.: Wang, K. J. (2013) Concentrating process of liquid digestate by disk tube-reverse osmosis system. *Desalination* 326, 30-36.
- Gonzalez-Martinez, A., Muñoz-Palazon, B., Rodriguez-Sanchez, A. and Gonzalez-Lopez, J. (2018) New concepts in anammox processes for wastewater nitrogen removal: recent advances and future prospects. *FEMS Microbiol. Lett.* 365(6).
- Grimont, F. and Grimont, P.A.D. (2006) *The Prokaryotes*, pp. 197-214.
- Grimont, P.A., Grimont, F. and Bouvet, P. (2000) *Salmonella in domestic animals*, pp. 1-17.
- Guerrero, L., Omil, F., Mendez, R. and Lema, J.M. (1999) Anaerobic Hydrolysis and Acidogenesis of Wastewaters From Food Industries With High Content of Organic Solids and Protein. *Water Res.* 33(15), 3281-3290.
- Guo, H., Oosterkamp, M.J., Tonin, F., Hendriks, A., Nair, R., van Lier, J.B. and de Kreuk, M.K. (2021) Reconsidering hydrolysis kinetics for anaerobic digestion of waste activated sludge applying cascade reactors with ultra-short residence times. *Water Res.* 202(1), 117398.

Gür, T.M. (2016) Comprehensive review of methane conversion in solid oxide fuel cells: Prospects for efficient electricity generation from natural gas. *Prog. Energy Combust. Sci.* 54, 1-64.

Haas, B.J., Gevers, D., Earl, A.M., Feldgarden, M., Ward, D.V., Giannoukos, G., Ciulla, D., Tabbaa, D., Highlander, S.K. and Sodergren, E. (2011) Chimeric 16S rRNA sequence formation and detection in Sanger and 454-pyrosequenced PCR amplicons. *Genome Res.* 21(3), 494-504.

Hahnke, S., Langer, T., Koeck, D.E. and Klocke, M. (2016) Description of *Proteiniphilum saccharofermentans* sp. nov., *Petrimonas mucosa* sp. nov. and *Fermentimonas caenicola* gen. nov., sp. nov., isolated from mesophilic laboratory-scale biogas reactors, and emended description of the genus *Proteiniphilum*. *Int. J. Syst. Evol. Microbiol.* 66(3), 1466-1475.

Hai, R., He, Y., Wang, X. and Li, Y. (2015) Simultaneous removal of nitrogen and phosphorus from swine wastewater in a sequencing batch biofilm reactor. *Chin. J. Chem. Eng.* 23(1), 303-308.

Hardy, G.A. and Dawes, E.A. (1985) Effect of oxygen concentration on the growth and respiratory efficiency of *Acinetobacter calcoaceticus*. *Microbiology* 131(4), 855-864.

Harris, P.W. and McCabe, B.K. (2015) Review of pre-treatments used in anaerobic digestion and their potential application in high-fat cattle slaughterhouse wastewater. *Appl. Energy* 155, 560-575.

Hartmann, H. and Ahring, B.K. (2005) Anaerobic digestion of the organic fraction of municipal solid waste: Influence of co-digestion with manure. *Water Res.* 39(8), 1543-1552.

Hassan, A. and Nelson, B. (2012) Invited review: anaerobic fermentation of dairy food wastewater. *J. Dairy Sci.* 95(11), 6188-6203.

He, Q., Tu, T., Yan, S., Yang, X., Duke, M., Zhang, Y. and Zhao, S. (2018) Relating water vapor transfer to ammonia recovery from biogas slurry by vacuum membrane distillation. *Sep. Purif. Technol.* 191, 182-191.

He, Q., Yu, G., Tu, T., Yan, S., Zhang, Y. and Zhao, S. (2017a) Closing CO₂ Loop in Biogas Production: Recycling Ammonia As Fertilizer. *Environ. Sci. Technol.* 51(15), 8841-8850.

He, Q., Yu, G., Wang, W., Yan, S., Zhang, Y. and Zhao, S. (2017b) Once-through CO₂ absorption for simultaneous biogas upgrading and fertilizer production. *Fuel Process. Technol* 166, 50-58.

Heo, J., Cho, H.Y., Heo, I., Hong, S.B., Kim, J.S., Kwon, S.W. and Kim, S.J. (2019) *Pulveribacter suum* gen. nov., sp. nov., isolated from a pig farm dust collector. *Int. J. Syst. Evol. Microbiol.* 69(7), 1864-1869.

Hernandez-Eugenio, G., Fardeau, M.-L., Cayol, J.-L., Patel, B.K., Thomas, P., Macarie, H., Garcia, J.-L. and Ollivier, B. (2002) *Sporanaerobacter acetigenes* gen. nov., sp. nov., a novel

acetogenic, facultatively sulfur-reducing bacterium. *Int. J. Syst. Evol. Microbiol.* 52(4), 1217-1223.

Hikmawati, D.N., Bagastyo, A.Y. and Warmadewanthi, I. (2019) Electrodialytic recovery of ammonium and phosphate ions in fertilizer industry wastewater by using a continuous-flow reactor. *J. Ecol. Eng.* 20(6), 255-263.

Hilares, R.T., Atoche-Garay, D.F., Pinto Pagaza, D.A., Ahmad, M.A., Andrade, G.J. and Santos, J.C. (2021) Promising physiochemical technologies for poultry slaughterhouse wastewater treatment: a critical review. *J. Environ. Chem. Eng.* 9, 105174.

Ho, Y.B., Zakaria, M.P., Latif, P.A. and Saari, N. (2013) Degradation of veterinary antibiotics and hormone during broiler manure composting. *Bioresour. Technol.* 131, 476-484.

Hofmann, G., Paroli, F. and Van Esch, J. (2009) Crystallization of Ammonium Sulphate: State of the Art and New Developments. *Chem. Eng. Trans.* 17, 657-662.

Holliger, C., Alves, M., Andrade, D., Angelidaki, I., Astals, S., Baier, U., Bougrier, C., Buffiere, P., Carballa, M., de Wilde, V., Ebertseder, F., Fernandez, B., Ficara, E., Fotidis, I., Frigon, J.C., de Lacroix, H.F., Ghasimi, D.S., Hack, G., Hartel, M., Heerenklage, J., Horvath, I.S., Jenicek, P., Koch, K., Krautwald, J., Lizasoain, J., Liu, J., Mosberger, L., Nistor, M., Oechsner, H., Oliveira, J.V., Paterson, M., Pauss, A., Pommier, S., Porqueddu, I., Raposo, F., Ribeiro, T., Rusch Pfund, F., Stromberg, S., Torrijos, M., van Eekert, M., van Lier, J., Wedwitschka, H. and Wierinck, I. (2016) Towards a standardization of biomethane potential tests. *Water Sci. Technol.* 74(11), 2515-2522.

Holloway, R.W., Childress, A.E., Dennett, K.E. and Cath, T.Y. (2007) Forward osmosis for concentration of anaerobic digester centrate. *Water Res.* 41(17), 4005-4014.

Holohan, B.C., Duarte, M.S., Szabo-Corbacho, M.A., Cavaleiro, A.J., Salvador, A.F., Pereira, M.A., Ziels, R.M., Frijters, C., Pacheco-Ruiz, S., Carballa, M., Sousa, D.Z., Stams, A.J.M., O'Flaherty, V., van Lier, J.B. and Alves, M.M. (2022) Principles, Advances, and Perspectives of Anaerobic Digestion of Lipids. *Environ. Sci. Technol.* 56(8), 4749-4775.

Hooper, D.U., Chapin III, F., Ewel, J.J., Hector, A., Inchausti, P., Lavorel, S., Lawton, J.H., Lodge, D., Loreau, M., Naeem, S., Schmid, B., Setälä, H., Symstad, A.J., Vandermeer, J. and Wardle, D.A. (2005) Effects of biodiversity on ecosystem functioning: a consensus of current knowledge. *Ecol. Monogr.* 75(1), 3-35.

Huang, H., Xiao, X. and Yan, B. (2009) Complex treatment of the ammonium nitrogen wastewater from rare-earth separation plant. *Desalin. Water Treat.* 8(1-3), 109-117.

Huang, H.M., Xiao, X.M., Yang, L.P. and Yan, B. (2011) Removal of ammonium from rare-earth wastewater using natural brucite as a magnesium source of struvite precipitation. *Water Sci. Technol.* 63(3), 468-474.

- Ippersiel, D., Mondor, M., Lamarche, F., Tremblay, F., Dubreuil, J. and Masse, L. (2012) Nitrogen potential recovery and concentration of ammonia from swine manure using electro dialysis coupled with air stripping. *J. Environ. Manage.* 95, S165-S169.
- Jabari, L., Gannoun, H., Cayol, J.-L., Hedi, A., Sakamoto, M., Falsen, E., Ohkuma, M., Hamdi, M., Fauque, G. and Ollivier, B. (2012) *Macellibacteroides fermentans* gen. nov., sp. nov., a member of the family Porphyromonadaceae isolated from an upflow anaerobic filter treating abattoir wastewaters. *Int. J. Syst. Evol. Microbiol.* 62(Pt_10), 2522-2527.
- Jabari, L., Gannoun, H., Khelifi, E., Cayol, J.-L., Godon, J.-J., Hamdi, M. and Fardeau, M.-L. (2016) Bacterial ecology of abattoir wastewater treated by an anaerobic digester. *Braz. J. Microbiol.* 47, 73-84.
- Jakubowski, H., Flatt, P., Agnew, H. and Larsen, D. (2022) Fundamentals of Biochemistry, a free and new LibreText book for Undergraduate Courses. *The FASEB Journal* 36(S1).
- Jazrawi, C., Biller, P., He, Y., Montoya, A., Ross, A.B., Maschmeyer, T. and Haynes, B.S. (2015) Two-stage hydrothermal liquefaction of a high-protein microalga. *Algal Res.* 8, 15-22.
- Jehmlich, N., Schmidt, F., von Bergen, M., Richnow, H.H. and Vogt, C. (2008) Protein-based stable isotope probing (Protein-SIP) reveals active species within anoxic mixed cultures. *ISME J.* 2(11), 1122-1133.
- Jenicek, P., Svehla, P., Zabranska, J. and Dohanyos, M. Factors affecting nitrogen removal by nitrification / denitrification. *Water Sci. Technol.* 49(5-6), 73-79.
- Jiang, Y., McAdam, E., Zhang, Y., Heaven, S., Banks, C. and Longhurst, P. (2019) Ammonia inhibition and toxicity in anaerobic digestion: A critical review. *J. Water Process. Eng.* 32, 100899.
- Jones, W.J., Nagle Jr, D. and Whitman, W.B. (1987) Methanogens and the diversity of archaeobacteria. *Microbiol. Rev.* 51(1), 135-177.
- Ju, T., Kong, J.Y., Stothard, P. and Willing, B.P. (2019) Defining the role of *Parasutterella*, a previously uncharacterized member of the core gut microbiota. *ISME J.* 13(6), 1520-1534.
- Ju, X., Gu, B., Wu, Y. and Galloway, J.N. (2016) Reducing China ' s fertilizer use by increasing farm size. *Glob. Environ. Change* 41(2016), 26-32.
- Kabdashi, I., Tünay, O., Öztürk, İ., Yılmaz, S. and Arıkan, O. (2000) Ammonia removal from young landfill leachate by magnesium ammonium phosphate precipitation and air stripping. *Water Sci. Technol.* 41(1), 237-240.
- Kampschreur, M.J., Temmink, H., Kleerebezem, R., Jetten, M.S.M. and van Loosdrecht, M.C.M. (2009) Nitrous oxide emission during wastewater treatment. *Water Res.* 43(17), 4093-4103.

- Karim, K., Klasson, K.T., Drescher, S.R., Ridenour, W., Borole, A.P. and Al-Dahhan, M.H. (2007) Mesophilic digestion kinetics of manure slurry. *Appl. Microbiol. Biotechnol.* 142, 231-242.
- Kayhanian, M. (1999) Ammonia inhibition in high-solids biogasification: An overview and practical solutions. *Environ. Technol.* 20(4), 355-365.
- Keucken, A., Habagil, M., Batstone, D., Jeppsson, U. and Arnell, M. (2018) Anaerobic Co-Digestion of Sludge and Organic Food Waste—Performance, Inhibition, and Impact on the Microbial Community. *Energies* 11(9), 2325.
- Khalid, A., Arshad, M., Anjum, M., Mahmood, T. and Dawson, L. (2011) The anaerobic digestion of solid organic waste. *Waste Manage.* 31(8), 1737-1744.
- Kim, B.-C., Jeon, B.S., Kim, S., Kim, H., Um, Y. and Sang, B.-I. (2015) *Caproiciproducens galactitolivorans* gen. nov., sp. nov., a bacterium capable of producing caproic acid from galactitol, isolated from a wastewater treatment plant. *Int. J. Syst. Evol. Microbiol.* 65(Pt_12), 4902-4908.
- Kim, D.H., Moon, S.-H. and Cho, J. (2002) Investigation of the adsorption and transport of natural organic matter (NOM) in ion-exchange membranes. *Desalination* 151(1), 11-20.
- Kim, J.K., Kim, J.B., Cho, K.S. and Hong, Y.K. (2007) Isolation and identification of microorganisms and their aerobic biodegradation of fish-meal wastewater for liquid-fertilization. *Int. Biodeterior. Biodegradation* 59(2), 156-165.
- Kobayashi, H., Hayakawa, A., Somarathne, K.D., Kunkuma A. and Okafor, Ekenechukwu C. (2019) Science and technology of ammonia combustion. *Proc. Combust. Inst.* 37(1), 109-133.
- Kobayashi, T., Wu, Y.P., Lu, Z.J. and Xu, K.Q. (2015) Characterization of anaerobic degradability and kinetics of harvested submerged aquatic weeds used for nutrient phytoremediation. *Energies* 8(1), 304-318.
- Kovács, E., Wirth, R., Maróti, G., Bagi, Z., Nagy, K., Minarovits, J., Rákhely, G. and Kovács, K.L. (2015) Augmented biogas production from protein-rich substrates and associated metagenomic changes. *Bioresour. Technol.* 178, 254-261.
- Kovács, E., Wirth, R., Maróti, G., Bagi, Z., Rákhely, G. and Kovács, K.L. (2013) Biogas Production from Protein-Rich Biomass: Fed-Batch Anaerobic Fermentation of Casein and of Pig Blood and Associated Changes in Microbial Community Composition. *PLoS ONE* 8(10), e77265-e77265.
- Krylova, N.I., Khabiboulline, R.E., Naumova, R.P. and Nagel, M.A. (1997) The influence of ammonium and methods for removal during the anaerobic treatment of poultry manure. *J. Chem. Technol. Biotechnol.* 70(1), 99-105.

Kundu, P., Debsarkar, A. and Mukherjee, S. (2013) Treatment of slaughterhouse wastewater in a sequencing batch reactor: Performance evaluation and biodegradation kinetics. *Biomed Res. Int.* 2013.

Kuntke, P., Sleutels, T.H.J.A., Rodríguez Arredondo, M., Georg, S., Barbosa, S.G., ter Heijne, A., Hamelers, H.V.M. and Buisman, C.J.N. (2018) (Bio)electrochemical ammonia recovery: progress and perspectives. *Appl. Microbiol. Biotechnol.* 102(9), 3865-3878.

Kuntke, P., Sleutels, T.H.J.A., Saakes, M. and Buisman, C.J.N. (2014) Hydrogen production and ammonium recovery from urine by a Microbial Electrolysis Cell. *Int. J. Hydrog. Energy* 39(10), 4771-4778.

Kuntke, P., Śmiech, K., Bruning, H., Zeeman, G., Saakes, M., Sleutels, T., Hamelers, H. and Buisman, C. (2012) Ammonium recovery and energy production from urine by a microbial fuel cell. *Water Res.* 46(8), 2627-2636.

Lackner, S., Gilbert, E.M., Vlaeminck, S.E., Joss, A., Horn, H. and van Loosdrecht, M.C.M. (2014) Full-scale partial nitrification/anammox experiences - An application survey. *Water Res.* 55, 292-303.

Ladd, J.N. and Jackson, R.B. (1982) Nitrogen in agricultural soils. Stevenson, F.J. (ed), pp. 173-228, American Society of Agronomy, Inc. Crop Science Society of America, Inc. Soil Science Society of America Inc.

Lan, R. and Tao, S. (2010) Direct Ammonia Alkaline Anion-Exchange Membrane Fuel Cells. *ECS Solid State Lett.* 13(8), B83-B86.

Lan, R. and Tao, S. (2014) Ammonia as a Suitable Fuel for Fuel Cells. *Front. Energy Res.* 2, 35.

Lang, X., Li, Q., Ji, M., Yan, G. and Guo, S. (2020) Isolation and niche characteristics in simultaneous nitrification and denitrification application of an aerobic denitrifier, *Acinetobacter* sp. YS2. *Bioresour. Technol.* 302, 122799.

Latham, K.G., Ferguson, A. and Donne, S.W. (2018) Influence of ammonium salts and temperature on the yield, morphology and chemical structure of hydrothermally carbonized saccharides. *SN Applied Sciences* 1(1), 54.

Laurení, M., Palatsi, J., Llovera, M. and Bonmatí, A. (2013) Influence of pig slurry characteristics on ammonia stripping efficiencies and quality of the recovered ammonium-sulfate solution. *J. Chem. Technol. Biotechnol.* 88(9), 1654-1662.

Leaković, S., Mijatović, I., Cerjan-Stefanović, Š. and Hodžić, E. (2000) Nitrogen removal from fertilizer wastewater by ion exchange. *Water Res.* 34(1), 185-190.

Ledda, C., Schievano, A., Salati, S. and Adani, F. (2013) Nitrogen and water recovery from animal slurries by a new integrated ultrafiltration, reverse osmosis and cold stripping process: A case study. *Water Res.* 47(16), 6157-6166.

- Ledezma, P., Jermakka, J., Keller, J. and Freguia, S. (2017) Recovering Nitrogen as a Solid without Chemical Dosing: Bio-Electroconcentration for Recovery of Nutrients from Urine. *Environ. Sci. Technol. Lett.* 4(3), 119-124.
- Lei, X., Sugiura, N., Feng, C. and Maekawa, T. (2007) Pretreatment of anaerobic digestion effluent with ammonia stripping and biogas purification. *J. Hazard. Mater.* 145(3), 391-397.
- Lei, Y., Wei, L., Liu, T., Xiao, Y., Dang, Y., Sun, D. and Holmes, D.E. (2018) Magnetite enhances anaerobic digestion and methanogenesis of fresh leachate from a municipal solid waste incineration plant. *Chem. Eng. J.* 348(March), 992-999.
- Lesmana, H., Zhang, Z., Li, X., Zhu, M., Xu, W. and Zhang, D. (2019) NH₃ as a Transport Fuel in Internal Combustion Engines: A Technical Review. *J. Energy Resour. Technol.* 141(7), 070703.
- Li, J., Rui, J., Yao, M., Zhang, S., Yan, X., Wang, Y., Yan, Z. and Li, X. (2015) Substrate type and free ammonia determine bacterial community structure in full-scale mesophilic anaerobic digesters treating cattle or swine manure. *Front. Microbiol.* 6, 1337.
- Li, Y., Shi, S., Cao, H., Wu, X., Zhao, Z. and Wang, L. (2016) Bipolar membrane electro dialysis for generation of hydrochloric acid and ammonia from simulated ammonium chloride wastewater. *Water Res.* 89, 201-209.
- Li, Y., Xu, Z., Xie, M., Zhang, B., Li, G. and Luo, W. (2020) Resource recovery from digested manure centrate: Comparison between conventional and aquaporin thin-film composite forward osmosis membranes. *J. Membr. Sci.* 593, 117436.
- Li, Z. and Stenstrom, M.K. (2018) Impacts of SRT on Particle Size Distribution and Reactor Performance in Activated Sludge Processes. *Water Environ. Res.* 90(1), 48-56.
- Liu, L., Yun, S., Ke, T., Wang, K., An, J. and Liu, J. (2023) Dual utilization of aloe peel: Aloe peel-derived carbon quantum dots enhanced anaerobic co-digestion of aloe peel. *Waste Manage.* 159, 163-173.
- Liu, Q., Liu, C., Zhao, L., Ma, W., Liu, H. and Ma, J. (2016a) Integrated forward osmosis-membrane distillation process for human urine treatment. *Water Res.* 91, 45-54.
- Liu, W., He, Z., Yang, C., Zhou, A., Guo, Z., Liang, B., Varrone, C. and Wang, A.-J. (2016b) Microbial network for waste activated sludge cascade utilization in an integrated system of microbial electrolysis and anaerobic fermentation. *Biotechnol. Biofuels* 9(1), 1-15.
- Liu, Y., Ngo, H.H., Guo, W., Peng, L., Wang, D. and Ni, B. (2019) The roles of free ammonia (FA) in biological wastewater treatment processes: A review. *Environ. Int.* 123, 10-19.
- Lubensky, J., Ellersdorfer, M. and Stocker, K. (2019) Ammonium recovery from model solutions and sludge liquor with a combined ion exchange and air stripping process. *J. Water Process. Eng.* 32, 100909.

- Luther, A.K., Desloover, J., Fennell, D.E. and Rabaey, K. (2015) Electrochemically driven extraction and recovery of ammonia from human urine. *Water Res.* 87, 367-377.
- Lymperatou, A., Gavala, H.N., Esbensen, K.H. and Skiadas, I.V. (2015) AMMONOX: Ammonia for Enhancing Biogas Yield and Reducing NOx—Analysis of Effects of Aqueous Ammonia Soaking on Manure Fibers. *Waste Biomass Valorization* 6(4), 449-457.
- Ma, Q., Peng, R., Tian, L. and Meng, G. (2006) Direct utilization of ammonia in intermediate-temperature solid oxide fuel cells. *Electrochem. Commun.* 8(11), 1791-1795.
- Macfarlane, G., Cummings, J. and Allison, C. (1986) Protein degradation by human intestinal bacteria. *Microbiology* 132(6), 1647-1656.
- Machdar, I., Depari, S., Ulfa, R., Muhammad, S., Hisbullah, A. and Safrul, W. (2018) Ammonium nitrogen removal from urea fertilizer plant wastewater via struvite crystal production, p. 012026, IOP Publishing.
- Magdalena, J.A., Ballesteros, M. and Gonz, C. (2018) Efficient Anaerobic Digestion of Microalgae Biomass : Proteins as a Key Macromolecule. *Molecules* 23, 1-16.
- Magoč, T. and Salzberg, S.L. (2011) FLASH: fast length adjustment of short reads to improve genome assemblies. *Bioinformatics* 27(21), 2957-2963.
- Magrí, A., Béline, F. and Dabert, P. (2013) Feasibility and interest of the anammox process as treatment alternative for anaerobic digester supernatants in manure processing - An overview. *J. Environ. Manage.* 131, 170-184.
- Mahato, N., Banerjee, A., Gupta, A., Omar, S. and Balani, K. (2015) Progress in material selection for solid oxide fuel cell technology: A review. *Prog. Mater. Sci.* 72, 141-337.
- Massé, D. and Massé, L. (2000) Treatment of slaughterhouse wastewater in anaerobic sequencing batch reactors. *Can. Agric. Eng.* 42(3), 1310137.
- Massé, D.I., Rajagopal, R. and Singh, G. (2014) Technical and operational feasibility of psychrophilic anaerobic digestion biotechnology for processing ammonia-rich waste. *Appl. Energy* 120, 49-55.
- Masse, L., Massé, D.I. and Pellerin, Y. (2007) The use of membranes for the treatment of manure: a critical literature review. *Biosyst. Eng.* 98(4), 371-380.
- Masse, L., Massé, D.I. and Pellerin, Y. (2008) The effect of pH on the separation of manure nutrients with reverse osmosis membranes. *J. Membr. Sci.* 325(2), 914-919.
- Masse, L., Mondor, M. and Dubreuil, J. (2013) Membrane filtration of the liquid fraction from a solid – liquid separator for swine manure using a cationic polymer as flocculating agent. *Environ. Technol.* 34(5), 671-677.

- Mata-Alvarez, J., Dosta, J., Romero-Güiza, M.S., Fonoll, X., Peces, M. and Astals, S. (2014) A critical review on anaerobic co-digestion achievements between 2010 and 2013. *Renew. Sust. Energ. Rev.* 36, 412-427.
- Mata-Alvarez, J., Macé, S. and Llabrés, P. (2000) Anaerobic digestion of organic solid wastes. An overview of research achievements and perspectives. *Bioresour. Technol.* 74(1), 3-16.
- Matassa, S., Batstone, D.J., Hulsen, T., Schnoor, J. and Verstraete, W. (2015) Can direct conversion of used nitrogen to new feed and protein help feed the world? *Environ. Sci. Technol.* 49(9), 5247-5254.
- Maturana, J.L. and Cárdenas, J.P. (2021) Insights on the evolutionary genomics of the *Blautia* genus: potential new species and genetic content among lineages. *Front. Microbiol.* 12.
- McInerney, M.J. (1988) Anaerobic hydrolysis and fermentation of fats and proteins. *Biology of Anaerobic Organisms*, 373-416.
- McMurdie, P.J. and Holmes, S. (2013) phyloseq: An R Package for Reproducible Interactive Analysis and Graphics of Microbiome Census Data. *PLOS ONE* 8(4), e61217.
- Meegoda, J.N., Li, B., Patel, K. and Wang, L.B. (2018) A Review of the Processes, Parameters, and Optimization of Anaerobic Digestion. *Int. J. Environ. Res. Public. Health.* 15(10).
- Mehta, C.M., Khunjar, W.O., Nguyen, V., Tait, S. and Batstone, D.J. (2015) Technologies to Recover Nutrients From Waste Streams: A Critical Review. *Crit. Rev. Environ. Sci. Technol.* 45, 385-427.
- Melkonian, E.A. and Schury, M.P. (2019) *Biochemistry, anaerobic glycolysis*, StatPearls, Treasure Island, FL.
- Meng, G., Jiang, C., Ma, J., Ma, Q. and Liu, X. (2007) Comparative study on the performance of a SDC-based SOFC fueled by ammonia and hydrogen. *J. Power Sources* 173(1), 189-193.
- Milani, C., Lugli, G.A., Duranti, S., Turrone, F., Bottacini, F., Mangifesta, M., Sanchez, B., Viappiani, A., Mancabelli, L. and Taminiu, B. (2014) Genomic encyclopedia of type strains of the genus *Bifidobacterium*. *Appl. Environ. Microbiol.* 80(20), 6290-6302.
- Miniaci, M.C., Irace, C., Capuozzo, A., Piccolo, M., Di Pascale, A., Russo, A., Lippiello, P., Lepre, F., Russo, G. and Santamaria, R. (2016) Cysteine prevents the reduction in keratin synthesis induced by iron deficiency in human keratinocytes. *J. Cell. Biochem.* 117(2), 402-412.
- Möller, K. and Müller, T. (2012) Effects of anaerobic digestion on digestate nutrient availability and crop growth: A review. *Eng. Life Sci.* 12(3), 242-257.
- Mondor, M., Ippersiel, D., Lamarche, F. and Masse, L. (2009) Fouling characterization of electro dialysis membranes used for the recovery and concentration of ammonia from swine manure. *Bioresour. Technol.* 100(2), 566-571.

Mondor, M., Masse, L., Ippersiel, D., Lamarche, F. and Massé, D.I. (2008) Use of electro dialysis and reverse osmosis for the recovery and concentration of ammonia from swine manure. *Bioresour. Technol.* 99, 7363-7368.

Montusiewicz, A., Bis, M., Pasieczna-Patkowska, S. and Majerek, D. (2018) Mature landfill leachate utilization using a cost-effective hybrid method. *Waste Manage.* 76, 652-662.

Morotomi, M., Nagai, F. and Watanabe, Y. (2012) Description of *Christensenella minuta* gen. nov., sp. nov., isolated from human faeces, which forms a distinct branch in the order Clostridiales, and proposal of Christensenellaceae fam. nov. *Int. J. Syst. Evol. Microbiol.* 62(1), 144-149.

Mosbæk, F., Kjeldal, H., Mulat, D.G., Albertsen, M., Ward, A.J., Feilberg, A. and Nielsen, J.L. (2016) Identification of syntrophic acetate-oxidizing bacteria in anaerobic digesters by combined protein-based stable isotope probing and metagenomics. *ISME J.* 10(10), 2405-2418.

Mulder, A. (2003) The quest for sustainable nitrogen removal technologies. *Water Sci. Technol.* 48(1), 67-75.

Münch, E.V. and Pollard, P.C. (1997) Measuring bacterial biomass-COD in wastewater containing particulate matter. *Water Res.* 31(10), 2550-2556.

Murat, S., Ateş Genceli, E., Taşlı, R., Artan, N. and Orhon, D. (2002) Sequencing batch reactor treatment of tannery wastewater for carbon and nitrogen removal. *Water Sci. Technol.* 46(9), 219-227.

Murat, S., Insel, G., Artan, N. and Orhon, D. (2006) Performance evaluation of SBR treatment for nitrogen removal from tannery wastewater. *Water Sci. Technol.* 53(12), 275-284.

Musa, M.A. and Idrus, S. (2021) Physical and biological treatment technologies of slaughterhouse wastewater: A review. *Sustainability* 13(9), 4656.

Mysoreammonia (2020) Aqueous Ammonia (Liquor Ammonia).

Nakakubo, R., Møller, H.B., Nielsen, A.M. and Matsuda, J. (2008) Ammonia Inhibition of Methanogenesis and Identification of Process Indicators during Anaerobic Digestion. *Environ. Eng. Sci.* 25(10), 1487-1496.

Nakamura, T., Yamada, K.D., Tomii, K. and Katoh, K. (2018) Parallelization of MAFFT for large-scale multiple sequence alignments. *Bioinformatics* 34(14), 2490-2492.

Nanninga, H., Drent, W. and Gottschal, J. (1987) Fermentation of glutamate by *Selenomonas acidaminophila* sp. nov. *Arch. Microbiol.* 147(2), 152-157.

Nesbø, C.L., Charchuk, R., Pollo, S.M., Budwill, K., Kublanov, I.V., Haverkamp, T.H. and Foght, J. (2019) Genomic analysis of the mesophilic Thermotogae genus *Mesotoga* reveals

phylogeographic structure and genomic determinants of its distinct metabolism. *Environ. Microbiol.* 21(1), 456-470.

Ni, M., Leung, D.Y.C. and Leung, M.K.H. (2008) Thermodynamic analysis of ammonia fed solid oxide fuel cells: Comparison between proton-conducting electrolyte and oxygen ion-conducting electrolyte. *J. Power Sources* 183(2), 682-686.

Ni, M., Leung, M.K.H. and Leung, D.Y.C. (2009) Ammonia-fed solid oxide fuel cells for power generation—A review. *Int. J. Energy Res.* 33(11), 943-959.

Nielsen, H., Mladenovska, Z., Westermann, P. and Ahring, B.K. (2004) Comparison of two-stage thermophilic (68 degrees C/55 degrees C) anaerobic digestion with one-stage thermophilic (55 degrees C) digestion of cattle manure. *Biotechnol. Bioeng.* 86(3), 291-300.

Nielsen, P.H., Saunders, A.M., Hansen, A.A., Larsen, P. and Nielsen, J.L. (2012) Microbial communities involved in enhanced biological phosphorus removal from wastewater—a model system in environmental biotechnology. *Curr. Opin. Biotechnol.* 23(3), 452-459.

Nightingale, A., Antunes, R., Alpi, E., Bursteinas, B., Gonzales, L., Liu, W., Luo, J., Qi, G., Turner, E. and Martin, M. (2017) The proteins API: accessing key integrated protein and genome information. *Nucleic Acids Res.* 45(W1), 539-544.

Niu, Q., Hojo, T., Qiao, W., Qiang, H. and Li, Y.-Y. (2014) Characterization of methanogenesis, acidogenesis and hydrolysis in thermophilic methane fermentation of chicken manure. *Chem. Eng. J.* 244, 587-596.

Niu, Q., Qiao, W., Qiang, H., Hojo, T. and Li, Y.Y. (2013) Mesophilic methane fermentation of chicken manure at a wide range of ammonia concentration: Stability, inhibition and recovery. *Bioresour. Technol.* 137, 358-367.

Noworyta, A., Koziol, T. and Trusek-Holownia, A. (2003) A system for cleaning condensates containing ammonium nitrate by the reverse osmosis method. *Desalination* 156(1), 397-402.

Numata, K. (2021) *Biopolymer Science for Proteins and Peptides*, Elsevier.

Oanh, N.T., Duc, H.D., Ngoc, D.T.H., Thuy, N.T.D., Hiep, N.H. and Van Hung, N. (2020) Biodegradation of propanil by *Acinetobacter baumannii* DT in a biofilm-batch reactor and effects of butachlor on the degradation process. *FEMS Microbiol. Lett.* 367(2), fnaa005.

Obaja, D., Mace, S., Costa, J., Sans, C. and Mata-Alvarez, J. (2003) Nitrification, denitrification and biological phosphorus removal in piggery wastewater using a sequencing batch reactor. *Bioresour. Technol.* 87(1), 103-111.

Obek, C.A., Ayittey, F.K. and Saptorio, A. (2019) Improved process modifications of aqueous ammonia-based CO₂ capture system. *MATEC Web Conf.* 268, 02004.

Okanishi, T., Okura, K., Srifa, A., Muroyama, H., Matsui, T., Kishimoto, M., Saito, M., Iwai, H., Yoshida, H., Saito, M., Koide, T., Iwai, H., Suzuki, S., Takahashi, Y., Horiuchi, T., Yamasaki, H., Matsumoto, S., Yumoto, S., Kubo, H., Kawahara, J., Okabe, A., Kikkawa, Y.,

Isomura, T. and Eguchi, K. (2017) Comparative Study of Ammonia-fueled Solid Oxide Fuel Cell Systems. *Fuel Cells* 17(3), 383-390.

Oksanen, J., Kindt, R., Legendre, P., O'Hara, B., Simpson, G.L., Solymos, P., Stevens, M.H.H. and Wagner, H. (2007) The vegan package. *Community ecology package* 10(631-637), 719.

Oladejo, J., Shi, K., Luo, X., Yang, G. and Wu, T. (2018) A Review of Sludge-to-Energy Recovery Methods. *Energies* 12(1), 60.

Oliviero, L., Barbier, J. and Duprez, D. (2003) Wet Air Oxidation of nitrogen-containing organic compounds and ammonia in aqueous media. *Appl. Catal. B* 40(3), 163-184.

Omar, R., Harun, R.M., Mohd Ghazi, T., Wan Azlina, W., Idris, A. and Yunus, R. (2008) Anaerobic treatment of cattle manure for biogas production. Annual meeting of American institute of chemical engineers, 1-10.

Palatsi, J., Viñas, M., Guivernau, M., Fernandez, B. and Flotats, X. (2011) Anaerobic digestion of slaughterhouse waste: Main process limitations and microbial community interactions. *Bioresour. Technol.* 102(3), 2219-2227.

Papadias, D.D., Ahmed, S. and Kumar, R. (2012) Fuel quality issues with biogas energy – An economic analysis for a stationary fuel cell system. *Energy* 44(1), 257-277.

Pasalari, H., Gholami, M., Rezaee, A., Esrafil, A. and Farzadkia, M. (2021) Perspectives on microbial community in anaerobic digestion with emphasis on environmental parameters: A systematic review. *Chemosphere* 270, 128618.

Pavlostathis, S.G. and Giraldo-Gomez, E. (1991) Kinetics of anaerobic treatment. *Water Sci. Technol.* 24(8), 35-59.

Pazouki, M., Shayegan, J. and Afshari, A. (2008) Screening of microorganisms for decolorization of treated distillery wastewater. *Iran. J. Sci. Technol. B.* 32, 53-60.

Pikaar, I., Matassa, S., Bodirsky, B.L., Weindl, I., Humpenöder, F., Rabaey, K., Boon, N., Bruschi, M., Yuan, Z., van Zanten, H., Herrero, M., Verstraete, W. and Popp, A. (2018) Decoupling Livestock from Land Use through Industrial Feed Production Pathways. *Environ. Sci. Technol.* 52(13), 7351-7359.

Pishchik, V.N., Chernyaeva, I.I., Semenova, E.A., Bel'kova, E.I., Vasser, N.R., Koval', G.N. and Turyanitsa, A.I. (1997) Metabolic features of bacteria of the genus *Klebsiella*. *Microbiology-New York* 66(1), 43-47.

Poulsen, J.S., de Jonge, N., Macedo, W.V., Dalby, F.R., Feilberg, A. and Nielsen, J.L. (2022) Characterisation of cellulose-degrading organisms in an anaerobic digester. *Bioresour. Technol.* 351, 126933.

Powar, C.B. and Chatwal, G.R. (2007) *Biochemistry*, Himalaya Publishing House, Mumbai, IN.

- Prather, M., Ehhalt, D., Dentener, F., Derwent, R. and Grubler, A. (2001) *Climate Change 2001: The Scientific Basis, Third Assessment Report*, pp. 239-289, Working Group I of the Intergovernmental Panel on Climate Change, Geneva, CH.
- Price, M.N., Dehal, P.S. and Arkin, A.P. (2010) FastTree 2--approximately maximum-likelihood trees for large alignments. *PLoS One* 5(3), e9490.
- Pronk, W., Biebow, M. and Boller, M. (2006a) Electrodialysis for Recovering Salts from a Urine Solution Containing Micropollutants. *Environ. Sci. Technol.* 40(7), 2414-2420.
- Pronk, W., Biebow, M. and Boller, M. (2006b) Treatment of source-separated urine by a combination of bipolar electrodialysis and a gas transfer membrane. *Water Sci. Technol.* 53(3), 139-146.
- Provolo, G., Perazzolo, F., Mattachini, G., Finzi, A., Naldi, E. and Riva, E. (2017) Nitrogen removal from digested slurries using a simplified ammonia stripping technique. *Waste Manage.* 69, 154-161.
- Pulami, D., Schauss, T., Eisenberg, T., Blom, J., Schwengers, O., Bender, J.K., Wilharm, G., Kampf, P. and Glaeser, S.P. (2021) *Acinetobacter stercoris* sp. nov. isolated from output source of a mesophilic german biogas plant with anaerobic operating conditions. *Antonie Van Leeuwenhoek* 114(3), 235-251.
- Qiao, W., Peng, C., Wang, W. and Zhang, Z. (2011) Biogas production from supernatant of hydrothermally treated municipal sludge by upflow anaerobic sludge blanket reactor. *Bioresour. Technol.* 102(21), 9904-9911.
- Qiu, T., Zhu, D., Fang, X., Zeng, Q., Gao, G. and Zhu, H. (2014) Leaching kinetics of ionic rare-earth in ammonia-nitrogen wastewater system added with impurity inhibitors. *J. Rare Earths* 32(12), 1175-1183.
- Quast, C., Pruesse, E., Yilmaz, P., Gerken, J., Schweer, T., Yarza, P., Pelplies, J. and Glochner, F.O. (2012) The SILVA ribosomal RNA gene database project: improved data processing and web-based tools. *Nucleic Acids Res.* 41(D1), D590-D596.
- Rahman, M.M., Salleh, M.A.M., Rashid, U., Ahsan, A., Hossain, M.M. and Ra, C.S. (2014) Production of slow release crystal fertilizer from wastewaters through struvite crystallization – A review. *Arab. J. Chem.* 7(1), 139-155.
- Rajab, A.R., Salim, M.R., Sohaili, J., Anuar, A.N. and Lakkaboyana, S.K. (2017) Performance of integrated anaerobic/aerobic sequencing batch reactor treating poultry slaughterhouse wastewater. *Chem. Eng. J.* 313, 967-974.
- Rajagopal, R., Massé, D.I. and Singh, G. (2013) A critical review on inhibition of anaerobic digestion process by excess ammonia. *Bioresour. Technol.* 143, 632-641.

- Ras, M., Lardon, L., Bruno, S., Bernet, N. and Steyer, J.P. (2011) Experimental study on a coupled process of production and anaerobic digestion of *Chlorella vulgaris*. *Bioresour. Technol.* 102(1), 200-206.
- Resch, C., Wörl, A., Waltenberger, R., Braun, R. and Kirchmayr, R. (2011) Enhancement options for the utilisation of nitrogen rich animal by-products in anaerobic digestion. *Bioresour. Technol.* 102(3), 2503-2510.
- Ripoll, V., Agabo-García, C., Solera, R. and Perez, M. (2022) Anaerobic digestion of slaughterhouse waste in batch and anaerobic sequential batch reactors. *Biomass Convers. Biorefin.*, 1-12.
- Rockström, J., Steffen, W., Noone, K., Persson, Å., Chapin, F.S., Lambin, E.F., Lenton, T.M., Scheffer, M., Folke, C. and Schellnhuber, H.J. (2009) A safe operating space for humanity. *Nature* 461(7263), 472-475.
- Rodríguez-Méndez, R., Le Bihan, Y., Béline, F. and Lessard, P. (2017) Long chain fatty acids (LCFA) evolution for inhibition forecasting during anaerobic treatment of lipid-rich wastes: Case of milk-fed veal slaughterhouse waste. *Waste Manage.* 67, 51-58.
- Rodríguez-Verde, I., Regueiro, L., Lema, J.M. and Carballa, M. (2018) Blending based optimisation and pretreatment strategies to enhance anaerobic digestion of poultry manure. *Waste Manage.* 71, 521-531.
- Rodríguez Arredondo, M., Kuntke, P., Jeremiasse, A.W., Sleutels, T.H.J.A., Buisman, C.J.N. and ter Heijne, A. (2015) Bioelectrochemical systems for nitrogen removal and recovery from wastewater. *Environ. Sci. Water Res. Technol.* 1(1), 22-33.
- Rognes, T., Flouri, T., Nichols, B., Quince, C. and Mahé, F. (2016) VSEARCH: a versatile open source tool for metagenomics. *PeerJ* 4, e2584.
- Rothrock Jr, M.J., Szögi, A.A. and Vanotti, M.B. (2010) Recovery of ammonia from poultry litter using gas-permeable membranes. *T. ASABE* 53(4), 1267-1275.
- Ruiz, C., Torrijos, M., Sousbie, P., Lebrato Martínez, J. and Moletta, R. (2001) The anaerobic SBR process: basic principles for design and automation. *Water Sci. Technol.* 43(3), 201-208.
- Ruiz, I., Veiga, M.C., de Santiago, P. and Blazquez, R. (1997) Treatment of slaughterhouse wastewater in a UASB reactor and an anaerobic filter. *Bioresour. Technol.* 60, 251-258.
- Saadabadi, S.A., Thallam Thattai, A., Fan, L., Lindeboom, R.E.F., Spanjers, H. and Aravind, P.V. (2019) Solid Oxide Fuel Cells fuelled with biogas: Potential and constraints. *Renew. Energy* 134, 194-214.
- Sadat-Mekmene, L., Genay, M., Atlan, D., Lortal, S. and Gagnaire, V. (2011) Original features of cell-envelope proteinases of *Lactobacillus helveticus*. A review. *Int. J. Food Microbiol.* 146(1), 1-13.

- Salminen, E. and Rintala, J. (2002) Anaerobic digestion of organic solid poultry slaughterhouse waste a review. *Bioresour. Technol.* 83, 13-26.
- Salveti, E., Torriani, S. and Felis, G.E. (2012) The genus *Lactobacillus*: a taxonomic update. *Probiotics Antimicrob. Proteins* 4(4), 217-226.
- Sanders, W.T.M. (2001) Anaerobic hydrolysis during digestion of complex substrates, Wageningen University, Wageningen, NL.
- Santillan, E., Seshan, H., Constancias, F., Drautz-Moses, D.I. and Wuertz, S. (2019) Frequency of disturbance alters diversity, function, and underlying assembly mechanisms of complex bacterial communities. *npj Biofilms Microbiomes* 5(1), 8.
- Schaubroeck, T., De Clippeleir, H., Weissenbacher, N., Dewulf, J., Boeckx, P., Vlaeminck, S.E. and Wett, B. (2015) Environmental sustainability of an energy self-sufficient sewage treatment plant: Improvements through DEMON and co-digestion. *Water Res.* 74, 166-179.
- Schoeman, J.J. and Strachan, L. (2009) Performance of tubular reverse osmosis for the desalination/ concentration of a municipal solid waste leachate. *Water SA* 35(3), 323-328.
- Scholz, W., Rouge, P., Bodalo, A. and Leitz, U. (2005) Desalination of mixed tannery effluent with membrane bioreactor and reverse osmosis treatment. *Environ. Sci. Technol.* 39(21), 8505-8511.
- Schwan, B., Abendroth, C., Latorre-Pérez, A., Porcar, M., Vilanova, C. and Dornack, C. (2020) Chemically stressed bacterial communities in anaerobic digesters exhibit resilience and ecological flexibility. *Front. Microbiol.* 11, 867.
- Serna-Maza, A., Heaven, S. and Banks, C.J. (2014) Ammonia removal in food waste anaerobic digestion using a side-stream stripping process. *Bioresour. Technol.* 152, 307-315.
- Shelly, Y., Kuk, M., Menashe, O., Zeira, G., Azerrad, S. and Kurzbaum, E. (2021) Nitrate removal from a nitrate-rich reverse osmosis concentrate: Superior efficiency using the bioaugmentation of an *Acinetobacter* biofilm. *J. Water Process. Eng.* 44, 102425.
- Shende, A.D. and Pophali, G.R. (2021) Anaerobic treatment of slaughterhouse wastewater: a review. *Environ. Sci. Pollut. Res.* 28(1), 35-55.
- Shi, L., Hu, Y., Xie, S., Wu, G., Hu, Z. and Zhan, X. (2018) Recovery of nutrients and volatile fatty acids from pig manure hydrolysate using two-stage bipolar membrane electro dialysis. *Chem. Eng. J.* 334, 134-142.
- Shi, L., Xie, S., Hu, Z., Wu, G., Morrison, L., Croot, P., Hu, H. and Zhan, X. (2019) Nutrient recovery from pig manure digestate using electro dialysis reversal: Membrane fouling and feasibility of long-term operation. *J. Membr. Sci.* 573, 560-569.
- Siegert, I. and Banks, C.J.P.B. (2005) The effect of volatile fatty acid additions on the anaerobic digestion of cellulose and glucose in batch reactors. *Process Biochem.* 40(11), 3412-3418.

- Siegrist, H., Salzgeber, D., Eugster, J. and Joss, A. (2008) Anammox brings WWTP closer to energy autarky due to increased biogas production and reduced aeration energy for N-removal. *Water Sci. Technol.* 57(3), 383-388.
- Sigurnjak, I., Michels, E., Crappé, S., Buysens, S., Tack, F.M. and Meers, E. (2016) Utilization of derivatives from nutrient recovery processes as alternatives for fossil-based mineral fertilizers in commercial greenhouse production of *Lactuca sativa* L. *Sci. Hort.* 198, 267-276.
- Silva, F.M.S., Mahler, C.F., Oliveira, L.B. and Bassin, J.P. (2018) Hydrogen and methane production in a two-stage anaerobic digestion system by co-digestion of food waste, sewage sludge and glycerol. *Waste Manage.* 76, 339-349.
- Silva, S.A., Cavaleiro, A.J., Pereira, M.A., Stams, A.J., Alves, M.M. and Sousa, D.Z. (2014) Long-term acclimation of anaerobic sludges for high-rate methanogenesis from LCFA. *Biomass Bioenergy* 67, 297-303.
- Silverman, A.P., Baron, E.J. and Kool, E.T. (2006) RNA-templated chemistry in cells: discrimination of *Escherichia*, *Shigella* and *Salmonella* bacterial strains with a new two-color FRET strategy. *ChemBioChem* 7(12), 1890-1894.
- Singh, M. and Srivastava, R.K. (2011) Sequencing batch reactor technology for biological wastewater treatment: a review. *Asia-Pac. J. Chem. Eng.* 6(1), 3-13.
- Sivakanesan, R. and Dawes, E.A. (1980) Anaerobic glucose and serine metabolism in *Staphylococcus epidermidis*. *Microbiology* 118(1), 143-157.
- Slavov, A.K. (2017) Dairy Wastewaters – General Characteristics and Treatment Possibilities – A Review. *Food Technol. Biotechnol.* 55(1), 14-28.
- Sleat, R., Mah, R.A. and Robinson, R. (1985) *Acetoanaerobium noterae* gen. nov., sp. nov.: an anaerobic bacterium that forms acetate from H₂ and CO₂. *Int. J. Syst. Evol. Microbiol.* 35(1), 10-15.
- Smil, V. (2004) *Enriching the earth: Fritz Haber, Carl Bosch, and the transformation of world food production*, MIT press.
- Smith, G.S., Walter, G.L. and Walker, R.M. (2013) Haschek and Rousseaux's Handbook of Toxicologic Pathology, pp. 565-594.
- Sotres, A., Cerrillo, M., Viñas, M. and Bonmatí, A. (2015) Nitrogen recovery from pig slurry in a two-chambered bioelectrochemical system. *Bioresour. Technol.* 194, 373-382.
- Stams, A. and Hansen, T. (1984) Fermentation of glutamate and other compounds by *Acidaminobacter hydrogenoformans* gen. nov. sp. nov., an obligate anaerobe isolated from black mud. Studies with pure cultures and mixed cultures with sulfate-reducing and methanogenic bacteria. *Arch. Microbiol.* 137(4), 329-337.

Staniforth, J. and Ormerod, R.M. (2003) Clean destruction of waste ammonia with consummate production of electrical power within a solid oxide fuel cell system. *Green Chem.* 5(5), 606-609.

Stelmangas (2020) *Liquour Ammonia*.

Stewart, E.J. (2012) Growing unculturable bacteria. *J. Bacteriol.* 194(16), 4145-4160.

Stoeckl, B., Preininger, M., Subotić, V., Gaber, C., Seidl, M., Sommersacher, P., Schroettner, H. and Hochenauer, C. (2019a) High Utilization of Humidified Ammonia and Methane in Solid Oxide Fuel Cells: An Experimental Study of Performance and Stability. *J. Electrochem. Soc.* 166(12), F774-F783.

Stoeckl, B., Preininger, M., Subotić, V., Megel, S., Folgner, C. and Hochenauer, C. (2020) Towards a wastewater energy recovery system: The utilization of humidified ammonia by a solid oxide fuel cell stack. *J. Power Sources* 450, 227608.

Stoeckl, B., Subotić, V., Preininger, M., Schwaiger, M., Evic, N., Schroettner, H. and Hochenauer, C. (2019b) Characterization and performance evaluation of ammonia as fuel for solid oxide fuel cells with Ni/YSZ anodes. *Electrochim. Acta* 298, 874-883.

Suzuki, S., Muroyama, H., Matsui, T. and Eguchi, K. (2012) Fundamental studies on direct ammonia fuel cell employing anion exchange membrane. *J. Power Sources* 208, 257-262.

Szymańska, M., Sosulski, T., Szara, E., Wąs, A., Sulewski, P., van Puijssen, G.W.P. and Cornelissen, R.L. (2019) Ammonium Sulphate from a Bio-Refinery System as a Fertilizer—Agronomic and Economic Effectiveness on the Farm Scale. *Energies* 12(24), 4721.

Tan, L.C., Peschard, R., Deng, Z., Ferreira, A.L.M., Lens, P.N.L. and Pacheco-Ruiz, S. (2021) Anaerobic digestion of dairy wastewater by side-stream membrane reactors: Comparison of feeding regime and its impact on sludge filterability. *Environ. Technol. Innov.* 22, 101482.

Tang, Y., Shigematsu, T., Morimura, S. and Kida, K. (2005) Microbial community analysis of mesophilic anaerobic protein degradation process using bovine serum albumin (BSA) -fed continuous cultivation. *J. Biosci. Bioeng.* 99(2), 150-164.

Tao, B., Passanha, P., Kumi, P., Wilson, V., Jones, D. and Esteves, S. (2016) Recovery and concentration of thermally hydrolysed waste activated sludge derived volatile fatty acids and nutrients by microfiltration, electro dialysis and struvite precipitation for polyhydroxyalkanoates production. *Chem. Eng. J.* 295, 11-19.

Tarpeh, W.A., Wald, I., Omollo, M.O., Egan, T. and Nelson, K.L. (2018) Evaluating ion exchange for nitrogen recovery from source-separated urine in Nairobi, Kenya. *Dev. Eng.* 3, 188-195.

Tassew, F.A., Bergland, W.H., Dinamarca, C. and Bakke, R. (2019) Settling velocity and size distribution measurement of anaerobic granular sludge using microscopic image analysis. *J. Microbiol. Methods* 159, 81-90.

Thalasso, F., Burgt, J.V.D., Flaherty, V.O. and Colleran, E. (1999) Large-scale anaerobic degradation of betaine. *J. Chem. Technol. Biotechnol.* 74, 1176-1182.

Thauer, R.K. (1988) Citric - acid cycle, 50 years on: modifications and an alternative pathway in anaerobic bacteria. *Europ. J. Biochem.* 176(3), 497-508.

Tilche, A., Bacilieri, E., Bortone, G., Malaspina, F., Piccinini, S. and Stante, L. (1999) Biological phosphorus and nitrogen removal in a full scale sequencing batch reactor treating piggery wastewater.pdf. *Water Sci. Technol.* 40(1), 199-206.

Ud-Din, A. and Wahid, S. (2015) Relationship among *Shigella* spp. and enteroinvasive *Escherichia coli* (EIEC) and their differentiation. *Braz. J. Microbiol.* 45(4), 1131-1138.

Udaondo, Z., Duque, E. and Ramos, J.L. (2017) The pangenome of the genus *Clostridium*. *Environ. Microbiol.* 19(7), 2588-2603.

Udert, K., Larsen, T.A. and Gujer, W. (2006) Fate of major compounds in source-separated urine. *Water Sci. Technol.* 54(11-12), 413-420.

Udert, K.M., Larsen, T.A., Biebow, M. and Gujer, W. (2003) Urea hydrolysis and precipitation dynamics in a urine-collecting system. *Water Res.* 37(11), 2571-2582.

Ukwuani, A.T. and Tao, W. (2016) Developing a vacuum thermal stripping - acid absorption process for ammonia recovery from anaerobic digester effluent. *Water Res.* 106, 108-115.

Usman, M., Zhao, S., Jeon, B.-H., Salama, E.-S. and Li, X. (2022) Microbial β -oxidation of synthetic long-chain fatty acids to improve lipid biomethanation. *Water Res.* 213, 118164.

Valera-Medina, A., Xiao, H., Owen-jones, M., David, W.I.F. and Bowen, P.J. (2018) Ammonia for power. *Prog. Energy Combust. Sci.* 69, 63-102.

van Groenestijn, J.W., Deinema, M.H. and Zehnder, A.J. (1987) ATP production from polyphosphate in *Acinetobacter* strain 210A. *Arch. Microbiol.* 148(1), 14-19.

van Lier, J.B., Mahmoud, N. and Zeeman, G. (2020) *Biological Wastewater Treatment, Principles, Modelling and Design*, 2nd Edition. Chen, G.H., van Loosdrecht, M.C.M., Ekama, G.A. and Brdjanovic, D. (eds), pp. 701-756, IWA Publishing, London, UK.

van Linden, N., Bandinu, G.L., Vermaas, D.A., Spanjers, H. and van Lier, J.B. (2020) Bipolar membrane electrodialysis for energetically competitive ammonium removal and dissolved ammonia production. *J. Clean. Prod.*, 120788.

van Linden, N., Spanjers, H. and van Lier, J.B. (2019) Application of dynamic current density for increased concentration factors and reduced energy consumption for concentrating ammonium by electrodialysis. *Water Res.* 163, 114856.

Vaneekhaute, C., Ghekiere, G., Michels, E., Vanrolleghem, P.A., Tack, F.M. and Meers, E. (2014) Assessing nutrient use efficiency and environmental pressure of macronutrients in

biobased mineral fertilizers: a review of recent advances and best practices at field scale. *Adv. Agron.* 128, 137-180.

Vaneekhaute, C., Lebuf, V., Michels, E., Belia, E., Vanrolleghem, P.A., Tack, F.M.G. and Meers, E. (2017) Nutrient Recovery from Digestate: Systematic Technology Review and Product Classification. *Waste Biomass Valorization* 8(1), 21-40.

Vanotti, M.B., Rashash, D.M.C. and Hunt, P.G. (2002) Solid-liquid separation of flushed swine manure with PAM: effect of wastewater strength. *T. ASAE* 45(6), 1959.

Varga, N., Hornok, V., Sebok, D. and Dekany, I. (2016) Comprehensive study on the structure of the BSA from extended-to aged form in wide (2-12) pH range. *Int. J. Biol. Macromol.* 88, 51-58.

Vasilaki, V., Massara, T.M., Stanchev, P., Fatone, F. and Katsou, E. (2019) A decade of nitrous oxide (N₂O) monitoring in full-scale wastewater treatment processes: A critical review. *Water Res.* 161, 392-412.

Verma, S. (2002) Anaerobic digestion of biodegradable organics in municipal solid wastes. Master Thesis, Columbia University New York, US.

Vesilind, P.A. (1968) Theoretical considerations: Design of prototype thickeners from batch settling tests. *Water Sew. Works* 115(7), 302-307.

Vitousek, P.M., Hattenschwiler, S., Olander, L. and Allison, S. (2002) Nitrogen and nature. *AMBIO: A Journal of the Human Environment* 31(2), 97-101.

Vivekanand, V., Mulat, D.G., Eijssink, V.G.H. and Horn, S.J. (2018) Synergistic effects of anaerobic co-digestion of whey, manure and fish ensilage. *Bioresour. Technol.* 249, 35-41.

Wang, D., Xin, Y., Shi, H., Ai, P., Yu, L., Li, X. and Chen, S. (2019) Closing ammonia loop in efficient biogas production: Recycling ammonia pretreatment of wheat straw. *Biosyst. Eng.* 180, 182-190.

Wang, L., Hao, J., Wang, C., Li, Y. and Yang, Q. (2022) Carbohydrate-to-protein ratio regulates hydrolysis and acidogenesis processes during volatile fatty acids production. *Bioresour. Technol.* 355, 127266.

Wang, L.K., Hung, Y.-T., Lo, H.H. and Yapijakis, C. (2005) Waste treatment in the food processing industry, CRC press, Boca Raton.

Wang, Q., Carrity, G.M., Tiedje, J.M. and Cole, J.R. (2007) Naïve Bayesian Classifier for Rapid Assignment of rRNA Sequences into the New Bacterial Taxonomy. *Appl. Environ. Microbiol.* 73(16), 5261-5267.

Wang, Q., Yang, P. and Cong, W. (2011) Cation-exchange membrane fouling and cleaning in bipolar membrane electro dialysis of industrial glutamate production wastewater. *Sep. Purif. Technol.* 79(1), 103-113.

Wang, X., Lu, X., Li, F. and Yang, G. (2014) Effects of temperature and Carbon-Nitrogen (C/N) ratio on the performance of anaerobic co-digestion of dairy manure, chicken manure and rice straw: Focusing on ammonia inhibition. *PLoS ONE* 9(5), 1-7.

Wang, Y., Pelkonen, M. and Kotro, M. (2010) Treatment of High Ammonium–Nitrogen Wastewater from Composting Facilities by Air Stripping and Catalytic Oxidation. *Water Air Soil Pollut.* 208(1), 259-273.

Wang, Y. and Serventi, L. (2019) Sustainability of dairy and soy processing: A review on wastewater recycling. *J. Clean. Prod.* 237, 117821.

Wang, Y., Zhang, Y., Wang, J. and Meng, L. (2009) Effects of volatile fatty acid concentrations on methane yield and methanogenic bacteria. *Biomass Bioenerg.* 33(5), 848-853.

Ward, A.J., Arola, K., Thompson Brewster, E., Mehta, C.M. and Batstone, D.J. (2018) Nutrient recovery from wastewater through pilot scale electrodialysis. *Water Res.* 135, 57-65.

Wasajja H., S.A.A. Al-Muraisy, A.L. Piaggio, P. Ceron-Chafla, P. V. Aravind, H. Spanjers, J.B. van Lier and Lindeboom, R.E.F. (2021) Improvement of biogas quality and quantity for small scale biogas-electricity generation application in off-grid settings: A field-based study. *Energies* 14(11), 3088.

Webster, G., Watt, L.C., Rinna, J., Fry, J.C., Evershed, R.P., Parkes, R.J. and Weightman, A.J. (2006) A comparison of stable - isotope probing of DNA and phospholipid fatty acids to study prokaryotic functional diversity in sulfate - reducing marine sediment enrichment slurries. *Environ. Microbiol.* 8(9), 1575-1589.

Wei, S.P., van Rossum, F., van de Pol, G.J. and Winkler, M.K.H. (2018) Recovery of phosphorus and nitrogen from human urine by struvite precipitation, air stripping and acid scrubbing: A pilot study. *Chemosphere* 212, 1030-1037.

Weissbrodt, D.G., Lochmatter, S., Ebrahimi, S., Rossi, P., Maillard, J. and Holliger, C. (2012) Bacterial Selection during the Formation of Early-Stage Aerobic Granules in Wastewater Treatment Systems Operated Under Wash-Out Dynamics. *Front. Microbiol.* 3, 332.

Welte, W., Nestel, U., Wacker, T. and Diederichs, K. (1995) Structure and function of the porin channel. *Kidney Int.* 48(4), 930-940.

White, M. (1975) Settling of activated sludge, Water Research Centre, Stevenhage. UK.

Whiteley, A.S., Manefield, M. and Lueders, T. (2006) Unlocking the ‘microbial black box’ using RNA-based stable isotope probing technologies. *Curr. Opin. Biotechnol.* 17(1), 67-71.

Wickham, H. (2011) ggplot2. *WIREs Computational Statistics* 3(2), 180-185.

- Wickham, H., Chang, W. and Wickham, M.H. (2016) Package ‘ggplot2’. Create elegant data visualisations using the grammar of graphics Version 2(1), 1-189.
- Wiegel, J., Tanner, R. and Rainey, F.A. (2006) The Prokaryotes: Volume 4: Bacteria: Firmicutes, Cyanobacteria. Dworkin, M., Falkow, S., Rosenberg, E., Schleifer, K.-H. and Stackebrandt, E. (eds), pp. 654-678, Springer US, New York, NY.
- Willems, A., Busse, J., Goor, M., Pot, B., Falsen, E., Jantzen, E., Hoste, B., Gillis, M., Kersters, K. and Auling, G. (1989) *Hydrogenophaga*, a new genus of hydrogen-oxidizing bacteria that includes *Hydrogenophaga flava* comb. nov. (formerly *Pseudomonas flava*), *Hydrogenophaga palleronii* (formerly *Pseudomonas palleronii*), *Hydrogenophaga pseudoflava* (formerly *Pseudomonas pseudoflava* and “*Pseudomonas carboxydoflava*”), and *Hydrogenophaga taeniospiralis* (formerly *Pseudomonas taeniospiralis*). *Int. J. Syst. Evol. Microbiol.* 39(3), 319-333.
- Wojcik, A., Middleton, H., Damopoulos, I. and Van herle, J. (2003) Ammonia as a fuel in solid oxide fuel cells. *J. Power Sources* 118(1-2), 342-348.
- Wu, L.J., Kobayashi, T., Li, Y.Y. and Xu, K.Q. (2015) Comparison of single-stage and temperature-phased two-stage anaerobic digestion of oily food waste. *Energy Convers. Manag.* 106, 1174-1182.
- Xie, M., Shon, H.K., Gray, S.R. and Elimelech, M. (2016) Membrane-based Processes for Wastewater Nutrient Recovery: Technology, Challenges, and Future Direction. *Water Res.* 89, 210-221.
- Xin, H., Worix, V., Burkhart, W. and Spremulli, L.L. (1995) Cloning and expression of mitochondrial translational elongation factor Ts from bovine and human liver. *J. Biol. Chem.* 270(29), 17243-17249.
- Xu, K., Qu, D., Zheng, M., Guo, X. and Wang, C. (2019) Water reduction and nutrient reconcentration of hydrolyzed urine via direct-contact membrane distillation: ammonia loss and its control. *J. Environ. Eng.* 145(3), 04018144.
- Yabuuchi, E., Kaneko, T., Yano, I., Wayne Moss, C. and Miyoshi, N. (1983) *Sphingobacterium* gen. nov., *Sphingobacterium spiritivorum* comb. nov., *Sphingobacterium multivorum* comb. nov., *Sphingobacterium mizutae* sp. nov., and *Flavobacterium indologenes* sp. nov.: glucose-nonfermenting gram-negative rods in CDC groups I1K-2 and I1b. *Int. J. Syst. Evol. Microbiol.* 33(3), 580-598.
- Yang, G., Zhang, P., Zhang, G., Wang, Y. and Yang, A. (2015a) Degradation properties of protein and carbohydrate during sludge anaerobic digestion. *Bioresour. Technol.* 192, 126-130.
- Yang, J., Molouk, A.F.S., Okanishi, T., Muroyama, H., Matsui, T. and Eguchi, K. (2015b) A Stability Study of Ni/Yttria-Stabilized Zirconia Anode for Direct Ammonia Solid Oxide Fuel Cells. *ACS Appl. Mater. Interfaces* 7(51), 28701-28707.

Yang, N., Yu, H., Li, L., Xu, D., Han, W. and Feron, P. (2014) Aqueous Ammonia (NH₃) Based Post Combustion CO₂ Capture: A Review. *Oil and Gas Science and Technology - Revue d'IFP Energies nouvelles* 69(5), 931-945.

Yang, Q., Yang, M., Zhang, S. and Lv, W. (2005) Treatment of wastewater from a monosodium glutamate manufacturing plant using successive yeast and activated sludge systems. *Process Biochem.* 40, 2483-2488.

Yara (2020) Choose the Ammonia grade that suits your industry

Yi, J., Dong, B., Jin, J. and Dai, X. (2014) Effect of increasing total solids contents on anaerobic digestion of food waste under mesophilic conditions: performance and microbial characteristics analysis. *PLoS ONE* 9(7), e102548.

Yu, H. and Fang, H.H.P. (2001) Acidification of mid-and high-strength dairy wastewaters. *Water Res.* 35(15), 3697-3705.

Yu, H. and Fang, H.H.P. (2003) Acidogenesis of gelatin-rich wastewater in an upflow anaerobic reactor: influence of pH and temperature. *Water Res.* 37, 55-66.

Yu, H., Yang, C., Maher, D., Green, P., Wardhaugh, L., Milani, D., Cottrell, A., Jiang, K., Li, K., Li, L., Fernandes, D. and Feron, P. (2018) Pilot Plant Demonstration of an Advanced Aqueous Ammonia-Based CO₂ Capture Technology, pp. 21-26, Melbourne.

Zamora, P., Georgieva, T., Ter Heijne, A., Sleutels, T.H., Jeremiasse, A.W., Saakes, M., Buisman, C.J. and Kuntke, P. (2017) Ammonia recovery from urine in a scaled-up microbial electrolysis cell. *J. Power Sources* 356, 491-499.

Zarebska, A., Romero Nieto, D., Christensen, K.V., Fjerbæk Søtoft, L. and Norddahl, B. (2015) Ammonium fertilizers production from manure: A critical review. *Crit. Rev. Environ. Sci. Technol.* 45(14), 1469-1521.

Zaru, R., Magrane, M., Orchard, S. and Consortium, U. (2020) Challenges in the annotation of pseudoenzymes in databases: the UniProtKB approach. *The FEBS Journal* 287(19), 4114-4127.

Zhang, C., Su, H., Baeyens, J. and Tan, T. (2014) Reviewing the anaerobic digestion of food waste for biogas production. *Renew. Sust. Energ. Rev.* 38, 383-392.

Zhang, H., Guo, S.H., Sun, B., Zhang, J., Cheng, M.G., Li, Q., Hong, Q. and Huang, X. (2015) *Mangrovibacter yixingensis* sp. nov., isolated from farmland soil. *Int. J. Syst. Evol. Microbiol.* 65(8), 2447-2452.

Zhang, L., Lee, Y.W. and Jahng, D. (2011) Anaerobic co-digestion of food waste and piggery wastewater: Focusing on the role of trace elements. *Bioresour. Technol.* 102(8), 5048-5059.

Zhang, Y. and Angelidaki, I. (2015) Submersible microbial desalination cell for simultaneous ammonia recovery and electricity production from anaerobic reactors containing high levels of ammonia. *Bioresour. Technol.* 177, 233-239.

Zhou, M., Yan, B., Wong, J.W.C. and Zhang, Y. (2018) Enhanced volatile fatty acids production from anaerobic fermentation of food waste: A mini-review focusing on acidogenic metabolic pathways. *Bioresour. Technol.* 248, 68-78.

Zhou, Z., Chen, L., Wu, Q., Zheng, T., Yuan, H., Peng, N. and He, M. (2019) The valorization of biogas slurry with a pilot dual stage reverse osmosis membrane process. *Chem. Eng. Res. Des.* 142, 133-142.

Ziels, R.M., Beck, D.A. and Stensel, H.D. (2017) Long-chain fatty acid feeding frequency in anaerobic codigestion impacts syntrophic community structure and biokinetics. *Water Res.* 117, 218-229.

Reference regulations

Directive 91/676/EEC, 1991. Council Directive 91/676/EEC of 12 December 1991 concerning the protection of waters against pollution caused by nitrates from agricultural sources, O. J. L 375, 1-8.

Regulation (EU) 2003/2003, 2003. Regulation (EC) No. 2003/2003 of the European Parliament and of the Council relating to fertilisers. O. J. L 304, 1-194.

Regulation (EU) 2019/1009, 2019. Regulation (EU) 2019/1009 of the European Parliament and of the Council of 5 June 2019 laying down rules on the making available on the market of EU fertilising products and amending Regulations (EC) No 1069/2009 and (EC) No 1107/2009 and repealing Regulation (EC) No 2003/2003.

ACKNOWLEDGEMENT

致谢

To my dear family and friends, I am thrilled to announce that I will be finishing my PhD this year, in 2023. This journey has been a long and unforgettable one, and I consider it to be the most valuable experience of my life. I am incredibly grateful for your constant support and company throughout this process, and I want to express my heartfelt appreciation to you all.

I would like to extend a special thank you to my wonderful supervisors, Henri Spanjers and Jules van Lier, who have been guiding me since my MSc days. Henri, I still remember how patiently you answered all my questions in the Fundamentals of Water Treatment course. You always made time for our discussions and never imposed your opinions on me, instead, you guided me to think independently and conceptually. You always show me your inclusiveness and encouragement during my research, and your gentle and meticulous supervision comforted me during times of frustration. Jules, your sharp mind and critical thinking challenged me in the best possible way, and I always felt I grew as a researcher after our discussions. You encouraged me to take on all challenges when I felt hesitant, and you offered me every opportunity to improve when it was needed. I will never forget the lessons on anaerobic digestion that you taught at IHE Delft, and I am also grateful for the postdoc position you offered during the final stage of my PhD. As someone who has always seen themselves as ordinary, I feel incredibly fortunate to have had the opportunity to learn and develop under your guidance. It has been an honour and a pleasure to work with you both, and I sincerely wish you all the best.

I would like to thank Ana and Santiago, who helped shaping my research plan, supervised my laboratory work, and guided me through practical issues. I would like to thank Patrick, Rewin, Menno, Sanjana, Lea, Rogelio, Timi, and all the interns worked with me in the Biothane lab. I learned about how a laboratory can function smoothly and efficiently, and I will always cherish the memories we created together. My thanks go out to my students Fabian and Jiahao for their hard work and dedication.

My deep gratitude to Niels van Linden, Elena Guillen, Jan Struckmann Poulsen, Jeppe Lund Nielsen, David Weissbrodt, Julian Muñoz Sierra, and David Cerqueda-Garcia for sharing their knowledge and enriching this work. Niels and Elena, our collaboration on TAN recovery was smooth and fruitful thanks to your thoughtful insights and discussions. Jan, Jeppe, and David, your lessons on microbiology and metaproteomics were incredibly

inspiring, and I learned a lot from your studies. Julian, thank you for your insights on anaerobic treatment of slaughterhouse wastewater and for helping analyse our complex data. I also want to thank Armand, Patricia, Jane and Jasper for your support in the Water Lab. I appreciate the help from Mariska, Sabrina, Tamara, and Riëlle in organizing all the administrative tasks, without which my research life would have been very difficult.

I want to give a shoutout to my fantastic office mates: Nan, Ran, Jawairia, Kajol, Liangfu, Yasmina, Ljiljana, Jawairia, Nessia, Devanita, and Ali. Working in room 4.44 was a pleasure, and I enjoyed all the relaxing time we had together. I am also grateful for my friends and colleagues: Sandra, Irene & Joris, Anke, Bianca, Iza & Damien, Zofia & Przemek, Xiang & Erik&Fiona, Antonella, Carina, Sara, Pamela, Magela, Javier, Adrian, Victor, Mona, Bruno, Diana, Raluca, and etc. I feel honoured to work with many colleagues in Sanitary Engineering: Merle, Ralph, Luuk, Jan Peter, Bas, Lisa, Doris, Boris, and many more.

I acknowledge the China Scholarship Council and Lamminga fund for their financial support.

感谢姜米花在我博士生涯中的鼓励，指导，帮助，和投喂。感谢大鱼成为我的好朋友。感谢学东大佬，刚哥，曾总，郭洪胖，商老板和 Jenny，菲菲姐和晓臣师兄，翠杰师姐和魏鹏师兄，家良师兄，国帅，刘宏波老师，老马，利华，亮哥，斌哥，硕哥和郎姐，还有所有的师弟师妹们。感谢中国好邻居梁福琪和羽毛球友们。感谢覃添，王勃和大妈，梁博士和马总，刘茜和邵教授，瓜哥和小李，老张和小黄，王三和小金。感谢我在动物森友会认识的朋友们和温柔的细细。感谢女明星摄影师佳星。感谢街霸，皮鸡和秋扣，Leo & Mickey，汤圆，马贱，肉包，小冰箱，还有村里每一只治愈过我的小猫咪。

感谢父母对我的养育，感谢刘泽宇无条件的爱。

邓哲 Zhe Deng

18th September, 2023

Delft

CURRICULUM VITAE

Personal information:

Family name: Deng 邓

Given name: Zhe 哲

Date of birth: 5th May 1991

Place of birth: Lipu, Guangxi Province, China

Email: dengzhe2017@hotmail.com

Education and experience:

- 2022 – 2024 Postdoctoral researcher at **Delft University of Technology**
- ProfED online course: High-rate anaerobic wastewater treatment.
- 2017 - 2023 Ph.D. researcher at **Delft University of Technology**
- Ph.D. thesis entitled: Anaerobic Protein Degradation for Resources Recovery from Nitrogen-Loaded Residual Streams.
- 2017 - 2017 Engineer at **Shenzhen Water Planning and Design Institute**
- Project: Planning of Integrated Water Management in Hezhou, China.
- 2016 - 2017 Researcher at **Institute of Karst Geology**
- Project: Geological Survey for National Poverty Alleviation.
- 2013 – 2015 Master Sanitary Engineering at **Delft University of Technology**
- Master thesis entitled: Online VFA monitoring for efficient VFA production in a two-phase anaerobic system.
- 2008 – 2012 Bachelor Hydrology and Water Resources Engineering at **Sun Yat-sen University**
- Bachelor thesis entitled: Investigation of the concentration and toxicity of Parabens in surface waters of Guangzhou, China.

Publication list:

Deng, Z., Poulsen, J.S., Nielsen, J.L., Weissbrodt, D.G., Spanjers, H., & van Lier, J.B. Identification of protein-degraders in an anaerobic digester by protein stable isotope probing combined with metagenomics. Under review.

Deng, Z., Muñoz Sierra, J., Ferreira, A.L.M., Cerqueda-Garcia, D., Spanjers, H., & van Lier, J.B. (2023). Effect of operational parameters on the performance of an anaerobic sequencing batch reactor (AnSBR) treating protein-rich wastewater. *Environmental Science and Ecotechnology* 17 (2024): 100296.

Deng, Z., Ferreira, A.L.M., Spanjers, H., & van Lier, Jules B. (2023) Anaerobic protein degradation: effects of protein structural complexity, protein concentrations, carbohydrates, and volatile fatty acids. *Bioresource Technology Reports* 22, 101501.

Deng, Z., Ferreira, A.L.M., Spanjers, H., & van Lier, J.B. (2022). Characterization of microbial communities in anaerobic acidification reactors fed with casein and/or lactose. *Applied Microbiology Biotechnology* 106, 6301–6316.

Deng, Z., van Linden, N., Guillen, E., Spanjers, H., & van Lier, J.B. (2021). Recovery and applications of ammoniacal nitrogen from nitrogen-loaded residual streams: A review. *Journal of Environmental Management*, 295, 113096.

Tan, L.C., Peschard, R., Deng, Z., Ferreira, A.L.M., Lens, P.N., & Pacheco-Ruiz, S. (2021). Anaerobic digestion of dairy wastewater by side-stream membrane reactors: Comparison of feeding regime and its impact on sludge filterability. *Environmental Technology & Innovation*, 22, 101482.